Semi-Synthesis of a Biologically Inspired Library of Sesquiterpene Derivatives, from the Lipophilic Marine Natural Product (+)-β-Gorgonene

A Thesis

Submitted to the Graduate Faculty

in Partial Fulfilment of the Requirements

for the Degree of Doctor of Philosophy

Molecular and Macromolecular Sciences

Department of Chemistry

Faculty of Science

University of Prince Edward Island

Beth Margaret Buchanan

Charlottetown, Prince Edward Island

April, 2014

Conditions for the Use of the Thesis

Permission to Use Postgraduate Thesis

Title of thesis: Semi-Synthesis of a Biologically Inspired Library of Sesquiterpene Derivatives, from the Lipophilic Marine Natural Product (+)-β-Gorgonene

Name of Author:	Beth Margaret Buchanan	
Department:	Chemistry	
Degree:	Doctor of Philosophy	Year: 2014

In presenting this thesis in partial fulfillment of the requirements for a postgraduate degree from the University of Prince Edward Island, I agree that the Libraries of this University may make this thesis freely available for inspection and give permission to add an electronic version of the thesis to the Digital Repository at the University of Prince Edward Island. Moreover the author agrees that permission for extensive copying of this thesis for scholarly purposes may be granted by the professor or professors who supervised my thesis work, or, in their absence, by the Chair of the Department or the Dean of the Faculty in which my thesis work was done. It is understood any copying or publication or use of this thesis or parts thereof for financial gain shall not be allowed without my written permission. It is also understood that due recognition shall be given to me and to the University of Prince Edward Island in any scholarly use which may be made of any material in my thesis.

Signature: _____

Address: Faculty of Science

University of Prince Edward Island

550 University Avenue, Charlottetown, PE

Canada C1A 4P3

Date: _____

University of Prince Edward Island

Faculty of Science

Charlottetown

CERTIFICATION OF THESIS WORK

We, the undersigned, certify that Beth M. Buchanan, candidate for the degree of Doctor of Philosophy has presented a thesis with the following title: Semi-Synthesis of a Biologically Inspired Library of Sesquiterpene Derivatives, from the Lipophilic Marine Natural Product (+)-β-Gorgonene, that the thesis is acceptable in form and content and that a satisfactory knowledge of the field covered by the thesis was demonstrated by the candidate through an oral examination held on April 4, 2014.

Examiners:

Dr. Russell Kerr (Supervisor) _____

Dr. Nola Etkin (Committee member) _____

Dr. Barry Linkletter (Committee member) _____

Dr. Richard Bethell (Committee member) _____

Dr. Darren Derksen (external examiner) _____

Dr. Jason Pearson - Chair _____

Date _____

Abstract

Natural products and their mimics have a high probability of engaging with biological targets. Hence, natural products have historically been a valuable source of medicines. They continue to inspire the synthesis of biologically relevant compound libraries, useful for drug discovery. Over 50 % of the small molecule drugs approved in the last 30 years are natural products or natural product derived. Sesquiterpenes are widespread in nature and exhibit a range of notable biological activities including antimicrobial, anti-inflammatory, anti-viral and lipid lowering activity. Therefore, sesquiterpene frameworks are suitable templates for biologically relevant screening libraries.

Inspired by selected natural bioactive sesquiterpenes, we have transformed a highly lipophilic, non-drug-like, marine natural product (+)-β-gorgonene, available as a by-product from the purification of pseudopterosins, into a library of more drug-like derivatives. Several semi-synthetic techniques were employed to attach suitable structures such as substituted aromatics and heteroaromatics to the gorgonene scaffold to increase its drug-likeness and probability of exhibiting biological activity. Each compound synthesized was chemically characterized, analyzed for drug-likeness and screened for PTP1B inhibition (potential therapeutic target for treatment of type 2 diabetes), antimicrobial activity and cytotoxic properties.

With the goal of incorporating the desired substructures in a minimum number of steps, a 2+3 dipolar cycloaddition reaction was used to attach selected motifs to the gorgonene framework *via* an isoxazoline linker. The series of synthesized isoxazoline derivatives included decahydroazulene and cyclopropane-containing compounds. Several members of the isoxazoline-containing collection displayed selective inhibition of the PTP1B enzyme and others exhibited modest cytotoxic activity.

Another family of gorgonene analogues was synthesized through a dione containing intermediate, a product of the ozonolysis of gorgonene. Carbonyl chemistry was then used to incorporate aromatic moieties into the structure such as the aldol reaction and nucleophilic addition. Gorgonene was observed to undergo an intramolecular Alder-ene reaction when catalyzed by $FeCl_3$ or BF_3 and produce novel tricyclic sesquiterpene-like hydrocarbons. A hydroboration/oxidation strategy highlighted the tendency for the 1,5-diene system to react intramolecularly to form additional five- and six-membered rings. A glycosyl-containing derivative was synthesized through a dihydroxy-gorgonene analogue. Biotransformation was used as an additional strategy to selectively oxidize synthetically inaccessible carbons on gorgonenes saturated decalin backbone to facilitate further transformations. Incubation of gorgonene with *Bionectria ochroleuca* resulted in the production of a novel trihydroxylated sesquiterpenoid.

Acknowledgements

I would like to take this opportunity to thank the individuals that have supported me in my intellectual journey. First, I would like to extend my gratitude to my supervisor, Dr. Russell Kerr, for providing the opportunity for me to develop my knowledge and skills in a state of the art laboratory while pursuing a doctoral degree. Russ fostered my interest for natural products chemistry providing guidance and wisdom throughout my time in his lab. I would also like to thank the research managers in the Kerr lab, Dr. Fabrice Berrue, Dr. Dave Overy and Brad Haltli for sharing your wealth of knowledge and supporting me from day one. A huge thank you to mentor and friend Dr. Malcolm McCulloch who provided many suggestions and insights for this project. I would like to acknowledge my supervisory and examining committee members Dr. Nola Etkin, Dr. Junzeng Zhang, Dr. Richard Bethell, Dr. Barry Linkletter, Dr. Michael Shaver Dr. Darren Derksen and Dr. Jason Pearson for their time, thoughtful insights and suggestions. To my lab mates, for great discussions and moral support thank you Erin, Krista, Alyssa, Stacey, Doug, Hebelin, Ghada and Amir. I am very grateful to funding agencies, especially NSERC and Dr. Regis Duffy for the financial support without which I would not have been able to pursue this dream.

Finally I would like to express my thanks and love to my family for believing in me and supporting me. My daughter Dahlia Buchanan has been my sunshine and motivation from beginning to end. My mother was the reason I got into science and my inspiration. I would like to thank my partner, Trevor, for your love through thick and thin. Thank you to Honey and Woody Mahaney for supporting me in immeasurable

ways and saw potential in me when no one else did. They consistently went far above and beyond what anyone would expect and are truly like a mother and father to me. My sisters, Heaz and Jenn, are my rock and my wings, my soft place to fall, and the ones that have kept me sane all of these years. Thank you to my lovely nieces: Taylor, Madison and Bailey for all the fun we have had and for sharing your inner beauty with me. Thank you finally to my father for all your love and patience. I love you all.

Dedication

To Honey, Woody and Dahlia.

Epigraph

What lies behind us and what lies before us are tiny matters compared to what lies within us.

Ralph Waldo Emerson

Table of Contents

Semi-Synthesis of a Biologically Inspired Library of Sesquiterpene Derivatives, from the Lipophilic Marine Natural Product (+)-β-Gorgonene ..... **i**

Conditions for the Use of the Thesis ..... **ii**

Permission to Use Postgraduate Thesis ..... **iii**

Certification of Thesis Work ..... **iv**

Abstract ..... **v**

Acknowledgements ..... **vii**

Dedication ..... **ix**

Epigraph ..... **x**

Table of Contents ..... **xi**

List of Figures ..... **xviii**

List of Tables ..... **xxiii**

Table of Abbreviations ..... **xxv**

Chapter 1 - General Introduction **1**

1.1 The Need for New Therapeutics 2

1.2 Sources of Screening Libraries 2

1.3 Natural Products 3
1.3.1 Marine Natural Products 4
1.3.2 Natural Product Isolation and Screening 5
1.3.3 Challenges and Solutions for Natural Product Chemistry 5
1.4 Combinatorial Chemistry 9
1.5 Biologically-Inspired Synthetic Strategies 9
1.5.1 Target-Oriented Synthesis and Diversity-Oriented Synthesis 9
1.5.2 Natural Product - Like Compounds 10
1.5.3 Target-Based Drug Discovery 11
1.5.4 Lead-Oriented Synthesis 11
1.5.5 Lead-Directed Semi-synthesis 12
1.5.6 Chemically Engineered Extracts 13
1.5.7 Biology-Oriented Synthesis (BIOS) 14
1.6 Diseases with a Need for New Drugs 14
1.6.1 The Global Diabetes and Obesity Problem 14
1.6.2 PTP1B as a Drug Target for Diabetes and Obesity 15
1.6.3 Need for New Antimicrobial Drugs 16
1.6.4 Need for New Cancer Drugs 17
1.7 Sesquiterpenoids and Meroterpenoids 17
1.7.1 Antimicrobial Decalin Containing Sesquiterpenoids and Meroterpenoids 18
1.7.2 Sesquiterpene and Meroterpenes that Inhibit the PTP1B Enzyme 28
1.7.3 Cytotoxic Sesquiterpenes 28

1.8 Precedent for Decalin Containing BIOS Libraries 29

1.8.1 Summary 31

1.9 Research Goals 32

1.9.1 (+)-β-Gorgonene 32

1.9.2 Hypothesis 34

1.9.3 Objectives 34

1.9.4 Experimental Design 35

Chapter 2 - Regioselective Intramolecular Alder-Ene Reaction of Un-activated Sesquiterpene (+)-β-Gorgonene 38

2.1 Introduction 39

2.1.1 Alder-Ene Reaction 39

2.1.2 Application of Alder-Ene Reaction to the Functionalization of Gorgonene .. 40

2.2 Results and Discussion 41

2.2.1 Thermal Alder-Ene Reaction 41

2.2.2 $FeCl_3$ Catalyzed Intramolecular Alder-Ene Rearrangement of (+)-β-Gorgonene 41

2.2.3 Proposed Mechanism for Intramolecular Alder-Ene Reaction of Gorgonene 43

2.2.4 Synthetic and Biocatalytic Work with **74** 44

2.2.5 BF_3 Catalyzed Intramolecular Alder-ene Rearrangement of (+)-β-Gorgonene 44

2.2.6 Stability Studies of Gorgonene 47

2.2.7 Biological Assessment of Gorgonene (**73**) and Synthetic Derivatives (**74**, **75**) 50

2.3 Significance and Future Work 53

2.4 Experimental Section 54

2.4.1 General Experimental 54

2.4.2 General Procedure for Anti-Microbial Assays 56

2.4.3 General Procedure for Cytotoxicity Assay 58

2.4.4 General Procedure for PTP1B Assays 60

Chapter 3 - Semi-synthesis and Biological Evaluation of Isoxazoline-Containing (+)-β-Gorgonene Derivatives 65

3.1 Introduction 66

3.1.1 Isoxazolines and Related Heterocycles 66

3.2 Results and Discussion 67

3.2.1 Preparation of Isoxazoline-Containing Compounds Using a 2+3 Dipolar Cycloaddition 67

3.2.2 Isoxazoline Containing Compound Library 69

3.2.3 Analysis of the Drug-Likeness of Isoxazoline Library 90

3.2.4 Biological Evaluation of Isoxazoline-Containing Compound Collection 92

3.3 Conclusion 94

3.4 Experimental Section 95

3.4.1 General Procedure for Synthesis of Isoxazoline Derivatives 95

Chapter 4 - Semi-Synthesis and Biological Analysis of β-Gorgonene Analogues Accessed through Ozonolysis Product 117

4.1 Introduction 118

4.2 Results and Discussion 119

4.2.1 Ozonolysis of Gorgonene 119

4.2.2 Synthesis of Gorgonene Analogues using the Aldol Reaction 128

4.2.3 Synthesis of Amine Containing Gorgonene Derivatives using Condensation and Reductive Amination Reactions 135

4.2.4 Nucleophilic Addition to Dione **118** 142

4.2.5 Biological Assessment of Compound Collection 145

4.3 Conclusion 148

4.4 Experimental Section 149

Chapter 5 - Route to a Novel Glycosylated Derivative *via* Hydroxylation of Gorgonene 168

5.1 Introduction 169

5.2 Results and Discussion 170

5.2.1 Dihydroboration / Oxidation of Gorgonene as a Route to Dihydroxygorgonene Derivatives 170

5.2.2 Synthesis of Glycosylated Analogue of (+)-β-Gorgonene 174

5.2.3 Reactivity of Gorgonene Derivatives **135** and **136** 176

5.2.3 Riley Allylic Selenium Dioxide Oxidation of Gorgonene 179

5.2.4 Biological Assessment of Compounds **135**, **136**, **141**, **145** and **147** 183

5.3 Conclusion and Significance 184

5.4 Experimental Section 185

Chapter 6 - Microbial Transformation of the Sesquiterpene (+)-β-Gorgonene.... 195

6.1 Introduction to the Use of Biotransformation in Organic Synthesis 196

6.2 Biotransformation Method Development 197

6.2.1 Extraction of Metabolites from Biotransformation Culture 198

6.2.2 GCMS as a Screening Tool for Biotransformation Extracts 198

6.2.3 Optimization of Substrate Concentration in Biotransformation Culture 199

6.2.4 Selection of Fungi for Biotransformation 199

6.2.5 Optimization of Duration of Fermentation 200

6.3 Large Scale Biotransformation Fermentation 203

6.3.1 *Bionectria ocroleuca* Biotransformation of **73** 203

6.3.2 Fermentation of *Beauveria geodes* with **74** 209

6.3.3 *Pleurotus djamor* Fermentation with **74** 209

6.4 Future work 209

6.5 Significance 210

6.6 Experimental Section 211

Chapter 7 - Conclusion and Future Work 215

7.1 Synthesis and Biological Evaluation of Gorgonene Derivatives 216

7.2 Reactivity of Gorgonene 216

7.3 Future Work 217

References 218

List of Figures

Figure 1.1 - Synthetic and Biological Sources of Small Molecule Screening Libraries... 3

Figure 1.2 - Bioassay-Guided Fractionation 5

Figure 1.3 - Target-Oriented and Diversity-Oriented Synthesis 10

Figure 1.4 - Natural Products as a Source of Drugs and Lead Compounds..... 13

Figure 1.5 - Antimicrobial Siphonodictyals and Siphonodictyols 19

Figure 1.6 - Ilimaquinone, Dictyoceratin and Avarol Derivatives..... 20

Figure 1.7 - Avarone and Related Synthetic Compounds..... 21

Figure 1.8 - Potent Antimicrobial Sesquiterpenes and Meroterpenes..... 22

Figure 1.9 - Antimicrobial Compounds Agelasine B, Ageline B and Prianicin B 23

Figure 1.10 - Kalihinol Family of Compounds..... 24

Figure 1.11 - Antimicrobial Terpenoids **47**-**50** 25

Figure 1.12 - Bicyclofarnesol Skeleton..... 26

Figure 1.13 - Biosynthesis of Bicyclofarnesol and Maaliane Sesquiterpenes 27

Figure 1.14 - Sesquiterpene Quinones that Inhibit PTP1B 28

Figure 1.15 - Eudesmanolide Backbone and Parthenolide 29

Figure 1.16 - Androphapholide Inspired BIOS Compound Collection 30

Figure 1.17 - Sulfricin 30

Figure 1.18 - Dysidiolide Inspired Inhibitors of 11-β-HSD..... 31

Figure 1.19 - Santonin Inspired Library of 5-Lipoxygenase Inhibitors 31

Figure 1.20 - Structure of (+)-β-Gorgonene..... 32

Figure 1.21 - Comparison of (+)-β-Gorgonene and Bicyclofarnesol Skeleton..... 33

Figure 1.22 - Strategy to Convert Gorgonene to Drug-Like Library of Natural Product Derivatives 34
Figure 1.23 - Modular Composition of Screening Libraries 36
Figure 2.1 - Alder-Ene Reaction Scheme 39
Figure 2.2 - Retrosynthetic Analysis of Desired Alder-Ene Product 40
Figure 2.3 - $FeCl_3$ Catalyzed Intramolecular Alder-Ene Reaction of (+)-β-Gorgonene. 43
Figure 2.4 - Proposed Mechanism for Formation of **74** 44
Figure 2.5 - BF_3 Catalyzed Intramolecular Alder-Ene Reaction 45
Figure 2.6 - Stereochemical Assignment of **75** 46
Figure 2.7 - Mechanism of BF_3 Catalyzed Production of **75** 47
Figure 2.8 - Acid-Induced Rearrangement of (+)-β-Gorgonene 48
Figure 2.9 - PTP Enzymes and their Subclasses Used in Bioassay 52
Figure 3.1 - Oxazole and Related Ring Systems 66
Figure 3.2 - Isoxazoline Reaction Scheme 67
Figure 3.3 - Aldehyde Starting Materials Containing Desired Substructures 68
Figure 3.4 - Synthesized Isoxazoline-Containing Compound Collection 71
Figure 3.5 - Stereochemical Assignment of Compound **92** 72
Figure 3.6 - Rational for Stereoselectivity Observed in Isoxazoline Library 74
Figure 3.7 - NOESY Supported Stereochemical Assignment of **90** 76
Figure 3.8 - Key 2-D NMR Data for Structure Elucidation of Compound **97** 78
Figure 3.9 - Stack Plot of ^1H NMR Spectra (600 MHz, $CDCl_3$) of Semi-synthetic Compounds **98** (bottom), **99** (middle) and **100** (top). (δ in ppm Relative to Solvent Signal) 81

Figure 3.10 - Enlarged Stack Plot of ^{1}H NMR Spectra (600 MHz, $CDCl_3$) of Semi-synthetic Compounds **98** (bottom), **99** (middle) and **100** (top). (δ in ppm Relative to Solvent Signal) 82

Figure 3.11 - Acid-Induced Rearrangement of Bicyclogermacrene (**110**) 84

Figure 3.12 - Theoretical Starting Materials for Cyclopropane and Decahydroazulene Containing Products 85

Figure 3.13 - Batch of Gorgonene Starting Materials ^{1}H NMR Spectrum in $CDCl_3$ 86

Figure 3.14 - Stereochemical Assignment of Chlorinated Analogue **102** 88

Figure 3.15 - Radical Mechanism for the Formation of Chlorinated Analogue **102** 89

Figure 3.16 - Addition/Elimination Mechanism for the Formation of **102** 89

Figure 3.17 - Cytotoxic Evaluation and Structure Activity Relationship of Isoxazoline Compounds (HTB-26) 94

Figure 4.1 - Retrosynthetic Analysis of Diverse Compound Libraries Accessible through Carbonyl Containing Gorgonene Derivative 118

Figure 4.2 - Mechanism of Ozonolysis 120

Figure 4.3 - Products of the Ozonolysis of (+)-β-Gorgonene 123

Figure 4.4 - Stack Plot of ^{1}H NMR Spectra (600 MHz, $CDCl_3$) of Semi-synthetic Compounds 118 (Top) and 119 (Bottom) (δ in ppm Relative to Solvent Signal) 125

Figure 4.5 - Key NMR Correlations for Structure Elucidation of **120** 126

Figure 4.6 - Proposed Mechanism for Formation of **120** 128

Figure 4.7 - Aldol Reaction Scheme 129

Figure 4.8 - Pyrrole-Containing Aldol Derivatives 130

Figure 4.9 - Furan-Containing Enone Derivative 132

Figure 4.10 - Dimethoxybenzene - Containing Aldol Derivatives 133

Figure 4.11 - Stable Chair Conformation of **125** 134

Figure 4.12 - Methoxybenzene-Containing Aldol Derivative 134

Figure 4.13 - Oxime Containing Drugs Milbemycin Oxime and Cloximate..... 136

Figure 4.14 - Oxime Synthesis..... 137

Figure 4.15 - Numbering and Key COSY and HMBC Correlations for **131**..... 139

Figure 4.16 - Proposed Mechanism for the Formation of **131**..... 141

Figure 4.17 - Grignard Reaction of Benzyl Magnesium-Bromide with **118** 143

Figure 4.18 - Key NOESY Correlation Supporting Stereochemistry of **132**..... 143

Figure 4.19 - Grignard Reaction with 1-Bromo-2,5-Dimethoxybenzene and **118** 144

Figure 5.1 - Retrosynthesis of Glycosylated Gorgonene Analogue..... 170

Figure 5.2 - Hydroboration / Oxidation of Gorgonene 172

Figure 5.3 - Crystal Structure of Hydroboration/Oxidation Product **136** 172

Figure 5.4 - Proposed Mechanism for the Formation of Products **135** and **136**..... 174

Figure 5.5 - Glycosylation Reaction Scheme..... 175

Figure 5.6 - Retrosynthetic Analysis of Aromatic Containing Derivative of Gorgonene 177

Figure 5.7 - Tosylation of **136** Produces Tricyclic Ether **145**..... 178

Figure 5.8 - Proposed Mechanism for Formation of **145**..... 178

Figure 5.9 - Synthesis of Tosylate Ester **146** 179

Figure 5.10 - Riley Allylic Selenium Dioxide Oxidation Mechanism..... 179

Figure 5.11 - Synthesis of Selenide Derivative of **73** 180

Figure 5.12 - Key NMR Correlations for **147**..... 181

Figure 6.1 - Fungal Biotransformations of (-)-Maalioxide (**77**) 197

Figure 6.2 - Biocatalysis of Valencene (**153**) by *Pleurotus sapidus*..... 197

Figure 6.3 - Key NMR Correlations for the Structure Elucidation of Biotransformation Product **157** 207

Figure 6.4 - Biotransformation of (+)-Nootkatone by *Aspergillus niger*..... 207

Figure 6.5 - Proposed Mechanism for Formation of Glycol in **157**..... 208

List of Tables

Table 2.1 - NMR Spectroscopic Data ($CDCl_3$) for Compound **74** 42

Table 2.2 - NMR Spectroscopic Data for Compound **75** ($CDCl_3$) 45

Table 2.3 - Reaction Conditions Employed to Analyze the Stability of Gorgonene to Acid and Heat Treatment 48

Table 2.4 - Reaction Conditions Employed to Analyze Gorgonenes Stability to Lewis Acid and Metal Catalysts. 49

Table 2.5 - PTP1B Inhibition of Gorgonene, **74** and **75** 52

Table 3.1 - NMR Spectroscopic Data for Compound **92** ($CDCl_3$) 73

Table 3.2 - Products Yields of 2+3 Cycloaddition Reaction with **73** 74

Table 3.3 - Spectroscopic Data for Compound **90** ($CDCl_3$)..... 77

Table 3.4 - NMR Spectroscopic Data for Compound **97** ($CDCl_3$) 79

Table 3.5 - Analysis of Drug-Like Properties of Isoxazoline Compound Collection..... 91

Table 3.6 - Cytotoxicity of Isoxazoline Collection (IC_{50})..... 93

Table 4.1 - Optimization of Ozonolysis Reaction Conditions 122

Table 4.2 - NMR Spectroscopic Data for Compounds **118** and **119** ($CDCl_3$) 124

Table 4.3 - NMR Spectroscopic Data for the Characterization of **120** ($CDCl_3$)..... 127

Table 4.4 - NMR Spectroscopic Data for Compound **122** ($CDCl_3$) 131

Table 4.5 - Toward Reductive Amination Optimization 138

Table 4.6 - NMR Spectroscopic Data for Compound **131** ($CDCl_3$) 140

Table 4.7 - Assessment of Drug-likeness of Compound Collection..... 145

Table 4.8 - Evaluation of Cytotoxicity of Ketone Derived Family (IC_{50}) 146

Table 4.9 - Results of PTP Inhibition Assay of Compounds **122-124**..... 147

Table 5.1 - NMR Spectroscopic Data for Compound **135** ($CDCl_3$) 171

Table 5.2 - NMR Spectroscopic Data for Compound **147** ($CDCl_3$) 182

Table 5.3 - Cytotoxicity Data for Compounds **135**, **136**, **141**, **145** and**147** (IC_{50})..... 183

Table 6.1 - Qualitative Analysis of Fungi Growth and Sporulation in Various Media 201

Table 6.2 - Evaluation of Biotransformation Conversion at Two Time Points Using GCMS 202

Table 6.3 - Masses of Biotransformation Extracts..... 203

Table 6.4 - NMR Spectroscopic Data for Compound **157** ($CDCl_3$) 206

Table of Abbreviations

11β-HSD	11β-hydroxysteroid dehydrogenase
3T3-L1	immortalised mouse-derived fibroblast cell line
Ac	acetyl
ACN	acetonitrile
AcOH	acetic acid
ATCC	American type culture collection
BIOS	biology-oriented synthesis
BSA	bovine serum albumin
Bz	benzoyl
C18	octadecyl silane
CdC25A	cell division cycle 25 homolog A , a dual-specificity phosphatase
COSY	correlation spectroscopy
DBU	1,8-diazabicyclo[5.4.0]undec-7-ene
DCE	dichloroethane
DCM	dichloromethane

de	diastereomeric excess
DMAP	4-dimethylaminopyridine
DME	dimethyl ether
DMF	dimethyl formamide
DMS	dimethyl sulfide
DMSO	dimethyl sulfoxide
DTT	dithiothreitol
eq	equivalents
EtOH	ethanol
ELSD	evaporative light scattering detector
FTIR	Fourier transform infrared spectroscopy
GC	gas chromatography
GC-MS	gas chromatography mass spectrometry
h	hours
HEPES	4-(2-hydroxyethyl)-1-piperazineethanesulfonic acid
HMBC	heteronuclear multiple-bond correlation spectroscopy
HOMO	highest occupied molecular orbital

HPLC	high-performance liquid chromatography
HRMS	high-resolution mass spectrometry
HRESIMS	high-resolution electrospray ionization-mass spectrometry
HSQC	heteronuclear single-quantum coherence spectroscopy
HTB-26	human breast adenocarcinoma cell line
Hz	hertz
IC_{50}	half maximal inhibitory concentration
IPA	isopropyl alcohol
J	coupling constant
JAK2	janus kinase 2, a non-receptor tyrosine kinase
LAR D1D2	leukocyte common antigen-related protein tyrosine phosphatase containing domains 1 and 2
LC-MS	liquid chromatography-mass spectrometry
LUMO	lowest unoccupied molecular orbital
M	monoisotopic mass
MeOH	methanol
MIC	minimum inhibitory concentration
MRSA	methicillin-resistant *Staphylococcus aureus*

MW	molecular weight
MKPX	dual specific protein tyrosine phosphatase
m/z	mass to charge ratio
NBS	*N*-bromosuccinimide
NCS	*N*-chlorosuccinimide
NMR	nuclear magnetic resonance
NOESY	nuclear Overhauser effect spectroscopy
PBISe	Se,Se'-1,4-phenylenebis(1,2-ethanediyl)bisisoselenourea
PCA	principal component analysis
pNPP	*para*-nitrophenylphosphate
ppm	parts per million
prep	preparatory
PRL2/AS	regenerating liver protein tyrosine phosphatase
PTP	protein tyrosine phosphatase
PTP1B	protein tyrosine phosphatase 1B
ROESY	rotating frame nuclear Overhauser effect spectroscopy
RPM	revolutions per minute

RT	room temperature
SAR	structure activity relationship
SIGMA D1D2	murine receptor-like protein tyrosine phosphatase containing domains 1 and 2
sm	starting materials
SHP-1	intracellular protein tyrosine phosphatase non-receptor type 6
TBME	*tert*-butyl methyl ether
TC-PTP	protein tyrosine phosphatase non-receptor type 2
TEA	triethylamine
Tf	trifluoromethanesulfonyl
TFA	trifluoroacetic acid
THF	tetrahydrofuran
TLC	thin-layer chromatography
Ts	4-toluenesulfonyl
UPLC	ultra-performance liquid chromatography
UV	ultraviolet
ν_{max}	wavenumber absorption maxima

V	volts
VRE	vancomycin-resistant *Enterococcus*

Chapter 1 - General Introduction

1.1 The Need for New Therapeutics

The pharmaceutical industry has made dramatic advances over the past hundred years, yet many diseases continue to lack efficacious treatments that are not associated with serious side effects, at a reasonable cost. There are urgent needs for novel therapeutics in the fields of oncology, medical microbiology and bariatrics providing vast opportunities for drug discovery and development. Cancer is consistently one of the two top causes of death in Canada and its treatments are plagued with low efficacy and painful side effects.[1] The emergence of multi-drug resistant pathogenic bacteria necessitate the development of alternatives to current therapeutics.[2] Obesity and diabetes are growing problems associated with major health complications and have few medical treatments.[3] These examples illustrate the need for research invested in the development of new drugs designed to treat diseases lacking attractive therapeutic options. The first step of drug discovery is often the identification of lead compounds in screening libraries using appropriate biological assays. These hits are then optimized to improve pharmacological properties.

1.2 Sources of Screening Libraries

In order to address the medical needs described above (diabetes, obesity and antibiotic resistant bacterial infections), screening libraries of small molecules are required for biological evaluation. Sources of screening libraries vary widely and there are many approaches to acquire compound collections likely to contain biologically active compounds.[4] Some of these sources of screening libraries are outlined in Figure 1.1.

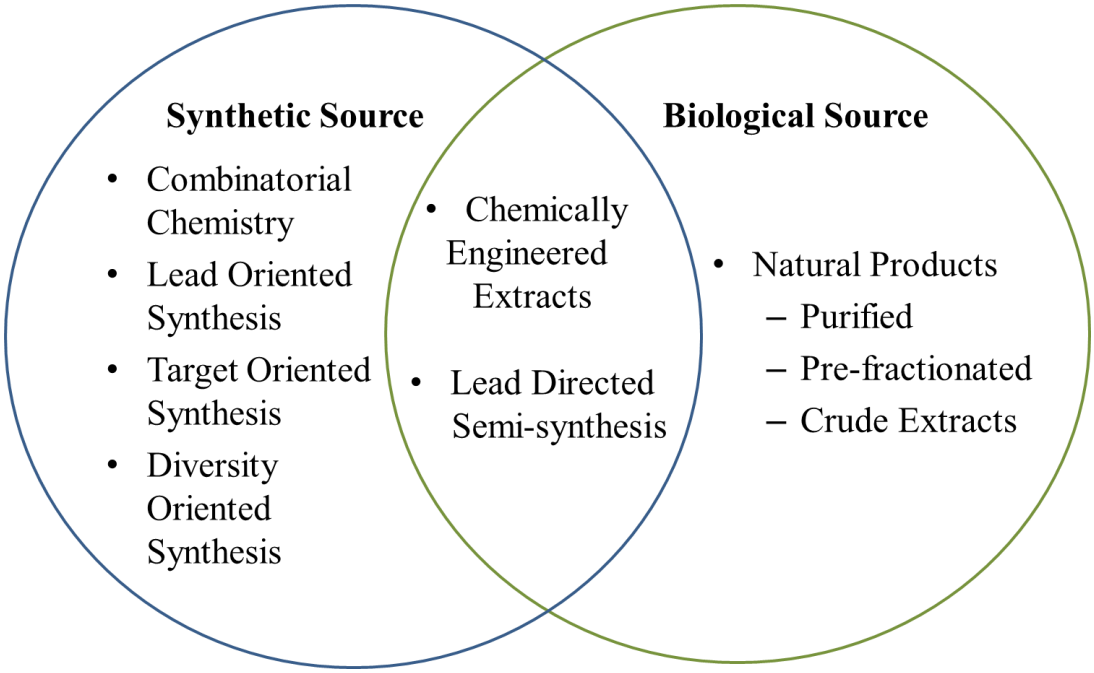

Figure 1.1 - Synthetic and Biological Sources of Small Molecule Screening Libraries

1.3 Natural Products

Natural products have been a great source of medicines over the course of history and continue to be invaluable in the production of new drugs.[5] Bioactive natural products often inspire the design and synthesis of libraries of molecules in the search for new pharmaceuticals[6] and these natural product-like libraries have been successful at producing new drug candidates.[7] Indeed, over 50 % of the drugs approved in the past 50 years have been natural products themselves, or derivatives of natural products.[8] Further, 19 new drugs were approved between the years 2005-2010 that fall in this category.[9]

Natural product based drug discovery programs produce a high percentage of bioactive compounds because natural products have evolved over millions of years to

interact with biological systems and control biological processes.[10] Due to the conservation of protein domains across taxonomic groups in nature, many natural products can interact with more than one biological target[10] and exhibit more than one type of biological activity within individual species or across species.[10] Due to the biological relevancy of natural products, they are considered ``pre-validated``, ``privileged`` structures for use in biological settings.[6] Some biologically active natural products may be unsuitable for therapeutic use due to insufficient activity, toxicity or supply issues, but in these cases they can be used as advanced lead compounds in the design of optimized bioactive libraries.[11]

1.3.1 Marine Natural Products

Oceans cover 70 % of the surface of the Earth and account for 95 % of the Earth's biosphere.[12] This rich biodiversity in turn produces chemical diversity.[13, 14] The marine environment has also been far less explored than the terrestrial environment, as many parts of the ocean were effectively inaccessible until the invention of scuba diving. Therefore, the marine environment is a promising source of novel biologically active compounds. Many marine organisms such as sponges and coral have little in the way of physical defense mechanisms (e.g. no mobility or physical protection) and often use chemical mechanisms in order to survive, such as the production of secondary metabolites that act as chemical defense against predation and pathogens.[5] Secondary metabolites may be produced by these organisms for other purposes as well such as communication, reproduction and adaptation to harsh marine environments.[15]

1.3.2 Natural Product Isolation and Screening

Due to the difficulty and time-consuming nature of purifying natural products from a crude extract it is impractical to purify each compound present in the extract prior to biological testing. Crude extracts or pre-fractionated libraries (partially purified extracts) are often screened for biological activity and only those fractions containing active components are purified further. The fractionation and biological testing processes are repeated until the bioactive compound is pure. This process is known as bioassay-guided fractionation (Figure 1.2).[16]

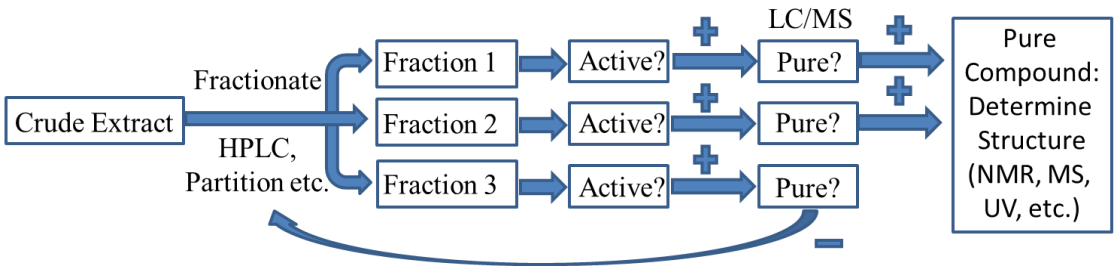

Figure 1.2 - Bioassay-Guided Fractionation[16]

1.3.3 Challenges and Solutions for Natural Product Chemistry

1.3.3.1 Supply of Natural Products

One of the major challenges associated with the use of natural products as therapeutics is the issue of supply. Several natural products with exceptional activity and potential have been delayed in development, or not developed due to a lack of supply.[17-20] These compounds are often produced in very small amounts from organisms which are limited in nature and difficult or impossible to farm using agriculture or aquaculture methods. Researchers have developed several solutions to address the supply problem and these are outlined in the following sections.

1.3.3.2 Total Synthesis of Natural Products

Developing total syntheses of natural products is a popular challenge for synthetic chemists. Natural products are often complex molecules with numerous stereocenters and their total synthesis provides value to the field in the form of improvement of synthetic methods. Total synthesis can also provide structure activity relationship information and new therapeutic leads.[21] Although great advances have been made in the recent past and amazing target molecules have been successfully constructed[22-24], total synthesis is frequently too expensive, time consuming and low yielding to use in the industrial scale production of natural products. Some chemists claim that developments in the scalability of synthetic methods will make the supply of natural products practical *via* total synthesis in the near future.[25]

1.3.3.3 Microbial Producers of Natural Products

A growing body of evidence supports the production of many natural products, traditionally attributed to the whole organism they were isolated from, to microbes living within the host organism.[26] If a microbial producer of a natural product can be identified and cultured, the production of the natural product can be accomplished *via* fermentation. Bacterial and fungal fermentation are often more financially viable than agriculture or aquaculture of the associated macro-organism host, when sufficient amounts of the host cannot be collected.

One example of the production of a compound by a microbe that had previously been associated with its associated host organism is that of the cancer drug paclitaxel (Taxol™). Paclitaxel was originally isolated from the pacific yew tree, but the limited supply of the yew tree and length of time to grow the trees was a limiting factor in the

production of the natural product.[27] Plant tissue culture has been since used to circumvent this issue and provides a significant portion of the industrially produced drug.[28] However, paclitaxel is also produced from several fungal species, including *Taxomyces andreanae*[29] and researchers are exploring this as a new potential source of the drug.[30]

1.3.3.4 Semi-Synthesis of Natural Products

Semi-synthesis of a complex natural product from a structurally simpler natural product which is readily available from other methods (e.g. microbial fermentation) is a useful production method. Ecteinascidin 743 is a potent antitumor natural product isolated from the tunicate *Ecteinascidia turbinata.*[31] A semi-synthesis of ecteinascidin 743 from safracin B, produced by fermentation of *Pseudomonas fluorescens* was developed by Cuevas *et al*. and is currently used in the production of the cancer drug.[31]

1.3.3.5 Agriculture and Aquaculture

Agriculture or aquaculture of natural product producers can be a viable source of natural products.[32, 33] There are many instances of these being unsuccessful when organisms are difficult to grow outside of their native environment, take many years to mature, or produce low concentrations of the desired metabolite.[34, 35]

1.3.3.6 Heterologous Production

Heterologous production of valuable and complex natural products is a promising alternative to large scale synthesis. It involves cloning the biosynthetic genes responsible for the production of the natural product from the natural producer into an easily fermented and well-studied host organism such as *E. coli* to enable the compound to be manufactured *via* fermentation.[36, 37]

1.3.3.7 Chemical Dereplication

A high percentage of organic extracts from marine invertebrates exhibit activity in antimicrobial or anticancer screening. The activity of many of these fractions is due to natural products that have been previously studied. Reisolation of known compounds is a recurring problem in natural products chemistry and tools such as LCMS and NMR can be used to "dereplicate" the extracts at an early stage. Dereplication is the process of identifying and eliminating those fractions that possess activity due to known bioactive compounds. LCMS can be used to create profiles for organisms or fractionated extracts, where molecular weight, UV absorbance and retention time can be used to identify known compounds. Many natural products are listed in databases such as MarinLit[38] and AntiBase[39] where the chemical characterization data is listed along with the taxonomy of the producing organism and known biological activity. The search options and information provided by the databases can be used to rapidly identify which fractions contain compounds that have been previously reported and can account for observed bioactivity. Computer software can be used to perform complicated mathematical transformations (e.g. principal component analysis, PCA)[40] to organize large sets of data generated by LCMS, group together similar compounds and identify unique chemical outliers.

The application of novel screening assays to known organisms increases the opportunity for the isolation of new compounds. New, active compounds are often found with the use of new biological targets.

1.4 Combinatorial Chemistry

Combinatorial chemistry is an approach which generates large numbers of compounds by applying reaction conditions to mixtures of reagents. This technique became very popular and has been successful at producing millions of compounds for high throughput screening campaigns; however, it has failed to live up to expectations and has only produced one drug since its conception (Sorafenib[41]). This is attributed to the nature of combinatorial libraries which commonly represent a small area of chemical space and lack the qualities of biological compounds such as stereogenic centers and complex ring systems.

1.5 Biologically-Inspired Synthetic Strategies

1.5.1 Target-Oriented Synthesis and Diversity-Oriented Synthesis

Target-oriented synthesis focuses on the production of a single compound (similar to total synthesis, *vide supra*). Diversity-oriented synthesis, alternatively, is a strategy to generate libraries of compounds with the aim of diversity (Figure 1.3), often with a focus on biologically relevant chemical space.[42]

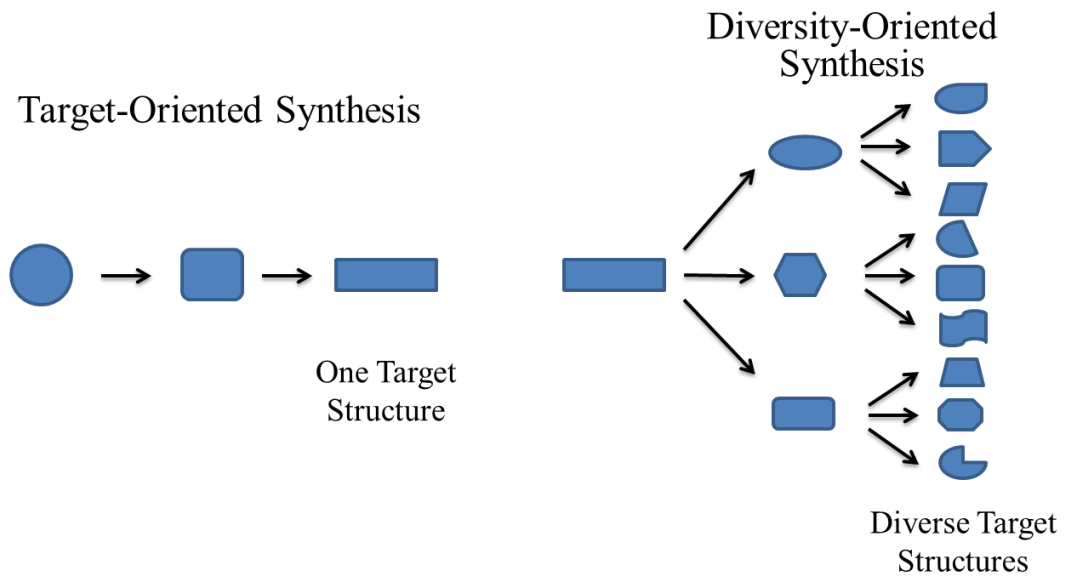

Figure 1.3 - Target-Oriented and Diversity-Oriented Synthesis[42]

1.5.2 Natural Product - Like Compounds

Compounds structurally resembling natural products are often designed to mimic natural product activity *in vivo*. Mimetic compounds often contain the entire natural product or the pharmacophore present in the parent natural product. The best examples of this approach are when the structure activity relationship studies allows the synthesis of simplified analogues that retain or increase potency of the natural product.[43] This often involves identifying the pharmacophore of the natural product and the design of families of compounds that contain the molecular features necessary for activity.

1.5.3 Target-Based Drug Discovery

This approach centers around the identification of a cellular target, such as a gene or a molecular mechanism, that is associated with a disease state and then small molecules are designed to interact with the active site specifically.[44] This is a promising approach, but has not achieved much success to date. Identification of a target that is altered in a disease state is relatively straightforward; validation of this target as a promising therapeutic target is far more challenging. The target must be established to have a therapeutic benefit and not be a consequence of the disease; this process is reported to be very complex and time consuming.[44]

Once a target is established, however, researchers can use computational chemistry and virtual screening methods to minimize the number of screening library members to synthesize.[45] Candidates for library synthesis can be analyzed using computational methods to assess their ability to interact with an active site on a known target. This narrows down the need for large screening libraries and can help drastically reduce synthetic time and resources required to arrive at a lead compound.

1.5.4 Lead-Oriented Synthesis

Lead-oriented synthesis focuses on the synthesis of molecules that have the pharmacological properties associated with bioavailability. Bioavailable compounds possess specific molecular properties associated with solubility and absorption that allow them to reach systemic circulation *in vivo*, making them good leads and/or good drugs.[46, 47]

Lipinski's rule of five[48] defines the characteristics of drug-like molecules as:

- Have no more than 5 hydrogen bond donors
- Have no more than 10 hydrogen bond acceptors
- Have a molecular mass less than 500
- Have a Log P between 0-5

Lead compounds have a separate set of rules for their optimal properties because they are to be further modified by definition. For example a lead compound should have a molecular weight less than 300 to allow for addition to the scaffold during lead optimization and ensure the final drug candidate has a molecular mass under 500 daltons. Lead-oriented synthesis focuses on the production of compounds that fit the criteria for bioavailability.

1.5.5 Lead-Directed Semi-synthesis

Natural products can act as a source of molecular scaffolds that can be converted to combinatorial libraries either by direct chemical modification of the natural product or by providing inspiration for organic synthesis. Lead-directed semi-synthesis involves modifying a natural product lead compound or compounds to generate libraries with improved pharmacological properties. An example of this is the semi-synthesis of β-lactam antibiotics that display greater resistance than their parent compound.[49]

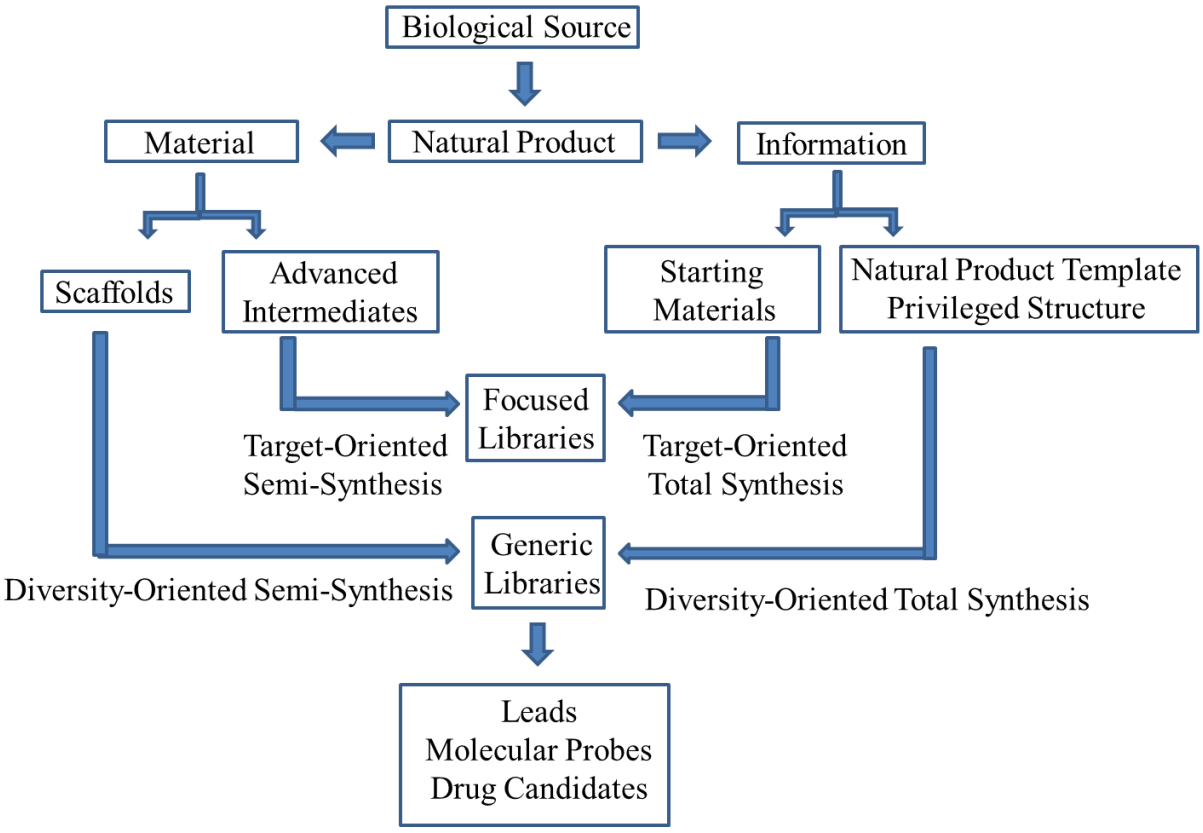

Figure 1.4 - Natural Products as a Source of Drugs and Lead Compounds[4]

1.5.6 Chemically Engineered Extracts

This process involves the treatment of a crude natural product extract or extract fraction with chemical reagents designed to perform specific transformations.[50] The semi-synthetic mixture is produced by transforming functional groups that are common in nature to moieties less common in nature. The resulting engineered extract is processed with bioassay-guided fractionation. Using this process, many diverse and even unknown inactive metabolites can be altered simultaneously and only those products that possess the desired activity are isolated and investigated. This strategy has not been widely used to date and few examples of bioactive compound generation have been reported.[51]

1.5.7 Biology-Oriented Synthesis (BIOS)

Natural products, as stated above, contain biologically relevant architectures. Natural products and similarly, their molecular targets (e.g. proteins) have evolved to occupy only a small fraction of vast chemical space. The biology-oriented synthesis approach focuses on creating libraries of compounds within the chemical space occupied by natural products and other biologically relevant molecules such as drugs.[6, 10, 42, 52, 53] Natural product frameworks are used as building blocks in the synthesis of libraries focused on biological relevancy. These high quality screening libraries have claimed hit rates in biological assays between 0.5-2%.[54] It is difficult to compare these rates to other drug discovery programs because the criteria that defines a hit differs between studies and is often defined based on the activity of the collection. Compound libraries designed using this method are often complex and synthetically demanding, however, higher hit rates reduce the size of libraries required to produce a lead compound. This may balance out the higher synthetic cost of the individual library members.

1.6 Diseases with a Need for New Drugs

1.6.1 The Global Diabetes and Obesity Problem

The rate of obesity worldwide has drastically increased in the past 50 years, and adiposity is widely recognized as one of the leading threats to human health.[55] Obesity is a major risk factor for many health problems such as cardiovascular disease, hypertension and type 2 diabetes.[56] Individuals diagnosed with type 2 diabetes have a higher risk of serious health complications such as cardiovascular disease, neuropathy (nerve damage), nephropathy (kidney damage) and retinopathy (eye damage) among

others.[57] Global instances of diabetes and obesity are expected to continue to grow in the next 10 years and cause a massive and growing burden on health systems.[3, 57]

1.6.2 PTP1B as a Drug Target for Diabetes and Obesity

Protein tyrosine phosphatase 1B (PTP1B), has been identified as a promising new therapeutic target for the treatment of diabetes and obesity.[58] Insulin resistance (failure of insulin receptors to recognize and respond to insulin in the body) is the major cause of type 2 diabetes. PTP1B is a negative regulator of the insulin signalling pathway, associating with and dephosphorylating activated insulin receptors or insulin receptor substrates, and contributing to insulin resistance.[58] Overexpression of the PTP1B enzyme in culture has been demonstrated to increase insulin resistance[59] and mice with under expressed PTP1B enzyme displayed increased insulin signaling[60], therefore, PTP1B is an exciting new target for the management of insulin-resistance related diabetes. Over 300 natural product inhibitors of PTP1B have been reported to date.[61]

Leptin is a hormone involved in the regulation of appetite and energy expenditure and leptin resistance has been linked to obesity in some cases.[51, 62] PTP1B is a negative regulator of JAK2, an enzyme downstream from the leptin receptor.[63] Negative regulation of PTP1B was predicted to increase an individual`s sensitivity to leptin because of the enzyme's role in leptin signaling. PTP1B knockout mice demonstrated resistance to diet induced obesity, which was attributed to increased sensitivity to leptin, resulting in increased energy expenditure.[64] Pre-treatment of leptin-resistant mice with a PTP1B inhibitor resulted in a suppression in food intake.[65] Thus PTP1B inhibitors are of interest in both diabetes and obesity indications.[58]

The major challenge associated with targeting the PTP1B enzyme for drug discovery is selectivity. There are over 100 protein tyrosine phosphatases in the body that possess widely varying biological functions and a high degree of sequence identity at the active site.[66] It is therefore important for PTP1B lead compounds to be tested for both activity and selectivity. The PTP1B active site is positively charged and has a side pocket adjacent to the main active site which causes the enzyme to favor bidentate ligands that can interact with both sites simultaneously.[58] Thusfar, most of the reported PTP1B inhibitors are negatively charged or highly polar molecules not suitable for drug use.[58]

A cysteine residue found in the active site of the PTP1B enzyme is susceptible to oxidation resulting in deactivation of the enzyme. Oxidative compounds are often associated with toxicity and are not good drug candidates. All active PTP1B inhibitors should be screened for oxidative behavior using other enzymes containing cysteine residues such as papain[61] to eliminate those acting *via* an oxidative mechanism.

1.6.3 Need for New Antimicrobial Drugs

Antibiotic resistance is a major threat to human health worldwide.[67] Bacterial resistance to antibiotics can develop through genetic mutation or acquisition of resistance genes from other bacteria through horizontal gene transfer.[68] Mechanisms of bacterial resistance include drug inactivation or modification, alteration of target site or metabolic pathway and decreasing drug accumulation by increasing efflux or decreasing drug permeability. A small population of bacteria containing antibiotic resistance genes existed before the discovery of penicillin in 1928[69], however, the increased prevalence of drug resistant and multi-drug resistant pathogens observed in recent years is largely

attributed to the overuse of antibiotics.[2] As the prevalence of antibiotic resistant bacteria increases and the appearance of bacteria resistant to newer antibiotics rises, so does the need for new antibiotics. Many of the antibiotics introduced in the past 20 years are "me too" drugs[70] and have similar structure and mechanism of action to current drugs. They are therefore ineffective against bacteria that have developed resistance to the original therapeutic and do not address the problem of resistance. With respect to this, Fenical stated "The fact is that no really new antibiotic has come out since the late 1980s. We are on a very dangerous collision course with a plague."[71] Scientists, health professionals and the world health organization have called for researchers to devote time and energy to the discovery and development of novel antimicrobial drugs and classes of drugs with new mechanisms of action.[72, 73]

1.6.4 Need for New Cancer Drugs

Cancer is second only to heart disease for the leading cause of death in Canada.[1] The number of different types and treatments for cancer is staggering. There have been many breakthroughs in the detection and treatment of cancer over the past decades, but many types of cancers remain without effective treatment options and many of those treatments involve serious risks.

1.7 Sesquiterpenoids and Meroterpenoids

Sesquiterpenes and sesquiterpenoids are ubiquitous in nature, isolated from plants[74, 75], insects[76], fungi[77, 78], bacteria[79, 80], sponges[81, 82] and coral.[83, 84] They have been reported to exhibit a broad range of bioactivity including antibacterial[85], antifungal[86], cytotoxic[87], antiviral[88] and anti-inflammatory[89] activities.

Meroterpenoids[90, 91] are natural products that have mixed biosynthetic origin and contain a terpenoid fragment. Many of the biologically interesting meroterpenoids are polyketide/terpenoid hybrids[92, 93] but alkaloid/terpenoid meroterpenes[94] are known as well.

1.7.1 Antimicrobial Decalin Containing Sesquiterpenoids and Meroterpenoids

Sesquiterpenes/meroterpenes containing two fused cyclohexane rings, a decalin skeleton, are common secondary metabolites isolated from marine sponges.[95] These sesquiterpenes, particularly derivatives of bicyclofarnesols with appended lactone[96], substituted aryl or quinone rings[97] commonly exhibit a range of biological activity including antimicrobial properties. The production of antibiotic and antifungal compounds protects the marine invertebrate against pathogenic or unwanted microorganisms and gives them an evolutionary advantage.[98] Sesquiterpene/aromatic, sesquiterpene/quinone and sesquiterpene/heterocycle skeleton are often discovered by researchers looking for antimicrobial compounds in marine sponges.[99]

The siphonodictyal (**1** – **4**, Figure 1.5) and siphonodictyol (**5**, **6**) family of compounds, isolated from the sponge *Siphonodictyon coralliphagum*, showed activity in disc diffusion assays against the Gram positive bacteria *Staphylococcus aureus* and *Bacillus subtilis.* Siphonodictyals C and D (**3** and **4**) were also active against the Gram negative bacterium *Vibrio anguillarum*.[100-102] These metabolites are of mixed biosynthetic origin containing a decalin skeleton connected to a hydroquinone moiety.

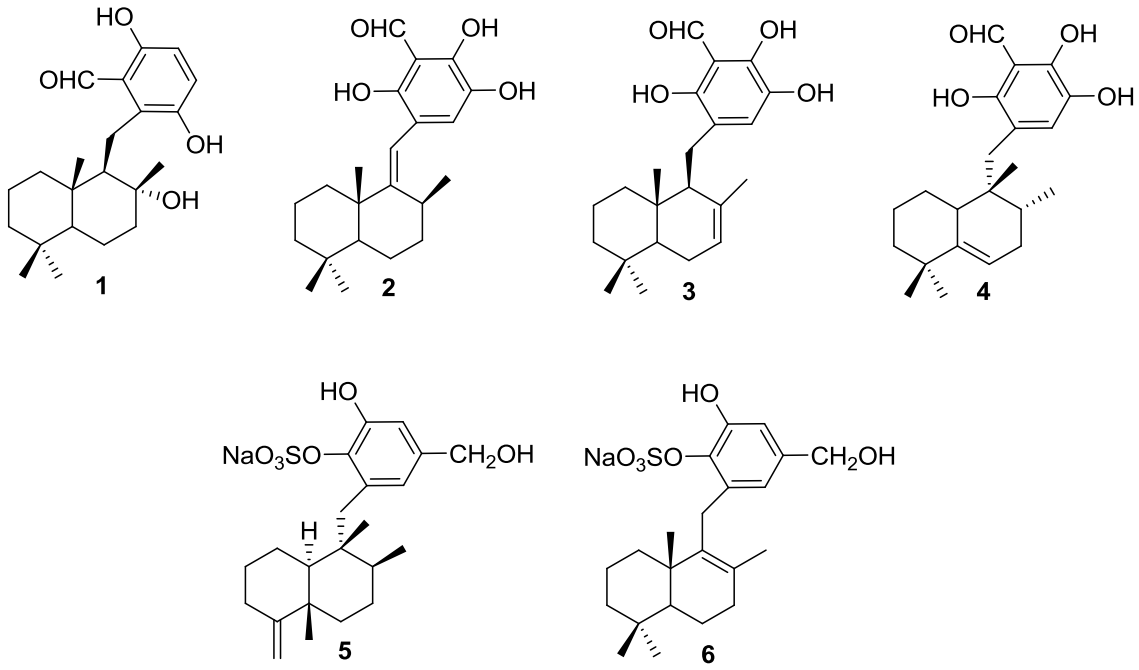

Figure 1.5 - Antimicrobial Siphonodictyals and Siphonodictyols

Ilimaquinone **7** and dictyoceratins A (**8**) and B (**9**), all isolated from marine sponge *Hippospongia sp*. display antimicrobial activity against *Staphylococcus aureus* and *Bacillus subtilis*[103] with dictyocaratin-A being the most potent with an MIC of 6.3 µg/ml against *S. aureus* and 3.1 µg/mL against *B. subtilis* (Figure 1.6). Ilimaquinone has a quinone moiety attached to the decalin skeleton and the dictyoceratins have phenols linked to the decalin scaffold.

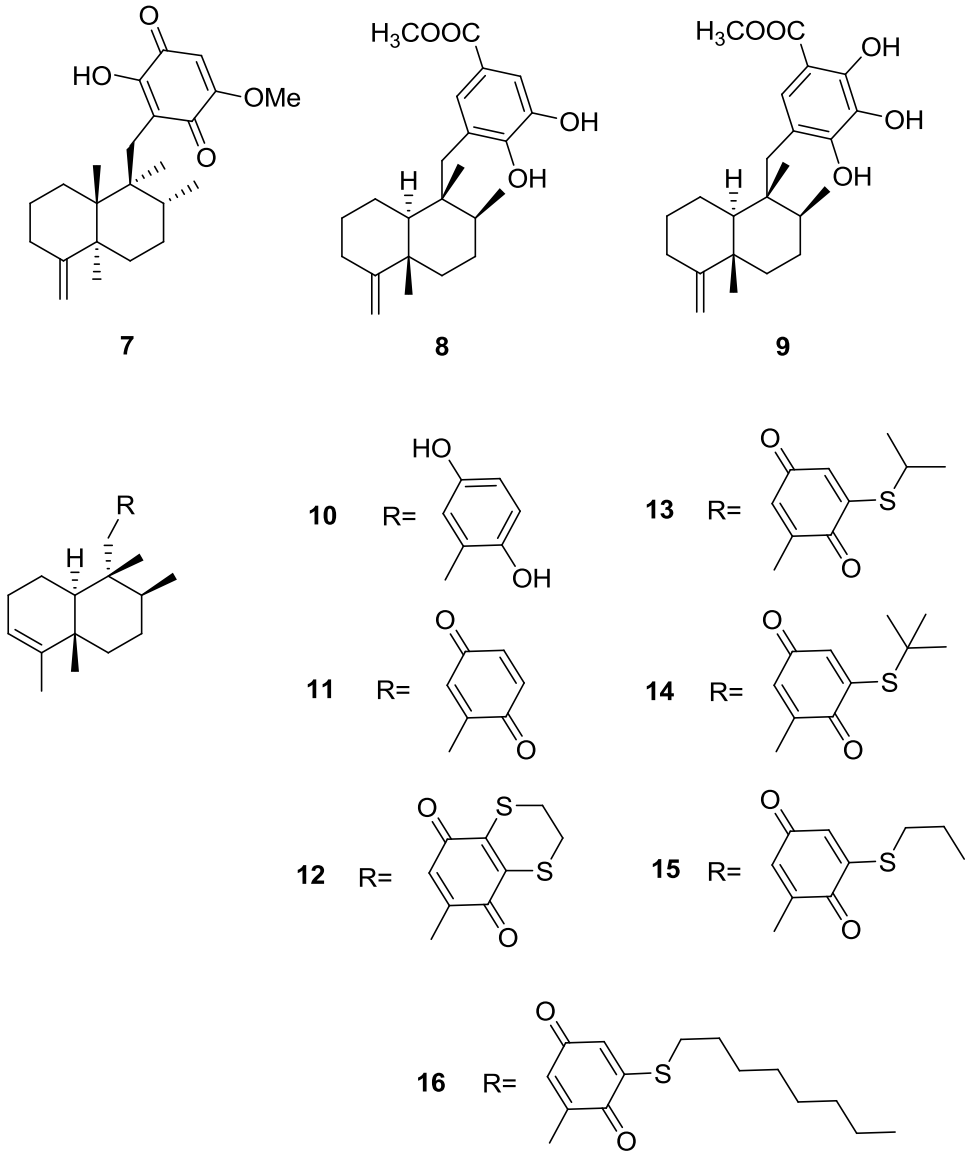

Figure 1.6 - Ilimaquinone, Dictyoceratin and Avarol Derivatives

Avarol (**10**) and avarone (**11**)[104], marine natural products isolated from the sponge *Dysidea avara* and their synthetic derivatives **12-16** (Figure 1.6) were tested for antimicrobial activity against marine bacteria *Cobetia marina*, *Marinobacterium stanieri*, *Vibrio fischeri* and *Pseudoalteromonas haloplanktis* by Tsoukatou *et al.*[104] and displayed MIC values of 0.5-5.0 µg/mL for *C. marina*, 0.5-5.0 µg/mL for *M. stanieri*, 1.0-10.0 µg/mL for *V. fischeri* and 1.0-10.0 µg/mL for *P. haloplanktis*. Sulfide

containing compounds **13** and **15** were found to be the most active against all strains. These compounds were also tested and found to have activity against the marine fungi *Halosphaeriopsis mediosetigera, Asteromyces cruciatus, Lulworthia uniseptata and Monodictys pelagica*.[104]

Avarone (**11**) showed antibacterial activity against *Staphylococcus aureus* with a reported MIC of 1.56 µg/mL.[105] Derivatives of avarone were synthesized (Figure 1.7), with a variety of amino appendages on positions R_1 and R_2, however these semi-synthetic compounds showed significantly weakened activity in *S. aureus* assays. Compounds **16** – **22** had MIC's of 50 µg/mL or greater, however, compounds **23**, **24** and **25** were more effective inhibitors of *S. aureus* with MIC's between 6.25 and 12.50 µg/mL.[105] The presence of a larger electron rich moiety at R_1 or R_2 appears to cause increased inhibition vs. primary or secondary amine substituents.

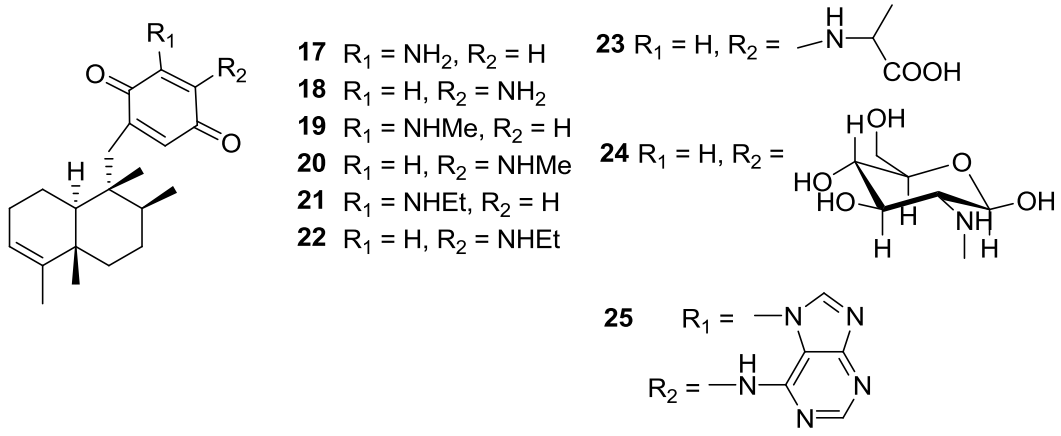

Figure 1.7 - Avarone and Related Synthetic Compounds

Sesquiterpenoid **26**, isolated from the tree *Pleodendron costaricense* is the only included example not containing a third ring. It was found to have antifungal activity against *Alternaria alternate*, *Candida albicans* D10 (azole resistant) and *Wangiella*

dermatidis with MICs of 3.9, 15.6, and 15.6 µg/mL respectively.[106] Compound **27**, isolated from the stem bark of the African tree of *Irvingia gabonensis* had an MIC value less than 5 µg/mL against Gram negative bacteria *E. cloacae*, *M. morganii*, *N. gonorrhoeae*, *N. flexneri* and *S. typhi* as well as Gram positive bacteria *B. cereus*, *B. megaterium*, *B. stearotherm* and *B. subtilis*.[107]

Compound **29** was tested in assays for bacterial inhibition and had an MIC of 15 µg/mL (*S. aureus, B. cereus, B. subtilis*), 20 µg/mL (*B. anthracis*) 17 µg/mL (*M. luteus*), 7 µg/mL (*M. smegmatis*) and 9 µg/mL (*M. phlei*). Interestingly, its close analogues, **28** and **30**, did not inhibit any bacterial growth at the 50 µg/mL level. The presence of the carboxylic acid or ester at this position may reduce activity for electronic or steric reasons.

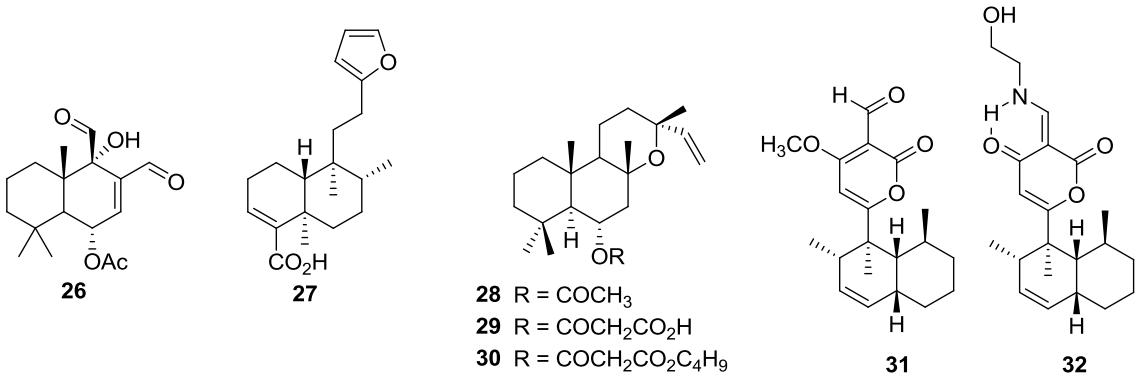

Figure 1.8 - Potent Antimicrobial Sesquiterpenes and Meroterpenes

Meroterpenoids containing a pyranone ring (**31** and **32**), isolated from an unidentified fungus, were active in antibiotic assays; **31** was found to have MICs of 20 and 24 µg/mL against *A. flavus* and *F. verticillioides* respectively and both showed clean

inhibition zones between 9 and 30 in disk diffusion assays against *F. verticillioides* (fungus), *S. aureus* and *C. albicans*.[109]

Antimicrobials with a decalin/methyladenine hybrid framework, agelasine B (**33**) and ageline B (**34**)[110], originating from an *Agelas* sponge, both inhibited *S. cerevisiae* at 10 µg/mL. Neither the inversion of the stereochemistry on C6 or C7 or the presence of the attached pyrrole ester appears to affect the activity of the compounds.

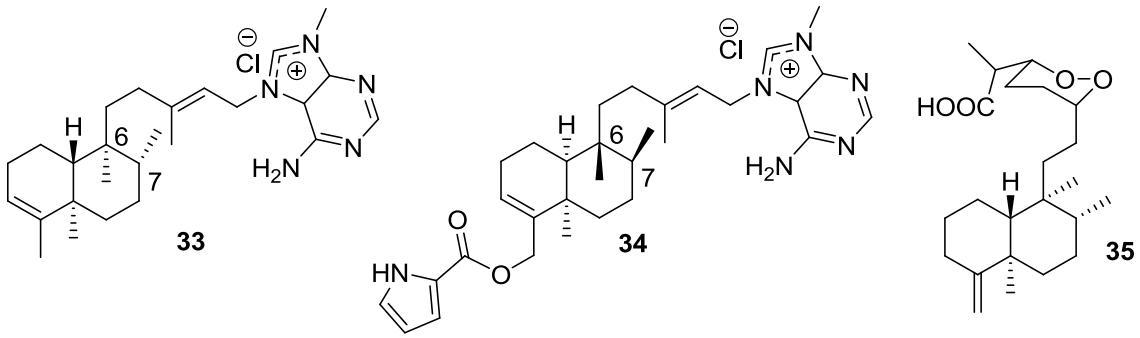

Figure 1.9 - Antimicrobial Compounds Agelasine B, Ageline B and Prianicin B

Prianicin B (**35**) has a unique peroxide containing ring attached to the bicyclic framework. It was isolated from the marine sponge *Diacarnus cf. spinopoculum* by Sokoloff *et al*.[111]and displayed promising inhibition against two β-hemolytic *Streptococcus* strains (MIC: 1.0 and 4.0 µg/mL).

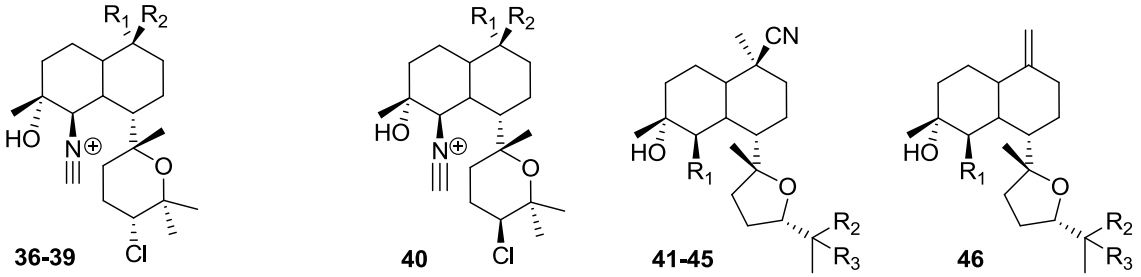

36 R_1 = CN R_2 = Me
37 R_1 = Me, R_2 = CN
38 R_1 = $=CH_2$
39 R_1 = Me, R_2= NCS
40 R_1 = CN R_2 = Me

41 R_1 = CN, R_2 = Me, R_3 = CN
42 R_1 = CN, R_2 = Me, R_3 = Cl
43 R_1 = CN, R_2 =
44 R_1 = Cl, R_2= Me, R_3 = CN
45 R_1 = CN, R_2 = Me, R_3 = NCS
46 R_1 = CN, R_2 = Me, R_3 = CN

Figure 1.10 - Kalihinol Family of Compounds

The kalihinol family of compounds (**36**-**46,** Figure 1.10) were isolated from a fraction of a sponge extract (*Acanthella sp.*) that displayed antibiotic activity against test strains *Bacillus subtilis, Staphylococcus aureus* and *Candida albicans*.[112, 113] The efficacy of the natural products was not reported. They are comprised of a decalin core with an attached tetrahydropyran or tetrahydrofuran heterocycle and an interesting isocyano-functional group that has been observed in natural products isolated from terrestrial microorganisms and marine sponges.

Sesquiterpene lactones, **47** and **48** (Figure 1.11)[96] are potent antimicrobial compounds. With MICs between 0.2-0.5 µg/mL against a panel of bacteria including *M. flavus, B. subtilis, P. tolaasii, S. epidermidis, S. enteritidis* and *E. coli* as well as fungi *A. flavus, A. niger, A. ochraceus, P. funiculosum, P. ochracholoron, T. viride, F. tricintum* and *A. alternate;* these are very intriguing skeletons.

A series of compounds represented by the scaffold **49** were major components from an antibacterial fraction extracted from the sponge *Spongia officinalis*.[114] The fraction was active against *S. aureus, P. aeruginasa* and *B. sphaericus.* Detailed analysis of the activity of each compound was not disclosed.

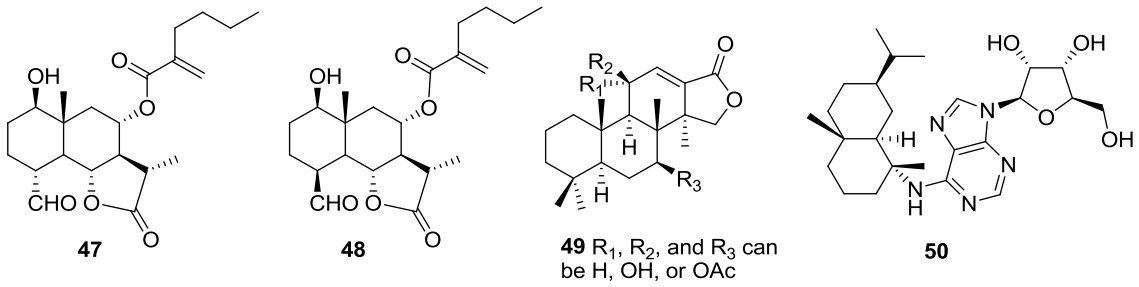

Figure 1.11 - Antimicrobial Terpenoids 47-50

The sesquiterpene sorangiadenosine (**50**)[115] was isolated from bacterium *Sorangium cellosum* and has moderate activity against Gram positive and Gram negative bacteria. MIC's of 25, 12.5, 6.25, 6.25 and 12.5 µg/mL were observed assays against *S. aureus, B. subtilis, M. leuteus, P. vulgaris* and *S. typhimurium*. Again we see an adenine moiety within the active structure and in this case a tetrahydrofuran group is present as well.

Summary

The sesquiterpenoids and meroterpenoids discussed above all contain a bicyclic decalin skeleton, but vary greatly in their substitution patterns, stereochemistry, unsaturation and functional groups attached. There are common substitution patterns; however, such as C5 and C10 (Figure 1.12); either one or both of which is substituted with a methyl group in every case except the kalihinols, **32** and **33**, however, the

stereochemistry varies among the examples. C1 is often substituted with one or two methyl groups, an olefin or another substituent and endo- and exocyclic unsaturation is found throughout the examples. The attached ring is commonly separated from C6 by a one-carbon linker, however, examples of 0, 2 and 5 carbons separating the decalin system from the attached ring are observed. The identity of the rings vary from substituted phenols, quinones, hydroquinones, furan, lactones, tetrahydropan, 1,2-dioxane and methyladenine units. These rings can also have two points of attachment to the main sesquiterpene unit creating a fourth ring.

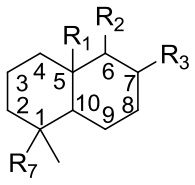

Figure 1.12 - Bicyclofarnesol Skeleton

As mentioned earlier, many of these compounds are part of a large subclass of sesquiterpenes called bicyclofarnesols based on their biosynthesis, outlined in Figure 1.13.

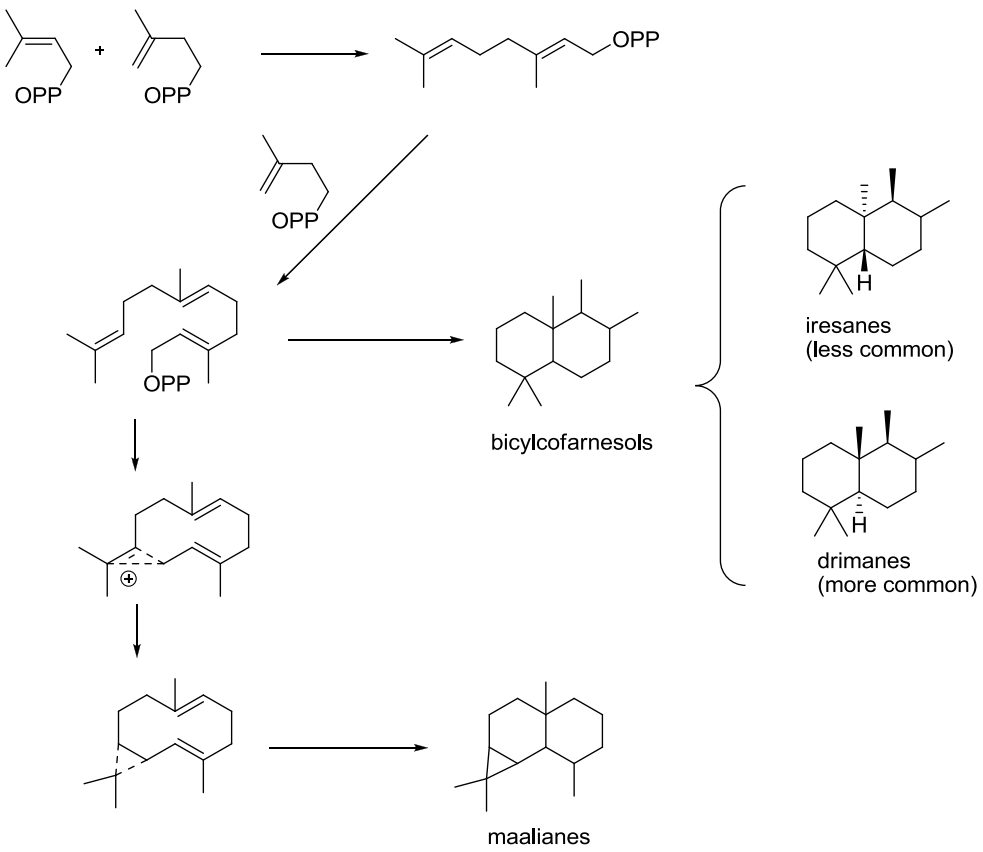

Figure 1.13 - Biosynthesis of Bicyclofarnesol and Maaliane Sesquiterpenes

1.7.2 Sesquiterpene and Meroterpenes that Inhibit the PTP1B Enzyme

In addition to antimicrobial activity, sesquiterpene quinones and hydroquinones are known to inhibit the PTP1B enzyme. Sesquiterpene quinones **51**-**54** were isolated from the Hainan sponge, *Dysidea villosa* and possess PTP1B inhibitory activity.

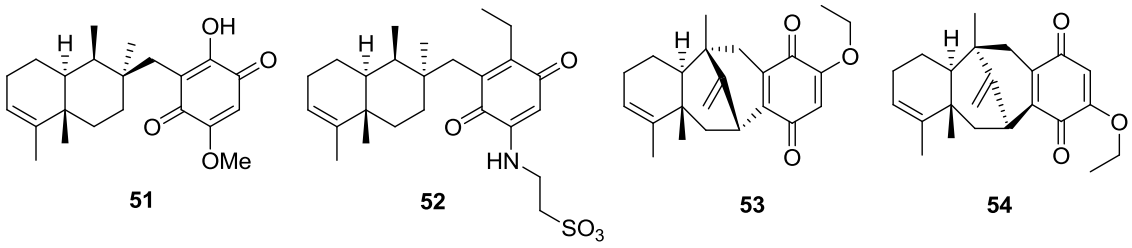

Figure 1.14 - Sesquiterpene Quinones that Inhibit PTP1B[116-118]

21-Dehydroxybolinaquinone (**51**, Figure 1.14) possesses moderate PTP1B inhibition, with an IC_{50} value of 39.5 μM. This compound is also cytotoxic with an IC_{50} of 19.5 μM.[116] Dysidine (**52**) was shown to activate the insulin signaling pathway, promote glucose uptake in 3T3-L1 cells and increase insulin sensitivity all of which was linked to PTP1B inhibition.[117] Dysidavarones A (**53**) and D (**54**) also showed inhibition of the PTP1B enzyme with IC_{50} values of 9.98 and 21.6 μM, respectively.[118]

1.7.3 Cytotoxic Sesquiterpenes

Cytotoxicity is extremely common among sesquiterpenoids, indeed there are too many examples to list here. Some of the most well-known of these are the terpene lactones[119] and terpene quinones/hydroquinones.[95] The reader is directed to several well written reviews and book chapters on the subject for more information.[120-123] Of notable mention are the eudesmanolides, a family consisting of hundreds of sesquiterpene lactones that contain a decalin scaffold[124] and have the general structure of the

eudesmane-12,6-olides (**55**) or eudesmane-12,8-olides (**56**, Figure 1.15). The sesquiterpene lactone parthenolide (**57**) is currently in clinical trials for cancer therapy (Figure 1.15).[120]

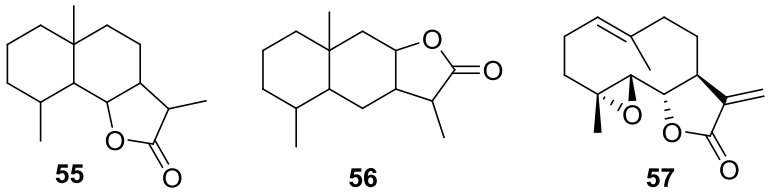

Figure 1.15 - Eudesmanolide Backbone and Parthenolide

1.8 Precedent for Decalin Containing BIOS Libraries

The abundance of biologically active, decalin-containing natural products suggests the decalin scaffold is a biologically validated building block useful for biologically inspired screening libraries. An illustrative example of a decalin containing BIOS collection is one containing 300 compounds that were synthesized in a three step sequence from andrographolide (**58**). Ozonolysis of andrographolide yielded the key synthetic intermediate **59** (Figure 1.16). This intermediate was used in parallel syntheses to generate a library of analogues containing a thiazole moiety (**60**). Further library diversification was established by esterification or amide formation of the carboxylic acid (**61**).[125] The library members were then assessed for their physiochemical properties and drug-likeness.

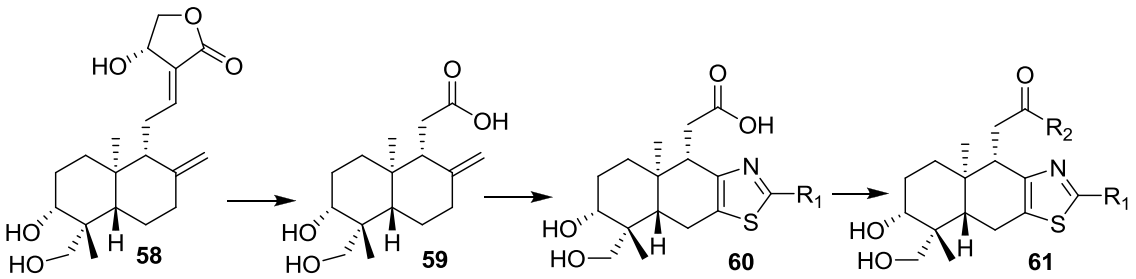

Figure 1.16 - Androphapholide Inspired BIOS Compound Collection[125]

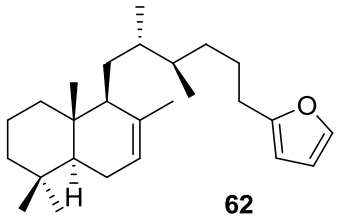

Figure 1.17 - Sulfricin

Sulfricin (**62**) is a natural product with Cdc25A (a protein phosphatase) inhibitory activity. A study replacing the decalin skeleton of the compound with benzimidazole, benzothiazole and naphthalene moieties produced analogues that lacked the activity of the parent natural product. This result supports the proposal that the decalin scaffold is indeed a privileged structure.[6]

One biologically relevant example of a BIOS library built around a decalin skeleton is the synthesis of a dysidiolide (**63**) inspired collection of 162 compounds and their biological evaluation for 11β-HSD (11β-hydroxysteroid dehydrogenase) inhibition. Thirty members of the synthetic library had IC_{50} values lower than 10 μM and four (**64-67)** showed inhibition in the nM range (Figure 1.18).[126]

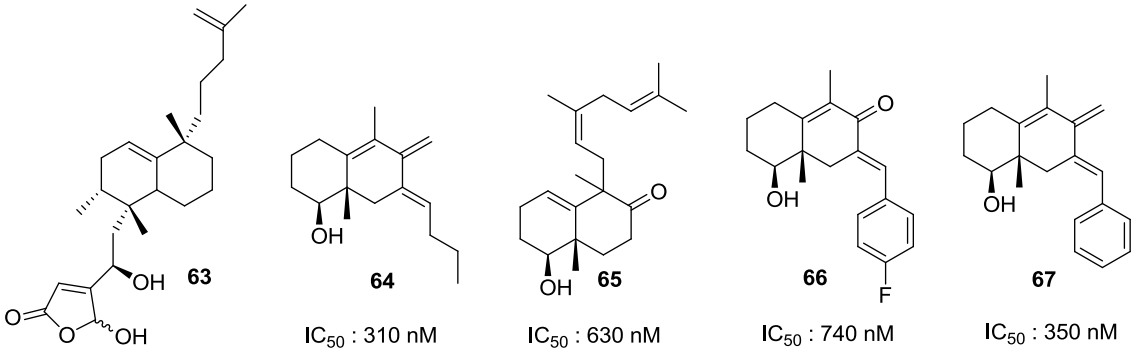

Figure 1.18 - Dysidiolide Inspired Inhibitors of 11-β-HSD[126]

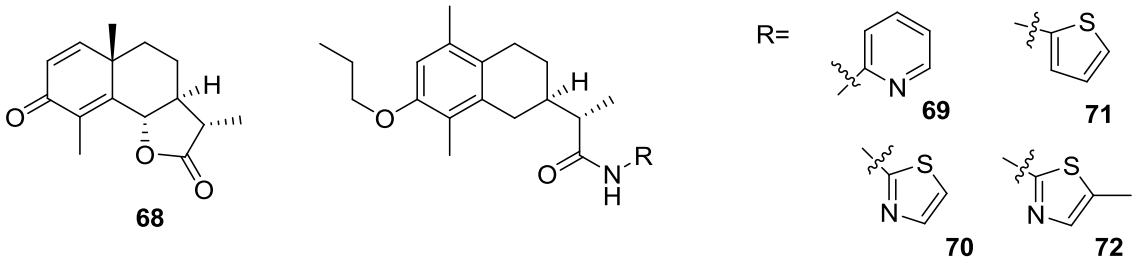

Figure 1.19 - Santonin Inspired Library of 5-Lipoxygenase Inhibitors

Santonin (**68**), a known inhibitor of 5-lipoxygenase (possible target for atheroclerosis, cancer, osteoporosis and inflammation) was used as inspiration for the synthesis of a natural product based combinatorial library.[127] Four out of the 23 synthesized analogues (**69** - **72**, Figure 1.19) showed potent inhibition of the enzyme with IC_{50}'s 0.8-8.0 μM.

1.8.1 Summary

Decalin containing sesquiterpenoids are common in nature and possess a range of pharmacological activity. Synthetic libraries inspired by these secondary metabolites have successfully produced pharmacologically relevant compound collections with a high hit rate for biological activity.

1.9 Research Goals

1.9.1 (+)-β-Gorgonene

The sesquiterpene (+)-β-gorgonene[128-130] (**73**, Figure 1.20) was isolated by Weinheimer *et al*. as a major component (55 %) of the sesquiterpene hydrocarbon mixture from *Pseudopterogorgia americana* and was identified as a non-isoprenoid sesquiterpene related to monoterpene sylvestrene. The biosynthesis resulting in the production of the scaffold was also proposed by Weinheimer in 1968.[128]

(+)-β-Gorgonene was isolated by our lab, from *Antillogorgia elisabethae* (formerly *Pseudopterogorgia elisabethae*), a sea whip found in the tropical West Atlantic, as a by-product of an industrial scale production of pseudopterosins (anti-inflammatory and analgesic family of diterpene glycosides used as additives in the cosmetic industry and being developed for therapeutic applications).[131-134]

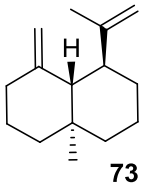

73

Figure 1.20 - Structure of (+)-β-Gorgonene

(+)-β-Gorgonene is a sesquiterpene hydrocarbon containing a decalin skeleton, three stereocenters and two exocyclic, terminal olefins (Figure 1.20). It is a member of the maaliane class of sesquiterpenes[135, 136]; a vastly understudied family with few examples reported in the literature.

The acquisition of a sustainable supply of gorgonene, coupled with the biological activity displayed by decalin containing sesquiterpenes and meroterpenes, warranted further investigation into the structure-activity relationship of this bicyclic framework. Semi-synthetic and biocatalytic manipulations allow exploration of the bioactive potential for a library containing a gorgonene backbone.

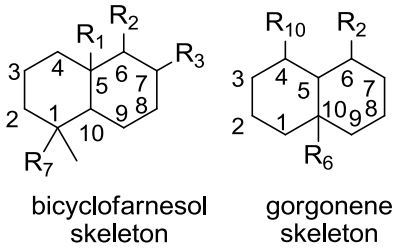

Figure 1.21 - Comparison of (+)-β-Gorgonene and Bicyclofarnesol Skeleton

Gorgonene is non-drug-like mainly due to its high log P value (lipophilicity), however, gorgonene contains a privileged decalin skeleton and is a great starting point for a semi-synthesis of a natural product-like collection of compounds. It was chosen as the foundation for the semi-synthetic BIOS library because it possesses a pre-validated structure, handles for reactivity and is readily available. A semi-synthetic family of natural product derivatives was designed according to the principles of lead-based drug discovery, complying with Lipinsky's rule of 5 for bioavailability (Figure 1.22).

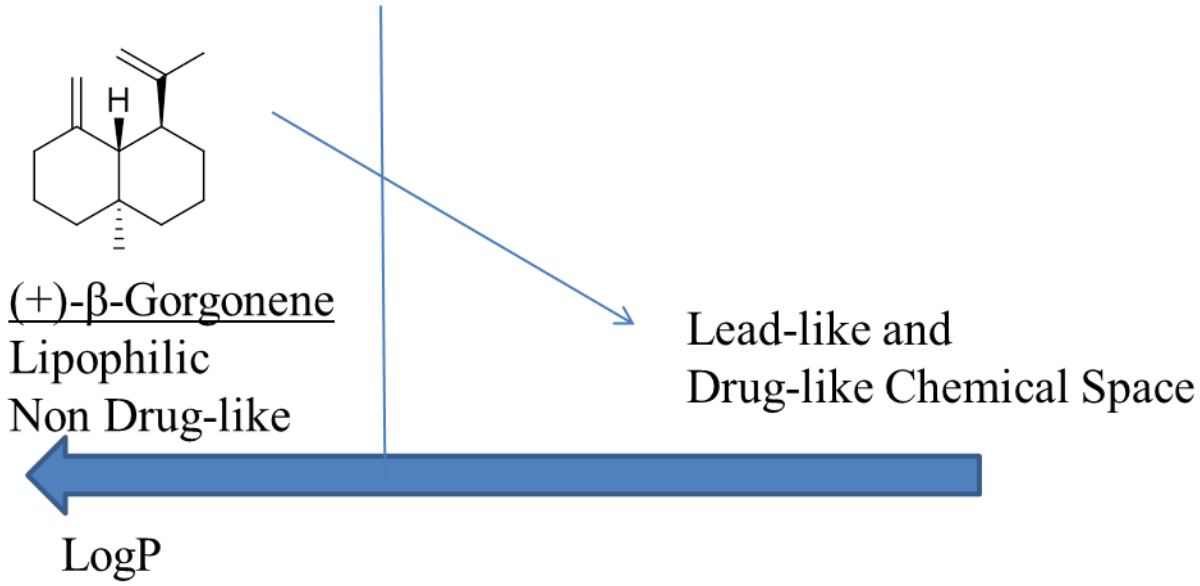

Figure 1.22 - Strategy to Convert Gorgonene to Drug-Like Library of Natural Product Derivatives

1.9.2 Hypothesis

A rationally designed semi-synthetic library of gorgonene derivatives will be efficient in producing biologically relevant compounds; specifically possessing PTP1B inhibition activity, antimicrobial and/or cytotoxic activity.

1.9.3 Objectives

Design, synthesize and biological evaluate families of natural product mimics derived from (+)-β-gorgonene.

1. Identify natural products with the desired biological properties and use these as inspiration for a semi-synthetic library of gorgonene derivatives.
2. Design and synthesize a library of new chemical entities containing the gorgonene skeleton by synthetically modifying the gorgonene framework following these fundamental principles:

- Produce a library of compounds with physiochemical properties associated with bioavailability.
- Synthetically incorporate desirable functionality using short linear sequences adaptable to parallel synthesis to produce a high quality, biologically relevant screening library.

3. Characterize each gorgonene derivative using 1 and 2D NMR, HRMS and IR.
4. Evaluate the semi-synthetic compound collection in bioassays for PTP1B inhibition, antimicrobial and cytotoxic activity.

1.9.4 Experimental Design

1.9.4.1 Strategy: Rapid Chemical Diversification

With the intention of rapidly creating a diverse library of compounds, several synthetic strategies are employed to produce a number of small libraries derived from (+)-β-gorgonene. Reactions were selected to produce families of compounds containing the desired substructures (present in biological molecules or derivatives thereof) in a minimum number of steps, varying only the linker and the position of attachment to gorgonene (Figure 1.23). The ideal syntheses may be performed in parallel to increase the diversity of the libraries. The semi-synthetic derivatives must have a reduced log P in comparison to the starting natural product.

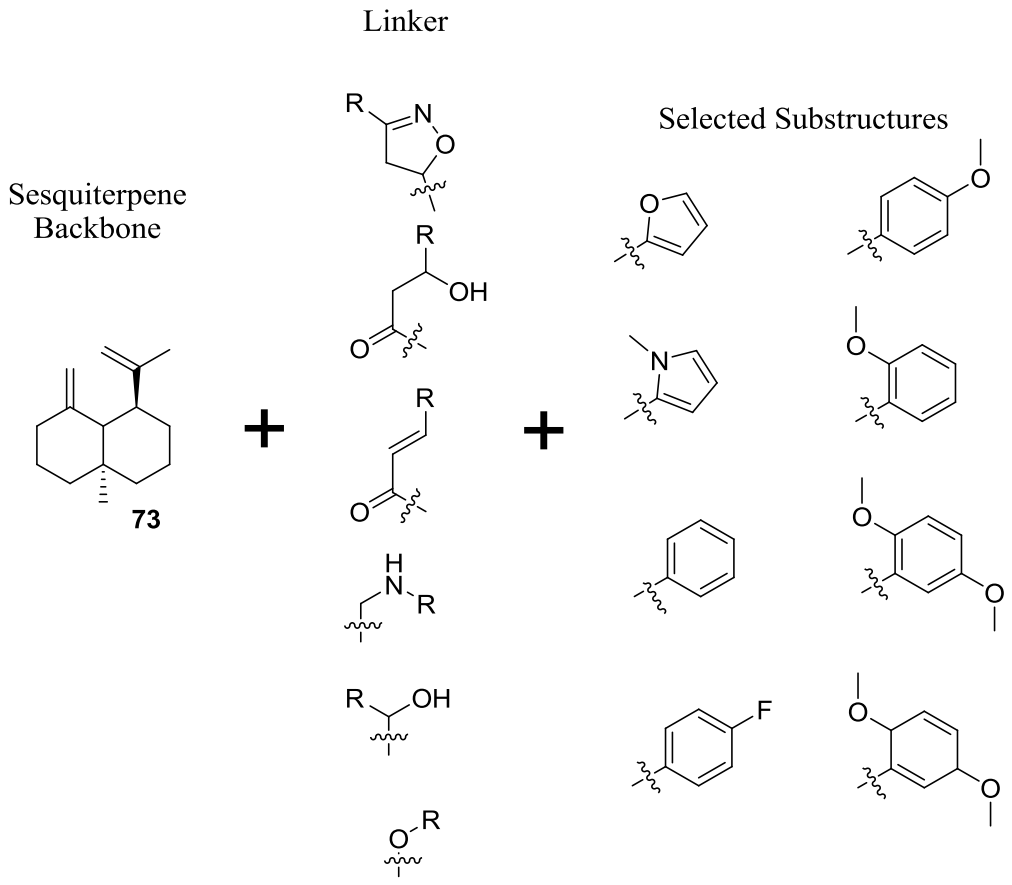

Figure 1.23 - Modular Composition of Screening Libraries

1.9.4.2 Building Block Selection

The decalin skeleton is a privileged scaffold because it is present in many biologically active ligands. In order to design the rest of the library, other privileged structures have been identified to use as complementary building blocks to combine with gorgonene and produce the derivatives. Molecule fragments that are present in numerous biologically active molecules and their congeners were chosen. Substituted aromatics and hetero-aromatics are ubiquitous in natural products and drugs. Quinones are present in some interesting natural compounds, but are also associated with oxidative behavior and toxicity and were therefore avoided. Glycosylated natural

products are also common and often some very active terpenes are glycosides.[134, 137] The selected substructures are to be attached to the gorgonene skeleton using several different synthetic strategies that will result a number of modular collections that vary in the identity of the linking moiety and the position of attachment to gorgonene (Figure 1.23).

Chapter 2 - Regioselective Intramolecular Alder-Ene Reaction of Un-activated Sesquiterpene (+)-β-Gorgonene

2.1 Introduction

2.1.1 Alder-Ene Reaction

The Alder-ene reaction is an electrocyclic group transfer reaction in which an olefin with an allylic hydrogen (the ene) reacts with a compound containing a double or triple bond (the enophile) to form an adduct having the two reactants connected by a new sigma bond (C3-C4, Figure 2.1).[138] The product contains one double bond located at the previous allylic position (C1-C2).

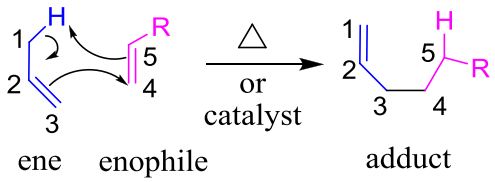

Figure 2.1 - Alder-Ene Reaction Scheme

The Alder-ene reaction, although similar to the Diels-Alder cyclization reaction mechanistically, is more energetically demanding and is performed at high temperatures or with the use of catalysts.[139] Several factors can affect the reactivity of the Alder-ene reaction. Methyl protons in the allylic position (C1, Figure 2.1) of the ene are more reactive than methylene protons which in turn are much more reactive than methine protons.[140] This is particularly pronounced in the case of thermal rearrangements, however, with catalyzed reactions methylene and methyl protons possess similar reactivity. The central atom (C2 - Figure 2.1) on the ene substrate bears a significant positive charge in the transition state and therefore disubstituted central vinylic carbons are more reactive than mono substituted or 1,2-disubstitutued ethylene groups.[139]

2.1.2 Application of Alder-Ene Reaction to the Functionalization of Gorgonene

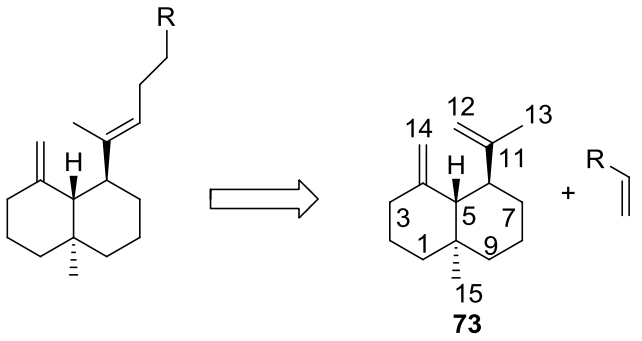

Figure 2.2 - Retrosynthetic Analysis of Desired Alder-Ene Product

Identifying reagents capable of modifying gorgonene in regio- and stereoselective manner is challenging due to the similarity of the two terminal alkenes. An Alder-ene reaction with **73** was predicted to favor the production of one major product or a minimum number of major products for the following reasons:

1. The C11-C12 double bond should be more reactive than the alternative alkene (C4-C14) for steric reasons.
2. No new stereocenters would be formed on the gorgonene scaffold during the reaction, reducing the number of possible products, although new stereocenters may be formed on the enophile segment and diastereomers may be formed.

Both alkenes in **73** are 1,1-disubstituted and therefore no difference in reactivity would be predicted to occur due to this. A series of new compounds was proposed to be synthesized by applying Alder-ene conditions to gorgonene (ene) and a variety of enophiles.

2.2 Results and Discussion

2.2.1 Thermal Alder-Ene Reaction

Maleic anhydride[141] was chosen as a reactive enophile to optimize the conditions of the ene reaction with **73**. The two reactants were heated to reflux temperature in a solution of xylenes (140 ^{o}C), however, no reaction was observed. The reaction was also attempted using other solvents such as dry benzene (80 ^{o}C) and 1-methyl-2-pyrrolodone (200 ^{o}C) however starting materials were recovered in each case.

2.2.2 $FeCl_3$ Catalyzed Intramolecular Alder-Ene Rearrangement of (+)-β-Gorgonene

After several unsuccessful attempts using thermal conditions, a Lewis acid catalyzed Alder-ene reaction was attempted. (+)-β-Gorgonene was treated with maleic anhydride and $FeCl_3$-$(H_2O)_6$ (catalytic) in DCM at room temperature. TLC showed the disappearance of **73** and the appearance of a less polar substance after stirring for only five minutes. After work-up, the crude product was analyzed using NMR and UPLC-HRMS and had a molecular formula identical to gorgonene ($C_{15}H_{24}$) with four degrees of unsaturation. The ^{13}C NMR spectrum contained 15 carbon signals, only two of which appeared in the alkene region at 141.7 and 128.9 ppm, a tetra-substituted alkene. The presence of only one double bond within the structure suggested a third ring must account for the other degree of unsaturation. Methylene hydrogen atoms, H14a and H14b, exhibited HMBC correlations with the C4 and C5 as well as two of the three singlet methyl groups, C12 and C13. This indicated that a new δ bond was formed between C14 and C11 to create the new five-membered ring. Further analysis of the 2D NMR data confirmed the structure of the product was **74** (Figure 2.3). The

intramolecular reaction was then attempted without the presence of the maleic anhydride and the Alder-ene reaction proceeded similarly to the initial conditions.

Table 2.1 - NMR Spectroscopic Data ($CDCl_3$) for Compound 74

	δ_C, type	δ_H (*J* in Hz)	COSY	HMBC
1	39.3, CH_2	1.54, m		2; 15
		1.28, m		
2	20.0, CH_2	1.66, m	3	
3	26.2, CH_2	1.88, m	2	2
4	128.9, C			14a,b; 3; 2
5	141.7, C			14a,b; 3; 1a; 15
6	53.1, CH	2.14, dd (2.0, 12.4)	7b	7b; 8a,b; 9b; 12; 13
7	30.0, CH_2	1.70, m		
		1.01, m	6; 7a	
8	22.9, CH_2	1.63, m		
		1.56, m	8a	
9	41.6, CH_2	1.50, m	9b	3a; 15
		1.10, m		
10	33.8, C			2; 3a; 15
11	38.3, C			12; 13
12	31.9, CH_3	1.07, s		14a,b; 13
13	25.5, CH_3	0.94, s		12; 14a,b
14	52.1, CH_2	2.03, d (15.4)		12; 13
		2.08, d (15.4)		
15	24.1, CH_3	1.03, s		3a

Data was obtained in $CDCl_3$ solution, δ in PPM relative to solvent signal. Assignments were aided by COSY, HSQC and HMBC experiments. HMBC correlations from the carbon stated to the indicated proton.

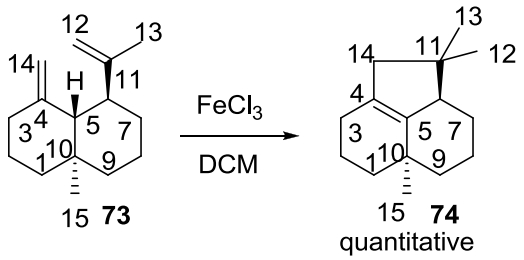

Figure 2.3 - $FeCl_3$ Catalyzed Intramolecular Alder-Ene Reaction of (+)-β-Gorgonene

Alder-ene reactions are typically performed in organohalide or aromatic solvents. To test whether the reaction would occur in an aromatic solvent, gorgonene was treated with $FeCl_3$-$(H_2O)_6$ in benzene; **74** was produced in quantitative yield after stirring for an hour at room temperature.

2.2.3 Proposed Mechanism for Intramolecular Alder-Ene Reaction of Gorgonene

The annulation reaction resulted in a single novel product containing a tricyclic core in quantitative yield. Unactivated alkenes (enophiles) are relatively unreactive in Alder-ene reactions.[140] Literature examples of intermolecular Alder-ene reaction with an unsubstituted hydrocarbon ene and enophile are rare.[139, 140, 141] This fact combined with the involvement of the sterically hindered methine allylic proton (H5) made this a surprising result, however, intramolecular Alder-ene reactions are more facile than intermolecular reactions due to their entropic advantage.[142] This is most likely the driving force for the exclusive formation of the intramolecular cyclization product, **74** .

Lewis acid catalyzed Alder-ene reactions can proceed through one of two mechanisms: (1) with a zwitterionic intermediate, or (2) in a concerted fashion with a polar transition state. The more reactive the ene or the enophile, the more likely the reaction is to occur in a stepwise fashion.[139] Neither the ene (C5-C4-C15, tertiary allylic

carbon) or the enophile (C11-C12, no polar functional groups) are exceptionally reactive and therefore this reaction likely proceeds through a concerted mechanism with a bridged bicyclic intermediate (Figure 2.4). According to the classification of Alder-ene reactions, this is a 1,4-ene cyclization. The involvement of the least reactive allylic proton present (H5) in the molecule is attributed to the geometry of the cyclic transition state.[142]

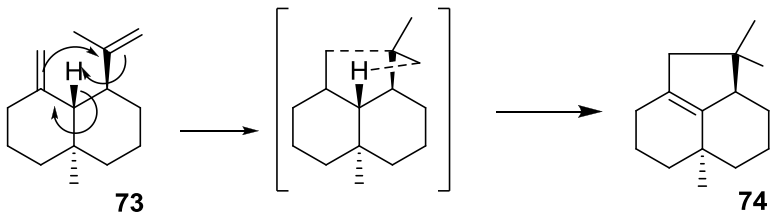

Figure 2.4 - Proposed Mechanism for Formation of 74

2.2.4 Synthetic and Biocatalytic Work with 74

The new skeleton **74** is a promising starting point for the semi-synthesis of another family of natural product mimics. All initial attempts to functionalize this compound, however (epoxidation, ozonolysis, addition reactions), resulted in extremely complex and inseparable mixtures of products that could not be isolated. Biocatalytic efforts to functionalize **74** are discussed in Chapter 6.

2.2.5 BF_3 Catalyzed Intramolecular Alder-ene Rearrangement of (+)-β-Gorgonene

In an effort to expand on the chemistry of the Alder-ene reaction, several other Lewis acids were used to try to promote a rearrangement. Catalytic BF_3-THF was combined with **73** in DCM which resulted in the production of a new compound that appeared from NMR to be very similar, but not identical to the previously isolated

intramolecular ene-product, **74**. The product had the molecular formula $C_{15}H_{24}$ according to HRMS and contained one tetrasubstituted alkene similar to compound **74**.

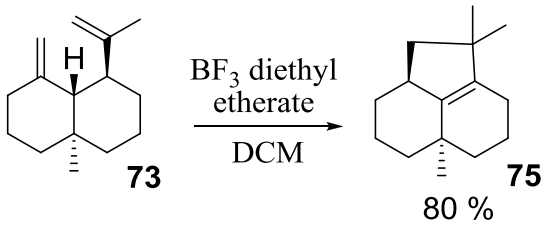

Figure 2.5 - BF_3 Catalyzed Intramolecular Alder-Ene Reaction

Table 2.2 - NMR Spectroscopic Data for Compound 75 ($CDCl_3$)

	δ_C, type	δ_H (*J* in Hz)	COSY	HMBC	NOESY
1	41.7, CH_2	1.07, m		15	
		1.52, m	2a,b		
2	22.3, CH_2	1.53, m	3b; 1b	1b	
3	37.0, CH_2	0.83, m			
		1.92, m	2		
4	39.5, CH	2.50, m	14a,b		3a; 2; 13; 14a,b; 15
5	140.6, C			14b; 9b; 15	
6	138.8, C			7; 8b; 12; 13; 14b	
7	21.8, CH_2	1.83, m	8a,b	8a,b; 9b	
8	20.1, CH_2	1.61, m	7	7	
		1.68, m	9a,b; 7		
9	39.3, CH_2	1.22, m	8b; 9b		15
		1.50, m	8b; 9a		
10	33.2, C			8b; 15	
11	45.1, C			12; 13	14b
12	28.1, CH_3	0.99, s		13	
13	27.2, CH_3	0.91, s		12	
14	47.9, CH_2	1.14, m	14b	12; 13	
		1.89, dd (7.8, 12.5)	4		
15	23.8, CH_3	0.98, s		9a	

Data was obtained in $CDCl_3$ solution, δ in PPM relative to solvent signal. Assignments were aided by COSY, HSQC and HMBC and NOESY experiments. HMBC correlations from the carbon stated to the indicated proton

The protons on the methylene bridging carbon (C14, Figure 2.6) exhibited COSY correlations to a proton on C4 that was not present in the structure of **74**. Similarly to **74**, C14 was HMBC coupled to the protons on C12 and C13; once again, a new five membered ring was formed to create a tricyclic structure. No other CH groups were present in the molecule and HBMC helped confirm the double bond was formed between C5 and C6. The newly formed stereocenter (C4) was assigned an S configuration using NOESY correlations between H4 and H15 (Figure 2.6).

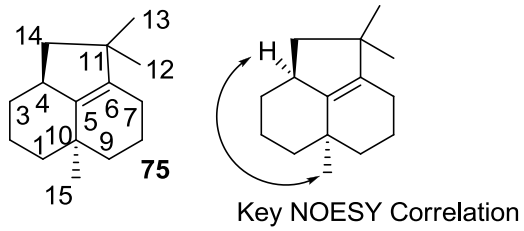

Figure 2.6 - Stereochemical Assignment of 75

The reaction was optimized by varying the ratio of solvent:**73**:BF_3 to give a maximum yield of 80 %. BF_3 is a known promoter of the Alder-ene reaction but is also known to lead to proton-catalyzed isomerization, as is seen in this case.[143, 144] The proposed mechanism for this isomerization is shown in Figure 2.7. The proton-scavenging nature of $FeCl_3$ and $AlCl_3$ minimizes the number of protons in solution that can catalyze such an isomerization and therefore reduces or eliminates the production of isomer by-products.[145]

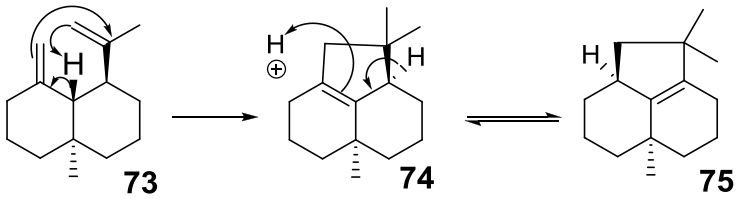

Figure 2.7 - Mechanism of BF_3 Catalyzed Production of 75

$AlCl_3$ and $FeCl_3$ are often used interchangeably in Lewis acid catalyzed Alder-ene reactions, as well as other Lewis acid catalyzed reactions (Friedel crafts, etc). Gorgonene was treated with catalytic and stoichiometric $AlCl_3$ in DCM at room temperature, however, no intramolecular Alder-ene reaction was observed. Since $AlCl_3$ was unable to catalyze the intramolecular Alder-ene reaction observed with $FeCl_3$, it was used to try to promote the intermolecular Alder-ene reaction between gorgonene and maleic anhydride. No reaction was observed between gorgonene and maleic anhydride when treated with $AlCl_3$ in DCM or benzene, at room temperature and at reflux temperature.

2.2.6 Stability Studies of Gorgonene

(+)-β-Gorgonene was reported to undergo acid induced rearrangement to give (+)-α-gorgonene (**76**) and (-)-maaloxide (**77**) when treated with an ion exchange resin in n-hexanes (Figure 2.8).[146] This prompted a study to try to repeat these results and help explore the reactivity of **73**. Gorgonene was treated with Amberlyst 15 in a solution of hexane:DCM at room temperature as per Hackl's protocol, however, no reaction was observed. Further treatment of gorgonene with Amberlyst 15 in a polar aprotic solvent (acetone) and a polar protic solvent (methanol), both with and without heating, resulted in recovery of starting materials.

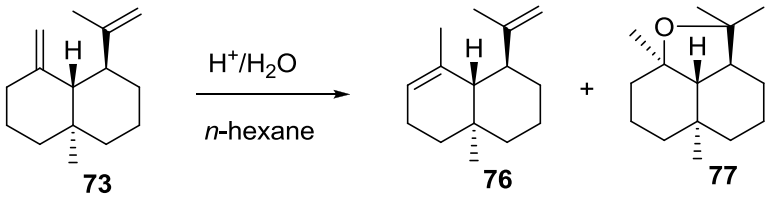

Figure 2.8 - Acid-Induced Rearrangement of (+)-β-Gorgonene[146]

The stability of gorgonene to Brønsted acid and heat treatment was further explored (Table 2.3). Combinations of heat and acid treatment of gorgonene in non-polar (hexane), polar aprotic (acetone) and polar protic (methanol) solvents were examined. Toluene sulfonic acid and hydrochloric acid were used as proton sources in addition to Amberlyst. Each example was performed using 30 mg of **73** in 5 mL of the indicated solvent. No changes to the starting material were observed in any of the reactions.

Table 2.3 - Reaction Conditions Employed to Analyze the Stability of Gorgonene to Acid and Heat Treatment

Acid	Mass acid	Temperature	Solvent
Amberlyst 15	5 mg	RT	Hexanes/DCM
None	0	Reflux	Hexanes
None	0	Reflux	Acetone
None	0	Reflux	Methanol
Amberlyst 15	5 mg	Reflux	Hexanes
Amberlyst 15	5 mg	RT/Reflux	Acetone
Amberlyst 15	5 mg	RT/Reflux	Methanol
Toluene sulfonic acid	5 mg	RT	Toluene
HCl (conc.)	50 µL	RT	Hexanes
HCl (conc.)	50 µL	RT	DCM

Migration of one of gorgonene's terminal double bonds could result in an endocyclic alkene or a more substituted olefin. This would be desirable for several reasons: (1) access to more diverse scaffold and (2) aid regioselectivity for future synthetic steps. Rh catalysts are known to promote olefin isomerization[147, 148] and Alder-

ene reactions[149], therefore **73** was treated with $RhCl_3$ in several solvents; no reaction, however, was observed (Table 2.4).

Iron chloride, being a strong Lewis acid, was tested with **73** in solvents not known to facilitate the Alder-ene reaction to determine if a rearrangement such as that observed by Hackl was possible. In an effort to further explore this chemistry, the substrate **73** was treated with catalytic $FeCl_3$ in a variety of solvents including methanol, tert-butyl methyl ether, acetone, ethyl acetate, diethyl ether and acetonitrile (Table 2.4) Starting material was recovered in each case. (+)-β-Gorgonene was also treated with a variety of other metals without any change being observed, see Table 2.4.

Table 2.4 - Reaction Conditions Employed to Analyze Gorgonenes Stability to Lewis Acid and Metal Catalysts.

Catalyst	Temperature	Solvent	Result
$FeCl_3$-$(H_2O)_6$	RT	MeOH	SM`s recovered
$FeCl_3$-$(H_2O)_6$	RT	MeOH/H_2O	SM`s recovered
$FeCl_3$-$(H_2O)_6$	Reflux	MeOH	SM`s recovered
$FeCl_3$-$(H_2O)_6$	RT	TBME	SM`s recovered
$FeCl_3$-$(H_2O)_6$	RT	Acetone	SM`s recovered
$FeCl_3$-$(H_2O)_6$	RT	Diethyl ether	SM`s recovered
$FeCl_3$-$(H_2O)_6$	RT	Acetonitrile	SM`s recovered
$AlCl_3$	RT	DCM	SM`s recovered
$CuCl_2$-$(H_2O)_2$	RT	DCM	SM`s recovered
$CuCl_2$-$(H_2O)_2$, Zn dust	RT	DCM	SM`s recovered
$ZnCl_2$	RT	DCM	SM`s recovered
$ZnCl_2$, Zn dust	RT	DCM	SM`s recovered
$FeCl_2$-$(H_2O)_6$	RT	DCM	SM`s recovered
RbCl	RT	DCM	SM`s recovered
Na_2MoO_4-$(H_2O)_2$	RT	DCM	SM`s recovered
$SrCl_2$-$(H_2O)_6$	RT	DCM	SM`s recovered
$MnCO_3$	RT	DCM	SM`s recovered
$RhCl_3$	Reflux	EtOH	SM's recovered
$RhCl_3$-(H_2O)	Reflux (N_2)	EtOH/DCM	SM`s recovered
$RhCl_3$-(H_2O)	RT	Acetone/DCM	SM`s recovered

2.2.7 Biological Assessment of Gorgonene (73) and Synthetic Derivatives (74, 75)

2.2.7.1 Evaluation of Antimicrobial Activity

Gorgonene (**73**) and compound **74** were tested for antibacterial and antifungal properties using four test organisms, two representing Gram positive bacteria: *Staphylococcus aureus* and *Enterococcus faecalis*, one Gram negative bacteria: *Pseudomonas aeruginosa* and a fungus: *Candida albicans*. The compounds did not inhibit the growth of these microorganisms at a concentration of 128 µg/mL. All antimicrobial assays were performed in conformance with the standards published in "Methods for Dilution Antimicrobial Susceptibility Tests for Bacteria that Grow Aerobically; Approved Standard – Sixth Edition" by Martin Lantaigne at UPEI.[150]

2.2.7.2 Evaluation of 73, 74 and 75 for Protein Tyrosine Phosphatase Inhibition

Gorgonene (**73**), **74**, and **75** were tested for inhibition and selectivity for the PTP1B enzyme. All PTP assays were performed by Michel Tremblay`s group at McGill University. The compounds were tested for inhibition of seven protein tyrosine phosphatases from class I. Testing the compounds for inhibition of PTP`s other than PTP1B gives an indication of the compounds' ability to selectively inhibit the PTP1B enzyme activity. The PTP class I subdivisions that are represented in the assay are: receptor-like (LAR D1D2 and SigmaD1D2), intracellular (PTP1B, TC-PTP, SHP-1) and dual-specific (MKPX, PRL2 A/S) (Figure 2.9).[66, 151]

The activity of the enzyme is measured by its ability to de-phosphorylate pNPP and produce *p*-nitrophenol, which generates an intense yellow color at an alkaline pH that can be measured at 405 nm using a spectrophotometer.[152] All pure compounds were

tested at a single concentration (25 µg/mL) for inhibition and IC_{50}`s were collected for compounds that showed activity at that concentration. The initial single data point collected describes the inhibitory effect the compound has on the enzyme at the concentration tested (25 µg/mL) with a numerical value between 0 and 1. A value of 1.0 in the assay indicates there is no inhibition of the enzyme and a value of 0.0 corresponds to complete inhibition.[152] Compounds were selected for further study if: (1) the PTP1B enzyme activity was reduced to 0.7 or less and (2) no inhibition of the other PTP enzymes was observed (value of 0.8 or greater). The exception to this was inhibition of the enzyme TC-PTP; TC-PTP inhibition did not exclude compounds from further study due to its similarity to PTP1B.

Compounds that exhibited selective inhibition of PTP1B were also screened for oxidative behavior in a papain assay. Papain, or papaya proteinase 1 is a cysteine proteinase unrelated to the protein tyrosine phosphatase family of enzymes and can be inactivated by oxidative compounds.[61] It is used in this context to identify compounds that inactivate PTP1B *via* an oxidative mechanism. Gorgonene did not show any inhibition of PTP1B or any of the other PTPs tested. Compound **74** showed modest inhibition and selectivity for the PTP1B and TC-PTP enzymes and produced a negative result for papain inactivation. Compound **74** was determined to have an IC_{50} of 62.05 µg/mL against PTP1B and 104.7 µg/mL against TC-PCP. Compound **75** showed even stronger inhibition of the panel of enzymes, but did not show specificity for the PTP1B enzyme and was not studied further.

The PTP1B inhibition observed by **74** and **75** is unprecedented. The active site in the PTP1B enzyme is known to be positively charged, electrophilic and the vast majority of

known PTP1B inhibitors are negatively charged molecules.[58] However, an allosteric site has been identified on the protein which is much less polar. This is a much more likely place where compound **74** and **75** could be binding to exert their effect. Table 2.5 summarizes the results of the PTP assay of gorgonene, **74** and **75**.

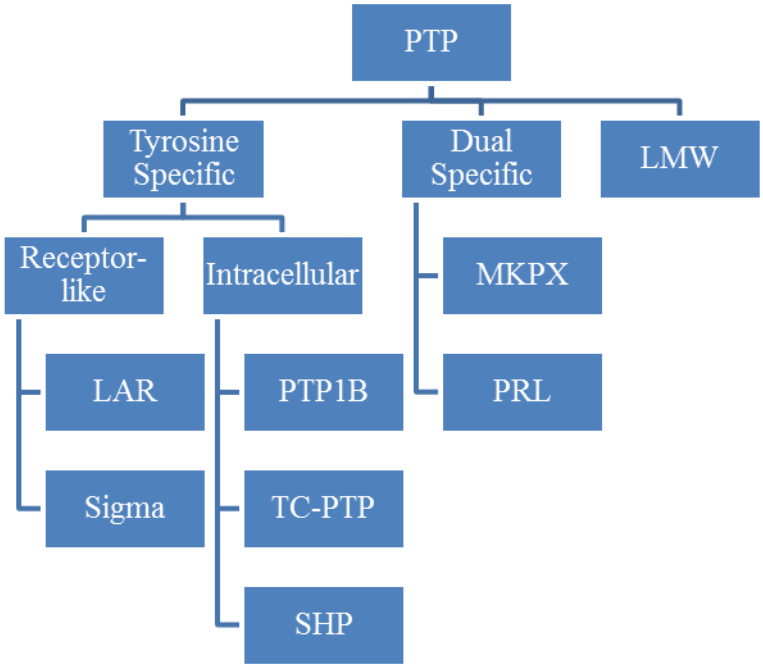

Figure 2.9 - PTP Enzymes and their Subclasses Used in Bioassay

Table 2.5 - PTP1B Inhibition of Gorgonene, 74 and 75

Enzyme	**Screening Relative Rate, % Control**		
	73	**74**	**75**
PTP1B	0.95	0.74	0.45
SigmaD1D2	1.06	0.88	0.73
SHP-1	0.94	0.88	0.57
MKPX	1.08	0.94	0.89
LAR D1D2	1.16	1.16	1.21
TC-PTP	0.84	0.61	0.42
PRL2 A/S	0.95	1.01	0.88
Papain	Not tested	Negative	Not tested

2.3 Significance and Future Work

Synthetic access to unactivated C-H bonds as well as regio- and stereoselective functionalization of substrates that lack directing groups are common goals for modern day organic chemists.[153-156] The intramolecular Alder-ene described in this chapter contributes to the scientific knowledge of the reaction scope to include unfunctionalized hydrocarbon reagents. The use of a safe and inexpensive catalyst, $FeCl_3$, adds to the attractiveness of this method.

The novel tricyclic scaffolds produced in this reaction may be used in future semi-synthesis of an expanded library of natural product mimics.

2.4 Experimental Section

2.4.1 General Experimental

All flash chromatographic separations were performed using prepackaged RediSep® columns (silica gel, diol and C18 stationary phases) and a CombiFlash® RF system with UV-dependent fraction collection. Thin layer chromatography was performed using aluminum-backed silica plates. Separation of products by HPLC was performed on a Thermo HPLC equipped with ELSD (Sedex 60 LT) and UV detectors. HPLC runs were performed with Phenomenex Luna C6-Phenyl 110 Å column (250 x 10 mm, 5 µ), Phenomenex Gemini 5 µ C18, 110 Å column (250 x 10 mm), Phenomenex Luna 5 µ silica column (2), 100 Å (250 x 10 mm) or Phenomenex Luna 5 µ PFP (2), 100 Å column (250 x 10 mm) columns at a flow rate of 2.5 mL/min. Analysis of samples by UPLC-HRESIMS with ELSD and UV detection was performed on a Thermo Scientific Exactive™ mass spectrometer, using Kinetex C18 (50 x 2.14 mm, 1.7 µm) column. The mass spectrometer was operated by Tricia Boland. GC-MS experiments were run on a Finnigan Polaris Q bench-top ion trap mass spectrometer with a Thermo Focus GC using an Agilent J&W DB-23 GC Column, (60 m, 0.25 mm, 0.15 µm). Infrared spectra were acquired with a Thermo Scientific 6700 FT-IR spectrometer.

All NMR data was collected by Dr. Chris Kirby, Lloyd Kerry or Maike Fischer on a Bruker Avance III 600 MHz NMR spectrometer operating at 600 and 150 MHz for ^{1}H and ^{13}C, respectively. Chemical shifts are reported in PPM relative to solvent signal $CDCl_3$ (^{1}H: 7.26 ppm, ^{13}C: 77.16 ppm) and CD_3OD (^{1}H: 3.31 ppm, ^{13}C: 49.05 ppm). 2D NMR experiments aided structural assignment, COSY, HSQC, HMBC, NOESY and

ROESY. Coupling constants are reported in Hz, with their multiplicity, singlet (s), doublet (d), triplet (t), quartet (q) and multiplet (m). Deuterated NMR solvents were purchased from Sigma-Aldrich. X-ray crystallography was performed by Dr. Andreas Decken at the University of New Brunswick on a Bruker AXS SMART 1000 CCD single crystal diffractometer at cryogenic temperatures. Melting points were collected on a Melt-Temp™ apparatus. Ozonolysis was performed using a Welsbach ozone generator operated at 70 V.

All solvents were ordered from Sigma-Aldrich or VWR and used as received unless otherwise noted. Anhydrous solvents were stored over molecular sieves. Molecular sieves (3Å pore size) were activated by microwave heating. All reagents were ordered from Sigma-Aldrich, VWR or Fischer Scientific and used as received and stored according to label instructions. Rotary evaporation was performed at room temperature.

2.4.2 General Procedure for Anti-Microbial Assays

Microbial assays were performed under sterile conditions and were performed by myself, or Martin Lantaigne at the AVC, UPEI. A single use cryovial of each organism was thawed and 20 µL was inoculated into 20 mL of sterile broth (CaMHB : DIFCO CA90000-602 for bacteria and DSD:DIFCO 0003-096 for fungi) in a 250 mL non-baffled, autoclaved Erlenmeyer flask. The cultures were incubated at 37 ^{o}C for 18 h at 220 rpm, then transferred by pipette into a sterile 50 mL falcon tube containing sterile beads, vortexed (30 seconds) and allowed to sit for 5 minutes. The supernatant (100 uL) was removed and combined with broth (5 mL; CaMHB : DIFCO CA90000-602 for bacteria and DSD:DIFCO 0003-096 for fungi) in a 15 mL glass tube. The turbidity of the dilution was adjusted to be visually equal to the McFarland Standard. This prepared dilution (25 µL)(1-2 x 10^8 CFU/mL) was added to broth (10 mL- CaMHB : DIFCO CA90000-602 for bacteria and DSD:DIFCO 0003-096 for fungi)) to give a concentration of 2.5 x 10^5 CFU (dilution **A** - for assay). **A** (100 µL) was added to 10 mL of broth (CaMHB : DIFCO CA90000-602 for bacteria and DSD:DIFCO 0003-096 for fungi) to give 2.5 x 10^3 CFU/mL (dilution **B** - for plate count) which was streaked (100 µL) onto prepared agar plates (bacteria - LB, fungus - SD) and incubated overnight (37 ^{o}C) to confirm CFU concentrations and purity of the cultures. Prepared assay stock solution (**A** - 80 µL) was added to each well of a sterile 96 well plate containing solution of test compound (0.7-25 µg in 20 µL solution 2:8 DMSO: H_2O) to give a final volume in the well of 200 µL. Each plate contained 3 positive controls (media + 10 % 2:8 DMSO: H_2O) 3 negative controls (Media + 10 % 2:8 DMSO: H_2O + cells) and a column containing a concentration range of antibiotic control (Penicillin G for *S. aureus*, vancomycin for *E. faecalis* and MRSA, gentamycin for *P. aeruginosa*, nystatin for *C.*

albicans). The plates were wrapped with parafilm and placed in an incubator (37 ^{o}C) for 20 hours. The OD600 (optical density at 600 nm) of the plates was measured using a BIOTEC plate reader before and after incubation to calculate the % inhibition of each test compound.

2.6.5.1 Kerr Lab Bioassay Strain Information

MRSA: ATCC 33591

VRE: Ef 379, Wyeth

S. aureus ATCC 375

E. faecalis: ATCC 10741

C. albicans: ATCC 14035

P. aeruginosa: ATCC 14210

P. vulgaris: ATCC 12454

M. furfur: ATCC 38593

P. acnes: ATCC 6919

S. warneri: ATCC 17917

2.4.3 General Procedure for Cytotoxicity Assay

The antiproliferative assays were performed using the reduction of rezasurin to resorufin (Alamar blue) as an indicator of cell health. These assays were performed by Martin Lantaigne and Kate McQuillan at the Kerr Research Laboratory, AVC, UPEI.[157]

Cell line and Growth Conditions

Human foreskin BJ fibroblast cells (ATCC CRL-2522) were grown and maintained in 15 mL of Eagle's minimal essential medium supplemented with 10 % fetal bovine serum and 100 µU penicillin and 0.1 mg/mL streptomycin in T75 cm^2 cell culture flasks at 37 ^oC in a humidified atmosphere of 5 % CO_2. Culture medium was refreshed every two to three days and cells were not allowed to exceed 80 % confluency.

Human breast adenocarcinoma cells (ATCC HTB-26) were grown and maintained in 15 mL of Dulbecco's Modified Eagle's Medium/Nutrient Mixture F-12 Ham (500 mL) supplemented with 10 % fetal bovine serum and 100 µU penicillin and 0.1 mg/mL streptomycin in T75 cm^2 cell culture flasks at 37 ^oC in a humidified atmosphere of 5 % CO_2. Culture medium was refreshed every two to three days and cells were not allowed to exceed 80 % confluency.

Cytotoxicity Assay

At 80% confluency, the cells were counted, diluted and plated into 96 well treated cell culture plates at a cell density of 10000 cells per well in 90 µL of respective growth medium. The assays were performed in the maintenance medium without the addition of antibiotics. The plates were incubated at 37 ^{o}C in a humidified atmosphere of 5% CO_2 to allow cells to adhere to the plates for 24 hrs before treatment. DMSO was used as the vehicle at a final concentration of 1 % in the wells. All compounds to be tested were resolublized in sterile DMSO and a dilution series was prepared for each cell line using the respective cell culture growth medium of which 10 µL were added to the respective assay plate well yielding eight final concentrations ranging from 128 µg/mL to 1 µg/mL per well (final well volume of 100 µL) and incubated at 37 ^{o}C in a humidified atmosphere of 5 % CO_2 for 24 hrs. All samples were tested in triplicate. Each plate contained eight uninoculated positive controls (media + 20% DMSO), eight untreated negative controls (Media +20 % DMSO + cells), and one column containing a concentration range of zinc pyrithione. Alamar blue was added, 24 hrs after treatment, to each well at 10 % of the culture volume (11 µL in 100 µL). Fluorescence was monitored using a BioTek Synergy HT plate reader at 530/25 excitation, 590/35 emission and 35 sensitivity at both time zero and 4 hours after Alamar blue was added. After subtracting the time zero emission 590 nm measurement from the final reading the inferred percentage of cell viability relative to vehicle control wells were calculated and the IC_{50} was determined.

2.4.4 General Procedure for PTP1B Assays

PTP assays were performed at McGill University by the Tremblay lab according to the following procedure:

A PTP enzyme solution (93.13 ng/mL) was prepared in the assay buffer (50 µM HEPES; pH 7.0; 0.1 mg/mL BSA; 3 mM DTT), and was transferred (50 µL) to each well in a 96 well plate containing a solution of test compound (1 µL, 10 µg/µL in DMSO). The plate was incubated at 30 ^{o}C for 2 mins and then the pNPP substrate solution (50 µL, 2x desired final concentration, 18.55 mg/mL for 50 mM) in assay buffer was added and the plate was incubated again at 30 ^{o}C for 2 minutes. The absorbance at 405 nM was recorded in 30 sec. intervals for 10 minutes. Enzyme activity is calculated from data that fall in the linear range.

Enzyme activity (µM/min µg) = 50 (vol) x OD405 nm x 1/time(min) x enzyme (µg) x 1/18000 (molar extinction coefficient)

Isolation of Gorgonene

Antillogorgia elisabethae was collected from the Tropical West Atlantic in early 2010, sun-dried and weighed (96.0 kg). The coral was then ground in 400 g batches and extracted with methanol (1.6 L) for 4 hour with shaking. The mixture was filtered through a Whatman # 4 filter and the solid cake was washed with methanol (0.8 L). A 2^{nd} filtration through glass frit funnel was performed on the extract. The solvent was removed *in vacuo* at 40 ^{o}C. The crude extract was separated on a C18 flash column into three fractions (50:50 MeOH:H_2O, 100 % MeOH and 100 % acetone). The acetone fraction was dried and was further separated using flash chromatography (diol stationary phase, 100 % hexanes) and the first fraction to elute was further purified using silica gel flash chromatography (100 % hexanes). The first compound to elute was a clear, colorless oil (0.79 % yield) and identified as (+)-β-gorgonene.[128]

^{1}H NMR (600 MHz, $CDCl_3$) δ 4.78 (s, 1H), 4.71 (s, 2H), 4.58 (s, 1H), 2.32 (dt, *J* = 4.0, 11.9 Hz, 1H), 2.27 (m, 1H), 1.99 (m, 1H), 1.86 (d, *J* = 11.3, 1H), 1.70 (m, 1H), 1.64 (m, 2H), 1.63 (s, 3H), 1.62 (m, 1H), 1.55 (m, 1H), 1.48 (m, 1H), 1.45 (m, 1H), 1.34 (m, 1H), 1.31 (m, 1H), 1.23, (dt, *J* = 3.8, 13.2, 1H), 0.83 (s, 3H).

^{13}C NMR (600 MHz, $CDCl_3$) δ 150.5, 148.6, 110.3, 107.8, 52.6, 43.0, 42.7, 41.7, 38.3, 36.8, 34.9, 24.5, 21.7, 19.3, 17.5.

FTIR (CH_2Cl_2): ν_{max} 3068.6, 2924.4 cm^{-1}.

Synthesis of **74**

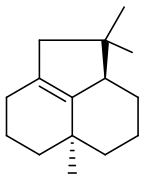

To a stirring solution of gorgonene (100 mg, 0.49 mmol) in DCM (10 mL) was added $FeCl_3$-$(H_2O)_6$ (15 mg, 0.056 mmol) at room temperature. After 5 minutes, complete conversion to a new product was observed by TLC. The solvent was removed *in vacuo* and the residue was re-suspended in hexanes and filtered through a plug of silica. The title compound (clear, colorless oil) was characterized without further purification (99.0 mg, 99 % yield).

^{1}H NMR (600 MHz, $CDCl_3$) δ 2.14 (dd, *J* = 2.0, 12.4 Hz, 1H), 2.08 (d, *J* = 15.4 Hz, 1H), 2.03 (d, *J* = 15.4 Hz, 1H), 1.88 - 1.85 (m, 2H), 1.71 – 1.67 (m, 1H), 1.66 – 1.63 (m, 2H), 1.65 – 1.62 (m, 1H), 1.58 – 1.55 (m, 1H), 1.55 - 1.52 (m, 1H), 1.50 - 1.47 (m, 1H), 1.30 - 1.28 (m, 1H), 1.29 - 1.26 (m, 1H), 1.11 - 1.09 (m, 1H), 1.07 (s, 3H), 1.03 (s, 3H), 0.94 (s, 3H).

^{13}C NMR (151 MHz, $CDCl_3$) δ 141.7, 128.9, 53.1, 52.1, 41.6, 39.3, 38.3, 33.8, 31.9, 30.0, 26.2, 25.5, 24.1, 22.9, 20.0.

FTIR (CH_2Cl_2): ν_{max} 3056.7, 2927.2 cm^{-1}.

(+) HRESIMS *m*/*z* 227.1753 $[M + Na]^+$ (calcd for $C_{15}H_{24}Na$, 227.1776)

Synthesis of **75**

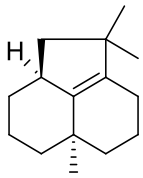

To a solution of gorgonene (100 mg, 0.49 mmol) in DCM (10 mL) was added 3 drops of BF_3-ethyl etherate (approx. 45 mg, 0.32 mmol) at room temperature with stirring. The solution was stirred for 1 hour during which time it turned a yellow color. The solution was washed with distilled water, the solvent was removed *in vacuo* and the product was purified using silica gel flash chromatography (100 % hexanes) to give **75** as a clear, colorless oil (80 mg, 80 % yield).

^{1}H NMR (600 MHz, $CDCl_3$) δ 2.54 – 2.47 (m, 1H), 1.95 – 1.90 (m, 1H), 1.88 (dd, *J* = 12.5, 7.8 Hz, 1H), 1.85 – 1.80 (m, 2H), 1.69 – 1.66 (m, 1H), 1.66 – 1.58 (m, 1H), 1.55 - 1.52 (m, 2H), 1.53-1.51 (m, 1H), 1.51 – 1.45 (m, 1H), 1.26 – 1.18 (m, 1H), 1.17 – 1.11 (m, 1H), 1.09 – 1.04 (m, 1H), 0.99 (s, 3H), 0.98 (s, 3H), 0.91 (s, 3H), 0.88 – 0.79 (m, 1H).

^{13}C NMR (151 MHz, $CDCl_3$) δ 140.6, 138.8, 47.9, 45.1, 41.7, 39.5, 39.3, 36.9, 33.2, 28.1, 27.2, 23.8, 22.3, 21.8, 20.1.

FTIR (CH_2Cl_2): ν_{max} 3162.18, 2929.2 cm^{-1}.

(+) HRESIMS *m*/*z* 205.1939 $[M + H]^+$ (calcd for $C_{15}H_{25}$, 205.1956)

General Procedure for Brønsted Acid/Heat Experiments

Gorgonene (30 mg) was dissolved in 5 mL of the indicated solvent (Table 2.3) and the acid (Table 2.3) was added with stirring. The reaction was allowed to stir for 3 hours at the indicated temperature (Table 2.3). The reactions were either filtered (Amberlyst™) or extracted with $NaHCO_{3(aq)}$ (HCl and toluene sulfonic acid), before the solvent was removed *in vacuo* and the crude product was analyzed using ^{1}H NMR.

General Procedure for Lewis Acid and Metal Catalysis Experiments

The Lewis acid or metal reagent (5 mg) was weighed and added to a solution of **73** (50 mg) in the specified solvent (Table 2.4, 10 mL). The reaction was stirred at the indicated temperature for one hour and monitored for changes using TLC.

Chapter 3 - Semi-synthesis and Biological Evaluation of Isoxazoline-Containing (+)-β-Gorgonene Derivatives

3.1 Introduction

3.1.1 Isoxazolines and Related Heterocycles

Isoxazolines (4,5-dihydro-1,2-oxazole) are members of the azole family of 5-membered heterocycles. Azoles contain one nitrogen atom and at least one other non-carbon atom within the ring. In a sub-class containing one nitrogen and one oxygen (oxazoles) the substitution pattern and number or of double bonds vary giving rise to the six congeners shown in Figure 3.1. These oxazole derivatives are commonly associated with biological activity including antibiotic and anti-proliferative activity and are present in a number of current drugs on the market.[158,159,160]

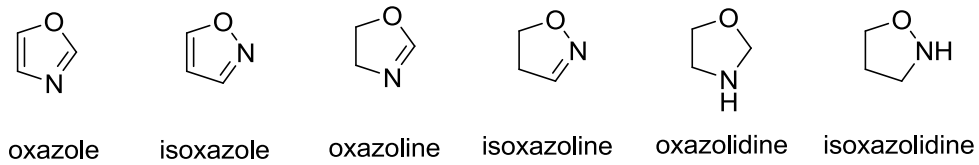

Figure 3.1 - Oxazole and Related Ring Systems

3.2 Results and Discussion

3.2.1 Preparation of Isoxazoline-Containing Compounds Using a 2+3 Dipolar Cycloaddition

In a strategy to attach biologically relevant molecular fragments to the gorgonene scaffold, an isoxazoline-containing compound collection was synthesized using a 2+3 dipolar cycloaddition reaction. This approach incorporated the desired substructures (substituted aromatics, heteroaromatics and aliphatic groups) in one step from gorgonene through an isoxazoline linker.[161-163] A series of aldehydes (Figure 3.3) was used in parallel syntheses to produce a collection of related compounds.

The first step in the synthesis of the natural product analogues was to convert the selection of aldehydes containing the desired substructures (Figure 3.3) to the corresponding oximes by treatment with hydroxyl amine hydrochloride in an ethanol/water solution. The oximes were then converted to nitrile oxides through a two-step process with a chloroxamic acid as a non-isolated intermediate (Figure 3.2). The nitrile oxide undergoes the cycloaddition reaction with the alkene.

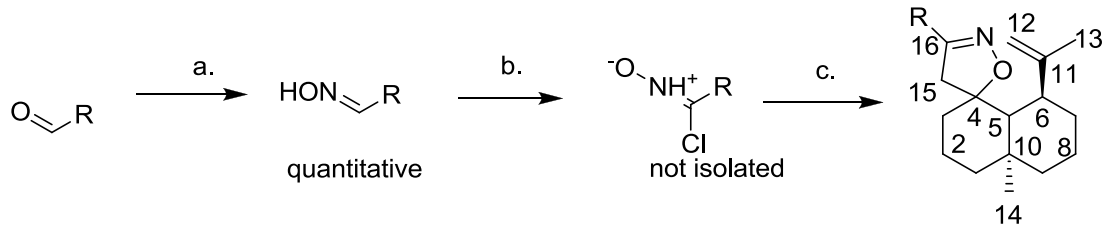

Reaction Conditions: 1: a. NH_2OH*HCl, H_2O/EtOH, b. NCS, Pyridine, DCM, c. gorgonene, Cs_2CO_3, TBME (0 ^oC – rt, 15 h).
2: a. NH_2OH*HCl, H_2O/EtOH, b. NCS, ACN c. gorgonene, TEA, ACN (0 ^oC – rt, 11 h).
3: a. NH_2OH*HCl, H_2O/EtOH, b. ACN, NCS c. gorgonene, DBU, ACN.
Figure 3.2 - Isoxazoline Reaction Scheme

Multiple isoxazoline-containing compounds were isolated from each reaction mixture including some containing unexpected carbon architectures. Three major products were typically isolated from each reaction with an average isolated individual yield of 6 %. Although this yield is low, much of the unreacted gorgonene was recovered for re-use. Aldehydes **76 - 84 (**Figure 3.3**)** produced the desired isoxazoline containing family members under the reaction conditions; however examples **85 - 88** resulted in no isoxazoline-containing products. These examples had no reaction observed and resulted in complete recovery of the starting sesquiterpene. This lack of reactivity was attributed to instability of the chloroxamic acid and nitrile oxide or solubility issues of the aldehydes.

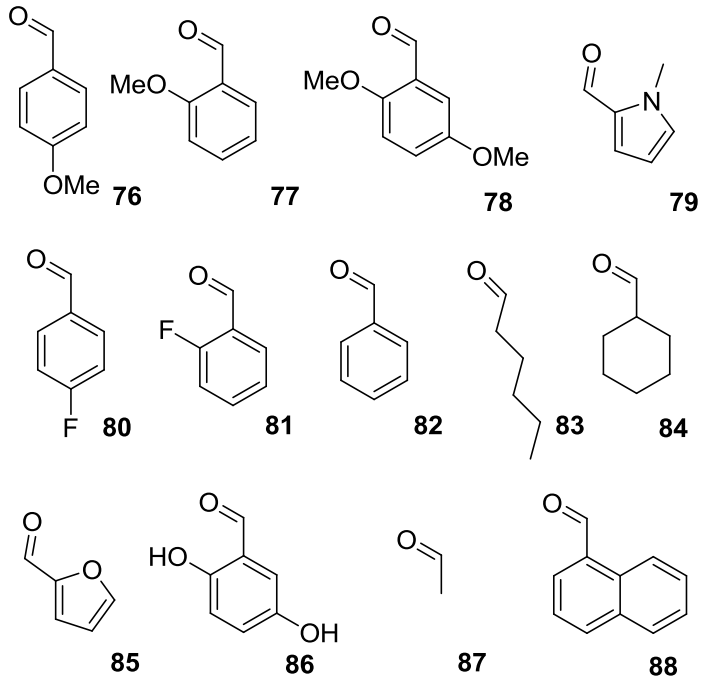

Figure 3.3 - Aldehyde Starting Materials Containing Desired Substructures

3.2.1.1 2+3 Cycloaddition Reaction Optimization

To improve the yield of the cycloaddition reaction, several strategies were explored. Bishta's conditions were applied, wherein steps b and c (Conditions 2, Figure 3.2) were performed in one pot in acetonitrile and TEA[164] replaced Cs_2CO_3 as the base. These conditions resulted in lower yield and increased recovery of starting materials. DBU[165] was also tested as a possible base for the reaction where steps b. and c. were performed, again, in one pot in acetonitrile (Conditions 3, Figure 3.2). These conditions also resulted in lower yields than the original reaction and were not explored further.

3.2.2 Isoxazoline Containing Compound Library

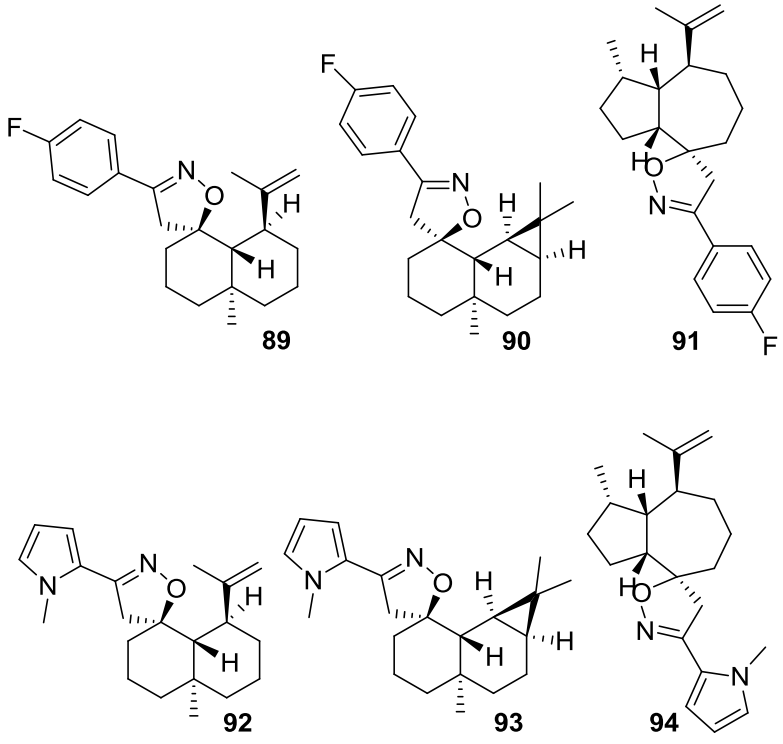

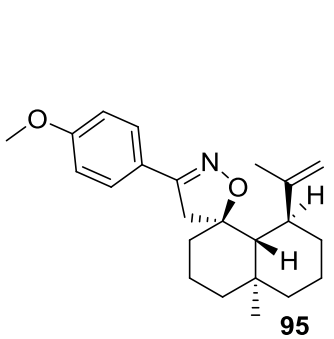

95

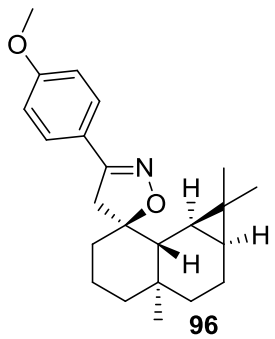

96

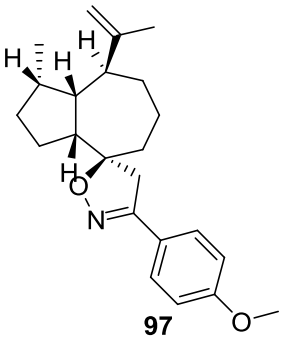

97

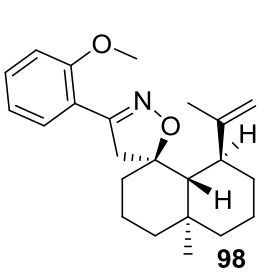

98

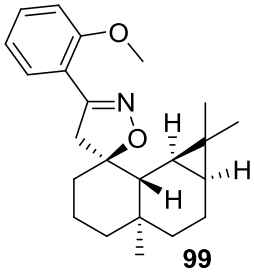

99

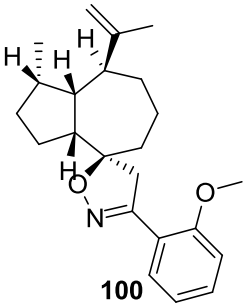

100

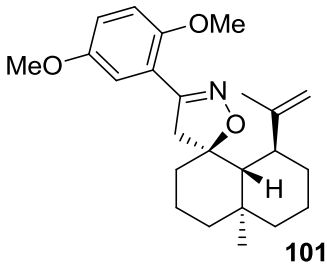

101

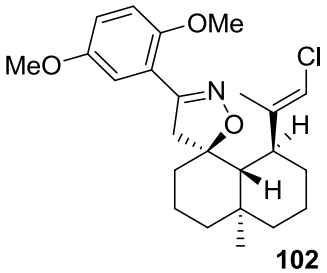

102

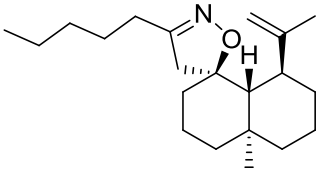

103

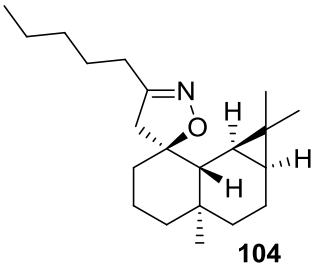

104

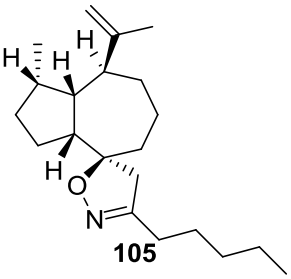

105

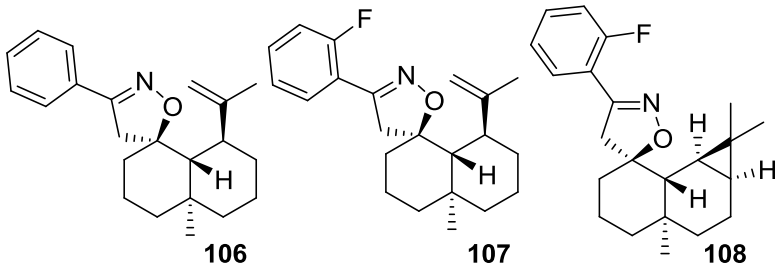

Figure 3.4 - Synthesized Isoxazoline-Containing Compound Collection

3.2.2.1 2+3 Cycloaddition Regioselectivity

The compound collection synthesized from the 2+3 cycloaddition is summarized in Figure 3.4. Similar regio- and stereoselectivity occurred in each example. The predicted configuration of the isoxazoline (oxygen attached to the more hindered carbon) was formed in each case. This is confirmed by the ^{13}C chemical shift of the sp^3 methylene carbon (C15, Figure 3.5) in the isoxazoline ring being more shielded (~50 ppm) than would be expected (~65 ppm) if attached to an oxygen atom. Also, the quaternary carbon (C4) would be expected to be much more shielded (~30 ppm) than observed (~90 ppm) if it was not attached to an oxygen atom.

The nitrile oxide dipole consistently cyclized regioselectively with the C4-C15 double bond preferentially over the iso-propylene moiety (C11-C12). This was determined by key HMBC correlations C3/H15 and C4/H15. This selectivity is attributed to elevated energy of the HOMO of the reactive caused by the angular strain associated with being connected to the cyclohexane ring. It therefore has a reduced energy of activation comparatively with the lower energy propylene HOMO void of angular strain.

3.2.2.2 2+3 Cycloaddition Stereoselectivity

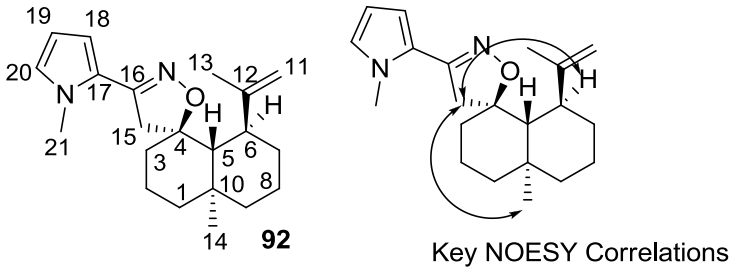

Figure 3.5 - Stereochemical Assignment of Compound 92

The key NOESY correlations that lead to the stereochemical assignment of the newly formed stereocenter (C4) in the isoxazolines **89**, **92**, **95**, **98**, **101**, **103**, **106** and **107** are shown in the representative example above (**92**, Figure 3.5). NOESY correlations between H15 and H6, as well as between H15 and H14 support the proposed stereochemistry. These correlations were present in each example mentioned above representing every library member that contained the isopropylene-substituted decalin skeleton.

The stereochemical outcome of the cyclization can be predicted by analysis of the reaction transition state. The two approaches of the dipole resulting in the two possible diastereomers are shown in Figure 3.6. The stereoisomer that is not observed would have the dipole approach the dipolarophile from the bottom face (**A**, Figure 3.6) which may be prevented due to steric hinderance between the methyl group (C14) and the approaching dipole. The observed diastereomer forms from the dipole approaching the top face (**B**) where there is less steric interaction and a favorable pi-pi interaction between the propylene group and the dipole (and aromatic groups in relevant examples). These two forces are enough to cause > 99 % de in every example.

Table 3.1 - NMR Spectroscopic Data for Compound 92 ($CDCl_3$)

	δ_C, type	δ_H (*J* in Hz)	COSY	HMBC	NOESY
1	43.4, CH_2	1.39, m			
		1.27, m			
2	18.4, CH_2	1.54, m		5	
3	39.7, CH_2	1.77, m		15a,b	
		1.52, m			
4	87.7, C			5; 15a,b	
5	50.5, CH	1.83, d (13.5)	6	14; 15a	15a
6	44.6, CH	2.35, ddd (4.1, 10.8, 10.8)		12; 13	
7	33.9, CH_2	1.56, m			
8	21.4, CH_2	1.61, m			
		1.55, m			
9	42.0, CH_2	1.37, m		14	
		1.25, m			
10	36.3, C			5; 14	
11	149.7, C			5; 13	
12	109.7, CH_2	4.34, s	13	13	
13	18.2, CH_3	1.73, s	12	6; 8; 12	
14	18.7, CH_3	0.94, s			15
15	40.9, CH_2	3.12, d (16.0)			5, 14
		2.73, d (16.0)			14
16	149.7, C			15a,b; 13	
17	124.087, C			18; 20; 21	
18	112.6, CH	6.30, m	20; 19	20	
19	107.7, CH	6.13, m		20	
20	126.8, CH	6.70, m	19; 18	21; 19	
21	37.6, CH_3	3.84, s			

Data was obtained in $CDCl_3$ solution, δ in PPM relative to solvent signal. Assignments were aided by COSY, HSQC and HMBC and NOESY experiments. HMBC correlations from the carbon stated to the indicated proton.

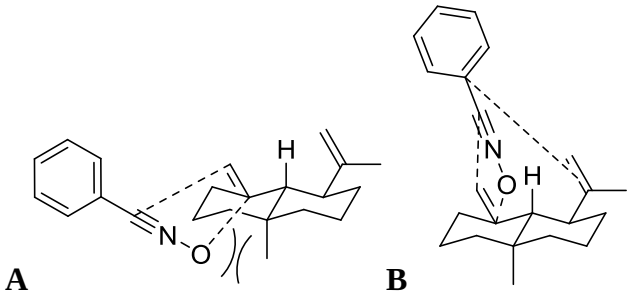

Figure 3.6 - Rational for Stereoselectivity Observed in Isoxazoline Library

3.2.2.3 Unexpected Products of Isoxazoline Reaction

Cyclopropane- (examples **90**, **93**, **96, 99**, **104 and 108**), and decahydroazulene containing analogues (examples **91**, **94**, **99**, **100**, **105**) were isolated from several reaction mixtures. The formation of a chlorinated analogue was observed in two cases (**102** and *m/z* ion consistent with the molecular formula $C_{22}H_{34}ClNO$ in the product mixture of reaction with **84**). The yield of the three major products formed (expected product, cyclopropane and decahydroazulene) was relatively consistent throughout each reaction and was close to a 1:1:1 ratio. The product distribution and yields are displayed in Table 3.2.

Table 3.2 - Products Yields of 2+3 Cycloaddition Reaction with 73

Aldehyde Starting Material	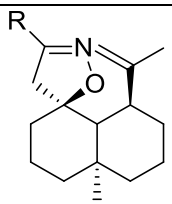	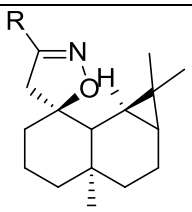	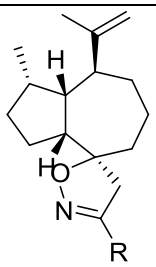	Chlorinated Product
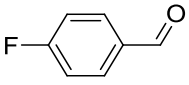	**89** >99 % pure Yield: 7.1 %	**90** >99 % pure Yield: 6.4 %	**91** >99 % pure Yield: 6.1 %	Not observed

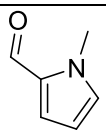	**92** >99 % pure Yield: 5.5 %	**93** >99 % pure Yield: 6.3 %	**94** 85-90 % pure	Not observed
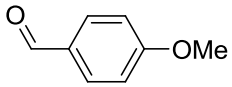	**95** >99 % pure Yield: 7.5 %	**96** 85-90 % pure Yield: 8.0 %	**97** >99 % pure Yield: 7.2 %	Not observed
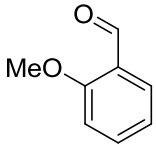	**98** >99 % pure Yield: 6.3 %	**99** >99 % pure Yield: 6.1 %	**100** >99 % pure Yield: 6.1 %	Not observed
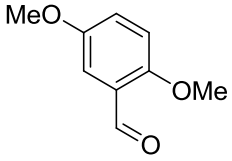	**101** >95 % pure Yield: 3.7 %	Not observed	Not observed	**102** >99% pure Yield: 6.1 %
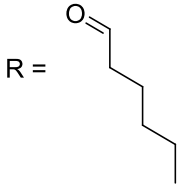	**103** 99 % pure Yield: 5.4 %	**104** 99 % pure Yield: 6.5 %	**105** 99 % pure Yield 4.8 %	Not observed
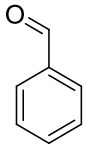	**106** 99 % pure Yield: 8.5 %	Not observed	Not observed	Not observed
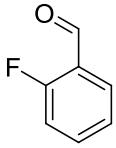	**107** 99 % pure Yield: 7.1 %	**108** 99 % pure Yield: 3.5 %	Not observed	Not observed
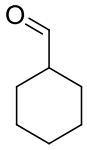	Not observed	Observed in inseparable product mixture	Observed in inseparable product mixture	Observed in product mixture

3.2.2.4 Cyclopropane-Containing Library Members

The $[M+H]^+$ of compound **90** was 342.2217 corresponding to the molecular formula $C_{22}H_{29}FNO$. Two signals with unexpected chemical shifts in the ^1H NMR spectrum of compound **90** (0.29 and 0.57 ppm) suggested the presence of a

cyclopropane ring. 2D NMR analysis, particularly COSY correlations H5/H6 and H6/H7 as well as HMBC correlations C6/H13, C7/H13, C11/H12, C11/H13, C11/H6 and C11/H7 aided assignment of the cyclopropane moiety (Table 3.3). Signals corresponding to the isoxazoline moiety and phenyl group were observed and HMBC correlations supported the connectivity shown in Figure 3.7. The stereochemistry at C4 was confirmed by NOESY correlations between H15/H14 and H15/H6. NOESY correlations between H5 and H12 confirmed the stereochemistry at C6. Similar observations for other cyclopropane-containing library members support a consistent stereochemical configuration in each example.

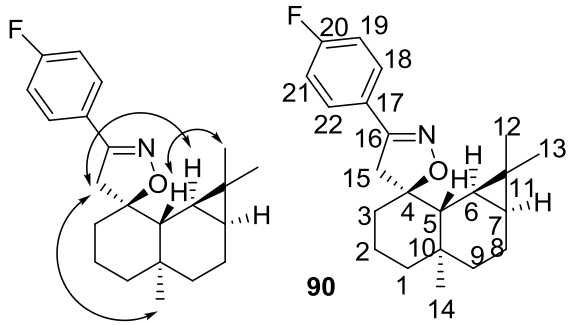

Figure 3.7 - NOESY Supported Stereochemical Assignment of 90

Table 3.3 - Spectroscopic Data for Compound 90 ($CDCl_3$)

	δ_C, type	δ_H (*J* in Hz)	COSY	HMBC	NOESY
1	39.1, CH_2	1.10,m	2; 1b	13	
		1.36, m	1a; 2		
2	19.2, CH_2	1.64, m	1a, b		
3	38.8, CH_2	1.60, m			3b
		1.94, m	3a		
4	90.8, C			15a,b; 5; 6	
5	44.8, CH	1.44, d (5.8)	6		
6	20.6, CH	0.29, m	5, 7	13	
7	19.0, CH	0.58, dd (8.5, 8.5)	6	13	8a,b; 6
8	15.7, CH_2	1.57, m			
		1.83, m	9a,b		8a; 9b; 7
9	39.9, CH_2	0.91, m		13	
		1.19, m		5	8a; 9a
10	33.9, C			5; 8; 9a, b; 14; 15	
11	17.5, C			12; 13; 6; 7	
12	15.6, CH_3	1.00, s		6; 13	
13	29.3, CH_3	0.98, s		12	
14	18.6, CH_3	0.92, s		1; 9; 5	8b; 2; 5; 9b
15	40.2, CH_2	2.96, d (16.6)	15b		14; 2; 3b; 15a
		3.33, d (16.6)	15a		6; 14; 15a
16	162.6, C			18; 22; 19	
17	154.6, C			18; 22; 15a,b	
18, 22	128.4, CH	7.68, m	19; 21	19, 21	15a
19, 21	115.9, CH	7.08, m	18; 22	18; 22	
20	164.2, C			18; 22; 19, 21	

Data was obtained in $CDCl_3$ solution, δ in PPM relative to solvent signal. Assignments were aided by COSY, HSQC and HMBC and NOESY experiments. HMBC correlations from the carbon stated to the indicated proton.

3.2.2.5 Isolation of Decahydroazulene-Containing Library Members

There is evidence in nearly all of the 2+3 cycloaddition reaction mixtures for a decahydroazulene containing product. 1D and 2D NMR supported the general structure represented by compound **97**, proposed in Figure 3.8. Compound **97** produced an

HRESIMS *m*/*z* ion of 354.2403 corresponding to a molecular formula of $C_{23}H_{32}NO_2$. The first indication that the products contained a decahydroazulene bicyclic scaffold was the appearance of the methyl group (H14) as a doublet in the ^{1}H NMR spectrum. Four aliphatic methine groups were present, two more than expected for the decalin containing product. COSY correlations H1/H2, H2/H3, H3/H4, H4/H5, H5/H6, H6/H7, H7/H8, H8/H9 and H5/H1 aided the elucidation of the new skeleton. HMBC correlations C10/H15, C10/H5 and C9/H15 helped assign the rest of the ring connectivity and indicated the isoxazoline was formed at C10. NOESY spectroscopy was extensively utilized to assign the stereochemistry of the **97** and the key correlations used are shown in Figure 3.8.

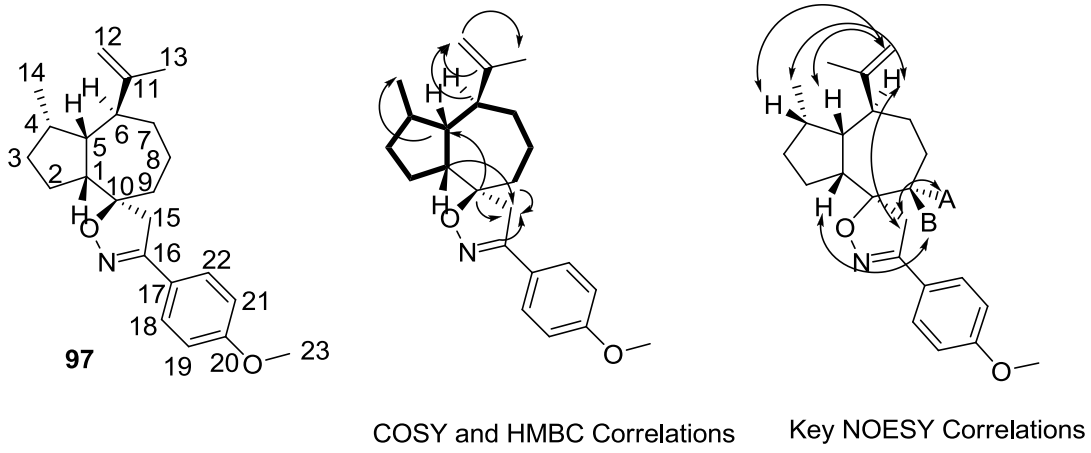

Figure 3.8 - Key 2-D NMR Data for Structure Elucidation of Compound 97

Table 3.4 - NMR Spectroscopic Data for Compound 97 ($CDCl_3$)

	δ_C, type	δ_H (*J* in Hz)	COSY	HMBC	NOESY
1	50.1, CH	2.74, m	2a, b; 5	15	2b; 5; 9a
2	27.8, CH_2	1.46, m	1, 3a		
		1.99, m	1		
3	33.0, CH_2	1.37, m	2a	14	14
		1.57, m	4		
4	36.4, CH	2.05, m	3b; 5; 14	5; 14	5; 14; 4
5	47.4, CH	2.32, ddd (12.3, 6.5, 6.5)	1; 4; 6	14	13; 3b; 12; 6; 1
6	47.9, CH	1.89, m	5; 7a	12; 13	13; 15; 14
7	36.4, CH_2	1.43, m	6		
		1.66, m	8b		
8	25.1, CH_2	1.50, m	9a,b		
		1.81, m	7b		
9	41.5, CH_2	1.77, m	8a	15	
		2.02, m	8a		15
10	92.7, C			5; 15	
11	149.7, C			22	
12	19.4, CH_3	1.69, s	13		13
13	109.7, CH_2	4.70, m	12	12	
14	15.8, CH_3	0.83, d (7.2)	4		
15	39.0, CH_2	3.15, s			18; 22; 6
16	155.2, C			15	
17	123.1, C			19; 21	
18, 22	128.1, 2xCH	7.64, m (8.9)			
19, 21	113.9, 2xCH	6.93, m (8.9)			
20	160.6, C			18; 19; 21; 22; 23	
23	55.5, CH_3	3.84, s			19; 21

Data was obtained in $CDCl_3$ solution, δ in PPM relative to solvent signal. Assignments were aided by COSY, HSQC and HMBC and NOESY experiments. HMBC correlations from the carbon stated to the indicated proton.

Stack plots of the ^{1}H NMR spectrum of the three isomers generated from the 2+3 dipolar cycloaddition of **73** with 2-methoxybenzene nitrile oxide (**98**, **99**, **100**) are shown in Figure 3.9 and Figure 3.10 (enlarged).

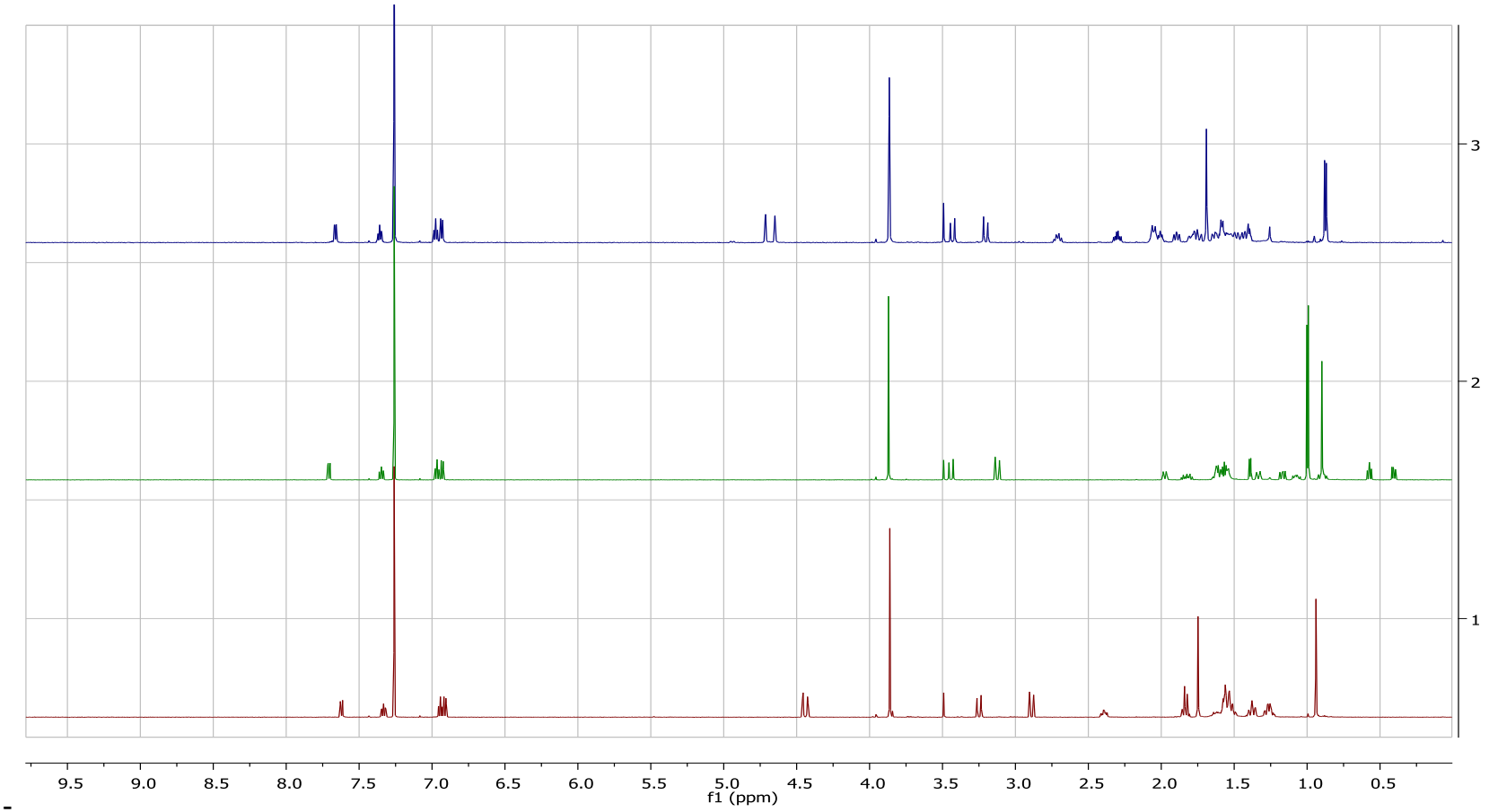

Figure 3.9 - Stack Plot of ^{1}H NMR Spectra (600 MHz, $CDCl_3$) of Semi-synthetic Compounds 98 (bottom), 99 (middle) and 100 (top). (δ in ppm Relative to Solvent Signal)

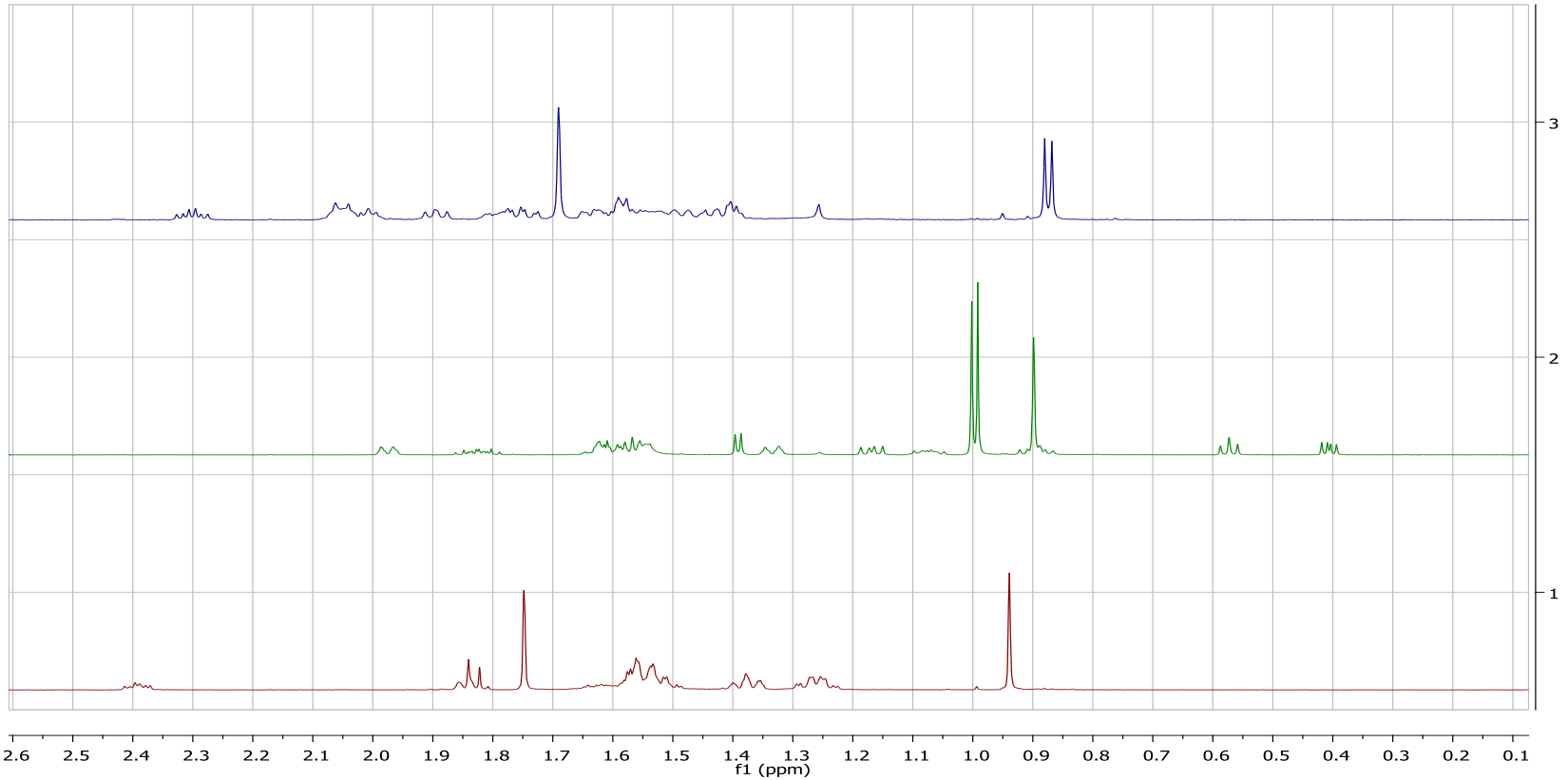

Figure 3.10 - Enlarged Stack Plot of ^{1}H NMR Spectra (600 MHz, $CDCl_3$) of Semi-synthetic Compounds 98 (bottom), 99 (middle) and 100 (top). (δ in ppm Relative to Solvent Signal)

3.2.2.6 - Source of Unexpected Cyclopropane and Decahydroazulene Products

The isolation of the unexpected cyclopropane and decahydroazulene containing products was originaly thought to be the result of a skeletal rearrangement of the gorgonene skeleton under the reaction conditions. The family of compounds biosynthetically related to gorgonene is reported to be very labile. Hackl, for example, reported that bicyclogermacrene A (**110**), underwent extensive rearrangements upon treatment with an acid ion exchange resin to produce known and unknown sesquiterpenes with widely varying skeletons (Figure 3.8).[130]

The unexpected sesquiterpenoid frameworks isolated from the reaction mixture may, alternatively, have arisen from the reaction of other hydrocarbons present in the coral extract. Naturally occurring sesquiterpene hydrocarbons produced within the coral from farnesyl pyrophosphate are a possible source of the unexpected products. Compound **115**, the logical synthetic precursor of the cyclopropane containing isoxazolines, belongs to the same biosynthetic class as gorgonene and was co-isolated with gorgonene from the sea whip *Antillogorgia americana* in a previous study performed by Hackl in a ratio of 8:55 (**115**: Gorgonene). The proposed precursor (**116**) to the decahydroazulene-isoxazoline products is not reported in the literature, but a similar scaffold was also isolated by Hackl from *Antillogorgia americana* (**117**), suggesting that the compound **116** could be present in the *Antillogorgia elisabethae* extract. The stereochemistry of the natural product precursers is consistent with the stereochemistry observed in the products.

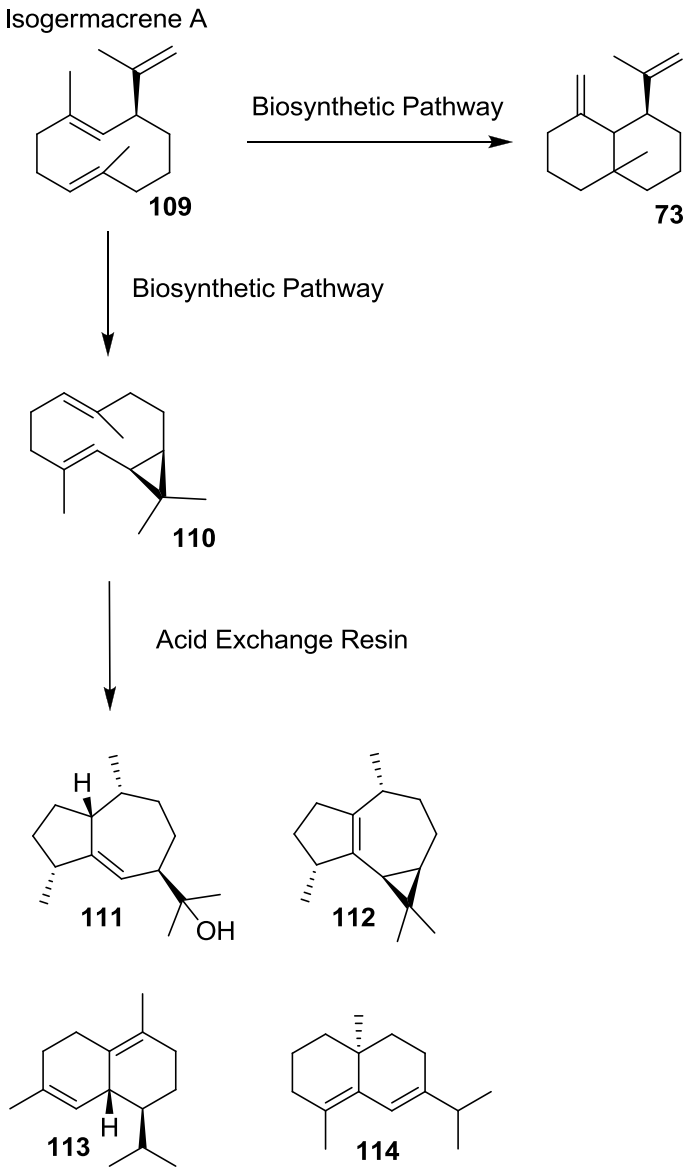

Figure 3.11 - Acid-Induced Rearrangement of Bicyclogermacrene (110)[130]

The purity of the gorgonene starting materials was thoroughly investigated and there was evidence of the presence of other minor sesquiterpene hydrocarbons components. There were several batches of starting materials that had NMR spectra containing signals that could be attributed to the presence of the proposed cyclopropane (**115**) and decahydroazulene (**116**) starting materials in 6-8 %.

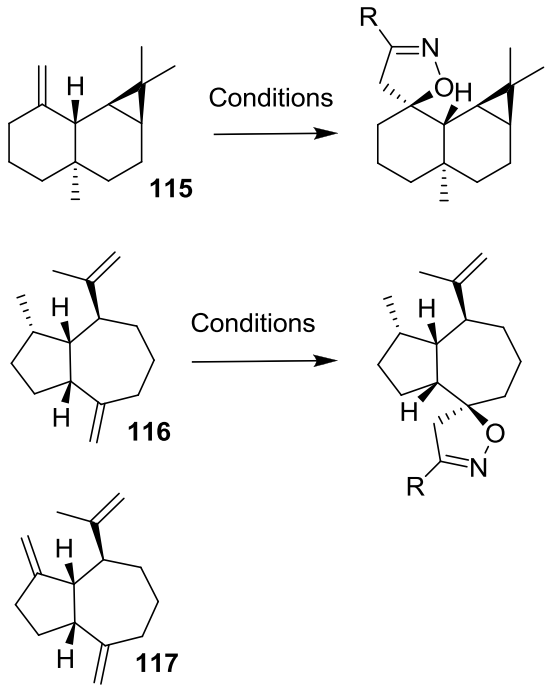

Figure 3.12 - Theoretical Starting Materials for Cyclopropane and Decahydroazulene Containing Products

The hydrocarbon skeletons of **73** and other sesquiterpene hydrocarbons present in the coral extract are not trivial to separate. Many of them share a molecular formula and contain no heteroatoms causing them to lack significant interaction with normal phase chromatography stationary phases. The hydrocarbons were not separable in our hands using reverse phase chromatography. Distillation was also attempted as mode of purification, however tandem diol-silica column flash chromatography resulted in the

highest purity of gorgonene out of all of the methods tested. The loss of purity in subsequent purifications of the starting materials is attributed to the repeated use of silica columns and variation in the mass of crude mixture loaded onto the column. Figure 3.9 shows an NMR spectrum recorded in deuterated chloroform of a concentrated sample of gorgonene used for synthetic starting materials. In it, in the ranges of 0.65, 0.8, 1.0-1.1 and 4.8-5.0 ppm, signals proposed to correspond to the putative starting materials, **115** and **116** are seen in 6-8 % composition.

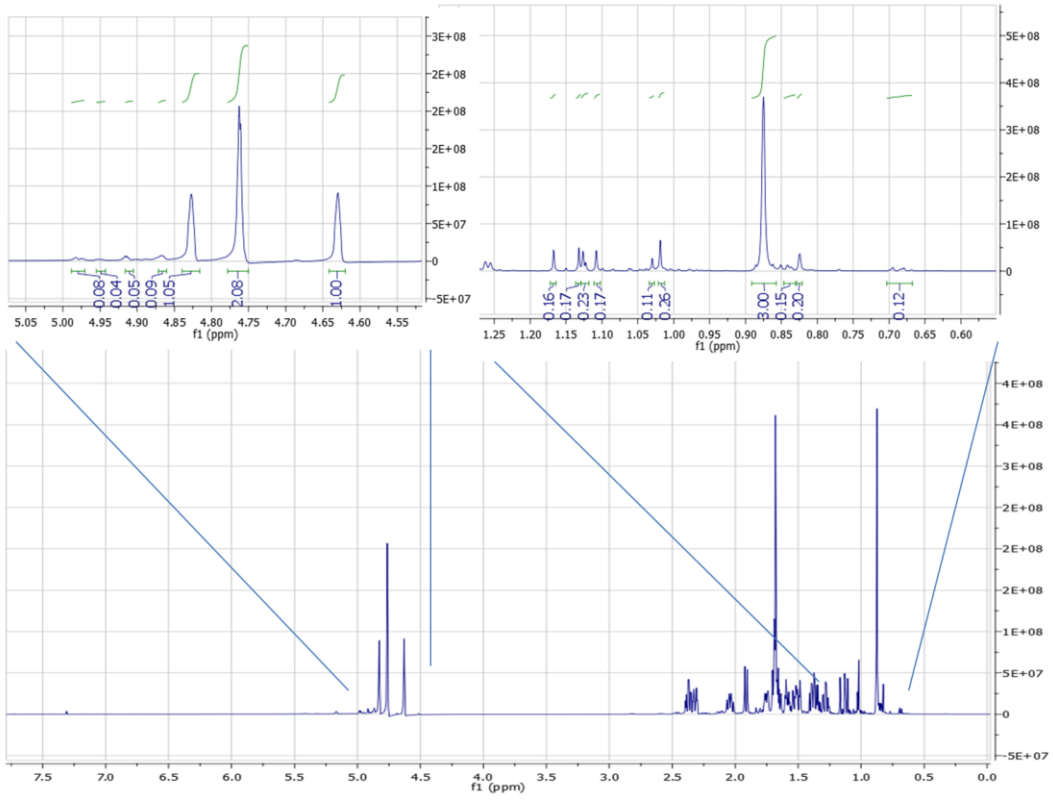

Figure 3.13 - Batch of Gorgonene Starting Materials ^{1}H NMR Spectrum in $CDCl_3$

Assuming the cyclopropane and decahydroazulene-containing products are the result of impurities present in the starting materials, those impurities evidently react much more readily than gorgonene under the reaction conditions. Indeed the impurities

must react in very high yield (approaching quantitative), whilst gorgonene reacts with a typical yield of 6 %. The reason for the vast difference in observed reactivity is not well understood, however both of these minor sesquiterpene components have terminal alkene motifs that are less sterically hindered than gorgonene. There may be an additional electronic interaction between the two alkenes in gorgonene that also leads to its lower reactivity compared with the two other two proposed starting materials.

3.2.2.7 Regio- and Stereochemical Assignment of Chlorine Containing Analogue

One of the products of the 2+3 cycloaddition reaction with dimethoxy-benzaldehyde contained a chlorine atom according to HRMS (*m/z* 418.2141, $C_{24}H_{33}ClNO_3$). Alkenyl carbon C13 appeared as a methine in the HSQC spectrum and the chemical shift of H13 was deshielded indicating the chlorine was substituted at this position. 1D and 2D NMR were used to assign the structure **102**; a key HMBC correlation was between C3/H15 indicated the isoxazoline had been formed at C4. The configuration of the chloro-substituted double bond of **102** was supported by a chemical shift in the ^{13}C NMR spectrum of 13.7 ppm corresponding to C12 which is closer to the predicted value for the *E* substituted double bond than the *Z*. An *E* configuration is also supported by NOESY correlations between H5 and H12. These details together suggest that the *E* isomer is a more likely structure than the *Z*. *Trans*- alkenes are more stable for steric reasons and the *trans*-geometry is more likely to be adopted in either mechanism proposed above.

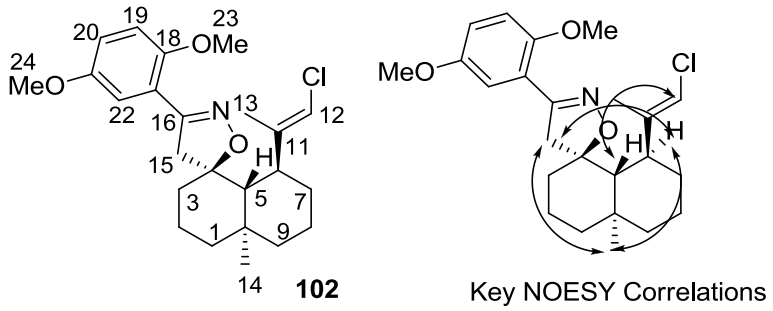

Figure 3.14 - Stereochemical Assignment of Chlorinated Analogue 102

3.2.2.8 Formation of Chlorinated Analogues

Several reaction conditions were used to explore the cause of the formation of the chlorinated analogues. Due to the instability of the chloro-oxamic acid, no purification step was performed on the intermediate before the next step (C, Figure 3.2: one-pot conversion to the nitrile oxide and cyclization). Residual NCS may be converted to radical chlorine under UV irradiation which could facilitate a radical substitution reaction, followed by a tautomerization to result in a chloro-substituted vinyl group (Figure 3.15). Allylic chlorination (similar to Wohl-Ziegler reaction with NBS (N-bromosuccinimide)) is most often performed in chlorinated solvents. To eliminate the possibility of residual NCS promoting radical allylic chlorination, gorgonene was treated with NCS in TBME (tert-butyl methyl ether) under UV irradiation. No reaction was observed, indicating that the residual NCS was not capable of causing the chlorination reaction to occur in TBME, even with UV irradiation. β-Gorgonene was then treated with NCS and Cs_2CO_3 in a solution of TBME to mimic the conditions used in the final step of the reaction with UV irradiation, again with no reaction. However, when β-gorgonene was treated with NCS in dichloromethane, allylic chlorination was observed. The possibility of a small amount of residual dichloromethane being present

in the final step of the reaction was considered as a cause for the radical formation, however is unlikely responsible for the production of the chlorinated analogues.

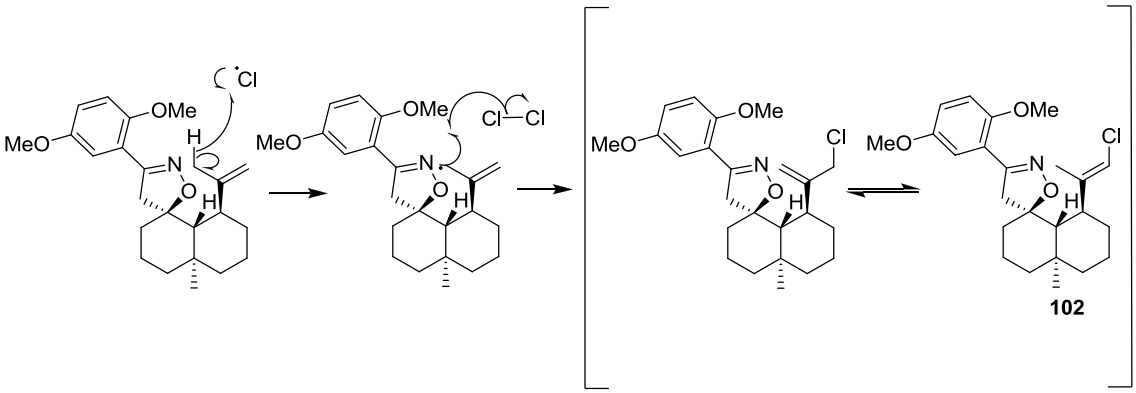

Figure 3.15 - Radical Mechanism for the Formation of Chlorinated Analogue 102

Since no chlorine radicals could be generated in the test reactions in the selected solvents, it is possible that the chlorination occurs *via* reaction of the alkene with Cl_2. The chlorine may add to the double bond, followed by an elimination reaction resulting in the observed product (Figure 3.16). Due to the fact that the chlorination did not occur under the test conditions without the nitrile oxide present, nor are any chlorinated derivatives present in the product mixture that do not also contain an isoxazole ring, it is likely that the chlorination occurs simultaneously with formation of the isoxazoline. The exact mechanism is not known.

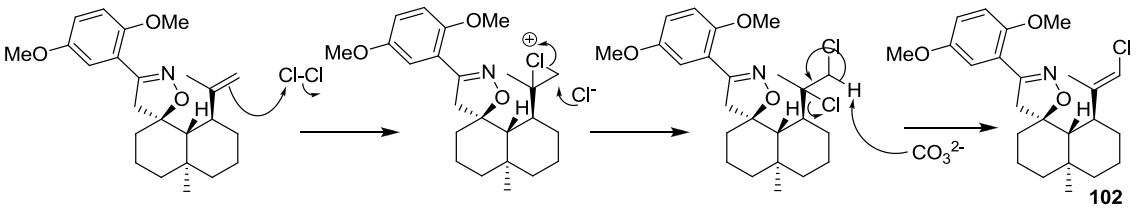

Figure 3.16 - Addition/Elimination Mechanism for the Formation of 102

3.2.3 Analysis of the Drug-Likeness of Isoxazoline Library

One of the primary aims of this study was to produce a compound library that was more drug-like than the starting material, gorgonene. Each compound was evaluated for characteristics associated with drug-likeness (physical properties consistent with the majority of known drugs).[175] These properties are associated with the compounds' solubility in both water and fat to facilitate absorption in the body, and molecular weight is important because small molecules diffuse more easily. Molecular flexibility is described using the number of rotatable bonds and decreased flexibility has been connected to better oral availability.[176] The results of the analysis are summarized in Table 3.5. For the purposes of these calculations, proton acceptors are any atom possessing a lone pair of electrons. LogP was calculated using the chemical software ChemDraw. According to Lipinski, a LogP value of less than 5 is appropriate for drugs, however, a more recent study done by Ghose *et al*. based on the compounds in the comprehensive medical chemistry database, an upper limit of 5.6 is more appropriate.[177]

Table 3.5 - Analysis of Drug-Like Properties of Isoxazoline Compound Collection

Compound Number	Hydrogen Bond Acceptors	Hydrogen Bond Donors	MW	LogP	Rotatable Bonds
89	3	0	341	5.64	2
90	3	0	341	5.53	1
91	3	0	341	5.5	2
92	3	0	303	4.26	2
93	3	0	326	4.15	1
94	3	0	326	4.12	2
95	3	0	353	5.35	3
96	3	0	353	5.24	2
97	3	0	353	5.21	3
98	3	0	353	5.35	3
99	3	0	353	5.24	2
100	3	0	353	5.21	3
101	4	0	383	5.23	4
102	5	0	417	5.63	4
103	2	0	317	6.24	5
104	2	0	317	6.13	4
105	2	0	317	6.1	5
106	2	0	323	5.48	2
107	3	0	341	5.64	2
108	3	0	341	5.53	2

Every library member is within Lipinski's limits for number of hydrogen donors (<5), hydrogen acceptors (<10) and molecular weight (<500).[48] Using the LogP parameters suggested by Ghose, 14 of the 20 isoxazolines have an appropriate LogP, although they are approaching the upper limit. The number of rotatable bonds is a description of the flexibility of the molecule and each compound in this set has less than the maximum suggested number of 10.

3.2.4 Biological Evaluation of Isoxazoline-Containing Compound Collection

3.2.4.1 Analysis of PTP1B Activity

The compounds described in this chapter were tested for inhibition of seven protein tyrosine phosphatases from class I to determine their activity and selectivity for the target PTP1B enzyme. All PTP assays were performed by Michel Tremblay`s group at McGill University. The compounds were tested for PTP inhibition at 50 µM (See Chapter 2-experimental details for procedure). Compound **90** showed modest selective inhibition of the PTP1B and TcPTP enzymes. The most potent inhibitors of PTP1B in the collection, however, were two decahydroazulene containing compounds (Compound **91**, 131.4 µg/mL and **105**, 105.1 µg/mL) and two ortho-fluoro phenyl containing members (**107**, 110.8 µg/mL and **108**, 95.3 µg/mL). This activity was approximately half as potent as the model compounds for this collection, ilimaquinone (68 µg/mL) and 5-epi-ilimaquinone (54 µg/mL).

5.2.4.2 Evaluation of Anticancer Activity

The compounds discussed in this chapter were tested for anticancer activity using a human foreskin BJ fibroblast cell line (ATC CRL-2522) and human breast adenocarcinoma cells (ATCC HTB-26) according to the procedure described in chapter 2. The most active compounds, **106** and **107** had IC_{50} values of 16-32 µg/mL against breast cancer cells and **107** showed growth inhibition of the fibroblast cell line as well. These two compounds are very similar structurally, the only difference being the replacement of a hydrogen atom with a fluorine atom in the ortho-position of the aromatic ring. Cytotoxic activity was not observed in similar compounds: **89** (replace para-H of aromatic ring of **106** with a fluorine atom) and **108** (propylene group in **107**

replaced by a cyclopropane ring - Figure 3.17). Perhaps a di-fluorobenzene, or a bromo- or chloro-substituted benzene derivative could possess increased cytotoxicity. Compounds **103-105** (N-hexyl isoxazoline substituent) each displayed activity between 32-64 µg/mL in the HTB cell line assay and **103** also inhibited the growth of the BJ cell line at 64 µg/mL. Compounds **92-94** were not included in the assay due to their instability. An IC_{50} of compound **98** was not calculated due to degradation of the compound.

Table 3.6 - Cytotoxicity of Isoxazoline Collection (IC_{50})

	Cancer Cell Line	
Compound	CRL-2522	HTB-26
89	>64 µg/mL	>64 µg/mL
90	>64 µg/mL	>64 µg/mL
91	>64 µg/mL	>64 µg/mL
95	NT	>100 µg/mL
97	NT	>100 µg/mL
98	NT	<100 µg/mL
99	NT	>100 µg/mL
100	NT	>100 µg/mL
101	>64 µg/mL	>64 µg/mL
102	>64 µg/mL	>64 µg/mL
103	32-64 µg/mL	32-64 µg/mL
104	>64 µg/mL	32-64 µg/mL
105	>64 µg/mL	32-64 µg/mL
106	>64 µg/mL	16-32 µg/mL
107	32-64 µg/mL	16-32 µg/mL
108	>64 µg/mL	>64 µg/mL

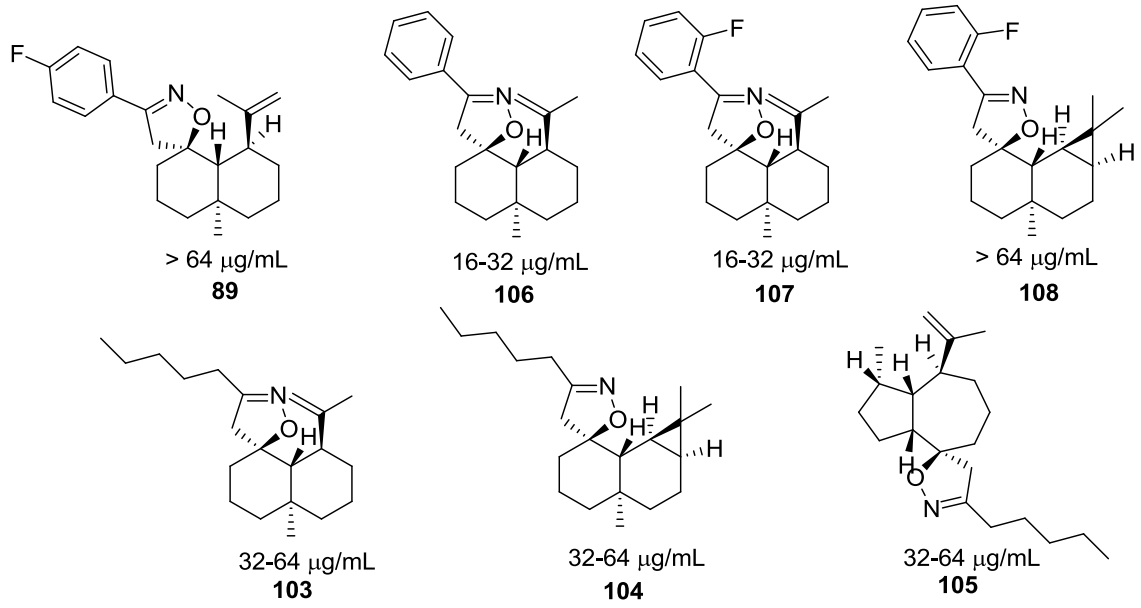

Figure 3.17 - Cytotoxic Evaluation and Structure Activity Relationship of Isoxazoline Compounds (HTB-26)

5.2.4.3 Evaluation of Antimicrobial Activity

The family of compounds described in this chapter was tested for antimicrobial activity against microbes: MRSA, VRE, *C. albicans*, *P. aeruginosa*, *P. vulgaris* and *S. warneri* using the assay protocol described in chapter 2. None of the compounds showed antimicrobial activity against any of the organisms up to 128 μg/mL.

3.3 Conclusion

A family of isoxazoline natural product mimics was synthesized from the marine sesquiterpene β-gorgonene using a 2+3 dipolar cycloaddition reaction. The resulting library was analyzed for PTP1B inhibition, anticancer and antimicrobial activities. The collection was then evaluated for drug-likeness. Several of the library members showed modest but selective inhibition of the PTP1B enzyme and modest cytotoxic activity.

3.4 Experimental Section

3.4.1 General Procedure for Synthesis of Isoxazoline Derivatives

An aqueous (5mL) solution of hydroxylamine hydrochloride (9.9 mmol) was added to a solution of aldehyde (4.6 mmol) in ethanol (5 mL) at room temperature with stirring. The reaction was monitored using TLC and was complete after 20 minutes. The reaction was diluted with distilled water (100 mL), extracted with chloroform (3 x 50 mL), dried with magnesium sulfate and the solvent was removed *in vacuo*. The oxime product **A** was used in the next step without further purification.

N-Chlorosuccinimide (1.1 mmol) and pyridine (5 µL) were added to a solution of oxime **A** (1.1 mmol) in dichloromethane (12 mL) in the dark and the reaction was stirred for one hour at room temperature. The solvent was then removed *in vacuo*. A solution of β-gorgonene (1.0 mmol) in diethyl ether (10 mL) was then added to the crude chloroxamic acid and the reaction was cooled to 0 ^{o}C. Cs_2CO_3 (1.0 mmol) was added as a solid and the reaction mixture was stirred vigorously for 15 hours while being allowed to come to room temperature. The reaction was then diluted with concentrated $NaHCO_3$ (25 mL) and extracted with ethyl acetate (3x30 mL). The organic layer was dried with $MgSO_4$ and the solvent was removed under a stream of air. The crude mixture was separated by C18 chromatography (50:50 H_2O: MeOH – 100 % MeOH) and the fractions containing the products were identified using UPLC/MS and were further purified using HPLC.

Compound **89**

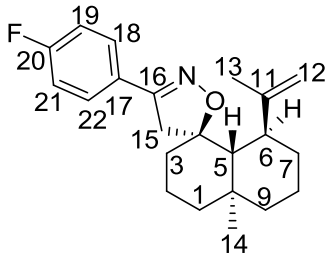

Compound **89** was synthesized according to the general procedure above and the product fraction purified using a semi-prep phenyl hexyl HPLC column (isocratic, 88:12 MeOH:H_2O, 2.5 mL/min) and was the first compound to elute (yield 7.1%).

^{1}H NMR (600 MHz, $CDCl_3$) δ 7.66 – 7.57 (m, 2H), 7.06 (m, 2H), 4.34 (s, 1H), 4.31 (s, 1H), 3.13 (d, *J* = 16.1 Hz, 1H), 2.72 (d, *J* = 16.1 Hz, 1H), 2.36 (ddd, *J* = 10.7, 4.6, 4.6 Hz, 1H), 1.85 (d, *J* = 11.1 Hz, 1H), 1.81 – 1.76 (m, 1H), 1.73 (s, 3H), 1.64 – 1.60 (m, 1H), 1.59 – 1.56 (m, 1H), 1.57 - 1.55 (m, 1H), 1.57 - 1.53 (m, 2H), 1.57 - 1.53 (m, 2H), 1.42 – 1.39 (m, 1H), 1.41 - 1.37 (m, 1H), 1.30 – 1.26 (m, 1H), 1.29 – 1.25 (m, 1H), 0.97 (s, 3H).

^{13}C NMR (151 MHz, $CDCl_3$) δ 163.6, 154.3, 149.6, 128.3, 128.2, 127.3, 115.8, 115.7, 110.1, 90.1, 50.6, 44.8, 43.4, 41.9, 39.8, 39.3, 36.3, 33.9, 21.5, 18.7, 18.4, 18.1.

FTIR (CH_2Cl_2): ν_{max} 3068.5, 2927.6, 2855.0, 1641.8 cm^{-1}.

(+) HRESIMS *m*/*z* 342.2217 $[M + H]^+$ (calcd for $C_{22}H_{29}FNO$, 342.2233).

Compound **90**

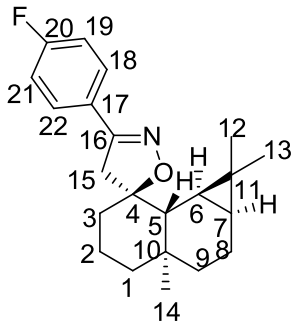

Compound **90** was synthesized according to the general procedure above and the product fraction was purified using a semi-prep phenyl hexyl HPLC column (isocratic, 88:12 MeOH:H_2O, 2.5 mL/min) and was the second compound to elute (yield 6.4 %).

^{1}H NMR (600 MHz, $CDCl_3$) δ 7.70 – 7.65 (m, 2H), 7.11 – 7.05 (m, 2H), 3.33 (d, *J* = 16.6 Hz, 1H), 2.96 (d, *J* = 16.6 Hz, 1H), 1.94 (m, 1H), 1.86 – 1.77 (m, 1H), 1.67 – 1.60 (m, 2H), 1.62 – 1.57 (m, 1H), 1.60 – 1.57 (m, 1H), 1.43 (d, *J* = 5.8 Hz, 1H), 1.36 (m, 1H), 1.18 (m, 1H), 1.09 (m, 1H), 0.99 (s, 3H), 0.98 (s, 3H), 0.91 (s, 3H), 0.94 – 0.87 (m, 1H), 0.57 (dd, *J* = 8.5, 8.5 Hz, 1H), 0.29 (m, 1H).

^{13}C NMR (151 MHz, $CDCl_3$) δ 164.4, 162.6, 154.6, 128.4, 128.4, 115.9, 115.7, 90.7, 44.8, 40.2, 39.9, 39.1, 38.8, 33.9, 29.2, 20.6, 19.2, 19.0, 18.6, 17.5, 15.7, 15.5.

FTIR (CH_2Cl_2): ν_{max} 3069.2, 2927.1, 2850.9, 1647.3 cm^{-1}.

(+) HRESIMS *m*/*z* 342.2217 $[M + H]^+$ (calcd for $C_{22}H_{29}FNO$, 342.2233).

Compound **91**

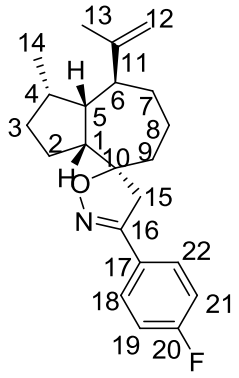

Compound **91** was synthesized according to the general procedure above and the product fraction purified using a semi-prep phenyl hexyl HPLC column (isocratic, 88:12 MeOH:H_2O, 2.5 mL/min) and was the fourth compound to elute (yield 6.1 %).

^{1}H NMR (600 MHz, $CDCl_3$) δ 7.71 – 7.66 (m, 2H), 7.09 (m, 2H), 4.73 (s, 1H), 4.66, (s, 1H), 3.15 (s, 2H), 2.79 – 2.68 (m, 1H), 2.32 (ddd, *J* = 12.3, 6.5, 6.5 Hz, 1H), 2.10 – 1.99 (m, 1H), 2.05 – 1.97 (m, 1H), 2.02 – 1.96 (m, 1H), 1.90 – 1.85 (m, 1H), 1.85 – 1.78 (m, 1H), 1.81 – 1.74 (m, 1H), 1.70 (s, 3H), 1.68 – 1.64 (m, 1H), 1.60-1.56 (m, 1H), 1.51 - 1.46 (m, 1H), 1.47 - 1.43 (m, 1m), 1.45 - 1.40 (m, 1H), 1.39 - 1.36 (m, 1H), 0.83 (d, *J* = 7.2 Hz, 3H).

^{13}C NMR (151 MHz, $CDCl_3$) δ 162.8, 154.8, 150.1, 128.4, 128.4, 126.8, 116.0, 115.8, 109.8, 93.3, 49.9, 48.0, 47.4, 41.7, 38.7, 36.5, 33.0, 27.8, 25.0, 19.1, 19.1, 15.7.

FTIR (CH_2Cl_2): ν_{max} 3071.8, 2924.2, 2856.2, 1643.6 cm^{-1}.

(+) HRESIMS *m*/*z* 342.2218 $[M + H]^+$ (calcd for $C_{22}H_{29}FNO$, 342.2233).

Compound **92**

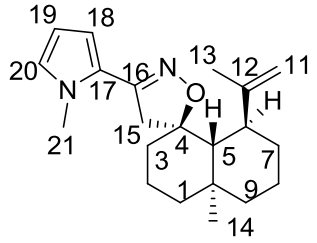

Compound **92** was synthesized according to the general procedure and the product fraction purified using a semi-prep phenyl hexyl HPLC column (Isocratic, 90:10 MeOH:H_2O, 2.5 mL/min) and was the first compound to elute (yield 5.5 %).

^{1}H NMR (600 MHz, $CDCl_3$) δ 6.70 (m, 1H), 6.30 (m, 1H), 6.16 – 6.08 (m, 1H), 4.34 (s, 2H), 3.83 (s, 3H), 3.12 (d, *J* = 15.9 Hz, 1H), 2.73 (d, *J* = 15.8 Hz, 1H), 2.34 (ddd, *J* = 4.1, 10.8 Hz, 10.8, 1H), 1.83 (d, *J* = 11.1 Hz, 1H), 1.77 (m, 1H), 1.73 (s, 3H), 1.64 – 1.58 (m, 1H), 1.57 (m, 1H), 1.56 – 1.53 (m, 2H), 1.55 – 1.52 (m, 2H), 1.48-1.52 (m, 1H), 1.39 (m, 1H), 1.37 (d, *J* = 10.8 Hz, 1H), 1.29 – 1.25 (m, 1H), 1.26 (m, 1H), 0.94 (s, 3H).

^{13}C NMR (151 MHz, $CDCl_3$) δ 149.7, 149.7, 126.8, 124.1, 112.6, 109.7, 107.7, 87.7, 50.5, 44.6, 43.4, 42.0, 40.9, 39.7, 37.6, 36.3, 33.9, 21.5, 18.7, 18.5, 18.2.

FTIR (CH_2Cl_2): ν_{max} 3066.7, 2927.3, 2854.6, 1641.4 cm^{-1}

(+) HRESIMS *m*/*z* 327.2420 $[M + H]^+$ (calcd for $C_{21}H_{31}N_2O$, 327.2436).

Compound **93**

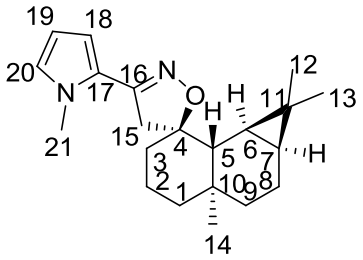

Compound **93** was synthesized according to the general procedure above and the product fraction purified using a semi-prep phenyl hexyl HPLC column (Isocratic, 90:10 MeOH:H_2O, 2.5 mL/min) and was the second compound to elute (yield 6.3 %).

^{1}H NMR (600 MHz, $CDCl_3$) δ 6.75 – 6.71 (m, 1H), 6.36 (dd, *J* = 3.8, 1.7 Hz, 1H), 6.15 (dd, *J* = 3.7, 2.7 Hz, 1H), 3.89 (s, 3H), 3.35 (d, *J* = 16.3 Hz, 1H), 2.96 (d, *J* = 16.3 Hz, 1H), 1.94 – 1.89 (m, 1H), 1.82 (m, 1H), 1.65 – 1.59 (m, 2H), 1.62 – 1.56 (m, 1H), 1.56-1.52 (m, 1H), 1.40 (d, *J* = 5.8 Hz, 1H), 1.34 (m, 1H), 1.17 (m, 1H), 1.11-1.05 (m, 1H), 0.99 (s, 3H), 0.98 (s, 3H), 0.89 (s, 3H), 0.94 – 0.85 (m, 1H), 0.56 (m, 1H), 0.32 (dd, *J* = 9.0, 5.8 Hz, 1H).

^{13}C NMR (151 MHz, $CDCl_3$) δ 150.0, 127.2, 123.8, 113.0, 107.9, 88.3, 44.7, 41.9, 40.0, 39.2, 38.7, 37.8, 33.8, 29.2, 20.6, 19.3, 19.0, 18.5, 17.4, 15.8, 15.5.

FTIR (CH_2Cl_2): ν_{max} 3068.7, 2927.3, 2854.6, 1641.5 cm^{-1}.

(+) HRESIMS *m*/*z* 327.2421 $[M + H]^+$ (calcd for $C_{21}H_{31}N_2O$, 327.2436).

Compound 94

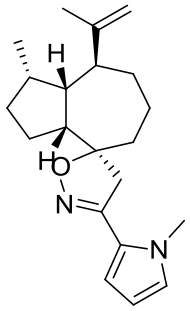

Proposed Structure

Compound **94** was synthesized according to the general procedure and the product fraction was partially purified using a semi-prep phenyl hexyl HPLC column (Isocratic, 90:10 MeOH:H_2O, 2.5 mL/min) and was the third compound to elute. The title compound was isolated as a white solid (Yield 6.1 % (90 % purity)).

(+) HRESIMS *m*/*z* 327.2423 $[M + H]^+$ (calcd for $C_{21}H_{31}N_2O$, 327.2436).

Compound **95**

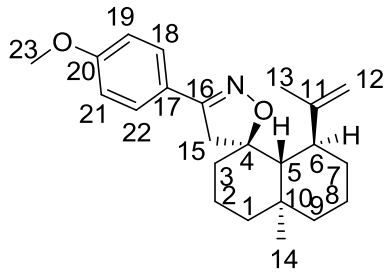

Compound **95** was synthesized according to the general procedure and purified using a semi-prep para-fluoro phenyl HPLC column (Isocratic, 12.5:85.5 H_2O:MeOH, 2.5 mL/min) and was the first compound to elute (yield 7.5 %).

^{1}H NMR (600 MHz, $CDCl_3$) δ 7.58 (m, 2H), 6.90 (m, 2H), 4.35 (d, *J* = 2.3 Hz, 1H) 4.27 (d, *J* = 2.3 Hz, 1H), 3.83 (s, 3H), 3.13 (d, *J* = 16.0 Hz, 1H), 2.72 (d, *J* = 16.0 Hz, 1H), 2.36 (ddd, *J* = 10.8, 10.8, 4.9 Hz, 1H), 1.84 (d, *J* = 11.1 Hz, 1H), 1.82 – 1.78 (m, 1H), 1.74 (s, 3H), 1.58 – 1.55 (m, 1H), 1.57 – 1.55 (m, 2H), 1.58 – 1.55 (m, 1H), 1.56 – 1.53 (m, 2H), 1.41-1.39 (m, 1H), 1.41 – 1.35 (m, 1H), 1.30 – 1.26 (m, 1H), 1.28 – 1.24 (m, 1H), 0.97 (s, 3H).

^{13}C NMR (151 MHz, $CDCl_3$) δ 160.4, 154.8, 149.6, 127.9 (2C), 123.6, 114.1 (2C), 110.2, 89.5, 55.5, 50.7, 44.8, 43.4, 42.0, 39.9, 39.4, 36.3, 34.0, 21.5, 18.7, 18.5, 18.1.

FTIR (CH_2Cl_2): ν_{max} 3065.4, 2927.6, 2854.6, 1641.4 cm^{-1}.

(+) HRESIMS *m*/*z* 354.2406 $[M + H]^+$ (calcd for $C_{23}H_{32}NO_2$, 354.2433).

Compound **96**

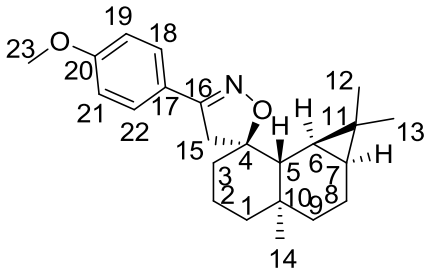

Compound **96** was synthesized according to the general procedure and purified using a semi-prep para-fluoro phenyl HPLC column (Isocratic, 12.5:85.5 H_2O:MeOH, 2.5 mL/min) and was the second compound to elute (85-90 % pure, 8.0 %).

^{13}C NMR (151 MHz, $CDCl_3$) δ 160.3, 155.3, 128.0 (2C), 114.1 (2C), 90.1, 55.5, 44.8, 40.3, 40.0, 39.2, 38.8, 33.9, 29.3, 20.7, 19.3, 19.0, 18.6, 15.8, 15.6.

FTIR (CH_2Cl_2): ν_{max} 3068.4, 2929.5, 2859.0, 1642.1 cm^{-1}.

(+) HRESIMS *m/z* 354.2407 $[M + H]^+$ (calcd for $C_{23}H_{32}NO_2$, 354.2433).

Compound **97**

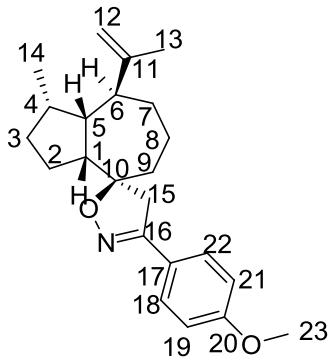

Compound **97** was synthesized according to the general procedure above and purified using a semi-prep para-fluoro phenyl HPLC column (Isocratic, 12.5:85.5 H_2O:MeOH, 2.5 mL/min) and was the third compound to elute (yield 7.2 %).

^{1}H NMR (600 MHz, $CDCl_3$) δ 7.64 (m, 2H), 6.93 (m, 2H), 4.73 (d, *J* = 2.0 Hz, 1H) 4.66 (d, *J* = 2.0 Hz, 1H), 3.84 (s, 3H), 3.15 (s, 2H), 2.79 – 2.69 (m, 1H), 2.31 (ddd, *J* = 12.3, 12.3, 6.5 Hz, 1H), 2.08 – 2.03 (m, 1H), 2.05 – 2.00 (m, 1H), 2.00 – 1.97 (m, 1H), 1.92 – 1.86 (m, 1H), 1.84 – 1.78 (m, 1H), 1.75 (m 1H), 1.70 (s, 3H), 1.66 (m, 1H), 1.57 (m, 1H), 1.51 – 1.47 (m, 1H), 1.48 – 1.44 (m, 1H), 1.46 – 1.41 (m, 1H), 1.37 (m, 1H), 0.83 (d, *J* = 7.2 Hz, 3H).

^{13}C NMR (151 MHz, $CDCl_3$) δ 160.6, 155.2, 149.7, 128.1 (2C), 123.2, 113.9 (2C), 109.7, 92.7, 55.5, 50.1, 47.9, 47.4, 41.5, 39.0, 36.4, 36.4, 33.0, 27.8, 25.1, 19.4, 15.8.

FTIR (CH_2Cl_2): ν_{max} 3067.9, 2924.2, 2857.1, 1643.2 cm^{-1}.

(+) HRESIMS *m*/*z* 354.2403 $[M + H]^+$ (calcd for $C_{23}H_{32}NO_2$, 354.2433).

Compound **98**

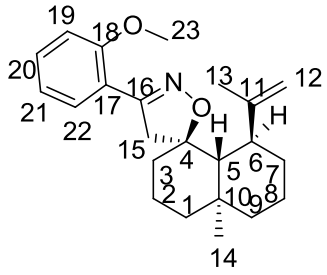

Compound **98** was synthesized according to the general procedure and purified using a semi-prep para-fluoro phenyl HPLC column (Isocratic 84:16 MeOH:H_2O, 2.5 mL/min) and was the first compound to elute (yield 6.3 %).

^{1}H NMR (600 MHz, $CDCl_3$) δ 7.62 (dd, *J* = 7.6, 1.7 Hz, 1H), 7.36 – 7.30 (m, 1H), 6.94 (dd, *J* = 7.5, 7.5 Hz, 1H), 6.91 (d, *J* = 8.3 Hz, 1H), 4.46 (d, *J* = 2.6 Hz, 1H), 4.42 (d, *J* = 2.6 Hz, 1H), 3.86 (s, 3H), 3.25 (d, *J* = 16.9 Hz, 1H), 2.89 (d, *J* = 16.9 Hz, 1H), 2.41-2.39 (m, 1H), 1.85 - 1.82 (m, 1H), 1.83 - 1.81 (m, 1H), 1.75 (s, 3H), 1.60 – 1.54 (m, 2H), 1.58 – 1.54 (m, 2H), 1.52 (m, 1H), 1.53 - 1.51 (m, 2H), 1.39 (m, 1H), 1.39 – 1.34 (m, 1H), 1.27 (m, 1H), 1.25 (m, 1H), 0.94 (s, 3H).

^{13}C NMR (151 MHz, $CDCl_3$) δ 157.3, 155.1, 149.7, 130.4, 129.6, 120.9, 119.6, 111.3, 109.9, 89.4, 55.7, 50.7, 44.7, 43.2, 41.9, 41.7, 39.5, 36.1, 33.8, 21.4, 18.6, 18.5, 18.3.

FTIR (CH_2Cl_2): ν_{max} 3067.2, 2932.2.6, 2866.9, 1640.9 cm^{-1}.

(+) HRESIMS *m*/*z* 354.2407 $[M + H]^+$ (calcd for $C_{23}H_{32}NO_2$, 354.2433).

Compound **99**

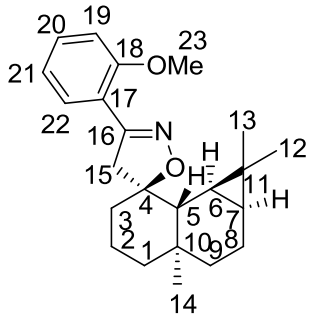

Compound **99** was synthesized according to the general procedure and purified using a semi-prep para-fluoro phenyl HPLC column (Isocratic 84:16 MeOH:H_2O, 2.5 mL/min) and was the second compound to elute (yield 6.1 %).

^{1}H NMR (600 MHz, $CDCl_3$) δ 7.71 (dd, *J* = 7.7, 1.7 Hz, 1H), 7.38 – 7.32 (m, 1H), 6.97 (dd, *J* = 7.5, 7.5 Hz, 1H), 6.93 (d, *J* = 8.3 Hz, 1H), 3.87 (s, 3H), 3.44 (d, *J* = 17.4 Hz, 1H), 3.12 (d, *J* = 17.4 Hz, 1H), 1.98 (m, 1H), 1.87 – 1.76 (m, 1H), 1.65 – 1.59 (m, 2H), 1.59 – 1.53 (m, 1H), 1.58-1.56 (m, 1H), 1.39 (d, *J* = 5.8 Hz, 1H), 1.33 (m, 1H), 1.17 (m, 1H), 1.11 – 1.03 (m, 1H), 1.00 (s, 3H), 0.99 (s, 3H), 0.90 (s, 3H), 0.93 – 0.86 (m, 1H), 0.58 (m, 1H), 0.40 (dd, 8.6, 8.6 Hz, 1H).

^{13}C NMR (151 MHz, $CDCl_3$) δ 157.4, 155.0, 130.9, 129.5, 120.9, 119.5, 111.5, 89.7, 55.9, 45.2, 43.1, 40.3, 39.4, 38.9, 33.7, 29.2, 20.7, 19.5, 19.0, 18.6, 17.7, 15.9, 15.6.

FTIR (CH_2Cl_2): ν_{max} 3064.2, 2925.3, 2856.4, 1640.4 cm^{-1}.

(+) HRESIMS *m*/*z* 354.2406 $[M + H]^+$ (calcd for $C_{23}H_{32}NO_2$, 354.2433).

Compound **100**

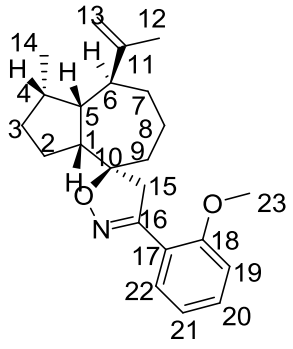

Compound **100** was synthesized according to the general procedure and purified using a semi-preparatory para-fluoro phenyl HPLC column (Isocratic 84:16 MeOH:H_2O, 2.5 mL/min) and was the fourth compound to elute (yield 6.1 %).

^{1}H NMR (600 MHz, $CDCl_3$) δ 7.66 (dd, *J* = 7.1, 1.5 Hz, 1H), 7.35 (dd, *J* = 7.1, 7.1 Hz, 1H), 6.97 (dd, *J* = 7.1, 7.1 Hz, 1H), 6.93 (d, *J* = 7.1 Hz, 1H), 4.71 (d, *J* = 1.8 Hz, 1H), 4.65 (d, *J* = 1.8 Hz, 1H), 3.86 (s, 3H), 3.43 (d, *J* = 17.5 Hz, 1H), 3.20 (d, *J* = 17.5 Hz, 1H), 2.71 (m, 1H), 2.30 (ddd, *J* = 12.3, 12.3, 6.5 Hz, 1H), 2.07 - 2.05 (m, 1H), 2.07 - 2.04 (m, 1H), 2.01 - 1.99 (m, 1H), 1.92 – 1.86 (m, 1H), 1.81 - 1.79 (m, 1H), 1.77 – 1.71 (m, 1H), 1.69 (s, 3H), 1.66 - 1.63 (m, 1H), 1.62 - 1.59 (m, 1H), 1.60 - 1.59 (m, 1H), 1.50 - 48 (m, 1H), 1.43 - 1.42 (m, 1H), 141 - 1.39 (m, 1H), 0.87 (d, *J* = 7.2 Hz, 3H).

^{13}C NMR (151 MHz, $CDCl_3$) δ 158.0, 155.4, 150.4, 130.9, 129.6, 121.1, 119.7, 111.5, 109.7, 92.4, 55.7, 50.2, 48.1, 47.5, 41.7, 41.6, 36.8, 36.6, 33.2, 27.9, 25.0, 19.3, 15.4.

FTIR (CH_2Cl_2): ν_{max} 3069.0, 2924.5, 2856.0, 1643.8 cm^{-1}.

(+) HRESIMS *m*/*z* 354.2403 $[M + H]^+$ (calcd for $C_{23}H_{32}NO_2$, 354.2433).

Compound **101**

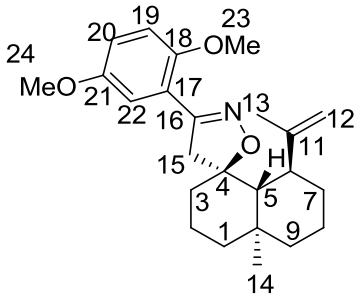

Compound **101** was synthesized according to the general procedure and the product fraction purified using para-fluoro phenyl semi-preparatory HPLC column (Isocratic 82:18 MeOH:H_2O) and was the fourth compound to elute (yield 3.7 %).

^{1}H NMR (600 MHz, $CDCl_3$) δ 7.30 – 7.22 (m, 1H), 6.94 – 6.86 (m, 1H), 6.92 – 6.82 (m, 1H), 4.48 (d, *J* = 2.4, 1H), 4.45 (d, *J* = 2.4, 1H), 3.83 (s, 3H), 3.79 (s, 3H), 3.27 (d, *J* = 16.9 Hz, 1H), 2.90 (d, *J* = 17.0 Hz, 1H), 2.41 (ddd, *J* = 10.9, 10.9, 5.1 Hz, 1H), 1.87-1.84 (m, 1H), 1.87-1.83 (m, 1H), 1.76 (s, 3H), 1.66 - 1.62 (m, 1H), 1.62 – 1.54 (m, 2H), 1.61 - 1.57 (m, 2H), 1.57 – 1.52 (m, 1H), 1.56 – 1.52 (m, 1H), 1.42 - 1.40 (m, 1H), 1.40 - 1.36 (m, 1H), 1.31 - 1.27 (m, 1H), 1.27 - 1.25 (m, 1H), 0.95 (s, 3H).

^{13}C NMR (151 MHz, $CDCl_3$) δ 155.2, 153.4, 151.4, 149.5, 120.8, 116.8, 113.7, 113.1, 110.1, 89.3, 56.4, 55.7, 50.6, 44.5, 43.4, 42.0, 41.5, 39.6, 36.0, 34.0, 21.2, 18.5, 18.4, 17.9.

FTIR (CH_2Cl_2): ν_{max} 3066.8, 2927.9, 2854.5, 1630.4 cm^{-1}.

(+) HRESIMS *m*/*z* 384.2533 $[M + H]^+$ (calcd for $C_{24}H_{34}NO_3$, 384.2538).

Compound **102**

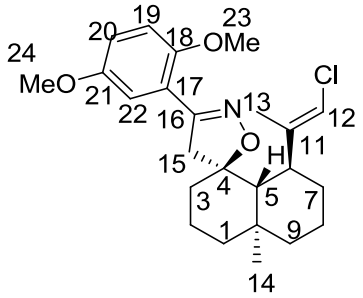

Compound **102** was synthesized according to the general procedure and the product fraction purified using para-fluoro phenyl semi-preparatory HPLC column (82:18 MeOH:H_2O) and was the first compound to elute (yield 6.2 %).

^{1}H NMR (600 MHz, $CDCl_3$) δ 7.29 (d, *J* = 3.1 Hz, 1H), 6.90 (dd, *J* = 9.0, 3.1 Hz, 1H), 6.85 (d, *J* = 9.0 Hz, 1H), 5.57 (s, 1H), 3.81 (s, 3H), 3.79 (s, 3H), 3.08 (d, *J* = 17.2 Hz, 1H), 3.04 (d, *J* = 17.2 Hz, 1H), 2.36 – 2.29 (m, 1H), 1.87 (d, *J* = 8.1 Hz, 1H), 1.85 (d, *J* = 11.1 Hz, 1H), 1.76 (d, *J* = 1.1 Hz, 3H), 1.62 - 1.59 (m, 1H), 1.61 – 1.55 (m, 2H), 1.58 - 1.54 (m, 1H), 1.56 – 1.53 (m, 2H), 1.56 – 1.49 (m, 1H), 1.42 – 1.37 (m, 1H), 1.39 – 1.35 (m, 1H), 1.29 – 1.24 (m, 1H), 1.29 - 1.23 (m, 1H), 0.92 (s, 3H).

^{13}C NMR (151 MHz, $CDCl_3$) δ 154.8, 154.0, 151.0, 142.5, 120.1, 117.3, 113.4, 112.8, 110.5, 88.9, 56.2, 55.6, 50.7, 43.0, 42.8, 41.6, 41.3, 39.6, 35.9, 33.1, 20.9, 18.1, 18.0, 13.7.

FTIR (CH_2Cl_2): ν_{max} 3066.1, 2928.8, 2855.3, 1643.3 cm^{-1}.

(+) HRESIMS *m*/*z* 418.2141 $[M + H]^+$ (calcd for $C_{24}H_{33}ClNO_3$, 418.2149).

Compound **103**

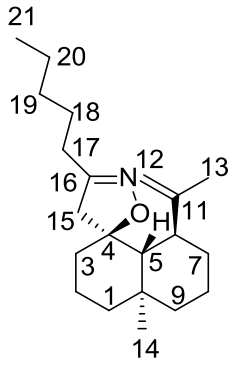

Compound **103** was synthesized according to the general procedure and the product fraction purified using a silica semi-prep HPLC column (96:4 hexanes:ethyl acetate) and was the second compound to elute (yield 5.4 %).

^{1}H NMR (600 MHz, MeOD) δ 4.46 (d, *J* = 2.1 Hz, 1H), 4.35 (d, *J* = 2.1 Hz, 1H), 2.87 (d, *J* = 16.9 Hz, 1H), 2.49 (d, *J* = 16.9 Hz, 1H), 2.39 (m, 1H), 2.27 (t, *J* = 7.6 Hz, 2H), 1.74 (d, *J* = 11.1 Hz, 1H), 1.71 – 1.68 (m, 1H), 1.66 (s, 3H), 1.67 – 1.64 (m, 1H), 1.63 – 1.59 (m, 1H), 1.58 – 1.50 (m, 2H), 1.56 - 1.53 (m, 1H), 1.56 - 1.52 (m, 2H), 1.51 – 1.47 (m, 1H), 1.44 – 1.39 (m, 1H), 1.40 - 1.36 (m, 1H), 1.38 – 1.34 (m, 1H), 1.37 – 1.34 (m, 2H), 1.36 - 1.30 (m, 2H), 1.30 – 1.24 (m, 1H), 1.27 – 1.22 (m, 1H), 0.93 (s, 3H), 0.91 (t, *J* = 7.1 Hz, 3H).

^{13}C NMR (151 MHz, MeOD) δ160.5, 150.8, 110.3, 89.5, 51.8, 45.8, 44.4, 43.0, 42.1, 40.8, 37.1, 35.1, 32.6, 28.9, 27.2, 23.3, 22.4, 19.2, 18.8, 18.3, 14.3.

FTIR (CH_2Cl_2): ν_{max} 3066.3, 2925.7, 2855.6, 1640.2 cm^{-1}.

(+) HRESIMS *m*/*z* 318.2795 $[M + H]^+$ (calcd for $C_{21}H_{36}NO$, 318.2797).

Compound **104**

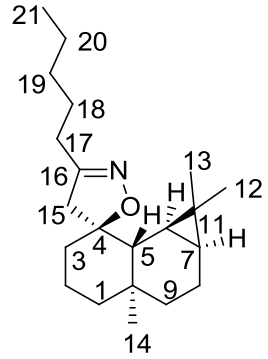

Compound **104** was synthesized according to the general procedure and the product fraction purified using a silica semi-prep HPLC column (96:4 hexanes:ethyl acetate) and was the third compound to elute (yield 6.5 %).

^{1}H NMR (600 MHz, MeOD) δ 3.04 (d, *J* = 17.5 Hz, 1H), 2.73 (d, *J* = 17.5 Hz, 1H), 2.33 (t, *J* = 7.4 Hz, 2H), 1.91 – 1.83 (m, 1H), 1.87 – 1.80 (m, 1H), 1.72 – 1.63 (m, 1H), 1.61 – 1.58 (m, 1H), 1.61 - 1.56 (m, 2H), 1.60 - 1.55 (m, 1H), 1.49 – 1.40 (m, 1H), 1.39 – 1.33 (m, 2H), 1.34 - 1.32 (m,1H), 1.33 – 1.28 (m, 2H), 1.31 – 1.28 (m, 1H), 1.21 – 1.14 (m, 1H), 1.05 (m, 1H), 0.98 (s, 3H), 0.97 (s, 3H), 0.94 – 0.87 (m, 3H), 0.89 (s 3H), 0.90 – 0.87 (m, 1H), 0.61 (dd, *J* = 8.6, 8.6 Hz, 1H), 0.31 (m, 1H).

^{13}C NMR (151 MHz, MeOD) δ 160.6, 90.1, 46.1, 43.1, 41.0, 40.1, 39.9, 34.8, 32.4, 29.5, 28.7, 27.0, 23.3, 21.9, 20.1, 20.0, 18.8, 18.1, 16.5, 15.7, 14.3.

FTIR (CH_2Cl_2): ν_{max} 3046.9, 2922.9, 2854.5, 1640.4 cm^{-1}.

(+) HRESIMS *m*/*z* 318.2796 $[M + H]^+$ (calcd for $C_{21}H_{36}NO$, 318.2797).

Compound **105**

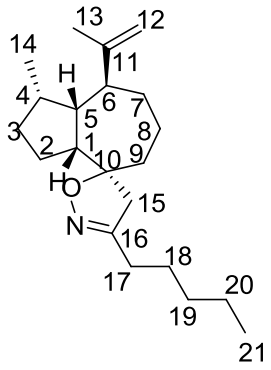

Compound **105** was synthesized according to the general procedure and the product fraction purified using Silica Semi-Prep HPLC column (96:4 hexanes:ethyl acetate) and was the fourth compound to elute (yield 4.8 %).

^{1}H NMR (600 MHz, MeOD) δ 4.71 (d, *J* = 1.3 Hz, 1H), 4.64 (d, *J* = 1.3 Hz, 1H), 2.93 (d, *J* = 17.6 Hz, 1H), 2.83 (d, *J* = 17.6 Hz, 1H), 2.67 – 2.58 (m, 1H), 2.37 – 2.32 (m, 1H), 2.37 – 2.28 (m, 1H), 2.04 (dt, *J* = 13.5, 6.8 Hz, 1H), 1.92 - 1.89 (m, 1H), 1.90 – 1.87 (m, 1H), 1.90 - 1.85 (m, 1H), 1.80 – 1.74 (m, 1H), 1.68 (s, 3H), 1.67 – 1.62 (m, 1H), 1.62 – 1.59 (m, 1H),1.61 - 1.56 (m, 1H), 1.61 - 1.56 (m, 1H), 1.53-1.49 (m, 1H), 1.46 – 1.41 (m, 1H), 1.46 - 1.39 (m, 2H), 1.40 - 36 (m, 1H), 1.38 - 1.34 (m, 2H), 1.37 – 1.32 (m, 2H), 0.92 (t, *J* = 7.0 Hz, 3H), 0.84 (d, *J* = 7.2 Hz, 3H).

^{13}C NMR (151 MHz, MeOD) δ 160.8, 151.5, 110.2, 92.6, 51.1, 49.0, 48.4, 42.8, 41.6, 37.7, 37.6, 33.8, 32.5, 28.8, 28.7, 27.1, 25.7, 23.3, 19.2, 16.0, 14.3.

FTIR (CH_2Cl_2): ν_{max} 3056.9, 2926.9, 2860.0, 1642.7 cm^{-1}.

(+) HRESIMS *m*/*z* 318.2801 $[M + H]^+$ (calcd for $C_{21}H_{36}NO$, 318.2797).

Compound **106**

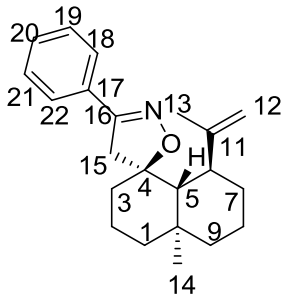

Compound **106** was synthesized according to the general procedure. The product fraction was purified using phenyl hexyl semi-prep HPLC column (Isocratic 75:25 ACN: H_2O) and was isolated as a white solid (yield 8.5 %).

^{1}H NMR (600 MHz, MeOD) δ 7.63 – 7.60 (m, 2H), 7.42 – 7.37 (m, 2H), 7.40 – 7.37 (m, 1H), 4.35 (d, *J* = 2.3 Hz, 1H), 4.27 (d, *J* = 2.3 Hz, 1H), 3.23 (d, *J* = 16.6 Hz, 1H), 2.94 (d, *J* = 16.6 Hz, 1H), 2.45 (ddd, *J* = 11.0, 11.0 4.3 Hz, 1H), 1.83 (d, *J* = 11.1 Hz, 1H), 1.80 – 1.75 (m, 1H), 1.69 (s, 3H), 1.74 – 1.64 (m, 1H), 1.71 – 1.64 (m, 1H), 1.60 – 1.52 (m, 2H), 1.58 – 1.48 (m, 1H), 1.56 – 1.51 (m, 1H), 1.55 – 1.51 (m, 1H), 1.43 – 1.38 (m, 1H), 1.41 – 1.37 (m, 1H), 1.32 – 1.25 (m, 1H), 1.30 – 1.23 (m, 1H), 1.01 (s, 3H).

^{13}C NMR (151 MHz, MeOD) δ 157.8, 150.5, 130.8, 129.7 (2C), 127.4 (2C), 110.7, 91.1, 69.1, 51.9, 45.7, 44.4, 42.9, 40.9, 40.2, 37.2, 35.0, 22.3, 19.2, 18.9, 18.4.

FTIR (CH_2Cl_2): ν_{max} 3066.0, 2925.4, 2853.8, 1641.1 cm^{-1}.

(+) HRESIMS *m*/*z* 324.2323 $[M + H]^+$ (calcd for $C_{22}H_{30}NO$, 324.2327).

Compound **107**

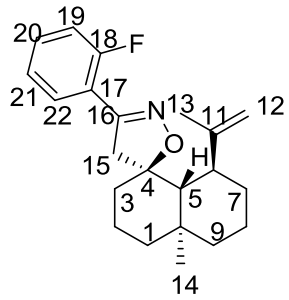

Compound **107** was synthesized according to the general procedure and the product fraction purified using silica gel semi-prep HPLC column (99:1, hexanes:ethyl acetate) and was the fourth compound to elute (yield 7.1 %).

^{1}H NMR (600 MHz, MeOD) δ 7.66 (td, *J* = 7.6, 1.6 Hz, 1H), 7.47 – 7.39 (m, 1H), 7.21 (td, *J* = 7.7, 1.0 Hz, 1H), 7.20 – 7.16 (m, 1H), 4.44 (d, *J* = 2.1 Hz, 1H), 4.32 (d, *J* = 2.1 Hz, 1H), 3.31 (d, *J* = 17.0 Hz, 1H), 2.99 (d, *J* = 17.0 Hz, 1H), 2.47 (ddd, *J* = 10.8, 10.8, 4.3 Hz, 1H), 1.86 (d, *J* = 11.1 Hz, 1H), 1.84 – 1.78 (m, 1H), 1.71 (s, 3H), 1.70 – 1.66 (m, 1H), 1.69 – 1.65 (m, 1H), 1.60-1.55 (m, 1H), 1.58-1.54 (m, 2H), 1.56-1.52 (m, 1H), 1.55 – 1.50 (m, 1H), 1.44 – 1.39 (m, 1H), 1.43 – 1.38 (m, 1H), 1.34 – 1.28 (m, 1H), 1.32-1.28 (m, 1H), 1.00 (s, 3H).

^{13}C NMR (151 MHz, MeOD) δ 161.5, 154.2, 150.6, 132.7, 130.2, 125.6, 118.2, 117.4, 110.7, 91.2, 51.9, 45.8, 44.4, 42.9, 41.9, 40.8, 37.2, 35.1, 22.4, 19.1, 18.9, 18.3.

FTIR (CH_2Cl_2): ν_{max} 3066.1, 2921.9, 2852.6, 1640.0 cm^{-1}.

(+) HRESIMS *m*/*z* 342.2242 $[M + H]^+$ (calcd for $C_{22}H_{29}FNO$, 342.2233).

Compound **108**

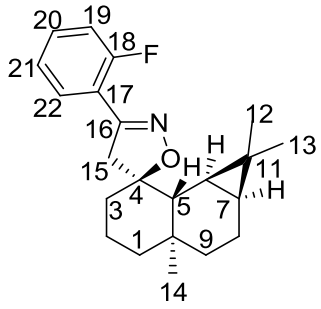

Compound **108** was synthesized according to the general procedure and the product fraction purified using a silica semi-prep HPLC column (99:1, hexanes:ethyl acetate) and was the third compound to elute (yield 3.5 %).

^{1}H NMR (600 MHz, MeOD) δ 7.74 (m, 1H), 7.50 – 7.41 (m, 1H), 7.25 – 7.22 (m, 1H), 7.22 – 7.17 (m, 1H), 3.48 (d, *J* = 17.3 Hz, 1H), 3.22 (d, *J* = 17.3 Hz, 1H), 1.99 – 1.95 (m, 1H) 1.79 – 1.69 (m, 1H), 1.66-1.59 (m, 1H), 1.60-1.52 (m, 1H), 1.42 (d, *J* = 5.9 Hz, 1H), 1.39 – 1.35 (m, 1H), 1.31-1.23 (m, 1H), 1.25 – 1.17 (m, 1H), 1.16 – 1.07 (m, 2H), 1.00 (s, 3H), 0.99 (s, 3H), 0.99-0.94 (m, 1H), 0.96 (s, 3H), , 0.66-0.61 (m, 1H), 0.39 (d, *J* = 6.0 Hz, 1H).

^{13}C NMR (151 MHz, MeOD) δ 159.3, 152.8, 131.4, 128.9, 124.4, 117.5, 116.3, 90.3, 44.6, 41.1, 39.8, 38.6, 38.5, 33.6, 29.2, 27.9, 20.4, 18.9, 18.6, 17.3, 15.2, 14.1.

FTIR (CH_2Cl_2): ν_{max} 3064.4, 2927.2, 2855.5, 1642.4 cm^{-1}.

(+) HRESIMS *m*/*z* 342.2234 $[M + H]^+$ (calcd for $C_{22}H_{29}FNO$, 342.2233).

General Procedure for Reaction of Gorgonene with NCS and Cs_2CO_3 in TBME

Gorgonene (100 mg, 0.49 mmol) was combined with NCS (150 mg, 1.2 mmol) and/or and Cs_2CO_3 (400 mg, 1.23 mmol) in a solution of TBME (10 mL) and the reaction was stirred at room temperature overnight. Analysis of the resulting solution using TLC and NMR indicated gorgonene was recovered in over 99 % yield.

Procedure for Reaction of Gorgonene with NCS in DCM

Gorgonene (100 mg, 0.49 mmol) was combined with NCS (200 mg, 1.5 mmol) in a solution of DCM (10 mL) and the reaction was stirred at room temperature overnight. TLC analysis showed no gorgonene left and the presence of two new products. The reaction was extracted with $NaHCO_{3(aq)}$, filtered through a plug of silica and analyzed using NMR and LCMS. The products were partially purified using silica chromatography and appeared as chlorinated derivatives, but did not ionize in the UPLC-HRMS.

Chapter 4 - Semi-Synthesis and Biological Analysis of β-Gorgonene Analogues Accessed through Ozonolysis Product

4.1 Introduction

Many of the natural products used as inspiration for the semi-synthetic compound collection described in this work have aromatic motifs attached to a decalin skeleton by a methylene group (compounds **1-26**, Chapter 1**)**. In the total synthesis developed for some of these natural products, the aromatic group is attached to the decalin skeleton using a nucleophilic addition to a carbonyl group.[178] Carbonyl chemistry is investigated in this chapter as a synthetic means to produce analogues of gorgonene with similar connectivity to aromatic moieties. A carbonyl containing gorgonene analogue also dramatically increases the number and types of transformations that can be performed on the scaffold. Several routes to new gorgonene derivatives were investigated such as aldol, nucleophilic addition and condensation reactions.

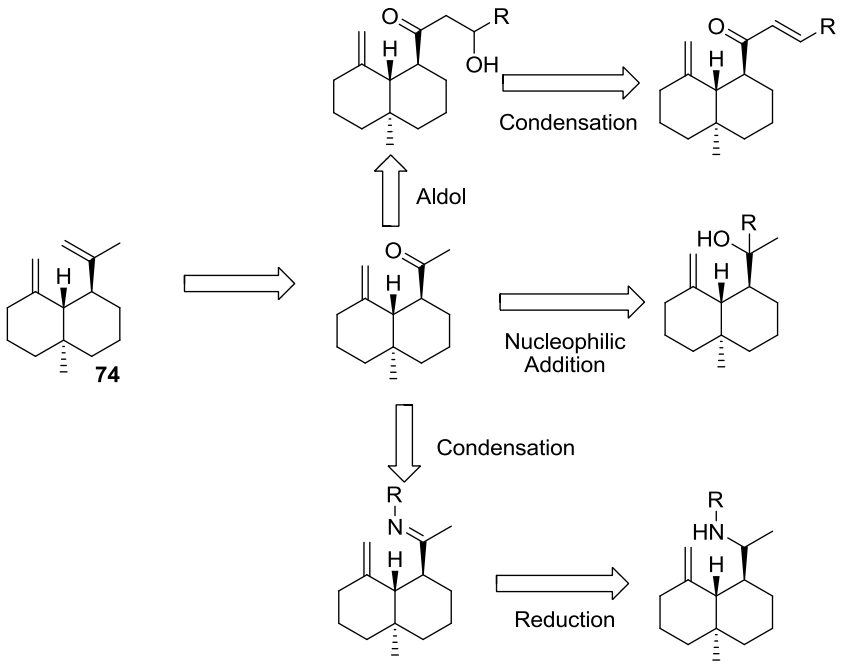

Figure 4.1 - Retrosynthetic Analysis of Diverse Compound Libraries Accessible through Carbonyl Containing Gorgonene Derivative

4.2 Results and Discussion

4.2.1 Ozonolysis of Gorgonene

The two terminal olefin moieties present in gorgonene are useful synthetic handles, however few known reactions will discriminate between the two 1,1-disubstituted alkenes. The absence of heteroatoms on the natural product scaffold makes stereoselectivity difficult to control as well. Traditional methods to direct stereoselectivity such as catalysis, chiral pool reagents and the use of chiral auxiliaries are largely useless in this case. Although reactions producing multiple products can be desirable for the generation of diversity (e.g. glycorandomization[179]), they come at a cost of low individual yield. In the first step of a multiple step synthesis, high yield is crucial.

A non-stereocenter generating reaction limits the number of possible products to regioisomers only. Ozonolysis was identified as a method to install a heteroatom into the scaffold without creating multiple stereoisomers. This maximizes the individual yield of the major product by minimizing the number of possible products.

Ozonolysis is a cyclization reaction between a molecule of ozone and an alkene, resulting in the cleavage of the carbon-carbon double bond and its replacement with two carbonyl groups. The reaction proceeds through the Criegee mechanism[180], shown in Figure 4.2. In the initial step, a 2+3-dipolar cycloaddition between the alkene and a molecule of ozone results in formation of molozonide, which decomposes (retro-cycloaddition) to form a carbonyl compound and a carbonyl oxide (the Criegee intermediate). The two intermediates recombine in another 2+3-dipolar cycloaddition to

form a trioxolane which is converted to the final carbonyl containing products *via* reductive or oxidative workup.

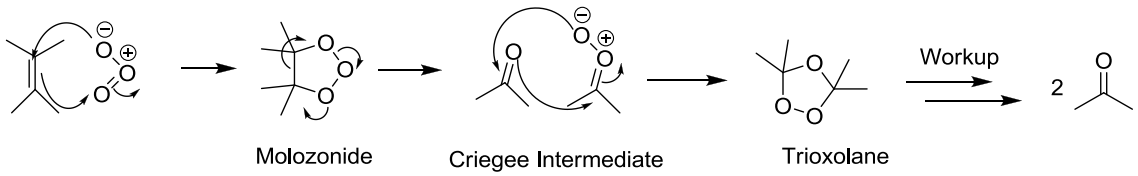

Figure 4.2 - Mechanism of Ozonolysis

Ozone was generated by passing compressed air through an ozonator at 70 V. During optimization, ozone was bubbled at a moderate flow rate through a solution of (+)-β-gorgonene (120 mg) in the solvent (15 mL), length of time and temperature specified in Table 4.1. The end of the reaction was initially monitored by a color change (colorless – violet) of an ozone quench solution containing KI at which time all of the gorgonene was assumed to be reacted. This monitoring method was determined to be ineffective due to the recovery of significant amounts of unreacted starting materials despite dramatic color change of the indicator solution after approximately 10 minutes. TLC and GC were then used to monitor the reaction progression (disappearance of starting materials) which typically took 30-40 min, after which N_2 was bubbled through the solution to displace dissolved O_3. A reducing or oxidizing agent was then added to the reaction and the resulting solution was allowed to come to room temperature and stirred overnight. The product mixture was purified using silica gel chromatography.

The traditional ozonolysis solvent, MeOH was unsuitable for the reaction due to insolubility of starting materials (A, Table 4.1). Triphenylphosphine was found to be inadequate at reducing the trioxolane and was difficult to separate completely from the product mixture (B-C).[181] Reactions B and C resulted in loss of significant product mass

during the chromatography step and this was attributed to incomplete reduction of the trioxolane, which then bound irreversibly to the silica and was lost on the column.

The mild triphenylphosphine reductant was replaced with more powerful acetic acid/zinc dust reductant in the next set of reactions (D-G).[182] The ozonolysis was performed in DCM or hexanes at -30 ^{o}C and 0 ^{o}C (30-60 min) after which a zinc/acetic acid slurry was added and the solution was stirred for 24 h. The product mixture was fractionated using silica gel chromatography and analyzed using GCMS and NMR. It was noted that some of the product fractions showed no signals in the alkene or carbonyl regions of the ^{13}C NMR spectrum indicating some unexpected compounds were being formed. A significant amount of the crude mass, again, was lost upon silica gel purification. Reaction and workup conditions were continually modified to optimize the production of one major ketone-containing product. The work-up was performed at 0 ^{o}C to try to reduce the number of products formed for kinetic reasons. This strategy did not affect the number of products or yield meaningfully (H). Several other workup conditions were used, both reductive (DMS (I, J))[181] and oxidative (H_2SO_4 (N) and H_2O_2(O))[183] but each produced a complex inseparable product mixture.

Several unconventional workup methods were attempted to optimize the reaction for the production of one product and simplify purification. Performing the ozonolysis in an acetone/H_2O solution has been successful in some literature examples to trap formed carbonyl oxides by water which then decompose under the reaction conditions resulting in the direct formation of the carbonyl from the alkene.[184] This approach (K-M) was attempted however unfortunately resulted in a complicated mixture.

Table 4.1 - Optimization of Ozonolysis Reaction Conditions

	Solvent	Temp	Time	Work-up Reagent	Result
A	Methanol	-30 ^{o}C	9 mins	Triphenyl phosphine	>90 % recovery of **73.**
B	Hexanes	-30 ^{o}C	19 mins	Triphenyl phosphine	Complex mixture / difficult to separate from reducing agent.
C	DCM	-30 ^{o}C	30 mins	Triphenyl phosphine	Complex mixture / difficult to separate from reducing agent.
D	DCM	-30 ^{o}C	30 mins	Zn/Acetic acid	Small amount of unreacted **73**. Complex product mixture.
E	DCM	-30 ^{o}C	60 mins	Zn/Acetic acid	Complex product mixture.
F	Hexanes	-30 ^{o}C	60 mins	Zn/Acetic acid	~70% recovery of **73.**
G	Hexanes	0 ^{o}C	60 mins	Zn/Acetic acid	Complex mixture with ~10 % unreacted **73.**
H	Hexanes	0 ^{o}C	60 mins	Zn/Acetic acid (0 ^{o}C)	Fewer Products than **G** workup, still complex mixture.
I	DCM/MeOH	-78 ^{o}C	15 mins	DMS	Complex product mixture. Some unreacted **73.**
J	DCM/MeOH	-78 ^{o}C	30 mins	DMS	Complex product mixture.
K	Acetone:H_2O	0 ^{o}C	8 mins	None	Major product **73.**
L	Acetone:H_2O	0 ^{o}C	20 mins	None	**73** still present in > 50 %. Complex product mixture.
M	Acetone:H_2O	0 ^{o}C	30 mins	None	Complex product mixture.
N	DCM	-78 ^{o}C	15 mins	H_2SO_4	Complex product mixture.
O	DCM	-78 ^{o}C	30 mins	H_2O_2	Complex product mixture.
P	DCM	-78 ^{o}C	30 mins	Triethyl amine	One major product (**118**).
Q	DCM	-78 ^{o}C	15 mins	Triethyl amine	30 % yield of **118.** 50 % recovery of **73**.

Finally, the use of basic work up conditions[185] using TEA was determined to be the most effective method at converting the olefins to the corresponding ketones and the reaction favored one major product, **118**, (P) with yields between 55-75 %. Compound

118 had an *m/z* ion consistent with the molecular formula of the diketone **118** and the product had two resonances in the ^{13}C NMR spectrum typical of a ketone (211.7 and 212.5 ppm, C4 and C11). Further analysis of the 1D and 2D NMR data confirmed the structure was **118** (Figure 4.3).

4.2.1.1 Unexpected Side Products of Ozonolysis

An enol tautomer of the diketone (**119,** Figure 4.3) was also isolated from the product mixture (P) in 11 % yield. The compound had the same molecular formula as **118** according to HRMS and contained two carbons that resonated in the carbonyl region of the ^{13}C spectrum (211.5 and 213.5 ppm). A set of peaks in the olefinic region of the ^{1}H NMR spectrum for the mono-enol (C12, **119,** Table 4.2**)** distinguished it from the dione **118** which instead had a singlet methyl group in the aliphatic region (C12, **118**, Compounds **118** and **119** were separable using flash chromatography and compound **119** was stable in chloroform solution for 24 hours at room temperature. This unusual stability of **119** is attributed to hydrogen bonding of the enolic proton (C11-OH) bridging the two oxygen atoms.

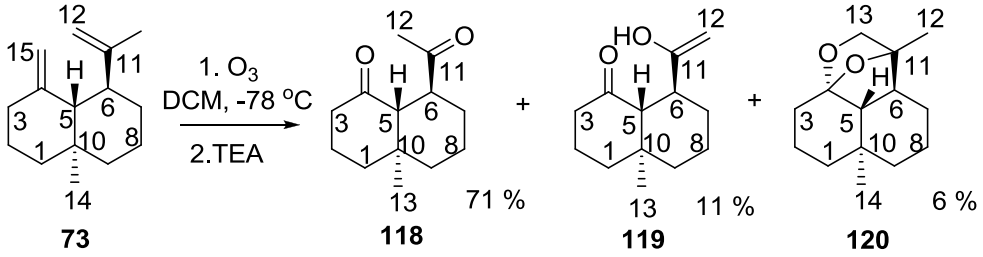

Figure 4.3 - Products of the Ozonolysis of (+)-β-Gorgonene

Table 4.2 - NMR Spectroscopic Data for Compounds 118 and 119 ($CDCl_3$)

118	δC, type	δH (J in Hz)	**119**	δC, type	δH (J in Hz)
1	39.9, CH_2	1.46, m	1	40.5, CH_2	1.69, m
		1.32, m			1.60, m
2	22.6, CH_2	1.92, m	2	22.4, CH_2	1.97, m
		1.85, m			1.9, m
3	41.1, CH_2	2.33, m	3	41.0	2.31, m
		2.24, m	4	211.6	
4	211.7, C		5	59.6	2.77, d (10.9)
5	59.4, CH	2.63, d (11.3)	6	40.8	2.67, ddd (3.8, 12.4, 12.4)
6	45.0, CH	2.69, ddd (12.0, 4.5, 3.0)	7	29.9	1.84, m
7	29.2, CH_2	1.90, m			1.23, m
		1.05, m	8	20.7	1.64, m
8	20.8, CH_2	1.58, m			1.56, m
		1.51, m	9	39.8	1.39, m
9	40.5, CH_2	1.52, m			1.54, m
		1.63, m	10	39.5	
10	39.4, C		11	213.5	
11	212.5, C		12	67.7	4.55, d (18.5)
12	29.7, CH_3	2.22, s			4.35, d (18.5)
13	17.5, CH_3	0.75, s	13	17.5	0.8, s

Data was obtained in $CDCl_3$ solution, δ in PPM relative to solvent signal. Assignments were aided by COSY, HSQC and HMBC experiments.

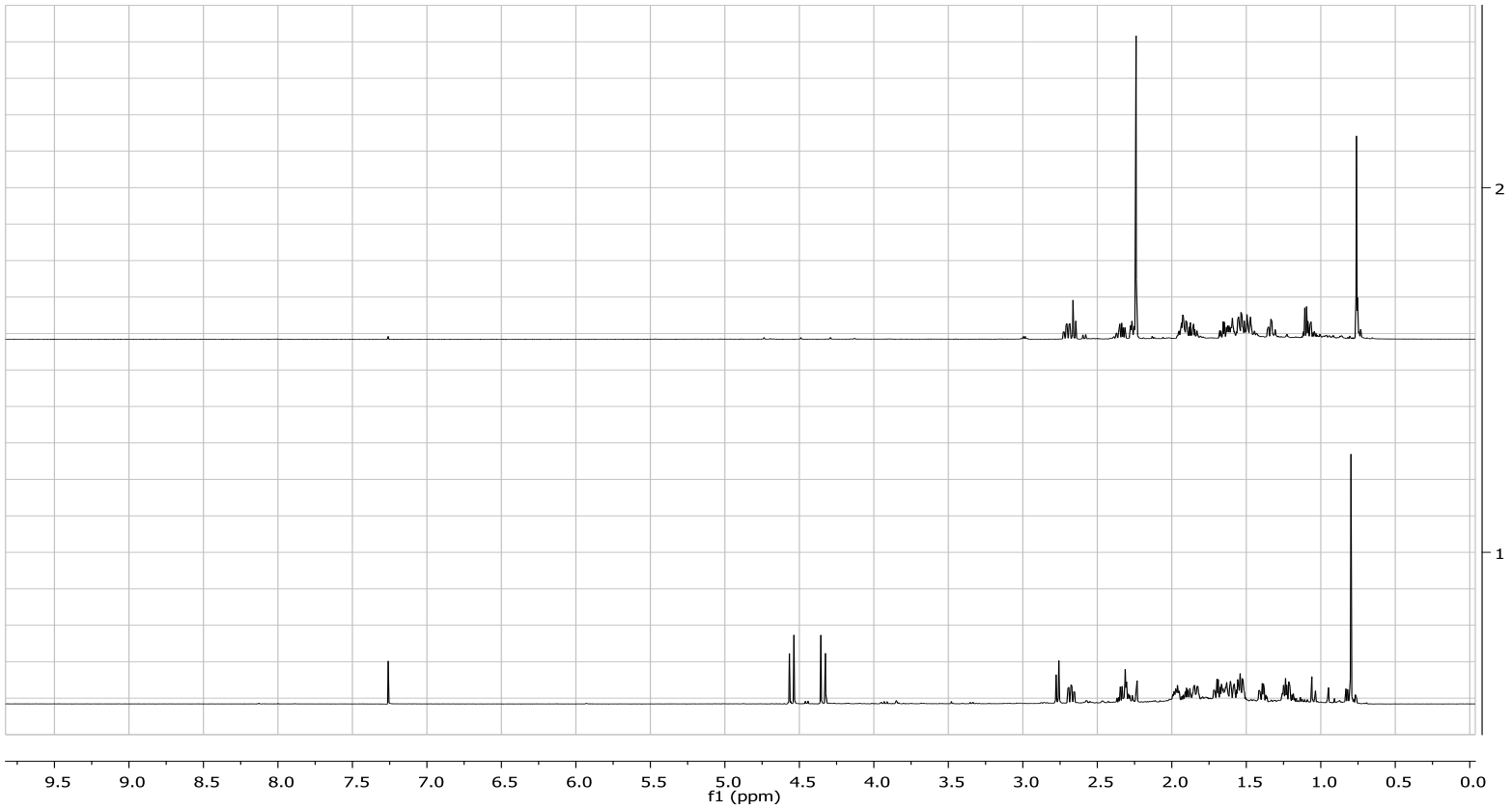

Figure 4.4 - Stack Plot of ^{1}H NMR Spectra (600 MHz, $CDCl_3$) of Semi-synthetic Compounds 118 (Top) and 119 (Bottom) (δ in ppm Relative to Solvent Signal)

Compound **120** was also isolated from the ozonolysis mixture as a colorless solid. It was determined to have a molecular formula of $C_{14}H_{23}O_2$ (M+H) by HRMS (*m/z* 223.1686) indicating it had only lost one carbon and possessed four degrees of unsaturation.

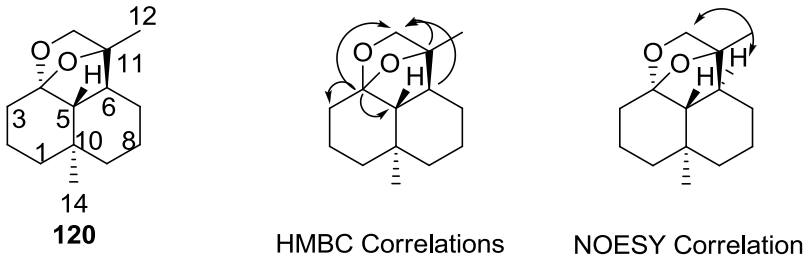

Figure 4.5 - Key NMR Correlations for Structure Elucidation of 120

No NMR resonances in the carbonyl or alkenyl region of the ^{13}C spectrum were present, however, two aliphatic singlet methyl groups were present (C12 and C14), as well as a ketal (96.6 ppm, C4) and two other C-O moieties (69.6 ppm – C13 and 69.7 ppm – C11). HMBC correlations were used to determine the position of the oxygen atom in the new six membered ring (**120,** Figure 4.5) and the stereochemistry indicated at C4 and C11 (Figure 4.5) was supported by NOESY correlations between protons H6 and H13.

Table 4.3 - NMR Spectroscopic Data for the Characterization of 120 ($CDCl_3$)

	δC, type	δH (*J* in Hz)	COSY	HMBC	NOESY
1	41.5, CH_2	1.13, m	2b	14	
		1.42, m		5	
2	19.3, CH_2	1.57, m			
		1.84, m	1a,b; 3b; 2a		14
3	40.1, CH_2	1.62, m			
		1.65, m	2b	2; 1	
4	96.6, C			5; 3b; 13	
5	48.5, CH	1.31, m		14, 1; 9	
6	37.0, CH	1.66, m	7a	13; 12	13
7	24.6, CH_2	1.78, m	6; 8		12
		1.31, m	8		
8	20.3, CH_2	1.53, m	9b; 7a, b	7; 6; 9	
9	43.2, CH_2	1.34, m		14	
		1.08, m	8		
10	34.0, C			5; 14	
11	69.7, C			13	
12	22.1, CH_3	1.06, s		6	5
13	69.6, CH_2	4.00, d (11.2)			3a; 6
		3.26, d (11.2)		6	
14	18.9, CH_3	1.00, s		1; 9; 5	6

Data was obtained in $CDCl_3$ solution, δ in PPM relative to solvent signal. Assignments were aided by COSY, HSQC and HMBC and NOESY experiments. HMBC correlations from the carbon stated to the indicated proton.

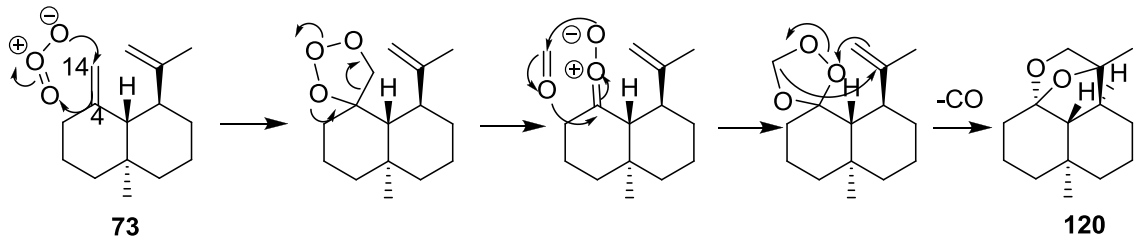

Figure 4.6 - Proposed Mechanism for Formation of 120

The proposed mechanism for the formation of **120** is shown in Figure 4.6. The ozone and the alkene (C4-C14) undergo a 1,3-dipolar cycloaddition as expected, followed by the retrocyclization and the second 1,3-dipolar cycloaddition to give a trioxolane intermediate. The trioxolane is proposed to undergo a reaction with the alkene (C11-C12) as shown in Figure 4.6 and there is a net loss of CO.

Once suitable conditions were developed to produce one major compound in greater than 70 % yield (**118**, P), the reaction time was halved to attempt to produce a mono-ketone derivative of gorgonene keeping all other reaction conditions constant. This resulted in lower yields of the dione **118** and increased recovery of starting materials. Mono-ketone containing derivatives were only detected in very small amounts (Q). This is presumed to be due to the ozone interacting with both olefinic groups simultaneously. This theory is supported by the production of the minor product **120**. The diketone **118** was therefore used as the starting materials for the next step of the semi-syntheses.

4.2.2 Synthesis of Gorgonene Analogues using the Aldol Reaction

The aldol reaction[186] is a staple in organic chemistry, combining two carbonyl-containing compounds to form a β-hydroxy ketone (aldol addition) or an enone (aldol

condensation). One of the carbonyl containing reagents must be enolizeable; that is, it must have an α-hydrogen atom which allows it to be converted to an enol (using an acid) or enolate ion (using a base). The electrons on the nucleophilic α-carbon of the enol(ate) are donated to the electrophilic carbonyl carbon (aldehyde), forming a new carbon-carbon bond. The resulting adduct is a β-hydroxy ketone that can be converted to an enone *via* condensation. The synthesis of a series of natural product derivatives with aromatic motifs attached to the decalin scaffold through a β-hydroxy ketone or an enone linker was achieved using the aldol reaction to combine several aldehydes with dione **118**.

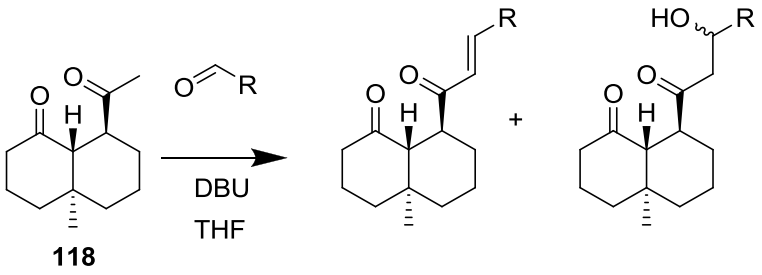

Figure 4.7 - Aldol Reaction Scheme

A solution of dione **118** and N-methyl-pyrrole carboxaldehyde in 1:1 molar ratio in anhydrous THF was treated with a base (NaOH or DBU). No reaction took place at room temperature and so the reaction mixture was heated to reflux temperature which caused the reaction to go to completion in 48 hours. DBU and NaOH both effectively catalyzed the reaction. Two major products (**121** and **122**, Figure 4.8) were isolated from the reaction mixture using DBU. Compound **121** had an *m/z* ion consistent with molecular formula $C_{19}H_{25}NO_2$. The disappearance of the methyl group C12 and HMBC correlations between C11/H13 confirmed the new carbon-carbon double bond was

formed at position C12. The olefin was determined to possess trans-geometry by the large vicinal ^{3}J coupling constant (15.5 Hz) between H12 and H13.

Another product was isolated from the reaction which had a molecular formula of $C_{19}H_{23}NO$ according to HRMS corresponding to a structure with nine degrees of unsaturation. The carbonyl carbon (C11) was slightly shielded in the ^{13}C NMR spectrum suggesting it is conjugated. Only one vinylic proton was present according to ^{1}H NMR other than the pyrrolic hydrogens. 2D NMR was used to assign the structure **122**. One other possible structure would have C4 attached to C13, however a HMBC correlation between C13 and H16 made the proposed structure the most likely. A cyclization had occurred resulting in the formation of a third, five membered ring (**122**, Figure 4.8).

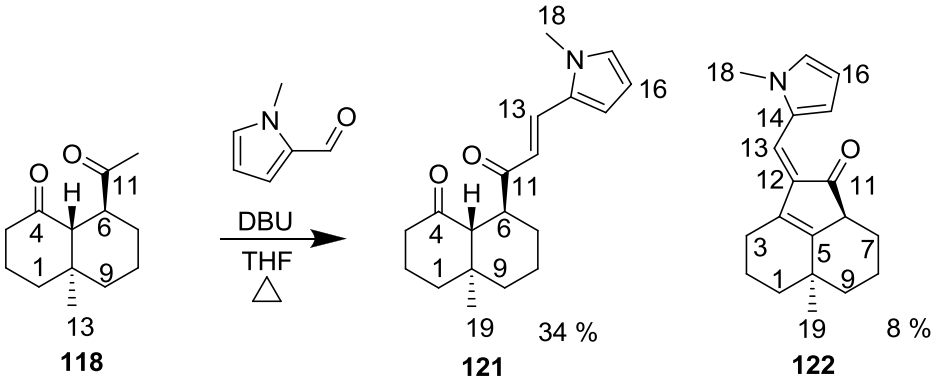

Figure 4.8 - Pyrrole-Containing Aldol Derivatives

In an attempt to optimize the yield of the aldol reaction, a more polar aprotic solvent was used. Highly polar solvents can affect the rate of the reaction by lowering the energy of the charged enolate intermediate.[187] The aldol reaction between *N*-methyl-2-pyrrolecarboxaldehyde and **118** was carried out in DMSO; after 24 hours, TLC indicated complete consumption of **118**. The mixture of products that was formed was

complex and complicated purification, this, combined with low individual yields discouraged the use of DMSO as a reaction solvent.

Table 4.4 - NMR Spectroscopic Data for Compound 122 ($CDCl_3$)

	δC, type	δH (J in Hz)	COSY	HMBC
1	39.4, CH_2	1.74, m	1b	19
		1.43, m	2b	
2	19.2, CH_2	1.74, m		
		1.63, m		
3	21.3, CH_2	2.29, m	2a, b	
		2.17, m	2a,b	
4	136.9, C			
5	174.9, C			19
6	40.7, CH	3.41, m	7a,b	13
7	31.4, CH_2	2.67, m	7b; 8a	
		0.83, m	8a	
8	21.7, CH_2	1.78, m	7b; 9b	
		1.68, m		
9	42.6, CH_2	1.80, m		19
		1.40, m	8a	
10	35.4, C			19; 9b; 1a
11	198.4, C			13
12	134.3, C			13
13	117.6, CH	7.26, s		
14	128.4, C			16; 18
15	109.5, CH	6.24, m		16
16	114.1, CH	6.55, m		13
17	126.1, CH	6.76, m		16; 18
18	34.5, CH_3	3.75, s		
19	24.2, CH_3	1.25, s		

Data was obtained in $CDCl_3$ solution, δ in PPM relative to solvent signal. Assignments were aided by COSY, HSQC and HMBC and NOESY experiments. HMBC correlations from the carbon stated to the indicated proton.

The aldol reaction was carried out with three additional aldehydes; two substituted aromatic aldehydes (anisaldehyde and 2,5-dimethoxybenzaldehyde) and another heteroaromatic aldehyde (furan-2-carbaldehyde) using the conditions established with the 2-formyl-1-methylpyrrole example. The product mixtures varied

slightly, however the enone-containing product resulting from reaction at the less sterically hindered C12 acetyl position was the major product in each example. Each newly formed olefin possessed the expected *E* geometry, indicated by ^{3}J coupling constants greater than 15 Hz between the vinylic hydrogens.

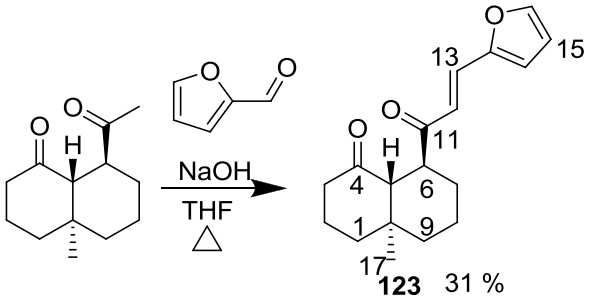

Figure 4.9 - Furan-Containing Enone Derivative

Treatment of **118** and furan-2-carbaldehyde with NaOH in THF and heating resulted in modest yield of the corresponding enone **123** (Figure 4.9). The structure was supported by the correct HRMS $M+H^{+}$ ion and contained two ketones and a trans, 1,2-disubstituted olefin as expected. The alkene hydrogen atoms were HMBC correlated to the ketone carbon C11, confirming the proposed connectivity.

The reaction of **118** with 2,5-dimethoxybenzaldehyde showed unique reactivity at the α-position of endocyclic ketone (C3, Figure 4.10) as indicated from COSY correlations between H3 and H14 (**125**) and produced the only observed β-hydroxy ketone in the collection.

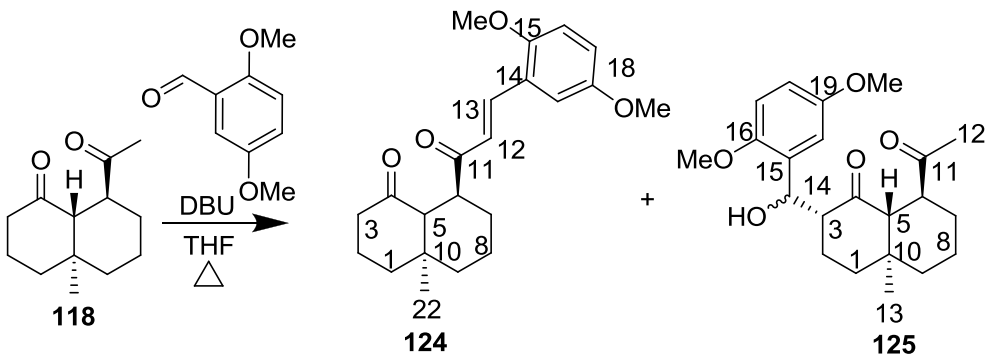

Figure 4.10 - Dimethoxybenzene - Containing Aldol Derivatives

Partial stereochemical assignment of compound **125** was performed using ^{3}J coupling constants between H3 and the adjacent methylene group H2. Coupling constants were calculated as 12.3 Hz (trans: axial-axial) and 6.7 Hz (cis: axial-equatorial) indicating the H3 must be in the axial position. The cyclohexane rings in decalin favor one chair conformation where the fused rings can occupy equatorial positions (C5, C10, Figure 4.11). Therefore the C3 carbon must have R geometry in order for the H3 to occupy an axial position. This is likely due to the steric bulk of the dimethoxybenzene group occupying to the more stable equatorial position. The stereochemistry on the secondary alcohol (C14) could not be determined using NMR spectroscopy due to free rotation about the C3-C14 bond, but could potentially be determined from a Mosher's ester of the compound. Due to the inactivity of this compound in biological assays, the determination of the stereochemistry was not a priority.

The enone derivative (**124**) was also formed, as detected using UPLC/HRMS and NMR but was inseparable from a minor contaminant in the reaction mixture.

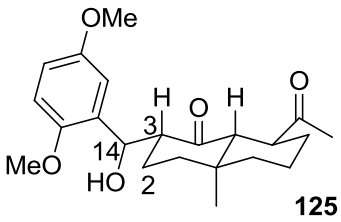

Figure 4.11 - Stable Chair Conformation of 125

Demethylation and oxidation of the dimethoxy-benzene containing products **124** and **125** was attempted by treatment with cerium ammonium nitrate[188], with the intention of producing a quinone containing library member. The reaction resulted in the formation of many products making isolation of the desired compound impossible.

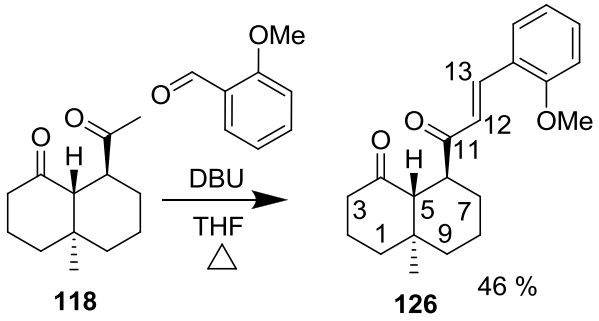

Figure 4.12 - Methoxybenzene-Containing Aldol Derivative

When anisaldehyde was combined with **118** under the aldol conditions, the major product was the *trans*-enone (**126**, Figure 4.12) and the reaction occurred at the expected C12 position. HRMS and 1 and 2D NMR confirmed the proposed structure.

4.2.2.1 Enone vs β-Hydroxy Ketone Formation

β-Hydroxy ketones are readily converted to the corresponding enones *via* dehydration. Due to the elevated temperatures required to produce the β-hydroxy ketones in the described syntheses, the elimination presumably occurs immediately upon formation of the β-hydroxy ketone at C12-13 which explains why β-hydroxy ketone derivatives are not observed at that position. The β-hydroxy ketone **125** did not undergo a condensation because the formed alkene would have increased energy due to steric hinderance (trisubstituted double bond) and strained bond angles (attachment to the ring system).

4.2.3 Synthesis of Amine Containing Gorgonene Derivatives using Condensation and Reductive Amination Reactions

Amines are ubiquitous in nature and in drugs. Nitrogen atoms are present in many drugs and drug candidates. The lone pair of electrons on nitrogen allows it to be protonated, so it may adopt a cationic charge and become more soluble in water. The synthesis of gorgonene derivatives that connect the sesquiterpene fragment with drug-like motifs with an amine linker and synthesis of amine containing derivatives of gorgonene was purpose of the next set of reactions.

4.2.3.1 Synthesis of Oxime Containing Derivatives of Gorgonene

Oximes are part of the imine family of compounds and are synthesized by condensation between an aldehyde or a ketone and hydroxyl amine. Several oxime containing therapeutics exist including the veterinary drug Milbemycin oxime[189]

(Interceptor™, Novartis), a broad spectrum anti-parasitic and Cloximate[190], an oxime ether containing anti-inflammatory drug (Figure 4.13).

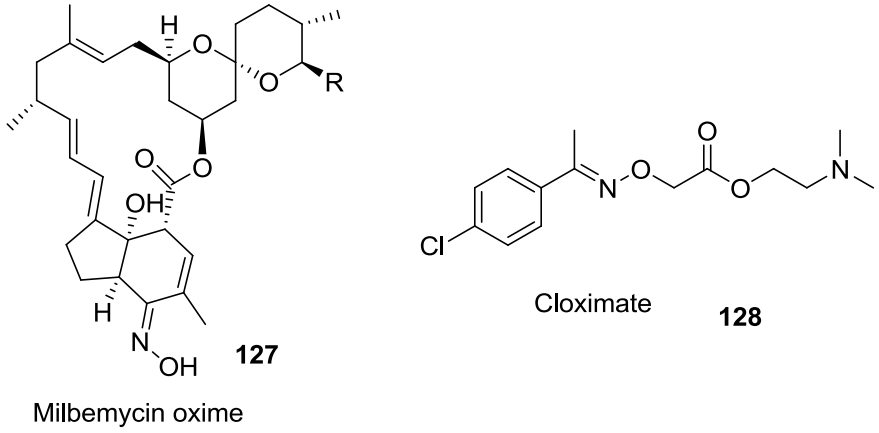

Figure 4.13 - Oxime Containing Drugs Milbemycin Oxime and Cloximate

Synthesis of oxime containing sesquiterpene derivatives was achieved by treatment of **118** with NH_2OH-HCl and K_2CO_3 in a solution of THF/MeOH/H_2O.[191] Two products were isolated from the product mixture that had the expected *m/z* ratio for a mono-oxime ($C_{13}H_{22}NO_2$) Compound **129** is an expected oxime containing product of reaction with the condensation occurring at C11 (162.2 ppm) (Figure 4.14) as determined from its HMBC correlations to H12. Compound **130** is the result of a similar condensation reaction occurring at C11 (159.3 ppm) but is followed by the addition of the oxime oxygen atom to the adjacent carbonyl carbon (C4 – 95.2 ppm) resulting in a new 6-membered oxime ether containing ring (**130**).

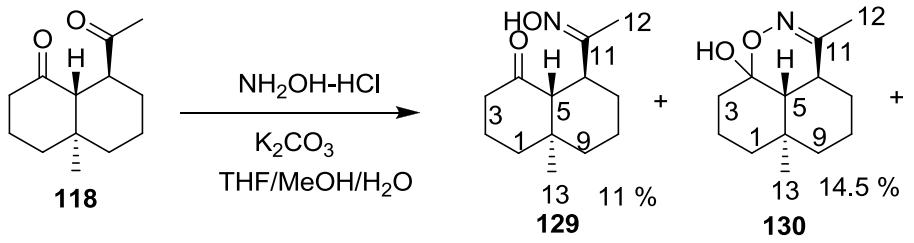

Figure 4.14 - Oxime Synthesis

4.2.3.2 Synthesis of Amine Derivatives of Gorgonene

Amine containing analogues were designed as an addition to the natural product derived library. Reductive amination is a two-step, one-pot reaction between a carbonyl containing compound and a primary or secondary amine. A mild reducing agent, $NaBH(OAc)_3$, which typically reduces imine bonds preferentially over carbonyl groups is used so that the reduction occurs upon formation of the imine. Reductive amination was used as a strategy to combine **118** with aromatic moieties through an amine linker.

Compound **118** was combined with benzylamine and $NaBH(OAc)_3$ in a solution of dry THF and heated to reflux temperature for 72 hours (A, Table 4.5).[192] This resulted in almost complete recovery of starting materials. Acid catalysts are used in condensation and reductive amination reactions to protonate the carbonyl group, increase the electrophilicity of the carbonyl carbon and facilitate the addition of the nitrogen and progression of the condensation. A stoichiometric amount of acetic acid was used to promote the reductive amination, keeping all other conditions from A constant, at room temperature (B, Table 4.5) and reflux temperature (C, Table 4.5), however, the reaction resulted in complete recovery of **118**. The use of the base NaOH was ineffective at catalyzing the reaction as well (D, Table 4.5). The reaction solvent DCE was used, with and without acid catalysis, under an atmosphere of N_2 and with

heating and no amine containing compounds were detected (E-I, Table 4.5). Molecular sieves were introduced combined with heating, polar solvents (THF and ACN) and acid catalysis (J, K, Table 4.5). In both of these examples, complex mixtures were formed including alcohol containing products, indicating that $NaBH(OAc)_3$ is capable of reducing the ketone moiety under these conditions.

Table 4.5 - Toward Reductive Amination Optimization

	Reducing agent	Solvent	Temp	Time	Acid	Result
A	$Na(OAc)_3BH$	THF	Reflux	72 H	None	**118** recovered
B	$Na(OAc)_3BH$	THF	RT	24 H	AcOH (1 eq)	**118** recovered
C	$Na(OAc)_3BH$	THF	Reflux	24 H	AcOH (1 eq)	**118** recovered
D	$Na(OAc)_3BH$	THF	0 ^oC - RT	24 H	NaOH	**118** recovered
E	$Na(OAc)_3BH$	DCE	RT	24 H	AcOH	**118** recovered
F	$Na(OAc)_3BH$	DCE	RT	24 H /N_2	None	**118** recovered
G	$Na(OAc)_3BH$	DCE	RT	24 H / N_2	AcOH (1 eq)	**118** recovered
H	$Na(OAc)_3BH$	DCE	Reflux	24 H / N_2	AcOH (1 eq)	**118** recovered
I	$Na(OAc)_3BH$	DCE	Reflux	24 H	None	**118** recovered
J	$Na(OAc)_3BH$	ACN Mol. Sieves	Reflux	72 H	AcOH	Complex mixture
K	$Na(OAc)_3BH$	THF Mol. Sieves	Reflux	24 H	AcOH	Mixture (alcohols and **131**)
L	$Na(OAc)_3BH$	can	RT	48 H	AcOH	**118** recovered, + mixture of products including **131**
M	$Na(OAc)_3BH$	DMF	RT	96 H	AcOH	Optimized for product **131**
N	$Na(OAc)_3BH$	IPA	RT	96 H	AcOH	Optimized for product **131**
O	$Na(OAc)_3BH$	THF	RT	96 H	TFA	**118** + **131**
P	$Na(OAc)_3BH$	DME	RT	96 H	TFA	**118** + **131**

Reaction K (Table 4.5) produced one amine containing compound, **131**. Compound **131** had an *m/z* of 294.1852 according to HRMS corresponding to the molecular formula $C_{20}H_{23}NO$; a compound with ten degrees of unsaturation. The HMBC spectrum of the new compound **131** indicated the presence of 4 disubstituted olefinic carbon atoms. HMBC correlations between C4 and H13 as well as C11 and H13 suggest that the nitrogen is attached to both C4 and C11 and their chemical shifts are consistent with this (Table 4.6). Other key HMBC correlations for the tetrasubstituted alkenes were C5/H20, C6/H7, C6/H12 and C11/H12. There were only 6 CH_2 groups in the structure (H1, H2, H7, H8, H9 and H13), none corresponding to C3 and no aliphatic CH groups were present in the molecule either. In addition to the presence of 6 aromatic carbons (C15-19), one far downfield carbon resonance at 186.6 ppm, typical of a conjugated ketone, was observed and was HMBC correlated to H2, suggesting it is at position C3. The proposed structure **131** best fit the observed chemical shift data for ^{1}H and ^{13}C as well as the 2D NMR and HRMS data.

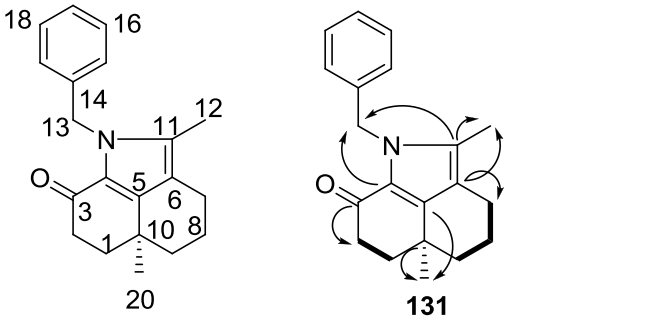

Figure 4.15 - Numbering and Key COSY and HMBC Correlations for 131

Table 4.6 - NMR Spectroscopic Data for Compound 131 ($CDCl_3$)

	δC, type	δH (J in Hz)	COSY	HMBC
1	40.1, CH_2	1.88, m	2a,b	20
		1.83, m		
2	36.5, CH_2	2.84, m	1a,b	
		2.39, m	1a,b	
3	186.6, C			2a
4	122.5, C			13
5	144.0, C			20
6	115.4, C			7b; 12
7	19.6, CH_2	2.31, m	8a,b; 7b	
		2.53, m	8b; 7a	4; 6; 9; 8
8	19.2, CH_2	1.92, m		
		2.02, m	7a,b; 9a	
9	36.9, CH_2	1.35, m	8b	
		1.72, m		
10	30.9, C			20
11	135.2, C			12; 13
12	10.0, CH_3	2.04, d		6; 11
13	47.8, CH_2	5.7, d (15.9)		15; 19; 14; 11; 17
		5.42, d (15.9)		
14	138.4, C			13; 16; 18
15;19	126.6, CH	7.06, m		17
18, 16	128.5, CH	7.3, m		14; 16; 18
17	126.9, CH	7.23, m		15; 19; 13
20	24.6, CH_3	1.3, s		10; 2; 1; 5

Data was obtained in $CDCl_3$ solution, δ in PPM relative to solvent signal. Assignments were aided by COSY, HSQC and HMBC and NOESY experiments. HMBC correlations from the carbon stated to the indicated proton.

The proposed mechanism for the formation of **131** is shown in Figure 4.16. In the first step a condensation occurs followed by isomerization of the imine bond to the C6-C11 position to form an alkene. The ketone migration from C4 to C3 is proposed to occur through an oxirene intermediate. Oxirenes have been proposed as intermediates in

the Wolff rearrangement as the result of a α-carbonyl carbene (formed from diazoketone).[193, 194] In this case the oxirene may be formed by rearrangement of an enolborane. The hydride H5 must be removed during the reaction, in an oxidative fashion, opposite of what is expected with the reagent used.

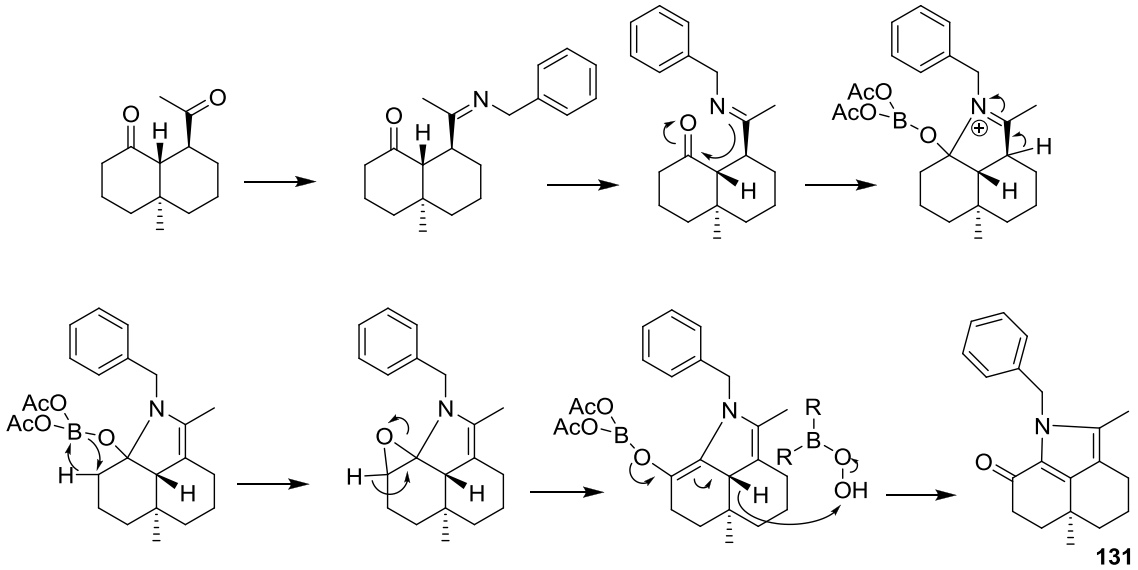

Figure 4.16 - Proposed Mechanism for the Formation of 131

Other polar solvents were used to increase yield, including DMF (M, Table 4.5) and isopropyl alcohol (N, Table 4.5); these reactions did optimize production of **16**, but no other major amine containing products were isolated.

Product fractions from several of the reductive amination reactions (H-K, Table 4.5) were analyzed using HRMS and observed *m/z* ions corresponding to the chemical formula $C_{22}H_{33}NO_2$ $(M+H)^+$ suggested that the acetic acid was being integrated into the molecule structure of some minor products. To prevent this, TFA replaced acetic acid as the catalyst for the reaction (O, P, Table 4.5) and the result of both was the production of compound **131** as the major amine containing product.

Due to the low yields of the reductive amination, the condensation and reduction steps were performed separately to probe which step was problematic in order to effectively optimize the conditions. The condensation reaction was performed under Dean Stark conditions with catalytic toluene sulfonic acid in toluene. The result of the condensation was the recovery of starting materials, suggesting the condensation is not occurring. No further attempts to optimize the reductive amination or produce new amine-containing analogues of gorgonene were made.

4.2.4 Nucleophilic Addition to Dione 118

Nucleophilic addition of an organometallic compound to a carbonyl group is a common method in the synthesis of natural products. Organocuprate, organolithium and Grignard reagents can add to aldehydes and ketones in powerful C-C bond forming reactions. Nucleophilic addition was explored as a route to add desired substructures to ketone containing compound **118**.

The Grignard reagent of benzyl bromide was prepared by treatment with magnesium turnings and an iodine crystal in a solution of anhydrous ether. A solution of compound **118** in ether was then added dropwise to the mixture with cooling. After addition of **118** was complete, the reaction was heated to reflux for 30 minutes. The major product was isolated from the reaction mixture and determined to have a molecular formula $C_{20}H_{28}O_2$ according to HRMS *m/z* ion at 283.2055 (M-OH). The quaternary carbon (C4) resonated at 73.9 and showed a HMBC correlation to H14. Carbonyl C11was HMBC coupled to methyl group protons of C12 and other key HMBC correlations used to assign the structure were between C3/H14 and C5/H14. The elucidation of **132** was completed using 1D- and 2D NMR.

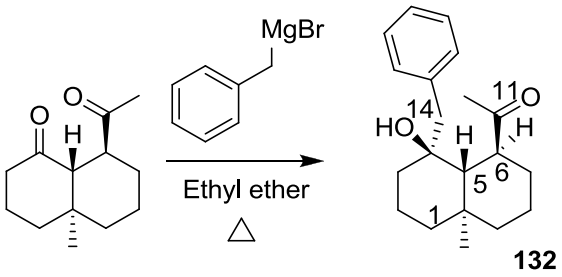

Figure 4.17 - Grignard Reaction of Benzyl Magnesium-Bromide with 118

The stereochemistry at the newly formed tertiary alcohol C4 was determined using NOESY correlations between H14 and H6 (Figure 4.18).

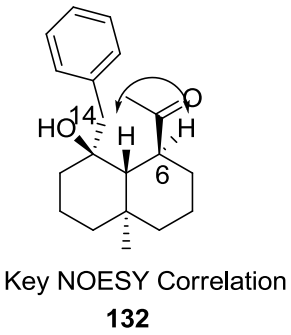

Figure 4.18 - Key NOESY Correlation Supporting Stereochemistry of 132

A Grignard reagent of 1-bromo-2,5-dimethoxybenzene was prepared and combined with **118** in the same manner as described for the preparation of **132**. The resulting mixture contained products with the desired molecular formula ($C_{21}H_{30}O_4$) according to UPLC-HRMS and the mixture was purified using flash chromatography and HPLC to give two major products (**133** and **134**, Figure 4.19).

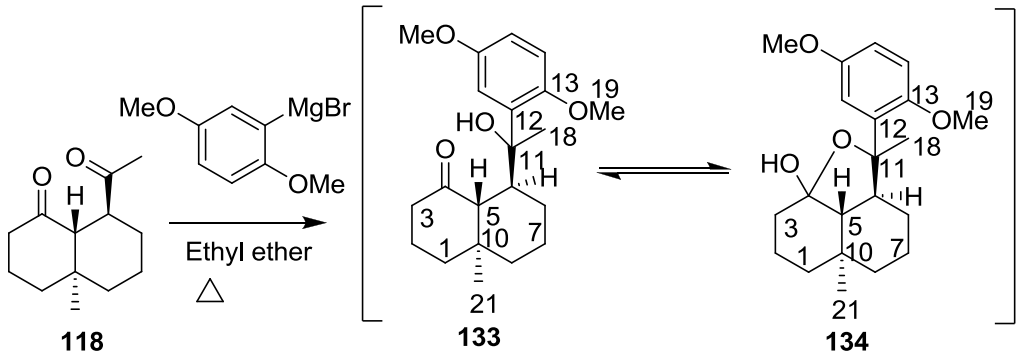

Figure 4.19 - Grignard Reaction with 1-Bromo-2,5-Dimethoxybenzene and 118

The two isolated compounds were analyzed using NMR, having the correct *m/z* ion and ^{1}H NMR data consistent with the products (e.g. aromatic and methoxy carbons, sesquiterpene backbone). After a short time in chloroform solution, however, the two products interconverted to a 50:50 ratio. The reaction was repeated and equilibration between the two products in a number of solvents made purification difficult and full characterization impossible. Compound **133** had HMBC correlations between the methyl hydrogens on C18 and several of the aromatic carbon atoms suggesting the regioselectivity shown in Figure 4.19. The carbonyl carbon C4 is observed in **133** but is replaced with a carbon with a chemical shift typical of a ketal in compound **134** suggesting the equilibrium is between compounds **133** and **134**. This interaction between the two oxygen containing groups (C4 and C11) is common among the reactions (**119**, **122** and **130**) and the ring formation not surprising based on the cyclizations seen under several other reaction conditions discusses in this work. Since compounds **133** and **134** could not be separated the mixture was carried forward for bioassay screening.

4.2.5 Biological Assessment of Compound Collection

4.2.5.1 Drug-Likeness of Compound Collection

One of the goals of the study was to synthesize compounds from gorgonene (**73**) that possess the properties associated with bioavailability. Each compound synthesized was assessed for pharmacological relevancy using 5 measurements: the number of proton donors and acceptors, molecular weight, Log P and rotatable bonds. Reported LogP's are theoretical and calculated using ChemDraw software. Every compound within this chapter fits the criteria for drug-likeness using the standards of Lipinski (Table 4.7).[48]

Table 4.7 - Assessment of Drug-likeness of Compound Collection

	Proton Acceptors	Proton Donors	MW	Log P	Rotatable Bonds
118	2	0	208	2.80	1
119	1	1	208	2.20	1
120	2	0	222	2.90	0
121	2	0	299	3.16	3
122	2	1	299	2.90	1
123	3	0	286	3.00	3
124	4	0	356	4.13	5
125	5	1	374	3.77	5
126	3	0	326	4.26	4
129	3	1	223	3.19	1
130	3	1	223	3.37	0
131	2	2	293	4.04	3
132	2	1	300	4.37	3
133	4	1	346	4.01	4
134	4	1	346	4.26	3

4.2.5.2 Evaluation of the Cytotoxicity of Semi-synthetic Derivatives 118-134

The compounds **118**, **120**, **121**, **122**, **124**, **125**, **126**, **129** and **131** to **134** were tested for cytotoxicity against a human foreskin BJ fibroblast cell line (ATTC CRL-2522) and/or human breast adenocarcinoma cells (ATCC HTB-26) according to the procedure described in Chapter 2. Compounds **119** and **123** were not tested due to stability issues. Compound **126** showed modest activity against the HTB-26 cell line. Due to its structural similarity to **126**, semi-pure **124** was screened for activity against HTB-26 and the 85 % pure mixture did show 99 % growth inhibition at of the cell line at 100 µg/mL, but IC_{50} data was not collected.

Table 4.8 - Evaluation of Cytotoxicity of Ketone Derived Family (IC_{50})

	Cell Line	
Compound Tested	HTB-26	CRL-2522
118	>64 µg/mL	>64 µg/mL
119	NT	NT
120	>64 µg/mL	>64 µg/mL
121	>64 µg/mL	>64 µg/mL
122	>64 µg/mL	>64 µg/mL
123	NT	NT
124	<100 µg/mL	NT
125	>64 µg/mL	>64 µg/mL
126	32-64 µg/mL	>64 µg/mL
129	>64 µg/mL	>64 µg/mL
130	NT	NT
131	>64 µg/mL	>64 µg/mL
132	>64 µg/mL	>64 µg/mL
133/134	>64 µg/mL	>64 µg/mL

4.2.5.3 Evaluation of Compounds 118-134 for Antimicrobial Activity

The family of compounds described in this Chapter were tested for a range of antimicrobial activity in an assay with four microbes representing Gram positive antibiotic resistant bacteria (MRSA, VRE), Gram negative bacteria (*Pseudomonas*

aeruginosa) and fungi (*Candida albicans*). The compounds did not inhibit the growth of these microorganisms at a concentration of 128 µg/mL.

4.2.5.4 Evaluation of Compounds 118-134 for PTP1B Inhibitory Activity

The compounds described in this chapter were tested for inhibition and selectivity for the inhibition of the PTP1B enzyme. All PTP assays were performed by Michel Tremblay`s group at McGill University. The compounds were tested for inhibition of seven protein tyrosine phosphatases from class I (Figure 2.9) including PTP1B at 50 µM.

Three compounds (**121**, **122** and **123**) containing five-membered heteroaromatic rings showed inhibition of the entire family of PTP enzymes. None of the other compounds discussed in this Chapter showed significant inhibition of the PTP1B enzyme at 50 µM. Table 4.9 shows the PTP inhibition of these compounds, calculated as the rate of pNPP de-phosphorylation, relative to the control. The compounds did not show sufficient selectivity for the PTP1B enzyme to be studied further.

Table 4.9 - Results of PTP Inhibition Assay of Compounds 122-124

Enzyme	**Screening Relative Rate, % Control**		
	122	**123**	**124**
PTP1B	0.57	0.67	0.35
SigmaD1D2	0.63	0.68	0.49
SHP-1	0.63	0.68	0.40
MKPX	0.72	0.73	0.65
LAR D1D2	0.96	0.94	1.05
TC-PTP	0.53	0.69	0.29
PRL2 A/S	0.94	0.84	0.94
Papain	Not tested	Negative	Not tested

4.3 Conclusion

A family of novel natural product-like compounds were designed, synthesized and characterized spectroscopically. The compound collection was evaluated biologically using pharmacological standards for drug likeness and screened for activity in bioassays for antimicrobial, anticancer and protein tyrosine phosphatase inhibition. One compound in the library showed moderate anticancer activity against a human breast cancer cell line HTB-26.

4.4 Experimental Section

General Procedure for Optimization of Ozonolysis of Gorgonene - Table 4.1

Ozone (formed by passing compressed air through ozonator at 70 V) was bubbled through a solution of **73** (300 mg, 1.47 mmol) in the indicated solvent (10 mL) at the specified temperature and length of time (Table 4.1). The ozone bubbler was removed from the solution and the workup reagent was added. The solution was allowed to warm to room temperature and stirring continued overnight and then the solvent was removed *in vacuo*. The crude product was purified using silica gel chromatography (gradient: 80:20 hexanes:ethyl acetate – 60:40 hexanes:ethyl acetate) and the fractions were analyzed using UPLC-HRMS and NMR.

Synthesis of Compound **118**, **119** and **120**

Ozone was bubbled through a solution of **73** (300 mg, 1.47 mmol) in dichloromethane (10 mL) at -78 ^{o}C for 1.5 hours until all starting materials were consumed according to TLC. The ozone bubbler was removed from the solution and triethyl amine (500 µL) was added at -78 ^{o}C. The solution was allowed to warm to room temperature and was stirred overnight and then the solvent was removed *in vacuo*. The crude product was purified using silica gel chromatography (gradient: 80:20 hexanes:ethyl acetate – 60:40 hexanes:ethyl acetate) and was further purified using reversed-phase C18 semi-prep HPLC (88:12 MeOH:H_2O) to give the three compounds **118**, **119** and **120**.

Compound **118**

(217 mg, 71.1 % yield).

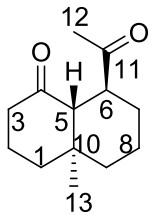

^{1}H NMR (600 MHz, $CDCl_3$) 2.69 (ddd, *J* = 12.0, 4.5, 3.0 Hz, 1H), 2.63 (d, *J* = 11.3 Hz, 1H), 2.33 (m, 1H), 2.24 (m, 1H), 2.22 (s, 3H), 1.92 (m, 1H), 1.90 (m, 1H), 1.85 (m, 1H), 1.63 (m, 1H), 1.58 (m, 1H), 1.52 (m, 1H), 1.51 (m, 1H), 1.46 (m, 1H), 1.32 (m, 1H), 1.05 (m, 1H), 0.75 (s, 3H).

^{13}C NMR (151 MHz, $CDCl_3$) 212.4, 211.6, 59.4, 45.0, 41.1, 40.5, 39.9, 39.4, 29.7, 29.2, 22.6, 20.8, 17.5.

FTIR (CH_2Cl_2): ν_{max} 2938.9, 1704.8 cm^{-1}.

(+) HRESIMS *m*/*z* 231.1373 $[M + Na]^+$ (calcd for $C_{13}H_{20}O_2Na$, 231.1361).

Compound **119**

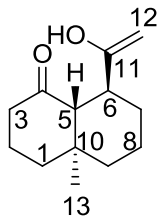

(33.6 mg, 11 % yield).

^{1}H NMR (600 MHz, $CDCl_3$) 4.55 (d, *J* = 18.5 Hz, 1H), 4.35 (d, *J* = 18.5 Hz, 1H), 2.77 (d, *J* = 10.9 Hz, 1H), 2.67 (ddd, *J* = 3.8, 12.4, 12.4 Hz, 1H), 2.31 (m, 2H), 1.97 (m, 1H), 1.97 (m, 1H), 1.84 (m, 1H), 1.69 (m, 1H), 1.64 (m, 1H), 1.60 (m, 1H), 1.54 (m, 1H), 1.39 (m, 1H), 1.23 (m, 1H), 0.80 (s, 3H), 1.90 (m, 1H), 1.56 (m, 1H).

^{13}C NMR (151 MHz, $CDCl_3$) 213.5, 211.6, 67.7, 59.6, 41.0, 40.8, 40.5, 39.8, 39.5, 29.9, 22.4, 20.7, 17.5.

FTIR (CH_2Cl_2): ν_{max} 3365.8, 2931.4, 1708.1 cm^{-1}.

(+) HRESIMS *m*/*z* 209.1530 $[M + H]^+$ (calcd for $C_{13}H_{20}O_2$, 209.1542).

Compound **120**

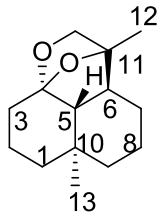

(19.8 mg, 6.0 %).

^{1}H NMR (600 MHz, $CDCl_3$) 4.00 (d, *J* = 11.3 Hz, 1H), 3.26 (d, *J* = 11.3 Hz, 1H), 1.84 (m, 1H), 1.78 (m, 1H) 1.66 (m, 1H), 1.65 (m, 1H), 1.62 (m, 1H), 1.57 (m, 1H) 1.53 (m, 2H), 1.42 (m, 1H), 1.34 (m, 1H), 1.31 (m, 1H), 1.31 (m, 1H), 1.13 (m, 1H), 1.08 (m, 1H), 1.06 (s, 3H), 1.00 (s, 3H).

^{13}C NMR (151 MHz, $CDCl_3$) 96.6, 69.7, 69.6, 48.4, 43.2, 41.5, 40.1, 37.0, 34.0, 24.6, 22.1, 20.3, 19.3, 18.9.

FTIR (CH_2Cl_2): ν_{max} 2924.5 cm^{-1}.

(+) HRESIMS *m*/*z* 223.1686 $[M + H]^+$ (calcd for $C_{14}H_{23}O_2$, 223.1698).

Synthesis of Compound **121** and **122**

All glassware was dried in an oven overnight prior to use. Compound **118** (62 mg, 0.21 mmol) and 1-methyl pyrrole 2-carbaldehyde (34 mg, 0.35 mmol) were dissolved in a solution of dry THF (10 mL) in a dry flask equipped with a condenser and drying tube. NaOH (38 mg) was added as a solid and the mixture was heated to reflux temperature for 24 hours with stirring. The reaction was cooled and diluted with ethyl acetate, washed with 0.1 % HCl (3 x 75 mL) and distilled water (2 x 75 mL) and dried with $MgSO_4$. The solvent was removed *in vacuo* and the crude product was purified using flash chromatography (C18, gradient 50:50 MeOH:H_2O – 100 % MeOH (0.1 % FA)), followed by HPLC purification (phenyl hexyl semi-prep column, isocratic, 92:8 MeOH:H_2O) to give major products **121** and **122**.

Compound **121**

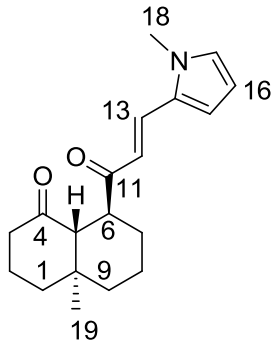

(21 mg, 34 % yield).

^{1}H NMR (600 MHz, $CDCl_3$) δ 7.53 (d, *J* = 15.5 Hz, 1H), 6.75 – 6.73 (m, 1H), 6.75 – 6.72 (m, 1H), 6.64 (d, *J* = 15.5 Hz, 1H), 6.18 – 6.14 (m, 1H), 3.70 (s, 3H), 2.89 – 2.82 (m, 1H), 2.86 – 2.77 (m, 1H), 2.46 – 2.40 (m, 1H), 2.32 – 2.26 (m, 1H), 2.01 – 1.92 (m, 2H), 1.97 – 1.82 (m, 2H), 1.75 – 1.66 (m, 1H), 1.66 – 1.56 (m, 2H), 1.57 – 1.49 (m, 1H), 1.54 – 1.44 (m, 1H), 1.41-1.39 (m, 1H), 0.81 (s, 3H).

^{13}C NMR (151 MHz, $CDCl_3$) δ 210.7, 201.7, 129.2, 128.5, 126.5, 119.7, 111.5, 108.7, 58.4, 43.4, 40.6, 39.9, 39.2, 38.9, 33.6, 29.0, 22.0, 20.1, 16.8.

FTIR (CH_2Cl_2): ν_{max} 3055.5, 2929.5, 1707.1 cm^{-1}.

(+) HRESIMS *m*/*z* 322.1782 $[M + Na]^+$ (calcd for $C_{19}H_{25}NO_2Na$, 322.1783)

Compound **122**

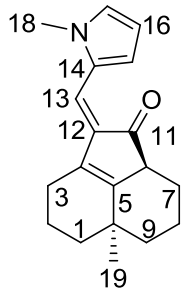

(5 mg, 8 % yield).

^{1}H NMR (600 MHz, $CDCl_3$) δ 7.26 (s, 1H), 6.76 (s, 1H), 6.55 (d, *J* = 3.8 Hz, 1H), 6.26 – 6.23 (m, 1H), 3.75 (s, 3H), 3.42 (m, 1H), 2.69 – 2.61 (m, 1H), 2.29 (m, 1H), 2.19 – 2.11 (m, 1H), 1.84 – 1.75 (m, 1H), 1.79 – 1.73 (m, 1H), 1.74 – 1.65 (m, 1H), 1.73 – 1.62 (m, 1H), 1.70 – 1.61 (m, 1H), 1.69 – 1.57 (m, 1H), 1.46 – 1.37 (m, 1H), 1.46 – 1.33 (m, 1H), 1.24 (s, 3H), 0.87 – 0.78 (m, 1H).

^{13}C NMR (151 MHz, $CDCl_3$) δ 198.4, 174.9, 137.0, 134.4, 128.4, 126.2, 117.7, 114.2, 109.6, 42.7, 40.8, 39.5, 35.5, 34.6, 31.5, 24.3, 21.8, 21.4, 19.3.

FTIR (CH_2Cl_2): ν_{max} 3059.9, 2928.6, 1680.0 cm^{-1}.

(+) HRESIMS *m*/*z* 282.1842 $[M + H]^+$ (calcd for $C_{19}H_{24}NO$, 282.1858)

Synthesis of **123**

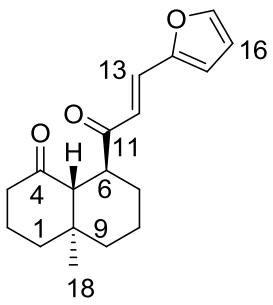

Glassware was dried in an oven overnight. Compound **118** (70.0 mg, 0.34 mmol), was combined with furanaldehyde (40 mg, 0.41 mmol) and NaOH (40 mg, 1.6 mmol) in anhydrous THF (10 mL) in a dry flask equipped with a condenser and a drying tube. The mixture was heated to reflux temperature for 24 hours with stirring. The reaction was allowed to cool, diluted with ethyl acetate and washed with 0.1 % HCl (3 x 75 mL) and distilled water (2 x 75 mL). The solvent was removed *in vacuo* and the crude product was purified using flash chromatography (C18 stationary phase, gradient 50:50 MeOH:H_2O – 100 % MeOH (0.1 % FA) and the product containing fraction was further purified using HPLC (phenyl hexyl semi-prep column, isocratic, 90:10 MeOH: H_2O) to give compound **123** as a white solid (30 mg, 31 % yield).

^{1}H NMR (600 MHz, $CDCl_3$) δ 7.48 (d, *J* = 1.4 Hz, 1H), 7.34 (d, *J* = 15.7 Hz, 1H), 6.76 (d, *J* = 15.7 Hz, 1H), 6.64 (d, *J* = 3.4 Hz, 1H), 6.46 (dd, *J* = 3.4, 1.8 Hz, 1H), 2.96 – 2.90 (m, 1H), 2.83 (d, *J* = 11.0 Hz, 1H), 2.41 (m, 1H), 2.29 (m, 1H), 2.01 – 1.97 (m, 1H), 1.98 – 1.94 (m, 1H), 1.93-1.89 (m, 1H), 1.71 (m, 1H), 1.65 – 1.56 (m, 2H), 1.60 – 1.55 (m, 1H), 1.55 – 1.51 (m, 1H), 1.40 (m, 1H), 1.17 (m, 1H), 0.83 (s, 3H).

^{13}C NMR (151 MHz, $CDCl_3$) δ 210.9, 203.1, 152.3, 144.8, 128.7, 123.5, 115.5, 112.6, 59.4, 43.8, 41.4, 40.8, 40.0, 39.8, 29.8, 22.9, 21.0, 17.7.

FTIR (CH_2Cl_2): ν_{max} 3053.8, 2930.1, 1708.7 cm^{-1}.

(+) HRESIMS *m/z* 309.1464 $[M + Na]^+$ (calcd for $C_{18}H_{22}O_3Na$, 309.1467).

Synthesis of Compound **124** and **125**

All glassware was dried in an oven overnight. Compound **118** (70.0 mg, 0.34 mmol) was combined with 2,5-dimethoxy-1-benzaldehyde (80 mg, 0.481 mmol) and NaOH (40 mg, 1.6 mmol) in anhydrous THF (10 mL) in a dry flask equipped with a condenser and a drying tube. The mixture was heated to reflux temperature for 24 hours with stirring, allowed to cool and diluted with ethyl acetate. The solution was washed with 0.1 % HCl (3 x 75 mL) and distilled water (2 x 75 mL). The solvent was removed *in vacuo* and the crude product was purified using flash chromatography (C18 stationary phase, gradient 50:50 MeOH:H_2O – 100 % MeOH (0.1 % FA) to give compounds **124** and **125**.

Compound **124**

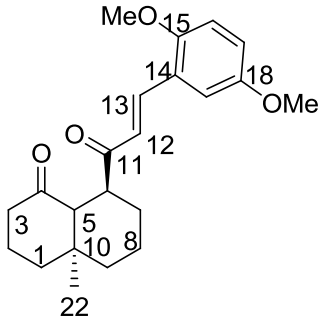

(46 mg, 32 % yield based on 85 % purity).

(+) HRESIMS *m/z* 357.2045 $[M + H]^+$ (calcd for $C_{22}H_{29}O_4$, 357.2066).

FTIR (CH_2Cl_2): ν_{max} 3057.2, 2923.1, 2853.4, 1705.9 cm^{-1}.

Compound **125**

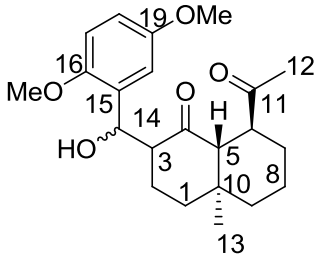

(36 mg, 26 % yield).

^{1}H NMR (600 MHz, $CDCl_3$) δ 7.06 (s, 1H), 6.74 (s, 1H), 6.74 (s, 1H), 5.55 (s, 1H), 3.77 (s, 3H), 3.74 (s, 3H), 3.13 (s, OH, 1H) 2.85 (m, 1H), 2.84 – 2.76 (m, 1H), 2.71 (d, *J* = 11.0 Hz, 1H), 2.32 (s, 3H), 2.03 – 1.96 (m, 1H), 1.98-1.94 (m, 1H), 1.68-1.64 (m, 1H), 1.61-1.55 (m, 1H), 1.60 – 1.55 (m, 2H), 1.50 – 1.45 (m, 1H), 1.44-1.41 (m, 1H), 1.35 – 1.28 (m, 1H), 1.10 (m, 1H), 0.78 (s, 3H).

^{13}C NMR (151 MHz, $CDCl_3$) δ 215.1, 212.6, 153.7, 149.7, 130.6, 113.4, 112.5, 110.9, 65.9, 59.6, 55.9, 55.8, 52.9, 45.3, 40.3, 40.0, 39.9, 29.6, 28.9, 21.8, 20.9, 17.6.

FTIR (CH_2Cl_2): ν_{max} 3521.8, 3063.6, 2925.5, 2853.6, 1701.12 cm^{-1}.

(+) HRESIMS *m*/*z* 397.2013 $[M + Na]^+$ (calcd for $C_{22}H_{30}O_5Na$, 397.1991).

Synthesis of Compound **126**

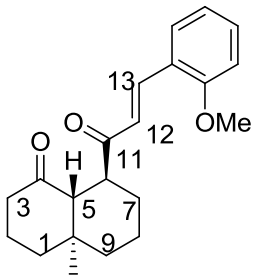

All glassware was dried in an oven overnight. Compound **118** (70.0 mg, 0.34 mmol) was combined with anisaldehyde (60 mg, 0.44 mmol) and NaOH (40 mg, 1.6 mmol) in anhydrous THF (10 mL) in a dry flask equipped with a condenser and a drying tube. The mixture was heated to reflux for 24 hours with stirring. The solution was allowed to cool and diluted with ethyl acetate before being washed with 0.1 % HCl (3 x 75 mL) and distilled water (2 x 75 mL). The solvent was removed *in vacuo* and the crude product was purified using flash chromatography (Diol stationary phase, isocratic, 20:80 ethyl acetate:hexanes) to give compound **126** as a white solid (51 mg, 46 % yield).

^{1}H NMR (600 MHz, $CDCl_3$) 7.92 (d, *J* = 16.2 Hz, 1H), 7.57 (m, 1H), 7.33 (m, 1H), 6.94 (m, 1H), 6.91 (d, *J* = 16.2 Hz, 1H), 6.90 (m, 1H), 3.87 (s, 3H), 3.01 (m, 1H), 2.86 (d, *J* = 10.9 Hz, 1H), 2.42 (ddd, *J* = 7.5, 13.5, 13.5 Hz, 1H), 2.29 (m, 1H), 2.02 (m, 1H), 1.96 (m, 1H), 1.90 (m, 1H), 1.71 (m, 1H), 1.63 (m, 2H), 1.58 (m, 1H), 1.53 (m, 1H), 1.40 (m, 1H), 1.19 (m, 1H), 0.85 (s, 3H).

^{13}C NMR (151 MHz, $CDCl_3$) 211.4, 203.4, 158.7, 137.6, 131.5, 128.9, 126.4, 124.0, 120.8, 111.2, 59.3, 55.6, 43.4, 41.4, 40.8, 40.1, 39.8, 30.0, 22.9, 21.0, 17.8.

FTIR (CH_2Cl_2): ν_{max} 3061.0, 2931.6, 1708.7, 1683.82 cm^{-1}.

(+) HRESIMS *m*/*z* 349.1776 $[M + Na]^+$ (calcd for $C_{21}H_{26}O_3Na$, 349.1780).

General Procedure for Demethylation/Oxidation of 124{{491 Jacob,Peyton. 1976;}}

To a solution of **124** (10 mg, 0.028 mmol) in 1:1 ACN:DMF (2 mL) was added a solution of cerium ammonium nitrate (70 mg, 0.132 mmol) in 1:1 (H_2O:ACN) (2 mL) slowly at room temperature. The mixture was heated to 70 ^oC overnight. The reaction was allowed to cool, diluted with ether (5 mL), washed with brine (2 x 5 mL), dried with $MgSO_4$ and the solvent removed *in vacuo*. The mixture was fractionated using C18 chromatography and analyzed using UPLC-HRMS and NMR spectroscopy.

Synthesis of Compounds **129** and **130**

Compound **118** (90 mg, 0.43 mmol) was combined with hydroxyl amine hydrochloride (167 mg, 2.40 mmol) and K_2CO_3 (332 mg, 2.40 mmol) in solution of THF (5 mL) H_2O (10 mL) and MeOH (10 mL). The reaction was stirred at room temperature overnight at which time it was partitioned between H_2O and ethyl acetate, dried with $MgSO_4$ and the solvent removed *in vacuo*. The crude product was fractionated using C18 flash chromatography (50:50 H_2O:MeOH-100 % MeOH) and the product containing fractions were combined and further purified using HPLC (C18 semi-prep column, isocratic, 70:30 MeOH:H_2O) and **129** was isolated as a white solid (11.4 mg, 12 % yield).

Compound **129**

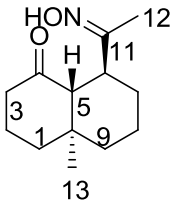

^{1}H NMR (600 MHz, $CDCl_3$) δ 7.83 (bs, 1H), 2.69 (d, *J* = 11.5 Hz, 1H), 2.41 – 2.34 (m, 1H), 2.37 – 2.29 (m, 1H), 2.25 (m, 1H), 1.99 – 1.95 (m, 1H), 1.96 – 1.85 (m, 2H), 1.92 (s, 3H), 1.65 (m, 1H), 1.59 – 1.51 (m, 1H), 1.60 – 1.49 (m, 2H), 1.53 – 1.47 (m, 1H), 1.35 (m, 1H), 1.15 – 1.06 (m, 1H), 0.78 (s, 3H).

^{13}C NMR (151 MHz, $CDCl_3$) δ 211.8, 162.2, 59.9, 42.2, 41.1, 40.9, 40.6, 39.0, 32.0, 23.6, 21.2, 17.4, 14.4.7

FTIR (CH_2Cl_2): ν_{max} 3355.9, 2929.6, 1711.6 (s), 1660.0 (w) cm^{-1}

(+) HRESIMS *m*/*z* 224.1640 $[M + H]^+$ (calcd for $C_{13}H_{22}NO_2$, 224.1651).

Compound **130**

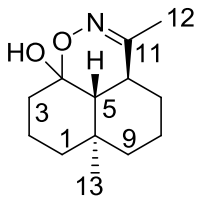

Compound **130** was purified using HPLC (C18 semi-prep column, isocratic 75:25 MeOH:H_2O) and was isolated as a white solid (14.0 mg, 14.5 % yield).

^{1}H NMR (600 MHz, $CDCl_3$) δ 2.44 (bs, OH), 2.20 – 2.12 (m, 1H), 2.13 – 2.07 (m, 1H), 1.89 (s, 3H), 1.86 – 1.82 (m, 1H), 1.83 – 1.77 (m, 1H), 1.67 – 1.63 (m, 1H), 1.66 – 1.59 (m, 2H), 1.62 – 1.55 (m, 1H), 1.52 – 1.46 (m, 1H), 1.40 (m, 1H), 1.34 (m, 1H), 1.18 – 1.10 (m, 1H), 1.14 – 1.08 (m, 1H), 1.08 (m, 1H), 1.01 (s, 3H).

^{13}C NMR (151 MHz, $CDCl_3$) δ 159.3, 95.2, 47.5, 42.0, 40.9, 37.2, 33.1, 29.4, 29.2, 21.4, 19.0, 18.7, 17.7.

FTIR (CH_2Cl_2): ν_{max} 3357.5, 2929.7 cm^{-1}, 1713.5 cm^{-1}.

(+) HRESIMS *m/z* $[M + H]^+$ 224.1634 (calcd for $C_{13}H_{22}NO_2$, 224.1651).

General Procedure for Optimization of Reductive Amination (Table 4.5)

All glassware was dried in an oven overnight, solvents were dried over molecular sieves and starting materials were dried in a desiccator overnight. To solution of **118** (40 mg, 0.19 mmol), benzylamine (100 mg, 0.93 mmol) and $NaBH(OAc)_3$ (100 mg, 0.47 mmol) in the specified solvent (under N_2 where indicated) was added acid,base and/or molecular sieves (if used) the reaction was stirred at the temperature and length of time stated in Table 4.5**.** The solution was then cooled, extracted with distilled water (neutral reaction conditions) 1M HCl (basic reaction conditions) or $NaHCO_{3(aq)}$ (acidic reaction conditions),dried with $MgSO_4$ and the solvent removed *in vacuo*. The reaction mixture was fractionated using silica or C18 flash chromatography before analysis using HRMS and ^1H NMR.

Dean Stark Condensation Reaction Procedure

In a Dean Stark apparatus a solution of **118** (50 mg, 0.24 mmol), benzylamine (25 mg, 0.23 mmol) and toluene sulfonic acid (10 mg, 0.06 mmol) in toluene (25 mL) was heated to reflux temperature for 4 hours. The reaction was then cooled, extracted with distilled water and filtered through a plug of C18 before the solvent was removed *in vacuo* and the product mixture was analyzed using UPLC-HRMS and NMR.

Synthesis of Compound **131**

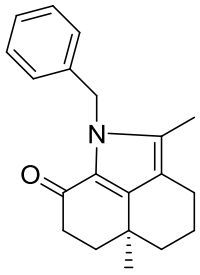

To a solution of **118** (75 mg, 0.36 mmol) and benzyl amine (50 mg, 0.46 mmol) in acetonitrile (3 mL) was added activated molecular sieves and glacial acetic acid (50 µL). The solution was stirred under an atmosphere of N_2 for 48 hours at room temperature and then filtered, diluted with ethyl acetate (15 mL) and washed with $NaHCO_{3(aq)}$ (2 x 15 mL). The solvent was removed *in vacuo* and the product was purified using C18 combiflash (50:50 MeOH:H_2O-100 % MeOH) followed by HPLC purification (phenyl hexyl semi-preparatory column, isocratic, 92:8 MeOH:H_2O, 2.5 ml/min) to give compound **131** as a white solid (36 mg, 34 % yield).

^{1}H NMR (600 MHz, $CDCl_3$) δ 7.30-7.24 (m, 2H), 7.24 – 7.17 (m, 1H), 7.06-7.02 (m, 2H), 5.77 – 5.65 (m, *J*=15.6 Hz, 1H), 5.47 – 5.35 (d, *J*=15.6 Hz, 1H), 2.89 – 2.76 (m, 1H), 2.57 – 2.47 (m, 1H), 2.43 – 2.35 (m, 1H), 2.35 – 2.25 (m, 1H), 2.03 (s, 3H), 2.02 – 1.96 (m, 1H), 1.96 – 1.90 (m, 1H), 1.90 – 1.79 (m, 1H), 1.74 – 1.68 (m, 1H), 1.61 – 1.53 (m, 1H), 1.39 – 1.32 (m, 1H), 1.30 (s, 3H).

^{13}C NMR (151 MHz, $CDCl_3$) δ 186.6, 144.0, 138.5, 135.2, 128.5 (2C), 126.9, 126.6 (2C), 115.4, 47.8, 40.1, 36.9, 36.5, 30.9, 24.6, 19.6, 19.2, 10.0.

(+) HRESIMS *m*/*z* $[M+H]^+$ 294.1852 (calcd for $C_{20}H_{24}NO$, 294.1858)

Synthesis of Compound **132**

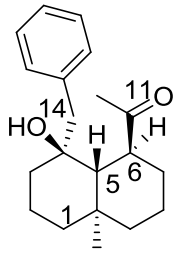

All glassware was dried in an oven overnight. In a two neck flask equipped with a condenser and drying tube, benzyl bromide (100 mg, 0.59 mmol) was dissolved in dry ethyl ether (5 mL) and a crystal of iodine was added to the flask. The solution began to bubble and after bubbling ceased the solution was heat to reflux for another 30 mins. A solution of **118** (37 mg, 0.178 mmol) in dry ethyl ether (10 mL) was added to the solution dropwise with cooling. After addition was complete the reaction was heated to reflux for another 30 mins and then cooled to room temperature. The reaction was diluted with ethyl acetate (20 mL), extracted with 1M HCl (15 mL) and brine (15 mL). The organic layer was dried with magnesium sulfate and the solvent was removed *in vacuo*. The mixture was purified using flash chromatography (silica gel, 80:20 - 100 % MeOH, and HPLC (phenyl hexyl column, isocratic 93:7 MeOH:H_2O) to give compound **132** as a colorless solid (40.5 mg, 76 %).

^{1}H NMR (600 MHz, $CDCl_3$) δ 7.28 – 7.24 (m, 2H), 7.20 (dd, *J* = 7.3, 7.0 Hz, 1H), 7.10 (d, *J* = 7.0 Hz, 2H), 3.08 – 3.00 (m, 1H), 2.54 (d, *J* = 13.0 Hz, 1H), 2.37 (s, 3H), 2.35 (d, *J* = 13.0 Hz, 1H), 2.16 (s, 1H), 1.89 (m, 1H), 1.76 (d, *J* = 11.1 Hz, 1H), 1.68 – 1.62 (m, 1H), 1.64 – 1.58 (m, 1H), 1.53 (m, 1H), 1.43 (m, 1H), 1.41 – 1.34 (m, 1H), 1.36-1.32

(m, 1H), 1.35-1.31 (m, 1H), 1.34 – 1.25 (m, 2H), 1.27 – 1.22 (m, 1H), 1.24 – 1.16 (m, 1H), 1.12 (s, 3H).

^{13}C NMR (151 MHz, $CDCl_3$) δ 214.5, 137.5, 130.7 (2C), 128. (2C), 126.3, 73.9, 53.1, 50.7, 47.5, 43.8, 41.8, 38.5, 34.6, 32.2, 31.1, 20.3, 19.9, 17.1.

FTIR (CH_2Cl_2): ν_{max} 3483.7, 3062.9, 2927.3, 1705.8 cm^{-1}.

(+) HRESIMS *m*/*z* 283.2055 $[M - OH]^+$ (calcd for $C_{20}H_{27}O$, 283.2062).

Synthesis of **133** and **134**

All glassware was dried in an oven overnight and assembled hot, the flask was equipped with a condenser and drying tube. A solution of 2,5-dimethoxy-1-bromobenzene (200 mg, 0.92 mmol) in dry ether (4 mL) was slowly added to a solution of Mg turnings (300 mg) and an iodine crystal in dry either. The solution was warmed slightly and the color disappeared and some bubbling occurred a white precipitate was observed. The solution was heated to reflux temperature for 30 minutes and then cooled to 0 ^oC. A solution of **118** (50 mg, 0.24 mmol) in ether (5 mL) was added dropwise to the reaction and the resulting solution was heated to reflux temperature for one hour before allowing to cool. The reaction was filtered and then extracted with $NaHCO_{3(aq)}$ (2 x 15 mL), dried with $MgSO_4$ and the solvent removed *in vacuo*. The crude mixture was purified using C18 flash chromatography (70 :30 MeOH:H_2O – 100 % MeOH) and then HPLC (Phenyl-hexyl semi-prep column, isocratic, 80:20 ACN:H_2O) to give compound **133** as a white solid (8.0 mg, 10 % yield).

Compound **133**

Proposed Structure

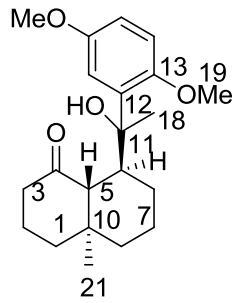

(+) HRESIMS *m*/*z* 329.2111 $[M - OH]^+$ (calcd for $C_{21}H_{29}O_3$, 329.2117).

Compound **134**

Proposed Structure

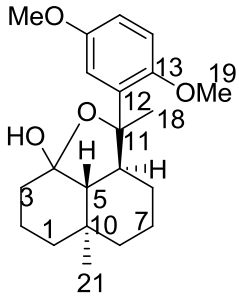

(8.0 mg, 10 % yield).

(+) HRESIMS *m*/*z* 329.2110 $[M - OH]^+$ (calcd for $C_{21}H_{29}O_3$, 329.2117).

Mixture of **133** and **134**: FTIR (CH_2Cl_2): ν_{max} 3461.3, 3072.5, 2927.3, 1700.5 (w) cm^{-1}.

General Procedure for Preparation of Organolithium Reagent and Reaction with 118

Reaction flasks and stir bars were dried in an oven overnight and cooled under an atmosphere of argon. *N*-BuLi was titrated prior to use to confirm concentration. 2,5-dimethoxy-1-bromobenzene (40 mg, 0.186 mmol) was weighed in the flask, dissolved in anhydrous THF (15 mL) and the solution was cooled to – 78 ^{o}C. *N*-Butyl lithium (2M in cyclohexane, 90 µL, 0.19 mmol) was added dropwise to the solution at -78 ^{o}C and the reaction was stirred for 20 min at this temperature. A solution of **118** (19 mg, 0.09 mmol) in anhydrous THF (5 mL) was added dropwise and the solution was stirred and monitored by TLC. The reaction was allowed to come to room temperature and stirred for 3 hours. Chilled isopropyl alcohol was slowly added to the reaction, which was then extracted with saturated $NaHCO_3$, dried with $MgSO_4$ and the solvent removed *in vacuo*. The product mixture was filtered through a plug of C18 and analyzed using UPLC-HRMS and NMR. Although a compound with the correct mass ionized in the HRMS, the NMR determined that the starting materials were the major product.

Chapter 5 - Route to a Novel Glycosylated Derivative *via* Hydroxylation of Gorgonene

5.1 Introduction

Terpene glycosides are natural products that very often possess excellent biological activity.[195] The pseudopterosin family of compounds[131, 132, 134, 196, 197], isolated from a sea whip, belong to this family and exhibit excellent anti-inflammatory and analgesic properties. The fuscosides (diterpene glycosides)[137,198] were also extracted from a sea whip and possess potent anti-inflammatory activity. Eleutherobin and its derivatives were isolated from an Australian coral and possess potent anticancer activity comparable to Taxol™.[199] Inspired by these molecules, a glycoside-affixed derivative of gorgonene (**73**) became a synthetic target.

A glycosylation reaction occurs between a carbohydrate moiety (glycosyl donor) and another molecule (glycosyl acceptor) typically containing a hydroxyl group that ultimately connects the two.[200] In order to prepare gorgonene for this type of reaction, a hydroboration/oxidation reaction was performed to install a hydroxyl motif (Figure 5.1). The hydroxyl moiety may then be used directly in a glycosylation reaction and also may be used as a starting point for syntheses targeting other functionalities. The regioselective hydroxylation of gorgonene is synthetically challenging, however, derivatives of gorgonene with glycosyl moieties at any position of attachment on the scaffold are desirable.

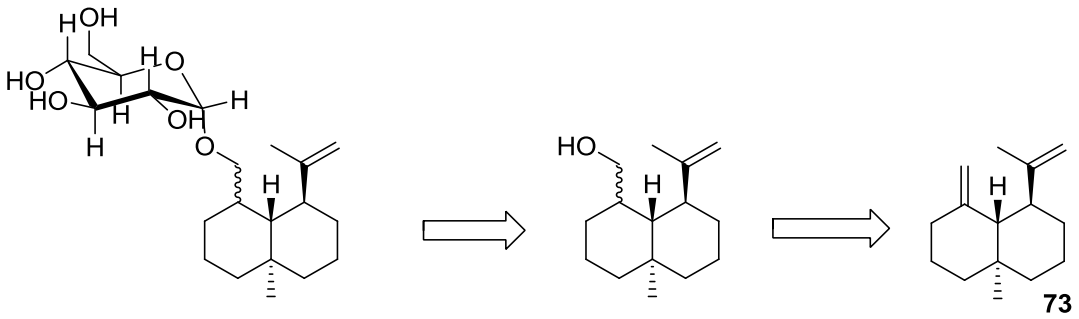

Figure 5.1 - Retrosynthesis of Glycosylated Gorgonene Analogue

5.2 Results and Discussion

5.2.1 Dihydroboration / Oxidation of Gorgonene as a Route to Dihydroxygorgonene Derivatives

A hydroboration/oxidation was performed on **73** in one pot. Gorgonene (**73**) was treated with BH_3 in THF, followed by the dropwise addition of NaOH and H_2O_2 at O ^oC. The resulting product mixture was complex but two major components were isolated, both with molecular formulae consistent with a dihydroxylation taking place ($C_{15}H_{28}O_2$). Compound **135** was an expected product with both alcohols adding in an anti-Markovnikov fashion. C12 and C15 of **135** are methylenes connected to an oxygen atom appearing at 61.0 and 64.0 ppm, whose hydrogen atoms are COSY correlated to H11 and H4 respectively; no alkenyl carbons remained in the molecule. The structure **135** was assigned based on the 1D and 2D NMR data listed in Table 5.1, however, the stereochemistry at C11 could not be assigned with certainty with the information available.

Table 5.1 - NMR Spectroscopic Data for Compound 135 ($CDCl_3$)

	δC, type	δH (J in Hz)	COSY	HMBC	NOESY
1	42.9, CH_2	1.38, m		15	1b
		1.07, ddd (4.75, 13.5, 13.5)			
2	17.4 CH_2	1.58, m		1b	
		1.39, m			
3	28.5 CH_2	1.97, m	3b; 2a	14a, b	3b
		1.30, m			
4	37.9 CH	1.93, m	14a; 3b	14a	12
5	38.7 CH	1.44, m	6; 4	6; 8b; 13	
6	48.9 CH	1.27, m	7a,b	15	
7	22.2 CH_2	1.40, m			
		1.49, m			
8	27.6 CH_2	1.82, m	8b	3	8b; 13
		0.82, m			
9	44.7 CH_2	1.22, m		1b; 15	13
		1.03, m			
10	34.6 CH		15		
11	34.4 CH	1.87, m	12a,b; 13		
12	64.1 CH_2	3.67, m		13	6; 11; 4
		3.22, m			
13	17.0 CH_3	1.03, d (6.8)	9	12a,b	
14	61.0 CH_2	3.57, m		6	15; 2a
		3.48, m			15; 5; 11
15	19.7 CH_3	0.74, s		1b; 5; 9b	1a; 7a; 14b

Data was obtained in $CDCl_3$ solution, δ in PPM relative to solvent signal. Assignments were aided by COSY, HSQC and HMBC and NOESY experiments. HMBC correlations from the carbon stated to the indicated proton.

The other major product **136** which crystallized easily from solution had one of the alcohols add to the more substituted position of the alkene (C4, **136**, Figure 5.2). This was supported by the quaternary substitution on the hydroxyl substituted carbon, C4 appearing at 74.6 ppm in the ^{13}C spectrum and the methyl protons on C15 appearing

as a singlet in the ^{1}H NMR spectrum. The structure of **136** was confirmed using X-ray crystallography (Figure 5.3).

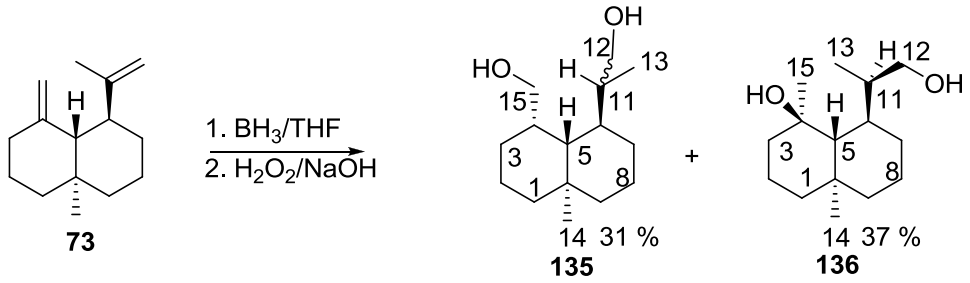

Figure 5.2 - Hydroboration / Oxidation of Gorgonene

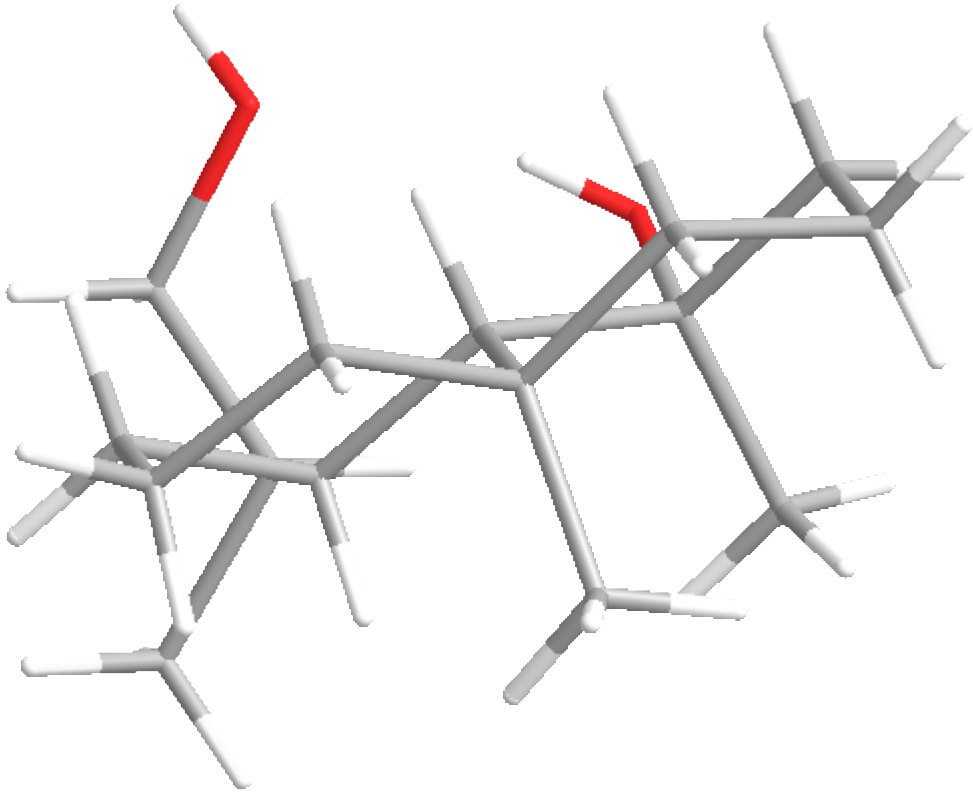

Figure 5.3 - Crystal Structure of Hydroboration/Oxidation Product 136

5.2.1.1 Mechanism of Dihydroboration of Gorgonene Resulting in the Formation of 136

To gain insight into the reaction mechanism favoring products **135** and **136**, a hydroboration reaction was performed using a 1:3 stoichiometric ratio of borane**:**gorgonene to facilitate the production of mono-hydroxylated derivatives. Interestingly, diols **135** and **136** were produced as the major alcohol-containing products, mono-hydroxy derivatives were only formed in minute yields and starting materials were re-isolated in greater than 50 % yield. This result confirms that dihydroboration occurs preferentially with BH_3 in gorgonene's 1,5-diene system.

The formation of products **135** and **136** suggested that the reaction does not proceed through a simple single-step mechanism. Figure 5.4 shows a putative mechanism for the formation of the borane-**73** complex that leads to the production of compound **136**. In the first step the hydroboration of the C11-C12 olefin occurs and then the C4-C14 double bond is ideally situated to undergo a rapid second hydroboration through a cyclic intermediate. The formation of the 1,5-diol (**136**) suggests that the intramolecular BH addition occurs forming a six membered cyclic organoborane (**136a**-Figure 5.4), but a seven membered ring (**135a**) is the proposed intermediate in the formation of **135**. Six membered rings are energetically favorable to seven membered rings due to reduced ring strain.[201] Anti-Markovnikov addition typically occurs during the hydroboration reaction because H-B adds to the carbon-carbon double bond in a concerted fashion with no carbocation intermediate being formed. Therefore the stereochemical outcome of the addition is determined mainly by steric effects with the larger boron atom adding to the less substituted carbon. The formation of **135** is the

result of both hydroborations occurring in the expected anti-Markovnikov way. The approximately equal formation of products **135** and **136** suggests that the two opposing forces (steric hindrance vs. ring strain) are approximately equal in their effect. Monohydroboration would presumably be favorable if a disubstituted hydroborane reagent was used containing one B-H bond such as chatecholborane.[202]

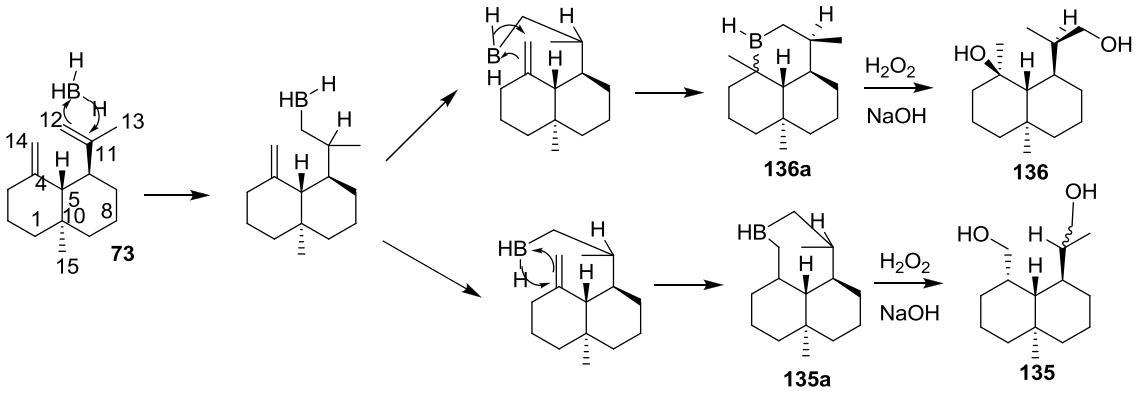

Figure 5.4 - Proposed Mechanism for the Formation of Products 135 and 136

5.2.2 Synthesis of Glycosylated Analogue of (+)-β-Gorgonene

Compound **136** was purified *via* crystallization and glycosyl donor **139** was prepared in two steps to couple with it. D-Glucose was first converted to the corresponding benzoyl protected sugar **138** by treatment with DMAP and subsequent addition of benzoyl chloride with stirring and cooling. After workup, the crude benzoylated sugar **138** was combined with an equivalent of acetyl bromide in methanol and DCM in the absence of light.[203] A second equivalent of acetyl bromide was required to complete the reaction according to TLC. ^{1}H NMR confirmed the production of the glycosyl bromide **139** which was unstable under ambient conditions and was used immediately in the next step without further purification.

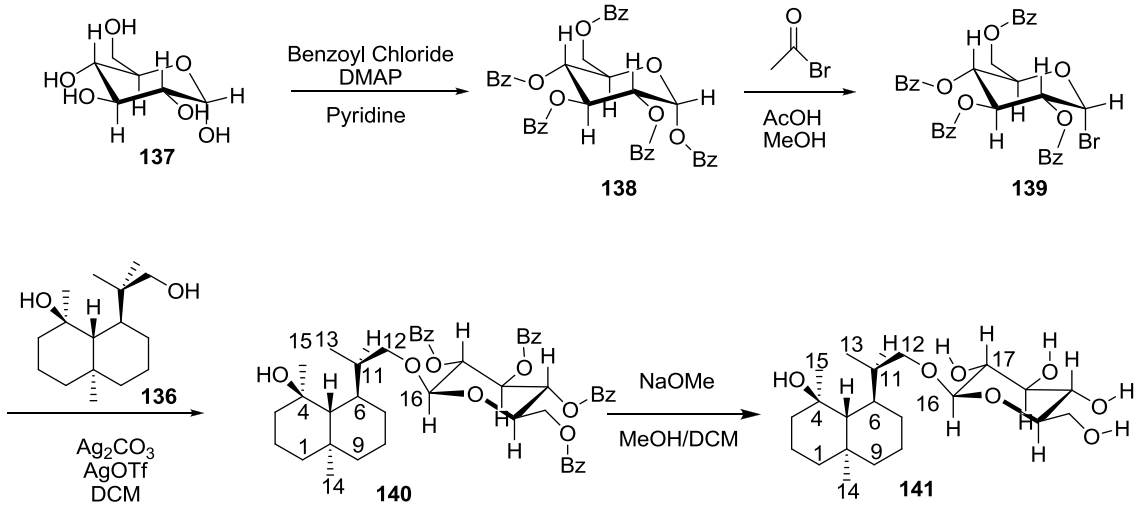

Figure 5.5 - Glycosylation Reaction Scheme

Glycosyl bromide (**139**) was coupled to glycosyl acceptor **136** using a modified Koenigs-Knorr reaction with a silver trifluoromethanesulfonate catalyst and silver carbonate under anhydrous conditions.[204] The product mixture was purified using C18 chromatography and the fraction containing the product **140** was identified using HRMS (*m/z* of 841.3606 $(M + Na)^+$ corresponding to the expected molecular formula $C_{49}H_{54}O_{11}$) . The product was further purified using HPLC to give a 7.1 % isolated yield.

In the final step of the synthetic sequence, the benzoyl deprotection of **140** was first attempted by treatment with K_2CO_3 in a methanol solution, but only partial deprotection was achieved.[204] Compound **140** was then treated with NaOMe in a DCM/MeOH solution until a pH of 12 was reached and the reaction was stirred for several hours before workup.[205] The glycoside **141** was purified using HPLC and analyzed using UPLC-HRMS and ^{1}H NMR. An *m/z* ion of 425.2508 confirmed the expected molecular formula of the product $C_{21}H_{38}NaO_7$. Many of the ^{13}C chemical shifts were identified using HSQC and HMBC, however limited material prevented a full ^{13}C

spectrum from being recorded. The structure and stereochemistry of the starting alcohol (**136**) was known before the reaction and is expected to be unchanged during the glycosylation. Primary alcohol glycosyl accepters are more reactive than tertiary alcohols due to steric reasons, directing the regioselectivity to favor attachment of the glycosyl moiety to the decalin scaffold at C12. Although the HMBC signals between the sugar moiety and the sesquiterpene fragment were too weak to be detected, ^{1}H NMR resonances for H12 and H13 were shifted downfield and H1, upfield, supporting reaction at position H12. The stereochemical outcome of the anomeric carbon of the sugar moiety is predicted to have the *S* configuration due to the neighboring group effects of the benzoyl group.[206] This would cause a *trans*-configuration between anomeric H16 and the adjacent H17 in the final product, (likely equatorial-equatorial, but possibly axial-axial). Vicinal hydrogen atoms with bond angles approaching 0 ^{o} or 180 ^{o} will display a large ^{3}J coupling constants (>7 Hz) according to the Karplus equation.[207] If the anomeric carbon has the reverse stereochemistry and H16-H17 are *cis*, then a bond angle closer to 90 ^{o} (axial-equatorial) would show a smaller ^{3}J coupling constant between the two vicinal protons (< 5 Hz). The anomeric proton is the most deshielded in the ^{1}H NMR spectrum and is clearly distinguishable from the other peaks. A coupling constant of 8.0 Hz is observed between H16 and H17, suggesting that the predicted trans geometry is indeed formed and confirming the structure of the product as **141** (Figure 5.5).

5.2.3 Reactivity of Gorgonene Derivatives 135 and 136

A retrosynthetic analysis of dimethoxybenzene derivative (**142**) of gorgonene is shown in Figure 5.6. A disconnection of the C13-C14 bond of structure **142** leads to

synthons **143** and **144**. Tosylate esters (**143**), which act as good leaving groups for a subsequent nucleophilic substitution reactions, can be synthesized from hydroxyl groups in one step by treatment with toluenesulfonyl chloride in pyridine. Novel analogues of gorgonene with attached aromatic groups *via* an ethylene or methylene linker were envisaged using this approach.

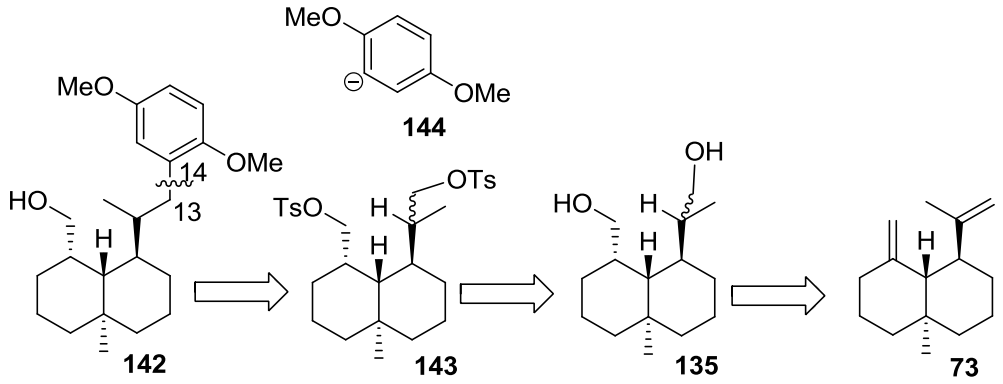

Figure 5.6 - Retrosynthetic Analysis of Aromatic Containing Derivative of Gorgonene

5.2.3.1 Unexpected Reactivity of Tosylation Reaction Leading to Cyclic Ether 145

In order to produce a tosylate containing intermediate, compound **136** was treated with toluenesulfonyl chloride in a solution of pyridine. The major isolated compound (C18 chromatography) of the reaction had a molecular formula of $C_{15}H_{23}O$ as indicated from HRMS (*m/z* ion of 223.2058 $(M + H)^+$). The compound contained 3 degrees of unsaturation but no peaks in the ^{13}C NMR spectrum more deshielded than 100 ppm indicated the absence of a tosyl moiety. Quaternary carbon C4 and methylene carbon C13 are attached to the ether oxygen with ^{13}C NMR chemical shifts of 74.1 and 67.4 ppm respectively. 1D and 2D NMR elucidation revealed the novel tricyclic compound **145** had been formed particularly a strong HMBC correlation between C4 and H13 as well as one between C13 and H15.

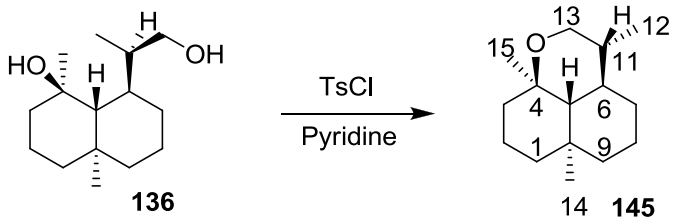

Figure 5.7 - Tosylation of 136 Produces Tricyclic Ether 145

The new 6-membered ether containing ring presumably formed as shown in Figure 5.8. The tosylate was likely first formed on C13, then deprotonation and nucleophilic attack of C4-O^- replacing the tosylate on C13 completed the formation of the ring.

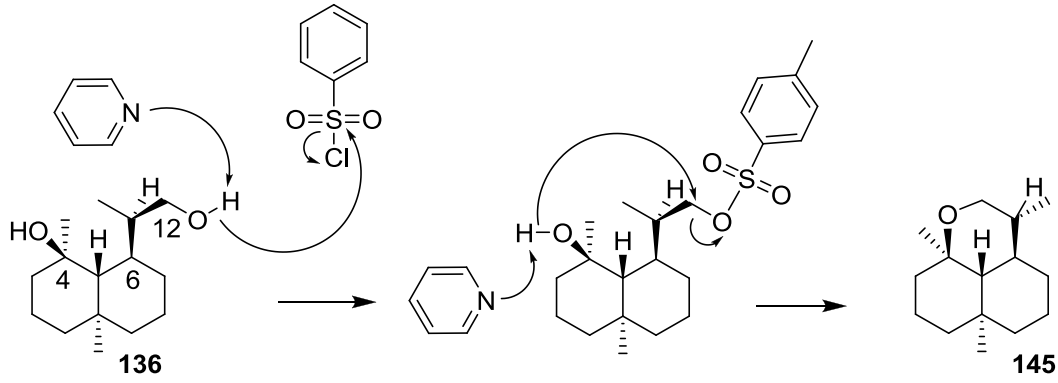

Figure 5.8 - Proposed Mechanism for Formation of 145

5.4.3.2 Tosylation of 135 as a Route to Aromatic Substituted Gorgonene Derivative

Tosylate ester **146** was successfully synthesized by treatment of **135** with toluenesulfonyl chloride in a pyridine solution, as indicated by an HRMS *m/z* ion of 566.2599 $(M+NH_4)^+$. Compound **146** was used in the next reaction after partial purification using silica gel flash chromatography.

A nucleophilic substitution reaction was attempted with **135** by addition of an organocuprate salt of dimethoxybenzene to an anhydrous solution of compound **135**,

however this resulted in recovery of starting materials. Treatment of **135** with Grignard reagent, 2,5 dimethoxyphenyl magnesium bromide also resulted in recovery of mainly starting materials and low yields of multiple products complicated purification. This phase of the study was not continued after multiple failed attempts.

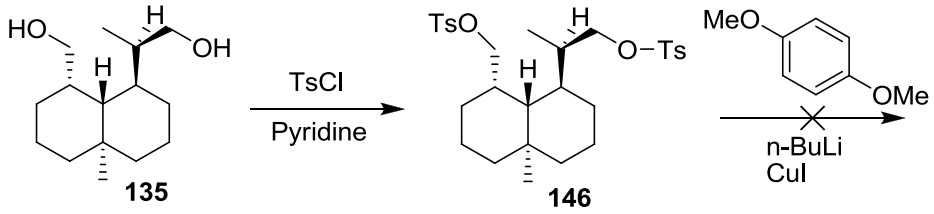

Figure 5.9 - Synthesis of Tosylate Ester 146

5.2.3 Riley Allylic Selenium Dioxide Oxidation of Gorgonene

The Riley allylic selenium dioxide oxidation was pursued as a route to a new hydroxy-derivative of gorgonene. Selenium dioxide allylic oxidations proceed through a two-step mechanism; first an ene-reaction occurs between the allylic group and the selenium dioxide, followed by a sigmatropic rearrangement with the net result of an allylic substituted alcohol (Figure 5.10).

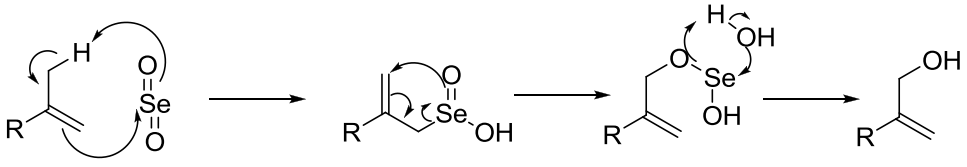

Figure 5.10 - Riley Allylic Selenium Dioxide Oxidation Mechanism

The major isolated product of the reaction of gorgonene (**73**) with selenium dioxide in a solution of 1,4-dioxane was compound **147**. After an aqueous workup the major product contained a selenium atom according to the HRMS *m/z* ions of 299.1073 and 301.1065 ($C_{15}H_{25}OSe$ $(M+H)^+$ for the two most abundant isotopes ^{78}Se and ^{80}Se).

The molecular formula indicated the compound had four degrees of unsaturation, but only two olefinic ^{13}C resonances appeared in the NMR spectrum (C11, C12), a 1,1-disubstituted alkene. The key HMBC correlation is between C4/H13 indicated there is a bridge between those two carbons. C3 and C4 are HMBC correlated to H13, placing the alcohol H13 at the C4 position. H15/OH COSY correlations indicate that the oxygen that is attached to H15 is an alcohol and not an ether or part of the bridge. The C13 is much more shielded (21.7 ppm) than would be expected if it was attached to two carbon atoms (~40-45 ppm) and there is significant literature precedent that carbon atoms attached to selenium atoms are more shielded than C-C atoms[208] suggesting that there is a selenium atom bridging the two atoms C13 and C4. The H13 hydrogens are more deshielded than expected (3.11, 3.57 ppm), but this may be due to their proximity to the C15-OH. Bridged selenanes have been reported to be formed from the reaction of dienes with selenium dioxide.[209] The proposed structure of **147** is based on the HRMS, 1D and 2D NMR data (Table 5.2) and the literature (Figure 5.11). The stereochemistry at C4 was assigned using a NOESY correlation between H6/H15.

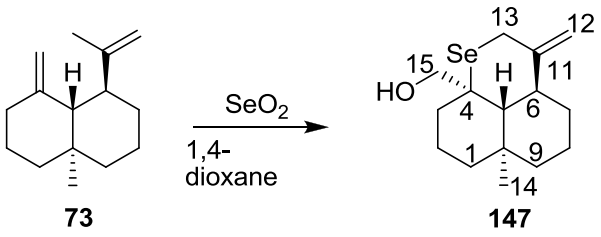

73 **147**

Figure 5.11 - Synthesis of Selenide Derivative of 73

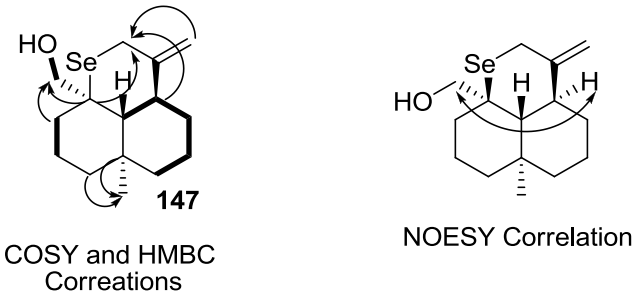

Figure 5.12 - Key NMR Correlations for 147

Selenium is found in biological systems in low quantities, although it is toxic in large amounts. Several commercial drugs contain selenium such as PBISe for the treatment of malignant melanoma.[210] For this reason compound **147** was tested for activity in cancer cell line assays.

Table 5.2 - NMR Spectroscopic Data for Compound 147 ($CDCl_3$)

	δC, type	δH (J in Hz)	COSY	HMBC	NOESY
1	45.2, CH_2	1.32, m		5; 14	
		1.21, m			
2	19.1, CH_2	1.60, m	3b	3b	
		1.40, m			
3	38.2, CH_2	2.33, m	3b	15b	3b
		1.80, m			
4	55.6, C			3; 5; 13; 15	
5	56.0, CH	2.04, d, (12.0)	6	14	3b
6	40.0, CH	2.44, ddd (3.2, 12.0, 12.0)	7a; 5	12; 13b; 5	5; 14
OH		2.27, dd (10.3, 3.3)	15a,b		
7	36.4, CH_2	1.50, m	6; 8		13a
		1.67, m			
8	21.9, CH_2	1.65, m	7a; 9		
9	42.1, CH_2	1.50, m		14	
		1.27, m			
10	36.5, C				
11	150, C			12; 13; 6	
12	109.9, CH_2	4.92, s	13a	13; 6	13b
		4.74, s			6
13	21.7, CH_2	3.57, d (10.0)	13b		13b; 5
		3.11, d (10.0)			
14	20.6, CH_3	0.99, s		5	6
15	62.7, CH_2	3.60, d, (11.3)	OH	3b; 5	14, oh
		3.70, m	OH, 15a		6

Data was obtained in $CDCl_3$ solution, δ in PPM relative to solvent signal. Assignments were aided by COSY, HSQC and HMBC and NOESY experiments. HMBC correlations from the carbon stated to the indicated proton.

5.2.4 Biological Assessment of Compounds 135, 136, 141, 145 and 147

5.2.4.1 Analysis of Cytotoxicity of Gorgonene Derivatives

Compounds **135**, **136**, **141**, **145**, **147** were tested for cytotoxicity against human foreskin BJ fibroblast cell line (ATCC CRL-2522) and human breast adenocarcinoma cell line (ATCC HTB-26) according to the procedure described in Chapter 2. Compound **136** did show inhibition of cancer cell growth in the initial screening at 100 µg/mL, but when an IC_{50} was performed it did not inhibit cancer growth at 64 µg/mL. Compound **135** and **145** did not show any activity in the anticancer assays up to 64 µg/mL. Compound **147** displayed modest anticancer activity in the 32-64 µg/mL range for both cell lines. Due to limited material, **141** was only tested in the assay at a concentration of 32-64 µg/mL and was not cytotoxic at that level.

Table 5.3 - Cytotoxicity Data for Compounds 135, 136, 141, 145 and147 (IC_{50})

	Cell Line	
Compound	BJ	HTB-26
135	>64 µg/mL	>100 µg/mL
136	>64 µg/mL	64-100 µg/mL
141	>32 µg/mL	>32 µg/mL
145	>64 µg/mL	>64 µg/mL
147	32-64 µg/mL	32-64 µg/mL

5.2.4.2 Antimicrobial Assessment of Gorgonene Derivatives

The compounds **135**, **136**, **141**, **145** and **147** were screened for antimicrobial activity and did display growth inhibition 128 µg/mL against Gram positive bacteria: MRSA or VRE, Gram negative bacterium: *Pseudomonas aeruginosa* or fungus: *Candida albicans*. The assays were performed according to the procedure described in Chapter 2.

5.2.4.3 Evaluation of Protein Tyrosine Phosphatase Inhibition of Gorgonene Derivatives

Compounds **135**, **136**, **141**, **145** and **147** were screened for protein tyrosine phosphatase inhibition according to the procedure described in Chapter 2. None of the compounds displayed inhibition at the concentration tested (50 μM).

5.3 Conclusion and Significance

Five new natural product derivatives of gorgonene were synthesized, fully characterized and screened for biological activity in three bioassays. The reactivity of **73** with BH_3 and SeO_2 gives insight into the tendency for the 1,5-diene to react intramolecularly through pericyclic rearrangements to favor the formation of 6 membered rings. The bioassays performed did not identify any significant activity, however, further biological screening of these compounds may reveal a biomedical application. Of particular interest would be to test glycoside **141** for anti-inflammatory properties.

5.4 Experimental Section

Synthesis of **135** and **136**

All glassware was dried in an oven overnight and allowed to cool to room temperature under an atmosphere of argon. To a solution of **73** (5g, 24.5 mmol) in anhydrous THF (100 mL) was added a 1M solution of BH_3-THF (20 mL, 20 mmol)) dropwise at 0 ^oC. The solution was allowed to come to room temperature and was stirred for two hours. The reaction was then cooled to 0 ^oC and a 3M solution of NaOH (15 mL, 45 mmol) was added dropwise, followed by the dropwise addition of H_2O_2 (35 %, 5 mL). The solution was then heated to 50 ^oC and stirred at that temperature for two hours. It was then allowed to cool and diluted with ethyl acetate, extracted with distilled water, dried with $MgSO_4$ and the solvent removed *in vacuo*. The product mixture was purified using C18 chromatography (70-85 % MeOH:H_2O) to give **135** as a white powder (1.8 g, 31 % yield). Compound **136** was crystallized from MeOH to give clear colorless crystals (2.2 g, 37 % yield).

Compound **135**

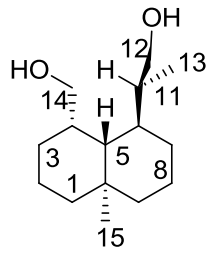

^{1}H NMR (600 MHz, $CDCl_3$) δ 3.67 (dd, *J* = 10.4, 2.9 Hz, 1H), 3.57 (ddd, *J* = 10.2, 10.2, 2.1 Hz, 1H), 3.48 (dd, *J* = 10.2, 1.3 Hz, 1H), 3.21 (dd, *J* = 15.9, 7.3 Hz, 1H), 2.89 (bs, 2OH), 1.97 (m, 1H), 1.91 (m, 1H), 1.86 (m, 1H), 1.80 (m, 1H), 1.61 – 1.52 (m, 1H), 1.50 - 1.48 (m, 1H), 1.48 - 1.42 (m, 1H), 1.43 – 1.38 (m, 1H), 1.41 - 1.38 (m, 1H), 1.40 - 1.36 (m, 1H), 1.34 - 1.29 (m, 1H), 1.30 - 1.26 (m, 1H), 1.25 - 1.21 (m, 1H), 1.11 – 1.06 (m, 1H), 1.08 – 1.04 (m, 1H), 1.03 (d, *J* = 6.8 Hz, 3H), 0.84 – 0.77 (m, 1H), 0.75 (s, 3H).

^{13}C NMR (151 MHz, $CDCl_3$) δ 64.0, 61.0, 48.9, 44.6, 42.8, 38.6, 37.9, 34.6, 34.4, 28.5, 27.6, 22.2, 19.7, 17.4, 17.0.

FTIR (CH_2Cl_2): ν_{max} 3310.1, 2921.9, 2854.5 cm^{-1}.

(+) HRESIMS *m*/*z* 223.2058 $[M - OH]^+$ (calcd for $C_{15}H_{27}O$, 223.2062).

Compound **136**

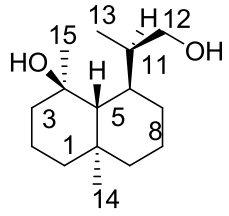

^{1}H NMR (600 MHz, $CDCl_3$) δ 3.54 (dd, *J* = 10.3, 10.3 Hz, 1H), 3.48 (dd, *J* = 10.3, 5.4 Hz, 1H), 2.96 – 2.86 (m, 1H), 1.82-1.80 (m, 1H), 1.72 – 1.69 (m, 1H), 1.67 (d, *J* = 11.2 Hz, 1H), 1.58 (OH, 2H), 1.58 - 1.55 (m, 1H), 1.56 - 1.54 (m, 1H), 1.56 - 1.53 (m, 1H), 1.52 – 1.48, (m, 1H), 1.51 - 1.49 (m, 1H), 1.50 – 1.46 (m, 1H), 1.34 – 1.30 (m, 1H), 1.32 - 1.29 (m, 1H), 1.31 - 1.29 (m, 1H), 1.25 (s, 3H), 1.25 – 1.19 (m, 1H), 1.16 - 1.13 (m, 1H), 0.91 (s, 3H), 0.83 (d, *J* = 7.1 Hz, 3H).

^{13}C NMR (151 MHz, $CDCl_3$) δ 74.6, 65.8, 56.2, 46.0, 45.3, 42.4, 40.0, 36.3, 33.7, 26.8, 24.3, 22.2, 19.7, 19.0, 17.4.

FTIR (CH_2Cl_2): ν_{max} 3254.3, 2928.4 cm^{-1}.

(+) HRESIMS *m*/*z* 241.2165 $[M + H]^+$ (calcd for $C_{15}H_{29}O_2$, 241.2164).

Mp. 216-217 ^{o}C.

Synthesis of **138**[211]

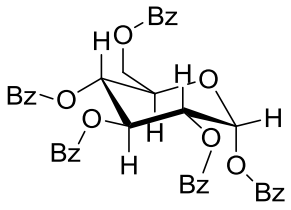

To a solution of glucose (3 g, 16.6 mmol) in pyridine (30 mL) was added DMAP (14 mg, 0.12 mmol). The solution was cooled in an ice bath and benzoyl chloride (17.6 g, 125.0 mmol) was added slowly with stirring. The reaction was stirred for 24 hours at room temperature and then the solvent removed *in vacuo*. The residue was dissolved in DCM and H_2O was added with cooling and stirring. The DCM layer was separated and the solvent removed *in vacuo*. The product was used in the formation of **139** without further purification.

Synthesis of **139**[203]

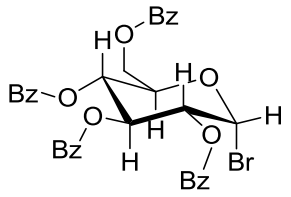

In the absence of light, a solution of acetyl bromide (0.05 mL, 1.4 mmol) and MeOH (0.03 mL, 1.4 mmol) was combined with DCM (5 mL) and the solution was stirred for 15 mins at room temperature. Compound **138** was added to the reaction and stirred overnight. A second equivalent of acetyl bromide/MeOH (0.05 mL/5mL) was added and the reaction was stirred overnight. The reaction was then washed with cold $NaHCO_3$ and

then brine. The organic phase was dried over $MgSO_4$ and the solvent removed *in vacuo*. The product was used in the next step without further purification.

Synthesis of **140**[204]

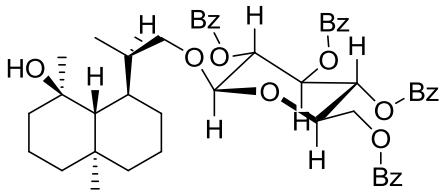

All glassware was dried in an oven overnight and allowed to cool under an atmosphere of N_2. All reagents were dried in a dessicator for 24 hours or more, and solvents were dried over 3Å molecular sieves. To a solution of AgOTf (15 mg, 0.05 mmol) and Ag_2CO_3 (193 mg, 0.7 mmol) in anhydrous DCM (20 mL) containing activated molecular sieves under an atmosphere of N_2 was added compound **135** (42 mg, 0.175 mmol). The resulting solution was stirred for 15 minutes at room temperature then cooled to -78 ^oC. A solution of **139** (480 mg, 0.728 mmol) in anhydrous DCM was added dropwise to the reaction and it was stirred for 4 days under N_2 and allowed to come to room temperature. The reaction was diluted with ethyl acetate and filtered through a plug of celite. The filtrate was washed with saturated Na_2SO_4 and then brine solution. The organic layer was dried with $MgSO_4$ and the solvent removed *in vacuo*. The product mixture was purified using silica gel flash chromatography (10:90 – 50:50 ethyl acetate:hexanes) and C18 flash chromatography (30:70 H_2O:MeOH-100 % MeOH) to give the product **140** (10.5 mg, 7.1 % yield).

(+) HRESIMS *m/z* 841.3606 $[M + Na]^+$ (calcd for $C_{49}H_{54}NaO_{11}$, 841.3564)

K_2CO_3 benzoyl group deprotection of **140**[204]

To a solution of **140** (10 mg) in methanol (1 mL) was added K_2CO_3 and the solution was stirred overnight, then neutralized with Amberlyst 15 resin, filtered, and the filtrate was evaporated to dryness *in vacuo*. The crude product mixture was analyzed using UPLC-HRMS and no ions corresponding to the desired product (fully deprotected glycoside **141**) were visible in the chromatogram.

Synthesis of **141**[205]

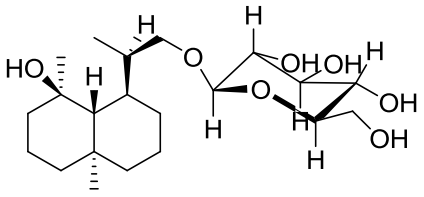

To a solution of **140** (3.5 mg, 0.004 mmol) in a 3:1 solution of MeOH:DCM (1 mL) was added a 1M solution of NaOMe in MeOH dropwise until the reaction reached a pH of 12. The reaction was then stirred for 4 hours at room temperature and the product mixture was neutralized using 1M HCl and purified using HPLC chromatography (phenyl-hexyl semi-preparatory column, isocratic, 80:20 MeOH:H_2O) to afford **141** (0.4 mg, 25 % yield).

^{1}H NMR (600 MHz, $CDCl_3$) δ 4.27 (d, *J* = 8.0 Hz, 1H), 4.08 - 4.06 (m, 1H), 3.87 (m, 1H), 3.83 (m, 1H), 3.61 – 3.52 (m, 1H), 3.51 - 3.48 (m, 1H), 3.49 (bs, OH), 3.38 (m, 1H), 3.28 - 3.32 (m, 1H), 3.21 - 3.16 (m, 1H), 2.89 - 2.84 (m, 1H), 1.82 (m, 1H), 1.75 (m, 1H), 1.63 (s, OH), 1.59 – 1.55 (m, 1H), 1.55 – 1.51 (m, 1H), 1.51 – 1.48 (m, 1H), 1.48 – 1.45 (m, 1H), 1.45 – 1.42 (m, 1H), 1.41 – 1.39 (m, 1H), 1.39 – 1.37 (m, 1H), 1.32 – 1.30 (m, 1H), 1.30 – 1.27 (m, 1H), 1.27 – 1.23 (m, 1H), 1.19 (s, 3H), 1.16 – 1.14 (m, 1H), 1.14 - 1.11 (m, 1H), 0.98 (d, *J* = 6.8 Hz, 3H), 0.89 (s, 3H).

FTIR (CH_2Cl_2): ν_{max} 3337.7, 2923.3, 2854.0 cm^{-1}.

(+) HRESIMS *m*/*z* 425.2508 $[M + Na]^+$ (calcd for $C_{21}H_{38}NaO_7$, 425.2515)

Synthesis of **145**

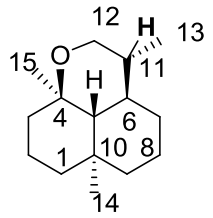

A solution of **136** (210 mg, 0.87 mmol) in pyridine (5 mL) was cooled in an ice bath and toluenesulfonyl chloride (498 mg, 2.6 mmol) was added as a solid. The reaction was stirred for 30 mins at 0 ^{o}C then placed in the fridge (5 ^{o}C) overnight. The solution was then carefully poured into a solution of ice water with stirring and extracted with TBME (3x25 mL). The organic layer was washed with cold 1M HCl (3x15 mL), dried with $MgSO_4$ and the solvent removed *in vacuo*. The product mixture was purified using silica gel chromatography (0-10 % ethyl acetate:hexanes) and **145** was isolated as a white solid (106 mg, 54.9 % yield).

^{1}H NMR (600 MHz, $CDCl_3$) δ 3.90 (dd, *J* = 11.7, 2.6 Hz, 1H), 3.32 (dd, *J* = 1.0, 11.8 Hz, 1H), 1.83 – 1.71 (m, 1H), 1.61 – 1.56 (m, 1H), 1.57 – 1.55 (m, 2H), 1.56 – 1.52 (m, 1H), 1.47 – 1.40 (m, 1H), 1.42 – 1.38 (m, 1H), 1.37 – 1.31 (m, 1H), 1.30 - 1.26 (m, 1H), 1.29 - 1.26 (m, 1H), 1.27 – 1.24 (m, 1H), 1.21 (s, 3H), 1.22 - 1.20 (m, 1H), 1.12 – 1.04 (m, 1H), 1.03 – 1.00 (m, 1H), 1.00 (d, *J* = 7.2 Hz, 3H), 0.81 (s, 3H).

^{13}C NMR (151 MHz, $CDCl_3$) δ 74.1, 67.4, 49.4, 45.2, 41.6, 40.7, 33.6, 33.5, 31.3, 30.6, 20.7, 20.0, 19.9, 19.8, 13.6.

FTIR (CH_2Cl_2): ν_{max} 2927.6, 2864.5 cm^{-1}.

(+) HRESIMS *m*/*z* 223.2058 $[M + H]^+$ (calcd for $C_{15}H_{27}O$, 223.2062).

Synthesis of **146**

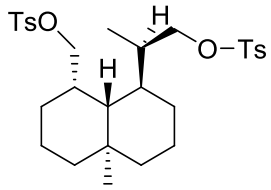

A solution of **135** (220 mg, 0.92 mmol) in pyridine (5 mL) was cooled in an ice bath and toluenesulfonyl chloride (522 mg, 2.75 mmol) was added as a solid. The reaction was stirred for 30 mins at 0 ^{o}C then placed in the fridge (5 ^{o}C) overnight. The solution was then carefully poured into a solution of ice water with stirring and extracted with TBME (3x25 mL). The organic layer was washed with cold 1M HCl (3x15 mL) dried with $MgSO_4$ and the solvent removed *in vacuo*. The product mixture was purified using silica gel chromatography (0-10 % ethyl acetate:hexanes) and isolated as a white solid (261 mg, 52 % crude yield).

(+) HRESIMS *m*/*z* 566.2598 $[M + NH_4]^+$ (calcd for $C_{29}H_{44}O_6NS_2$, 566.2610)

Synthesis of **147**[212]

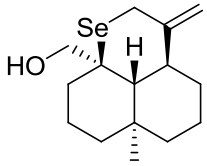

To a solution of **73** (200 mg, 0.98 mmol) in 1,4-dioxane (7 mL) under an atmosphere of N_2 at room temperature was added SeO_2 (140 mg, 1.26 mmol) as a solid. The reaction was stirred for 16 hours at which time the solution had changed to an orange-yellow color. The reaction was diluted with H_2O and extracted with DCM. The organic layer was washed with H_2O (3 x 15 mL), dried with $MgSO_4$ and the solvent removed *in vacuo*. The title compound was purified using silica gel flash chromatography (0-10% acetone:hexanes) and isolated as a yellow solid (172.2 mg, 54 % yield).

^{1}H NMR (600 MHz, $CDCl_3$) δ 4.92 (s, 1H), 4.74 (s, 1H), 3.73 - 3.67 (m, 1H), 3.62 – 3.57 (d, *J* = 11.3 Hz, 1H), 3.58 – 3.55 (d, *J* = 10.0 Hz, 1H), 3.11 (d, *J* = 10.0 Hz, 1H), 2.44 (ddd, *J* = 3.2, 10.0, 10.0 Hz, 1H), 2.33 (m, 1H), 2.27 (bs, OH), 2.04 (d, *J* = 12.0 Hz, 1H), 1.80 (m, 1H), 1.70 - 1.64 (m, 1H), 1.66 - 1.64 (m, 1H), 1.62 - 1.58 (m, 1H), 1.56 - 1.54 (m, 1H), 1.53 – 1.46 (m, 1H), 1.52 - 1.48 (m, 1H), 1.43 - 1.37 (m, 1H), 1.34 – 1.30 (m, 1H), 1.30 – 1.25 (m, 1H), 1.25 – 1.18 (m, 1H), 0.99 (s, 3H).

^{13}C NMR (151 MHz, $CDCl_3$) δ 150.0, 109.9, 62.7, 56.0, 55.6, 45.2, 42.1, 40.0, 38.2, 36.5, 36.4, 21.9, 21.7, 20.6, 19.0.

FTIR (CH_2Cl_2): ν_{max} 3402.5, 3063.5, 2926.3, 2846.9 cm^{-1}.

(+) HRESIMS *m*/*z* 301.1065 $[M + H]^+$ (calcd for $C_{15}H_{25}OSe$, 301.1071).

Chapter 6 - Microbial Transformation of the Sesquiterpene (+)-β-Gorgonene

6.1 Introduction to the Use of Biotransformation in Organic Synthesis

Biocatalysis is a useful tool for generating complexity in organic synthesis[213] and can be performed by whole organisms (biotransformation), isolated enzymes or cell-free extracts. Biotransformation can be an attractive alternative to traditional synthetic methods and is desirable for this project for the following reasons:

- Regio- and stereoselective functionalization of gorgonene.
- Functionalization of sites within the gorgonene skeleton that are otherwise inaccessible using synthetic methods.
- Environmentally friendly alternative to harsh chemicals, catalysts and organic solvents.

Problems associated with selectively synthetically modifying gorgonene prompted the use of microbial transformation as a method of introducing oxygen atoms to **73** and the synthetic compound **74** in a stereo- and regio-selective manor. Fungi are the most commonly used microorganism for hydroxylation of terpenes and sesquiterpenes in the literature.[214-216] No biocatalytic studies on gorgonene have been reported, however, the biohydroxylation of (-)-maalioxide (**77**), a sesquiterpene with a similar framework to gorgonene (**73**), using *Mucor plumbeus*,[214] *Aspergillus cellulosae* and *Aspergillus niger*[215] indicated they all had the biosynthetic hardware required to hydroxylate terpenoids (Figure 6.1).

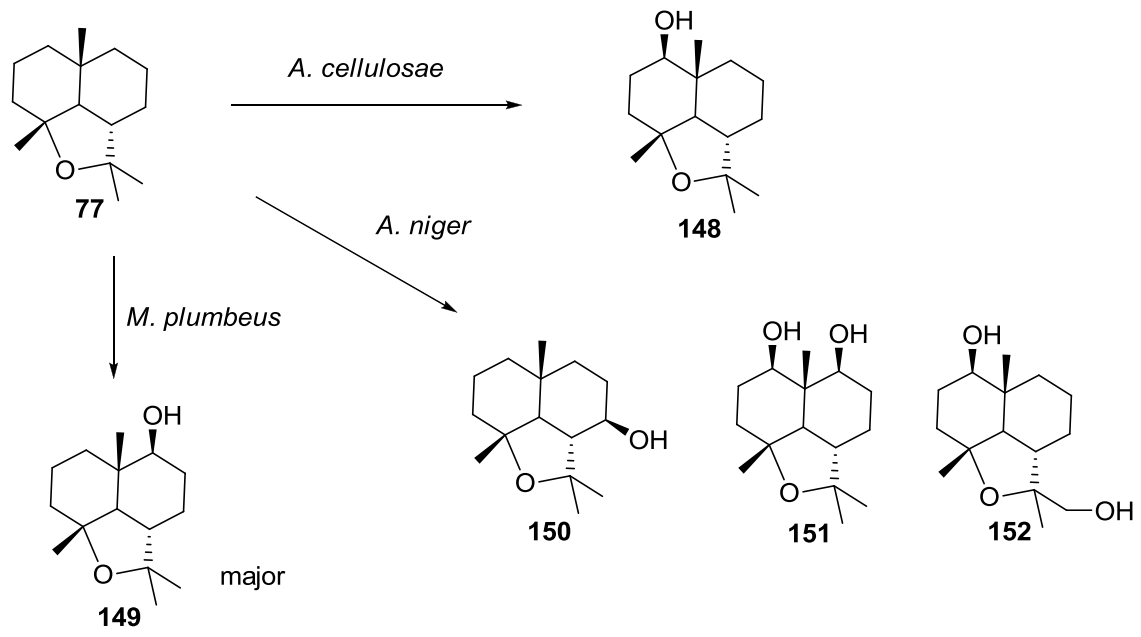

Figure 6.1 - Fungal Biotransformations of (-)-Maalioxide (77)

Enzymes isolated from *Pleurotus sapidus*, an edible mushroom[216], were capable of hydroxylating valencene (**153**), a sesquiterpene hydrocarbon containing a decalin core (Figure 6.2). Based on these literature precedents, the metabolism of **73** and **74** by select fungi was investigated.

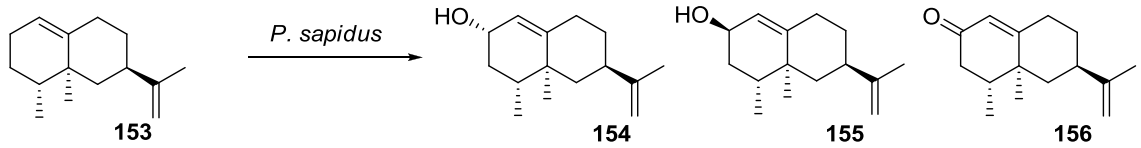

Figure 6.2 - Biocatalysis of Valencene (153) by *Pleurotus sapidus*

6.2 Biotransformation Method Development

Several experiments were performed to optimize culture conditions (type of media, duration of incubation, surfactant use and concentration of substrate) prior to large scale fermentation.

6.2.1 Extraction of Metabolites from Biotransformation Culture

Freeze-drying is a technique used to remove water from a sample at low temperatures under reduced pressure. It was identified as a way to prepare the biotransformation cultures for solvent extraction without using elevated temperatures and risk degrading the metabolites. There was concern that the freeze-drying process would also evaporate the volatile starting materials (**73** or **74**) and biotransformation products along with the water. In order to determine if gorgonene would remain after the sample was freeze-dried, three samples containing media (5 mL) and **73** (50, 20 and 2 µL) were freeze-dried and extracted with DCM (5 mL). The crude extract was then filtered and visualized using ^{1}H NMR. The gorgonene was recovered in > 90 % yield and freeze-drying did not affect the mass recovered of **73**.

6.2.2 GCMS as a Screening Tool for Biotransformation Extracts

GCMS was an ideal tool for biotransformation screening for several reasons. Only low-boiling compounds elute on the GCMS, resulting in a relatively clean chromatogram due to the media components and primary metabolites not being detected. Gorgonene and its related metabolites, however, are volatile and observable using GCMS. Minimal processing of the fermentations is therefore required and no purification step need be performed to prepare the extracts for injection onto the GCMS. This is desirable when large numbers of extracts are to be screened. The hydrophobic nature of the starting materials **73** and **74** also makes them poor candidates for reversed-phase LCMS analysis. The *m/z* data provided in the GCMS chromatogram aids the identification of gorgonene and any related biotransformation products which would have predictable molecular ions corresponding to formula: $C_{15}H_{24} + O_{(n)} +/- H_{(n)}$.

6.2.3 Optimization of Substrate Concentration in Biotransformation Culture

The optimal concentration of substrate **73** and **74** in the biotransformation was investigated. Oversaturation of the starting compound can prevent detection of metabolites due to low relative abundance of the new compounds. A minimal amount of starting compound should be used, slightly above what the organism is capable of processing. To determine the range of concentration to use in the fermentations, the compounds were incubated with *Aspergillus aculeatus* in three concentrations of **73** and **74**: 0.4, 3.0 and 10 mg per 5 mL culture. After incubation for 7 days the fermentations were freeze-dried, extracted and 0.1 mg of the crude extract was dissolved in 1 mL of hexanes and analyzed using GCMS. No starting material or metabolites were reliably detected in the GCMS profile of the culture containing 0.4 mg of **73** or **74**. In the more concentrated examples, **73** and **74** were both consistently detected in the GCMS however no transformation products were observed in either case. This experiment did not give insight into the rate of biotransformation but a concentration on the lower end of the range between the two was chosen for use in future biotransformations to avoid oversaturation.

6.2.4 Selection of Fungi for Biotransformation

The Kerr Lab collection of fungal isolates has over 1300 members. Five fungi from this library were selected, based on their taxonomic similarity to fungi known to perform oxidations on compounds structurally related to gorgonene (e.g. sesquiterpene hydrocarbons and decalin containing sesquiterpenes). Known pathogens were avoided.

The five species of fungi that were chosen to screen for biotransformation of **73** and **74** were *Pleurotus djamor, Beauveria geodes*, *Curvularia lunata, Aspergillus*

aculeatus and *Bionectria ochroleuca*. *Pleurotus djamor* was chosen for its genus-level similarity to *Pleurotus sapidus*, a fungus known to contain peroxidases and to regio-specifically transform (+)-valencene (**153**), a sesquiterpene, to a flavor compound, (+)-nootkatone.[216] *Aspergillus aculeatus* was included because many *Aspergillus* species are known to perform oxidations on sesquiterpenes including *Aspergillus niger*[217] and *Aspergillus cellulosae*.[218] *Beauveria geodes* was chosen for its relation to *Beauveria bassiana*, known to transform aryltetralone.[219] *Curvularia lunata* is known to perform oxidations on several substrates including the 6β-acetoxyeudesmanols and 6β-acetoxyeudesmanones.[217, 220, 221]

6.2.5 Optimization of Duration of Fermentation

A study investigating the effect of the duration of fermentations on the product yields of the biotransformation was undertaken. Fermentations were shaken for 18 and 32 days from the addition of the sesquiterpene (**73** and separately **74**) before GCMS analysis and comparison. The five species of fungi were each cultured in five different liquid media and each was analyzed at the two time points. The five media were chosen based on fungal biotransformation studies in the literature.[217, 218, 222, 223]Two of the five (C and D) media contained low concentrations of nutrients and A, B and D were comparatively rich in nutrients with different nutrient sources and metal salts. All media recipes are included in the experimental section.

The biotransformations of **73** and **74** were performed in 5 mL of culture media in 15 mL glass tubes. The growth of the fungi was evaluated visually and the extent of biotransformation of **73** and **74** was assessed using GCMS. The samples were processed using the established freeze-dry/extraction method to prepare for evaluation by GCMS.

Each was compared to fungal cultures not containing either of the sesquiterpenes. Table 6.1 summarizes the results of the qualitative growth evaluation and Table 6.2 displays the percent conversion of starting materials to biotransformed products as estimated using GCMS.

Table 6.1 - Qualitative Analysis of Fungi Growth and Sporulation in Various Media

		Fungi									
		Beauveria geodes		*Pleurotus djamor*		*Curvularia lunatus*		*Aspergillus aculateus*		*Bionectria ochroleuca*	
Media	**73** and **74**	growth	sporulation	growth	sporulation	growth	sporulation	growth	sporulation	growth	sporulation
A	Blank	8	ns	5	s	8	s	9	s	5	s
	73	8	ns	2	ns	8	ns	7	s	6	s
	74	7	ns	4	ns	7	ns	7	s	6	s
B	Blank	8	s	7	s	7	s	7	s	5	s
	73	5	ns	5	ns	6	s	6	s	5	s
	74	5	ns	5	ns	7	s	8	s	6	s
C	Blank	10	s	2	ns	8	s	10	s	9	s
	73	10	s	1	ns	7	ns	10	s	9	s
	74	10	s	1	ns	8	u	10	s	8	s
D	Blank	6	s	7	s	6	s	6	s	4	s
	73	6	ns	5	ns	4	ns	5	s	4	s
	74	7	s	4	ns	5	s	5	s	5	s
E	Blank	9	s	6	s	9	s	10	s	8	s
	73	9	s	4	ns	9	ns	10	s	7	s
	74	9	s	2	ns	8	ns	10	s	8	s

- Qualitative Visual Rating of Fungal Growth (1 (very little growth) - 10 (significant growth)); s - Spores Visible; ns - No Spores Visible; u - Unable to Determine if Spores are Present.

Four of the fungi experienced optimal growth on media C and E although *Pleurotus djamor* grew best on media B and D. The growth ratings of the fungi did not directly correlate to the extent of biotransformation measured by GCMS. Low-nutrient media appeared to promote biotransformation better than richer nutrient broths. This observation may be due to the fungus processing the compound as a food source in an environment with low abundance of carbon sources, removing them from the extract and increasing the observed (GCMS) ratio of hydroxylated products.

Table 6.2 - Evaluation of Biotransformation Conversion at Two Time Points Using GCMS

		Fungi									
		Beauveria geodes		*Pleurotus djamor*		*Curvularia lunatus*		*Aspergillus aculateus*		*Bionectria ochroleuca*	
Media	**73** or **74**	t1	t2	t1	t2	t1	t2	t1	t2	t1	t2
A	**73**	0	0	0	0	0	0	0	0	0	2
	74	0	2	3	3	0	N	2	1	0	1
B	**73**	0	0	N	0	0	N	0	0	3	3
	74	3	4	3	3	3	N	1	3	N	N
C	**73**	0	0	0	0	0	0	0	0	N	N
	74	0	0	1	2	0	0	0	3	2	3
D	**73**	0	0	0	0	0	0	0	0	N	0
	74	2	4	3	3	3	4	3	3	0	N
E	**73**	0	0	0	0	0	0	0	0	4	N
	74	0	0	1	1	0	0	2	2	N	N

0 – No Transformation (Only Sm Visible). 1 - New Compound(s) Visible but Starting Material is Largest Peak in the GCMS Chromatogram. 2 - New Compound(s) Visible in GCMS Chromatogram, Approximately Equal in Height to Starting Material Signal. 3 - New Compounds(s) Present in GCMS Chromatogram, in Higher Intensity than Starting Materials. 4 - New Compounds Visible and Little or No Starting Materials Visible in the GCMS Chromatogram. N – No Starting Materials or Transformation Products Visible in the GCMS Chromatogram. T1 – 18 days. T2 – 32 days.

Incubation of compound **73** with *Bionectria ochroleuca* resulted in new metabolites visible in the GC eluting at 7.62, 8.23 and 8.66 minutes. Within the *Bionectria* fermentations, media had very little effect on the ratio of product formation and low-nutrient media B was chosen to use in the large scale fermentation. No transformation of **73** was observed by any of the other four fungi.

The GCMS analysis of the fermentation extracts suggested that **74** was more susceptible to biotransformation by multiple fungi than **73**. Two fungi were chosen to do large-scale biotransformations that produced different metabolites: *Pleurotus djamor* and *Beauveria geodes*. Again, no significant difference was observed between types of media used and media B was chosen for the large-scale fermentation.

6.3 Large Scale Biotransformation Fermentation

The fungi were innoculated into 1 L of media B in a 2.2 L flask and incubated for 7 days before 1 g of the reagent (**73** or **74**) was added. The flask was shaken at ambient temperature for 30 days before the cultures were freeze-dried and extracted sequentially with DCM, ethyl acetate and methanol. The solvent was removed from the extracts and the mass was recorded (Table 6.3).

Table 6.3 - Masses of Biotransformation Extracts

	Beauveria geodes	*Pleorotus djamour*	*Bionectria ochroleuca*
DCM Extract	52.1 mg	40.5 mg	129.2 mg
DCM Extract after C18 Filteration	44.6 mg	30.9 mg	101.3 mg
Ethyl Acetate Extract	13.0 mg	23.0 mg	21.0 mg
Methanol Extract	8617.9 mg	6593.5 mg	6380.9 mg

6.3.1 *Bionectria ocroleuca* Biotransformation of 73

The DCM extract of the *Bionectria ochroleuca* culture was separated into two major fractions using HPLC and the desired metabolites were present in fraction 1 according to LCMS and NMR data. Fraction 1 was further purified using HPLC and the compound mixture ionized in the LCMS with *m/z* ions of 237.184 $(C_{15}H_{25}O_2)^+$, (**73**+2O+H)$^+$ and 277.1776 $(C_{15}H_{26}O_3Na)^+$- (**73**+3O+2H+Na)$^+$ and appeared to have peaks typical of sesquiterpenoids in the ^{1}H NMR spectrum. Although peak 1 appeared to contain compounds derived from **73**, it was not analyzed further due the low product yield and complexity of the product mixture.

6.3.1.1 Structure Elucidation of *Bionectria ocroleuca* Biotransformation Product

The second compound to elute was a compound that accounted for 40 % of the crude DCM extract. Metabolite **157** was obtained as a white amorphous solid and was determined to have a molecular formula of $C_{15}H_{26}O_3$ with a *m/z* $(M+Na)^+$ ion of 277.177 corresponding to **73**+3O+2H+Na^+.

Table 6.4 shows the data from the 1D and 2D NMR that assisted in the elucidation of the structure of **157**. Indeed the final structure has a skeleton modified from **73**. The compound containined 15 carbons according to the ^{13}C NMR spectrum, three of which had chemical shifts typical of aclohols, C9, C11 and C12. Methine carbon C9 appeard at 79.3 ppm and was HMBC correlated to H15 and its connected hydrogen was COSY correlated to H8. C11 was a quaternary carbon resonating at 76.6 ppm in the ^{13}C spectrum and had HMBC correlations to H6 and H13. C12 was a bound to two hydrogen atoms (67.8 ppm) and had HMBC correlations to H6 and H13. The C4-C14 olefin remained in the molecule and the alkene hydrogens appeared between 4.9 and 5.2 ppm in the ^1H NMR spectrum. The planar structure elucidation of **157** was completed using the COSY and HMBC data shown in (Figure 6.3) The stereochemistry of the tertiary alcohol at C9 was assigned using NOESY correlations between the H9 and both H1b and H7b. The stereochemistry of C11was more difficult to assign due to free rotation around the C7-C11 bond making the use of through-space coupling in 2D NMR as a means of stereochemical assignment more challenging and the quaterinary geometry of C11 prevents the use of typical chiral shift reagents. NOESY and ROESY data however do support the stereochemistry assigned in Figure 6.3. Neither H12 or H13 have NOESY correlations to H14 suggesting that they are positioned away from the

olefin in the global energy minimum conformation and this is further supported by NOESY correlations H12/H7b and H13/H7a. H13 is also correlated to H6 suggesting it is positioned on the back side of the decalin skeleton (as drawn, Figure 6.3). Correlations between between H12 and H5 complement those results and place C12 on the front side of the decalin skeleton. These correlations are summarized in Figure 6.3 and support an *S* configuration at C11.

Table 6.4 - NMR Spectroscopic Data for Compound 157 ($CDCl_3$)

	δ_C, type	δ_H (*J* in Hz)	COSY	HMBC	NOESY	ROESY
1	38.0, CH_2	1.92, m	1b; 2b	15		
		1.27, m				
2	25.7, CH_2	1.82, m	1b; 2b; 8b	3a,b; 1b		
		1.64, m	1b			
3	39.4, CH_2	2.35, m	2b; 3b	14a,b		
		2.09, m	2a,b			
4	153.1, C			5; 3b		
5	52.1, CH	2.22, m	6	3; 6; 14; 15		1b; 9
6	39.9, CH	2.05, m	5; 7a,b	8a; 13		
7	26.1, CH_2	1.95, m	8a, 7b	8a,b; 13		
		1.33, m				12a,b
8	29.0, CH_2	1.71, m	7b; 9	7a,b	7b	
		1.59, m	7b; 9		7b	
9	79.3, CH	3.34, m	8a,b	7a; 15	1b; 8b	1b; 7b
10	43.5, C			1b; 5; 8a; 15		
11	76.6, C			6; 13		
12	67.8, CH_2	3.63, d (11.0 Hz)		6; 13	5; 7b	5
		3.40, d (11.0 Hz)			7b	
13	25.3, CH_3	1.19, s		9; 12a	6; 7a	
14	109.4, CH_2	5.16, s	3b	5; 3b		3a
		4.93, s	5			8
15	11.4, CH_3	0.80, s		1b; 5; 9	1a; 5; 6; 14b	
	OH	2.29, m		12a,b		

Data was obtained in $CDCl_3$ solution, δ in PPM relative to solvent signal. Assignments were aided by COSY, HSQC and HMBC, NOESY and ROESY experiments. HMBC correlations from the carbon stated to the indicated proton.

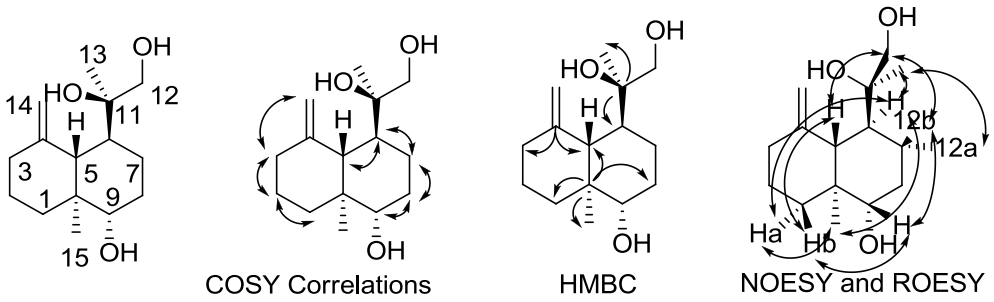

Figure 6.3 - Key NMR Correlations for the Structure Elucidation of Biotransformation Product 157

6.3.1.2 Metabolic Conversion of 73 to 157

The conversion of an olefin (C11-C12, **73**) to a glycol (C11-C12, **157**) by a fungus is similar to a result Asakawa *et al*. observed when transforming (+)-Nootkatone with *Aspergillus niger* (Figure 6.4).[224]

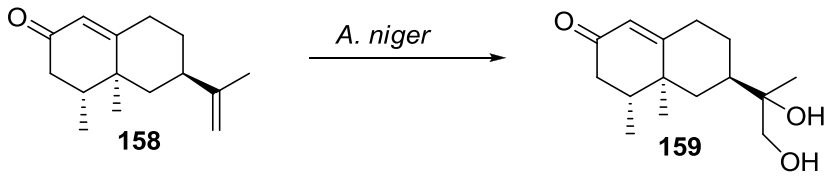

Figure 6.4 - Biotransformation of (+)-Nootkatone by *Aspergillus niger*

Asakawa *et al*. proposed that cytochrome P450 is responsible for the conversion of the alkene to an epoxide in an initial step which is then readily converted to the glycol moiety (**159**) in water. They concluded that a cytochrome P450 is involved based on the ability of 1-aminobenzotriazole, an inhibitor of cytochrome P450, to hinder the transformation. A cytochrome P450 may be responsible for the production of the glycol moiety in **157** as well. Below is a proposed mechanism for the dihydroxylation extrapolated from Asakawa's findings (Figure 6.5).

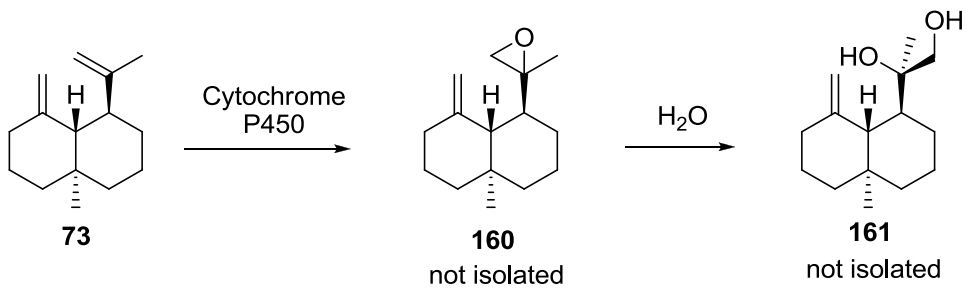

73 **160** not isolated **161** not isolated

Figure 6.5 - Proposed Mechanism for Formation of Glycol in 157

There are no examples of a biotransformation of (+)-β-gorgonene (**73**) in the literature, however, hydroxylation of C9 on similar decalin containing terpenoids is known (Figure 6.1) .[214, 215]

The regio- and stereoselective hydroxylation of gorgonene was successfully performed by *Bionectria ochroleuca.* The resulting metabolite **157** was obtained in a 4 % isolated yield. Although this is low for the purposes of this project, yields between 1-10 % are typical for this type of transformation.[219, 223] The disappearance of starting materials, however suggests that the product is being completely degraded by the fungus. This result is supported by the pathogenic nature of *B. ochroleuca* to plants[225] since sesquiterpenes are known to be major components of plants.[226]

6.3.1.3 Evaluation of Biological Activity of Compound 157

Compound **157** was tested for antimicrobial activity against a panel of 6 microbes (MRSA, VRE, *C. albicans*, *P. aeruginosa*, *P. vulgaris* and *S. warneri*) using the assay protocol described in Chapter 2 and was not active at 128 µg/mL. Compound **157** did not display cytotoxicity at a concentration of 64 µg/mL against human foreskin BJ fibroblast cell line (ATCC CRL-2522) or human breast adenocarcinoma cells (ATCC

HTB-26) when tested according to the procedure described in Chapter 2. Finally, compound **157** was not an inhibitor of the PTP1B enzyme at 50 µg/mL.

6.3.2 Fermentation of *Beauveria geodes* with 74

The DCM extract of the fermentation of *Beauveria geodes* with **74** was analyzed using UPLC-HRMS and several compounds ionized with *m/z* values within the range for predicted products (e.g. 277.131 (**74**+3O-4H)). HPLC purification of the crude extract was initiated but not successful due to exceptionally low yields of multiple product containing fractions.

6.3.3 *Pleurotus djamor* Fermentation with 74

The DCM extract from the *Pleurotus djamor* fermentation with compound **74** was analyzed using UPLC-HRMS and some promising ions were observed. There were two separate compounds that ionized with an *m/z* of 219.173, which are consistent with by the molecular formula $C_{15}H_{23}O^+$ (**74**+O-2H). There was also a compound with an *m/z* of 217.158, corresponding to the molecular formula $C_{15}H_{21}O$ (**74**+O-4H). Further attempts to purify the compounds were unsuccessful due to the complexity of the product mixture.

6.4 Future work

The successful production of one trihydroxylated metabolite was achieved and several other related metabolites were observed in amounts too low to fully characterize. The low yield of **157** prevented the use of biotransformation as an initial step of a semi-synthesis. Further optimization of this transformation would be necessary to warrant this as useful first step in a synthetic route.

A time trial experiment would be a logical next step in this study. Quantitative monitoring of disappearance of starting materials and the appearance of biotransformation products on a daily basis would provide more insight into the optimal end-time for the fermentations and perhaps help reduce loss of starting material. Should an optimized yield be achieved, this compound would be a candidate for further chemical modification.

The metabolite **157** did not show any biological activity in the assays tested. It may possess activity in another indication and should be included in a screening library for other indications.

6.5 Significance

Decalin containing sesquiterpenes are of interest for their varying biological activity and are often studied for their fragrance. Relatively little is known about the biotransformation of sesquiterpene hydrocarbons. Biocatalysis is an emerging field with great potential but much more exploratory work is warranted to establish an advanced understanding of the topic such as ability to predict the reactivity of specific organisms with substrates and make it a more useful tool for chemists. *Bionectria ochroleuca*, also known by several other names including *Clonostachys rosea* and *Gliocladium roseum* has been reported to perform an ester cleavage of an estrogenic compound[227] and hydroxylate sesquiterpenoids.[228]

6.6 Experimental Section

Procedure for Concentration Optimization and Use of Tween

Each fermentation was performed in duplicate and compared to a blank fermentation of the fungus. A cryovial containing *A. aculeatus* was thawed and 0.5 mL was inoculated into a sterile tube of seed media (E) and incubated for 7 days at ambient temperature. 1 mL of the seed inoculum was then transferred *via* pipette to a prepared, autoclaved 15 mL glass tube containing 5 mL media A. The tubes were shaken at 150 rpm at 22 ^{o}C for 4 days. Compound **73** or **74** was added to the cultures in the stated amount (2, 15 or 50 µL). Quadruplicates were performed of each compound at each concentration. The fermentations were allowed to stand for 7 days at 22 ^{o}C, then were freeze-dried and extracted with DCM (2x5 mL) with sonication. The extracts were combined, the solvent removed *in vacuo*, weighed and then injected to the GCMS at a concentration of 100 µg/mL in hexanes.

General Procedure for Optimization of Duration, Fungi and Media

Each fermentation was performed in duplicate and compared to a blank fermentation of the fungus. A cryovial containing the fungus (*Pleurotus djamor, Beauveria geodes*, *Curvularia lunata*, *Aspergillus aculeatus* or *Bionectria ochroleuca*) was thawed and 0.5 mL was inoculated into a sterile tube of seed media (E, 15 mL) and incubated for 7 days at ambient temperature. The seed inoculum (1 mL) was transferred *via* pipette to a prepared, autoclaved 15 mL glass tube containing 5 mL media (A-E). The tubes were shaken at 150 rpm at 22 ^{o}C for 4 days. Compound **73** or **74** (20 µL) was

added to the culture. The fermentations were allowed to stand for 14 days at 22 ^{o}C and duplicates of each fungus and media type were freeze-dried and extracted with DCM (2x5 mL). The extracts were combined, weighed and the injected to the GCMS at a concentration of 100 µg/mL in hexanes. The remaining fermentations (2 replicates of each fungi and media) were left to stand for a further 14 days before being rated for growth and sporulation, freeze-dried and extracted with DCM (2x5 mL). The solvent was removed from the extracts *in vacuo* and a 100 µL/mL solution in hexanes was prepared and injected to GCMS for analysis.

General Procedure for Large-Scale Biotransformation

A cryovial containing the fungus (*Bionectria ochroleuca, Pleorotus djamor or Beauveria geodes*) was thawed and innoculated (0.5 mL) into a autoclaved glass tube containing media E (15 mL) and microscope slides. The seed fermentation was allowed to shake (200 rpm, 25 ^{o}C) for 5 days. Media B (1 L) (autoclaved) was placed in a 2.2 L fernbach flask and media B (100 mL) was placed in a 250 mL earlenmeyer flask for a control. The seed fermenation was transferred *via* pipette to the 250 mL flask (1mL) and the fermbach flask (14 mL). The flasks were incubated with shaking (200 rpm) for 7 days at 25 ^{o}C. Gorgonene (1 mL) or **74** (1 mL) was added (neat) to the fernbach. The fungi were continually shaken at 200 rpm and 25 ^{o}C for 5 weeks. The fermentations were freeze-dried, extracted with DCM (2x 300 mL with sonication at 35 ^{o}C, 1 x 300 mL with soaking (12 hours)). The filtrates were decanted and combined and the solvent removed *in vacuo*. The freeze-dried cultures were then extracted with ethyl acetate (2 x 250 mL) and methanol (2 x 250 mL). The ethyl acetate fractions were combined and the methanol fractions were combined, the solvent removed and weighed. All of the extracts

were screened using GCMS and those with promising profiles were analyzed using NMR.

Biosynthesis of **157**

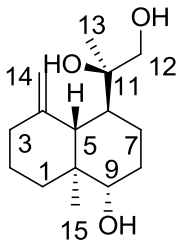

The biotransformation of **73** was performed according to the general procedure described above using *Bionectria ochroleuca*. The DCM and ethyl acetate fractions we combined and fractionated using reversed-phase HPLC (phenyl hexyl semi-prep column, isocratic, 75:25 MeOH:H_2O) and the second fraction to elute was further purified using reversed-phase HPLC (phenyl hexyl semi-prep column, isocratic 55:45, MeOH:H_2O). The second compound to elute was a pure white amorphous solid (4 % yield, 40 mg).

^{1}H NMR (600 MHz, $CDCl_3$) δ 5.16 (s, 1H), 4.94 (s, 1H), 3.63 (d, *J* = 11.0 Hz, 1H), 3.41 (d, *J* = 11.0 Hz, 1H), 3.34 (m, 1H), 2.35 (m, 1H), 2.21 (m, 1H), 2.11 – 2.06 (m, 1H), 2.08 – 2.01 (m, 1H), 1.97 – 1.92 (m, 1H), 1.94 – 1.89 (m, 1H), 1.84-1.80 (m, 1H), 1.74 – 1.68 (m, 1H), 1.65-1.61 (m, 1H), 1.60 – 1.53 (m, 1H), 1.36 – 1.30 (m, 1H), 1.28-1.23 (m, 1H), 1.19 (s, 3H), 0.80 (s, 3H).

^{13}C NMR (151 MHz, $CDCl_3$) δ153.0, 109.4, 79.2, 76.6, 67.7, 52.0, 43.4, 39.9, 39.3, 37.9, 29.0, 26.1, 25.6, 25.3, 11.4.

(+) HRESIMS *m*/*z* 277.1766 $[M + Na]^+$ (calcd for $C_{15}H_{26}O_3$, 277.1780)

Media Recipes

Media A[218]

1.5 % Sucrose, 1.5 % glucose, 0.5 % polypeptone, 0.1 % K_2HPO_4, 0.05 % KCl, 0.001 % $FeSO_4$-$7H_2O$, in distilled water.

Media B[222]

0.5 % Glucose, 0.5 % malt extract, 0.2 % peptone, 0.5 % yeast extract and1.8 % instant ocean in distilled water.

Media C[217]

3 % Glucose, 3 % glycerol, 1.5 % peptone, 1.5 % yeast extract, 1.5 % K_2HPO_4 and 1.5 % instant ocean in distilled water

Media D [223]

0.5 % Glucose, 0.1 % peptone, 0.1 % yeast, 0.1 % beef extract and distilled water. Adjust to pH 5.7 with NaOH.

Media E (SYMA)

4.0 % Maltose, 1.0 % peptone, 1.0 % yeast extract, 0.1 % agar and 1.8 % instant ocean in distilled water.

Chapter 7 - Conclusion and Future Work

7.1 Synthesis and Biological Evaluation of Gorgonene Derivatives

Several small collections of compounds derived from the sesquiterpeneoid (+)-β-gorgonene were synthesized, purified and characterized using HRMS, NMR and IR. A number of synthetic strategies were applied to produce the analogues, none of which were more than four steps from gorgonene. The series of non-natural sesquiterpene-like compounds were screened for biological activity in three assays for PTP inhibition, cytotoxicity and antimicrobial activity and analyzed for drug-likeness. Several of the library members showed modest cytotoxicity, the most potent of which displayed IC_{50}'s between of 16-32 μg/mL (**106** and **107**) against human breast adenocarcinoma cells. Although many of the gorgonene derivatives displayed inhibition of the PTP1B enzyme, those that were selective for the PTP1B enzyme were only modest inhibitors.

7.2 Reactivity of Gorgonene

One recurring observation in this project was intramolecular cyclizations of gorgonene and its derivatives, particularly the dione and glycol-containing analogues. The proximal functional groups (terminal alkenes, ketones, hydroxyl groups) are positioned to interact with each other instead of intermolecularly. Gorgonene can be viewed as a unactivated 1,5-diene model system providing precedence for other comparable systems to react similarly under the same synthetic conditions. Pericyclic reactions within gorgonene have produced several novel tri- and tetracyclic structures, useful for the expansion of the synthetic library and providing new routes to these desirable frameworks in other systems.

7.3 Future Work

Although a high hit rate of compounds possessing modest biological activity in the cytotoxicity and PTP assays were observed, none of the compounds were potent enough to warrant a second generation library based on a single lead compound. Synthesis of a library of similarly functionalized compounds based on the more common bicyclofarnesol sesquiterpene skeleton may produce derivatives with more potent activity and provide insight on the effect of the substitution pattern of the decalin skeleton on biological activity.

This semi-synthetic collection described in this work has been archived and a large portion of it is available for future screening in additional bioassays.

References

(1) Statistics Canada, Health Statistics Division **2011**.

(2) Anderson, D. I.; Levin, B. R. *Curr. Opin. Microbiol.* **1999**, *2*, 489-493.

(3) Smyth, S.; Heron, A. *Nat. Med.* **2006**, *12*, 75-80.

(4) Abel, U.; Koch, C.; Speitling, M.; Hansske, F. G. *Curr. Opin. Chem. Biol.* **2002**, *6*, 453-458.

(5) Jimeno, J.; Faircloth, G.; Sousa-Faro, J. F.; Scheuer, P.; Rinehart, K. *Marine Drugs* **2004**, *2*, 14-29.

(6) Kumar, K.; Waldmann, H. *Angewandte Chemie International Edition* **2009**, *48*, 3224-3242.

(7) Paterson, I.; Anderson, E. A. *Science* **2005**, *310*, 451-453.

(8) Newman, D. J.; Cragg, G. M. *J. Nat. Prod.* **2012**, *75*, 311-335.

(9) Mishra, B. B.; Tiwari, V. K. *Eur. J. Med. Chem.* **2011**, *46*, 4769-4807.

(10) Wetzel, S.; Bon, R. S.; Kumar, K.; Waldmann, H. *Angew. Chem. Int. Ed.* **2011**, *50*, 10800-10826.

(11) Bauer, A.; Bronstrup, M. *Nat. Prod. Rep.* **2014**.

(12) Jimeno, J.; Faircloth, G.; Sousa-Faro, J. F.; Scheuer, P.; Rinehart, K. *Marine Drugs* **2004**, *2*, 14-29.

(13) Mayer, A. M.; Glaser, K. B.; Cuevas, C.; Jacobs, R. S.; Kem, W.; Little, R. D.; McIntosh, J. M.; Newman, D. J.; Potts, B. C.; Shuster, D. E. *Trends Pharmacol. Sci.* **2010**, *31*, 255-265.

(14) Newman, D. J. Hill, R. T. *J. Ind. Microbiol. Biotechnol.* **2006**, *33*, 539-544.

(15) Galeano, E.; Rojas, J. J.; Martinez, A. *Nat. Prod. Commun.* **2011**, *6*, 287-300.

(16) Koehn, F. E.; Carter, G. T. *Nat Rev Drug Discov.* **2005**, *4*, 206-220.

(17) Paterson, I.; Florence, G. J. *Top. Curr. Chem.* **2009**, *286*, 73-119.

(18) DeChristopher, B. A.; LoyBrian A.; MarsdenMatthew D.; Schrier, A. J.; Zack, J. A.; Wender, P. A. *Nat. Chem.* **2012**, *4*, 705-710.

(19) Halford, B. *Chem. Eng. News Archive* **2011**, *89*, 10-17.

(20) Long, B. H.; Carboni, J. M.; Wasserman, A. J.; Cornell, L. A.; Casazza, A. M.; Jensen, P. R.; Lindel, T.; Fenical, W.; Fairchild, C. R. *Cancer Res.* **1998**, *58*, 1111-1115.

(21) Nicolaou, K. C.; van Delft, F.; Ohshima, T.; Vourloumis, D.; Xu, J.; Hosokawa, S.; Pfefferkorn, J.; Kim, S.; Li, T. *Angew. Chem. Int. Ed Engl.* **1997**, *36*, 2520-2524.

(22) Holton, R. A.; Kim, H. B.; Somoza, C.; Liang, F.; Biediger, R. J.; Boatman, P. D.; Shindo, M.; Smith, C. C.; Kim, S. *J. Am. Chem. Soc.* **1994**, *116*, 1599-1600.

(23) Corey, E. J.; Gin, D. Y.; Kania, R. S. *J. Am. Chem. Soc.* **1996**, *118*, 9202-9203.

(24) Marshall, J. A.; Johns, B. A. *J. Org. Chem.* **1998**, *63*, 7885-7892.

(25) Kuttruff, C. A.; Eastgate, M. D.; Baran, P. S. *Nat. Prod. Rep.* **2014**, ASAP

(26) Piel, J.; Hui, D.; Wen, G.; Butzke, D.; Platzer, M.; Fusetani, N.; Matsunaga, S. *Proc. Natl. Acad. Sci. U. S. A.* **2004**, *101*, 16222-16227.

(27) Campbell, E.; Nicholson, A. C.; British Columbia. Ministry of Forests. Research Branch In *A summary of western yew biology with recommendations for its management in British Columbia;* Province of British Columbia, Ministry of Forests Research Program: **1995**

(28) *Phyton News Release* - DFB Pharmaceuticals Acquires Phyton Inc.,World's Largest Plant Cell Fermentation Facility, **2006**.

(29) Stierle, A.; Strobel, G.; Stierle, D. *Science* **1993**, *260*, 214-216.

(30) Malik, S.; Cusidó, R. M.; Mirjalili, M. H.; Moyano, E.; Palazón, J.; Bonfill, M. *Process Biochemistry* **2011**, *46*, 23-34.

(31) Cuevas, C.; Perez, M.; Martin, M. J.; Chicharro, J. L.; Fernandez-Rivas, C.; Flores, M.; Francesch, A.; Gallego, P.; Zarzuelo, M.; de La Calle, F.; Garcia, J.; Polanco, C.; Rodriguez, I.; Manzanares, I. *Org. Lett.* **2000**, *2*, 2545-2548.

(32) Ruiz, C.; Valderrama, K.; Zea, S.; Castellanos, L. *Mar. Biotechnol. (NY)* **2013**, *15*, 571-583.

(33) Leal, M. C.; Calado, R.; Sheridan, C.; Alimonti, A.; Osinga, R. *Trends Biotechnol.* **2013**, *31*, 555-561.

(34) Nadeem, M.; Rikhari, H. C.; Kumar, A.; Palni, L. M.; Nandi, S. K. *Phytochemistry* **2002**, *60*, 627-631.

(35) Proksch, P.; Edrada-Ebel, R.; Ebel, R. *Marine Drugs* **2003**, *1*, 5-17.

(36) Zhang, H.; Wang, Y.; Pfeifer, B. A. *Mol. Pharm.* **2008**, *5*, 212-225.

(37) Galm, U.; Shen, B. *Expert Opin. Drug Discov.* **2006**, *1*, 409-437.

(38) MarinLit Database, University of Canterbury, ChristChurch. **2009**.

(39) Antibase Database, Wiley-VCH Verlag GmbH & Co. KGaA. **2012**.

(40) Abdi, H.; Williams, L. J. *WIREs Comp Stat* **2010**, *2*, 433-459.

(41) Vin, H.; Ching, G.; Ojeda, S.; Adelmann, C. H.; Chitsazzadeh, V.; Dwyer, D.; Ma, H.; Ehrenreiter, K.; Baccarini, M.; Ruggieri, R.; Curry, J.; Ciurea, A. M.; Duvic, M.; Busaidy, N. L.; Tannir, N. M.; Tsai, K. Y. *Mol. Cancer. Ther.* **2013**.

(42) Kaiser, M.; Wetzel, S.; Kumar, K.; Waldmann, H. *Cell Mol. Life Sci.* **2008**, *65*, 1186-1201.

(43) Kennedy, J. *Nat. Prod. Rep.* **2008**, *25*, 25-34.

(44) Sams-Dodd, F. *Drug Discov. Today* **2005**, *10*, 139-147.

(45) Sliwoski, G.; Kothiwale, S.; Meiler, J.; Lowe, E. W.,Jr *Pharmacol. Rev.* **2013**, *66*, 334-395.

(46) Lupfert, C.; Reichel, A. *Chem. Biodivers* **2005**, *2*, 1462-1486.

(47) Nadin, A.; Hattotuwagama, C.; Churcher, I. *Angew. Chem. Int. Ed.* **2012**, *51*, 1114-1122.

(48) Lipinski, C. A.; Lombardo, F.; Dominy, B. W.; Feeney, P. J. *Adv. Drug Deliv. Rev.* **2001**, *46*, 3-26.

(49) Boldi, A. M. *Curr. Opin. Chem. Biol.* **2004**, *8*, 281-286.

(50) Ramallo, I. A.; Salazar, M. O.; Mendez, L.; Furlan, R. L. *Acc. Chem. Res.* **2011**, *44*, 241-250.

(51) López, S. N.; Ramallo, I. A.; Sierra, M. G.; Zacchino, S. A.; Furlan, R. L. E. *Proceedings of the National Academy of Sciences* **2007**, *104*, 441-444.

(52) Breinbauer, R.; Manger, M.; Scheck, M.; Waldmann, H. *Curr. Med. Chem.* **2002**, *9*, 2129-2145.

(53) Breinbauer, R.; Vetter, I. R.; Waldmann, H. *Angewandte Chemie International Edition* **2002**, *41*, 2878-2890.

(54) Lee, M. L.; Schneider, G. *J. Comb. Chem.* **2001**, *3*, 284-289.

(55) Caballero, B. *Epidemiologic Reviews* **2007**, *29*, 1-5.

(56) Mokdad, A. H.; Ford, E. S.; Bowman, B. A.; Dietz, W. H.; Vinicor, F.; Bales, V. S.; Marks, J. S. *JAMA* **2003**, *289*, 76-79.

(57) Caro, J. J.; Ward, A. J.; O'Brien, J. A. *Diabetes Care* **2002**, *25*, 476-481.

(58) Zhang, S.; Zhang, Z. *Drug Discovery Today* **2007**, *12*, 373-381.

(59) Kenner, K. A.; Anyanwu, E.; Olefsky, J. M.; Kusari, J. *J. Biol. Chem.* **1996**, *271*, 19810-19816.

(60) Zinker, B. A.; Rondinone, C. M.; Trevillyan, J. M.; Gum, R. J.; Clampit, J. E.; Waring, J. F.; Xie, N.; Wilcox, D.; Jacobson, P.; Frost, L.; Kroeger, P. E.; Reilly, R. M.; Koterski, S.; Opgenorth, T. J.; Ulrich, R. G.; Crosby, S.; Butler, M.; Murray, S. F.; McKay, R. A.; Bhanot, S.; Monia, B. P.; Jirousek, M. R. *Proceedings of the National Academy of Sciences}* **2002**, *99*, 11357-11362.

(61) Carr, G.; Berrue, F.; Klaiklay, S.; Pelletier, I.; Landry, M.; Kerr, R. G. *Methods* **2014**, *65*, 229-238

(62) Enriori, P. J.; Evans, A. E.; Sinnayah, P.; Cowley, M. A. *Obesity* **2006**, *14*, 254S-258S.

(63) Zabolotny, J. M.; Bence-Hanulec, K. K.; Stricker-Krongrad, A.; Haj, F.; Wang, Y.; Minokoshi, Y.; Kim, Y. B.; Elmquist, J. K.; Tartaglia, L. A.; Kahn, B. B.; Neel, B. G. *Dev. Cell.* **2002**, *2*, 489-495.

(64) Bence, K. K.; Delibegovic, M.; Xue, B.; Gorgun, C. Z.; Hotamisligil, G. S.; Neel, B. G.; Kahn, B. B. *Nat. Med.* **2006**, *12*, 917-924.

(65) Tsou, R. C.; Zimmer, D. J.; De Jonghe, B. C.; Bence, K. K. *Endocrinology* **2012**, *153*, 4227-4237.

(66) Zhang, Z. Y. *Annu. Rev. Pharmacol. Toxicol.* **2002**, *42*, 209-234.

(67) Levy, S. B.; Marshall, B. *Nat. Med.* **2004**.*10*, S122-S129

(68) Ochman, H.; Lawrence, J. G.; Groisman, E. A. *Nature* **2000**, *405*, 299-304.

(69) Abraham, E. P.; Chain, E. *Rev. Infect. Dis.* **1988**, *10*, 677-678.

(70) Garattini, S. *J. Nephrol.* **1997**, *10*, 283-294.

(71) Marris, E. *Nature* **2006**, *443*, 904-905.

(72) Jasarevic, T. WHO: Urgent action needed to prevent the spread of untreatable gonorrhea. **2012**.

(73) Wise, J. *BMJ* **2010**, 341

(74) Portero, A. G.; González-Coloma, A.; Reina, M.; Díaz, C. E. *Phytochemistry Reviews* **2012**, *11*, 391-403.

(75) Lin, X.; Ji, S.; Li, R.; Dong, Y.; Qiao, X.; Hu, H.; Yang, W.; Guo, D.; Tu, P.; Ye, M. *J. Nat. Prod.* **2012**, *75*, 2121-2131.

(76) Krasulova, J.; Hanus, R.; Kutalova, K.; Sobotnik, J.; Sillam-Dusses, D.; Tichy, M.; Valterova, I. *J. Chem. Ecol.* **2012**, *38*, 557-565.

(77) Zhang, H. X.; Tan, J. L.; Wei, L. X.; Wang, Y. L.; Zhang, C. P.; Wu, D. K.; Zhu, C. Y.; Zhang, Y.; Zhang, K. Q.; Niu, X. M. *J. Nat. Prod.* **2012**, *75*, 1419-1423.

(78) Stierle, D. B.; Stierle, A. A.; Girtsman, T.; McIntyre, K.; Nichols, J. *J. Nat. Prod.* **2012**, *75*, 262-266.

(79) Che, Q.; Zhu, T.; Qi, X.; Mándi, A.; Kurtán, T.; Mo, X.; Li, J.; Gu, Q.; Li, D. *Org. Lett.* **2012**, *14*, 3438-3441.

(80) Citron, C. A.; Gleitzmann, J.; Laurenzano, G.; Pukall, R.; Dickschat, J. S. *Chembiochem* **2012**, *13*, 202-214.

(81) Shubina, L. K.; Kalinovsky, A. I.; Makarieva, T. N.; Fedorov, S. N.; Dyshlovoy, S. A.; Dmitrenok, P. S.; Kapustina, I. I.; Mollo, E.; Utkina, N. K.; Krasokhin, V. B.; Denisenko, V. A.; Stonik, V. A. *Nat. Prod. Commun.* **2012**, *7*, 487-490.

(82) Wright, A. D.; Schupp, P. J.; Schror, J. P.; Engemann, A.; Rohde, S.; Kelman, D.; de Voogd, N.; Carroll, A.; Motti, C. A. *J. Nat. Prod.* **2012**, *75*, 502-506.

(83) Su, J. H.; Huang, C. Y.; Li, P. J.; Lu, Y.; Wen, Z. H.; Kao, Y. H.; Sheu, J. H. *Arch. Pharm. Res.* **2012**, *35*, 779-784.

(84) Tseng, Y. J.; Shen, K. P.; Lin, H. L.; Huang, C. Y.; Dai, C. F.; Sheu, J. H. *Mar. Drugs* **2012**, *10*, 1572-1581.

(85) Tamemoto, K.; Takaishi, Y.; Chen, B.; Kawazoe, K.; Shibata, H.; Higuti, T.; Honda, G.; Ito, M.; Takeda, Y.; Kodzhimatov, O. K.; Ashurmetov, O. *Phytochemistry* **2001**, *58*, 763-767.

(86) Chang, S.; Wang, S.; Wu, C.; Chen, P.; Kuo, Y.*Holzforschung*, **2005**, *54*, 241-245.

(87) Chen, Q. F.; Liu, Z. P.; Wang, F. P. *Mini Rev. Med. Chem.* **2011**, *11*, 1153-1164.

(88) Song, A. R.; Sun, X. L.; Kong, C.; Zhao, C.; Qin, D.; Huang, F.; Yang, S. *Arch. Virol.* **2013**, 1-8.

(89) Lyss, G.; Schmidt, T. J.; Merfort, I.; Pahl, H. L. *Biol. Chem.* **1997**, *378*, 951-961.

(90) Geris, R.; Simpson, T. J. *Nat. Prod. Rep.* **2009**, *26*, 1063-1094.

(91) Menna, M.; Imperatore, C.; D'Aniello, F.; Aiello, A. *Mar. Drugs* **2013**, *11*, 1602-1643.

(92) Simpson, T. J.; Ahmed, S. A.; Rupert McIntyre, C.; Scott, F. E.; Sadler, I. H. *Tetrahedron* **1997**, *53*, 4013-4034.

(93) Iida, M.; Ooi, T.; Kito, K.; Yoshida, S.; Kanoh, K.; Shizuri, Y.; Kusumi, T. *Org. Lett.* **2008**, *10*, 845-848.

(94) Takada, K.; Kajiwara, H.; Imamura, N. *J. Nat. Prod.* **2010**, *73*, 698-701.

(95) Gordaliza, M. *Mar. Drugs* **2010**, *8*, 2849-2870.

(96) Djeddi, S.; Karioti, A.; Sokovic, M.; Stojkovic, D.; Seridi, R.; Skaltsa, H. *J. Nat. Prod.* **2007**, *70*, 1796-1799.

(97) Urban, S.; Capon, R. J. *J. Nat. Prod.* **1992**, *55*, 1638-1642.

(98) Pawlik, J. R. *Chem. Rev.* **1993**, *93*, 1911-1922.

(99) Menna, M.; Imperatore, C.; D'Aniello, F.; Aiello, A. *Marine Drugs* **2013**, *11*, 1602-1643.

(100) Sullivan, B.; Djura, P.; McIntyre, D. E.; Faulkner, D. J. *Tetrahedron* **1981**, *37*, 979-982.

(101) Sullivan, B. W.; Faulkner, D. J.; Matsumoto, G. K.; Cun-heng, H.; Clardy, J. *J. Org. Chem.* **1986**, *51*, 4568-4573.

(102) Sullivan, B.; Faulkner, D. J.; Webb, L. *Science* **1983**, *221*, 1175-1176.

(103) Nakamura, H.; Deng, S.; Kobayashi, J.; Ohizumi, Y. *Tetrahedron* **1986**, *42*, 4197-4201.

(104) Tsoukatou, M.; Maréchal, J. P.; Hellio, C.; Novaković, I.; Tufegdzic, S.; Sladić, D.; Gašić, M. J.; Clare, A. S.; Vagias, C.; Roussis, V. *Molecules* **2007**, *12*, 1022-1034.

(105) Cozzolino, R.; De Giulio, A.; De Rosa, S.; Strazzullo, G.; Gasić, M. J.; Sladić, D.; Zlatović, M. *J. Nat. Prod.* **1990**, *53*, 699-702.

(106) Amiguet, V. T.; Petit, P.; Ta, C. A.; Nuñez, R.; Sánchez-Vindas, P.; Alvarez, L. P.; Smith, M. L.; Arnason, J. T.; Durst, T. *J. Nat. Prod.* **2006**, *69*, 1005-1009.

(107) Kuete, V.; Wabo, G. F.; Ngameni, B.; Mbaveng, A. T.; Metuno, R.; Etoa, F. -.; Ngadjui, B. T.; Beng, V. P.; Meyer, J. J. M.; Lall, N. *J. Ethnopharmacol.* **2007**, *114*, 54-60.

(108) Da Silva, L. L. D.; Nascimento, M. S.; Cavalheiro, A. J.; Silva, D. H. S.; Castro-Gamboa, I.; Furlan, M.; Bolzani, V. D. S. *J. Nat. Prod.* **2008**, *71*, 1291-1293.

(109) Schmidt, L. E.; Gloer, J. B.; Wicklow, D. T. *J. Nat. Prod.* **2007**, *70*, 1317-1320.

(110) Fu, X.; Schmitz, F. J.; Tanner, R. S.; Kelly-Borges, M. *J. Nat. Prod.* **1998**, *61*, 548-550.

(111) Sokoloff, S.; Halevy, S.; Usieli, V.; Colorni, A.; Sarel, S. *Experientia* **1982**, *38*, 337-338.

(112) Chang, C. W. J.; Patra, A.; Baker, J. A.; Scheuer, P. J. *J. Am. Chem. Soc.* **1987**, *109*, 6119-6123.

(113) Chang, C. W. J.; Patra, A.; Roll, D. M.; Scheuer, P. J.; Matsumoto, G. K.; Clardy, J. *J. Am. Chem. Soc.* **1984**, *106*, 4644-4646.

(114) Gonzalez, A. G.; Estrada, D. M.; Martin, J. D. *Tetrahedron* **1984**, *40*, 4109-4113.

(115) Ahn, J. -.; Jang, K. -.; Chung, S. -.; Oh, K. -.; Shin, J. *Org. Lett.* **2008**, *10*, 1167-1169.

(116) Li, Y.; Zhang, Y.; Shen, X.; Guo, Y. W. *Bioorg. Med. Chem. Lett.* **2009**, *19*, 390-392.

(117) Zhang, Y.; Li, Y.; Guo, Y. W.; Jiang, H. L.; Shen, X. *Acta Pharmacol. Sin.* **2009**, *30*, 333-345.

(118) Jiao, W. H.; Huang, X. J.; Yang, J. S.; Yang, F.; Piao, S. J.; Gao, H.; Li, J.; Ye, W. C.; Yao, X. S.; Chen, W. S.; Lin, H. W. *Org. Lett.* **2012**, *14*, 202-205.

(119) Rodriguez, E.; Towers, G. H. N.; Mitchell, J. C. *Phytochemistry* **1976**, *15*, 1573-1580.

(120) Kreuger, M. R.; Grootjans, S.; Biavatti, M. W.; Vandenabeele, P.; D'Herde, K. *Anticancer Drugs* **2012**, *23*, 883-896.

(121) Merfort, I. *Curr. Drug Targets* **2011**, *12*, 1560-1573.

(122) Chaturvedi, D. In *Sesquiterpene lactones: Structural diversity and their biological activities;* Opportunity, Challenge and Scope of Natural Products in Medicinal Chemistry; Ari Puji Astuti: Kerala, India, 2011; pp 313.

(123) Sharma, A.; Bajpai, V.; Shukla, S. In *Sesquiterpenes and Cytotoxicity;* Ramawat, K., Merillon, J., Eds.; Natural Products; Springer Reference: 2013; pp 3515-3550.

(124) Wu, Q.; Shi, Y.; Jia, Z. *Nat. Prod. Rep.* **2006**, *23*, 699-734.

(125) Mang, C.; Jakupovic, S.; Schunk, S.; Ambrosi, H.; Schwarz, O.; Jakupovic, J. *J. Comb. Chem.* **2006**, *8*, 268-274.

(126) Koch, M. A.; Schuffenhauer, A.; Scheck, M.; Wetzel, S.; Casaulta, M.; Odermatt, A.; Ertl, P.; Waldmann, H. *Proc. Natl. Acad. Sci. U. S. A.* **2005**, *102*, 17272-17277.

(127) Schwarz, O.; Jakupovic, S.; Ambrosi, H. D.; Haustedt, L. O.; Mang, C.; Muller-Kuhrt, L. *J. Comb. Chem.* **2007**, *9*, 1104-1113.

(128) Weinheimer, A. J.; Washecheck, P. H.; Van Der Helm, D.; Hossain, M. B. *Chemical Communications (London)* **1968**, 1070-1071.

(129) Boeckman Jr., R. K.; Silver, S. M. *J. Org. Chem.* **1975**, *40*, 1755-1759.

(130) Hackl, T.; König, W. A.; Muhle, H. *Phytochemistry* **2004**, *65*, 2261-2275.

(131) Correa, H.; Valenzuela, A. L.; Ospina, L. F.; Duque, C. *J. Inflamm. (Lond)* **2009**, *6*, 5-9255-6-5.

(132) Mayer, A. M. S.; Jacobson, P. B.; Fenical, W.; Jacobs, R. S.; Glaser, K. B. *Life Sci.* **1998**, *62*, PL401-PL407.

(133) Roussis, V.; Wu, Z.; Fenical, W.; Strobel, S. A.; Van Duyne, G. D.; Clardy, J. *J. Org. Chem.* **1990**, *55*, 4916-4922.

(134) Look, S. A.; Fenical, W.; Jacobs, R. S.; Clardy, J. *Proceedings of the National Academy of Sciences* **1986**, *83*, 6238-6240.

(135) Ciminiello, P.; Fattorusso, E.; Magno, S.; Mayol, L. *J. Nat. Prod.* **1985**, *48*, 64-68.

(136) Wu, T. S.; Damu, A. G.; Su, C. R.; Kuo, P. C. *Nat. Prod. Rep.* **2004**, *21*, 594-624.

(137) Jacobson, P. B.; Jacobs, R. S. *J. Pharmacol. Exp. Ther.* **1992**, *262*, 866-873.

(138) Alder, K.; Pascher, F.; Schmitz, A. *Ber. Dtsch. Chem. Ges.* **1943**, *76*, 27.

(139) Snider, B. B. *Acc. Chem. Res.* **1980**, *13*, 426-432.

(140) Mikami, K.; Shimizu, M. *Chem. Rev.* **1992**, *92*, 1021-1050.

(141) Hoffmann, H. M. R. *Angew. Chem. Int. Ed Engl.* **1969**, *8*, 556-577.

(142) Paderes, G. D.; Jorgensen, W. L. *J. Org. Chem.* **1992**, *57*, 1904-1916.

(143) Blomquist, A. T.; Himics, R. J. *J. Org. Chem.* **1968**, *33*, 1156-1159.

(144) Blomquist, A. T.; Passer, M.; Schollenberger, C. S.; Wolinsky, J. *J. Am. Chem. Soc.* **1957**, *79*, 4972-4976.

(145) Snider, B. B.; Rodini, D. J.; Conn, R. S. E.; Sealfon, S. *J. Am. Chem. Soc.* **1979**, *101*, 5283-5293.

(146) Hackl, T.; König, W. A.; Muhle, H. *Phytochemistry* **2004**, *65*, 2261-2275.

(147) Harrod, J. F.; Chalk, A. J. *J. Am. Chem. Soc.* **1964**, *86*, 1776-1779.

(148) Stahl, P.; Kissau, L.; Mazitschek, R.; Huwe, A.; Furet, P.; Giannis, A.; Waldmann, H. *J. Am. Chem. Soc.* **2001**, *123*, 11586-11593.

(149) Okamoto, R.; Okazaki, E.; Noguchi, K.; Tanaka, K. *Org. Lett.* **2011**, *13*, 4894-4897.

(150) Hecht, D.; Aldridge, K.; Roe-Carpenter, D.; Citron, D.; Rosenblatt, J.; Cox, M.; Webb, D.; Jacobus, N.; Wexler, H.; Onderdonk, A. **2006**.

(151) Wang, W. Q.; Sun, J. P.; Zhang, Z. Y. *Curr. Top. Med. Chem.* **2003**, *3*, 739-748.

(152) Lorenz, U. In *Protein Tyrosine Phosphatase Assays;* John Wiley & Sons, Inc: **2001**.

(153) Strom, A. E.; Hartwig, J. F. *J. Org. Chem.* **2013**, *78*, 8909-8914.

(154) Voica, A.; Mendoza, A.; Gutekunst, W. R.; Fraga, J. O.; Baran, P. S. *Nat Chem* **2012**, *4*, 629-635.

(155) Kaufman, M. D.; Grieco, P. A.; Bougie, D. W. *J. Am. Chem. Soc.* **1993**, *115*, 11648-11649.

(156) Yang, D.; Wong, M.; Wang, X.; Tang, Y. *J. Am. Chem. Soc.* **1998**, *120*, 6611-6612.

(157) Marchal, E.; Uddin, M. I.; Smithen, D. A.; Hawco, C. L. A.; Lanteigne, M.; Overy, D. P.; Kerr, R. G.; Thompson, A. *RSC Adv.* **2013**, *3*, 22967-22971.

(158) Hulin, B.; Clark, D. A.; Goldstein, S. W.; McDermott, R. E.; Dambek, P. J.; Kappeler, W. H.; Lamphere, C. H.; Lewis, D. M.; Rizzi, J. P. *J. Med. Chem.* **1992**, *35*, 1853-1864.

(159) Greenblatt, D. J.; Matlis, R.; Scavone, J. M.; Blyden, G. T.; Harmatz, J. S.; Shader, R. I. *British Journal of Clinical Pharmacology* **1985**, *19*, 373-378.

(160) Barst, R. J.; Langleben, D.; Frost, A.; Horn, E. M.; Oudiz, R.; Shapiro, S.; McLaughlin, V.; Hill, N.; Tapson, V. F.; Robbins, I. M.; Zwicke, D.; Duncan, B.; Dixon, R. A. F.; Frumkin, L. R. *Am. J. Respir. Crit. Care Med.* **2004**, *169*, 441-447.

(161) Illescas, B. M.; Martín, N. *J. Org. Chem.* **2000**, *65*, 5986-5995.

(162) Bull, J.; Balskus, E.; Horan, R. .; Langner, M.; Ley, S. *Chem. Eur. J.* **2007**, *13*, 5515-5538.

(163) Conti, P.; De Amici, M.; Grazioso, G.; Roda, G.; Barberis Negra, F. F.; Nielsen, B.; Stensbøl, T. B.; Madsen, U.; Bräuner-Osborne, H.; Frydenvang, K.; De Sarro, G.; Toma, L.; De Micheli, C. *J. Med. Chem.* **2004**, *47*, 6740-6748.

(164) Bishta, S. S.; Ajay, A.; Sinhab, S. K.; Chaturvedic, V.; Tripathia, R. P. *International Journal of Drug Design and Discovery* **2010**, *1*, 11-18.

(165) Mishra, R. C.; Tewari, N.; Verma, S. S.; Tripathi, R. P.; Kumar, M.; Shukla, P. K. *J. Carbohydr. Chem.* **2004**, *23*, 353-374.

(166) Meijere, A.,de *Angewandte Chemie-international Edition* **1979**, *18*, 809-826.

(167) Carey, F.; Sundberg, R. In *Concerted Pericyclic Reactions;* Springer US: **2007**; pp 833-964.

(168) Aoyama, Y.; Araki, Y.; Konoike, T. *Synlett* **2001**, 1452-1454.

(169) Majerski, Z.; Hamersak, Z.; Mlinaric-Majerski, K. *J.Chem.Soc.Chem.Commun.* **1985**, 1830-1831.

(170) Li, Y.; Huang, J.; Zhou, Z.; Che, C. *J. Am. Chem. Soc.* **2001**, *123*, 4843-4844.

(171) Simmons, H. E.; Smith, R. D. *J. Am. Chem. Soc.* **1958**, *80*, 5323-5324.

(172) Pines, H.; Sih, N. C.; Lewicki, E. *J. Org. Chem.* **1965**, *30*, 1457-1462.

(173) Bülow, N.; König, W.,A. *Phytochemistry* **2000**, *55*, 141-168.

(174) Mehta, G.; Singh, B. P. *J. Org. Chem.* **1977**, *42*, 632-638.

(175) Walters, W. P.; Murcko, M. A. *Adv. Drug Deliv. Rev.* **2002**, *54*, 255-271.

(176) Veber, D. F.; Johnson, S. R.; Cheng, H.; Smith, B. R.; Ward, K. W.; Kopple, K. D. *J. Med. Chem.* **2002**, *45*, 2615-2623.

(177) Ghose, A. K.; Viswanadhan, V. N.; Wendoloski, J. J. *J. Comb. Chem.* **1999**, *1*, 55-68.

(178) Kuan, K. K. W.; Pepper, H. P.; Bloch, W. M.; George, J. H. *Org. Lett.* **2012**, *14*, 4710-4713.

(179) Yang, J.; Hoffmeister, D.; Liu, L.; Fu, X.; Thorson, J. S. *Bioorg. Med. Chem.* **2004**, *12*, 1577-1584.

(180) Criegee, R. *Angew. Chem. Int. Ed Engl.* **1975**, *14*, 745-752.

(181) Trost, B. M.; Fleming, I. In *Comprehensive Organic Synthesis: Reduction;* Elsevier Science \& Technology Books: **1991**

(182) Borowitz, I. J.; Rapp, R. D. *J. Org. Chem.* **1969**, *34*, 1370-1373.

(183) Van Ornum, S. G.; Champeau, R. M.; Pariza, R. *Chem. Rev.* **2006**, *106*, 2990-3001.

(184) Schiaffo, C. E.; Dussault, P. H. *J. Org. Chem.* **2008**, *73*, 4688-4690.

(185) Hon, Y.; Lin, S.; Lu, L.; Chen, Y. *Tetrahedron* **1995**, *51*, 5019-5034.

(186) Wurtz, C. A. *Bull. Soc. Chim. Fr.* **1872**, *17*, 436-442.

(187) Reichardt, C.; Welton, T. In *Solvents and Solvent Effects in Organic Chemistry;* Wiley: **2011**.

(188) Jacob, P.; Callery, P. S.; Shulgin, A. T.; Castagnoli, N. *J. Org. Chem.* **1976**, *41*, 3627-3629.

(189) Bienhoff, S. E.; Kok, D. J.; Roycroft, L. M.; Roberts, E. S. *Vet. Parasitol.* **2013**, *195*, 102-105.

(190) Van Dijk, J.; Zwagemakers, J. M. A. *J. Med. Chem.* **1977**, *20*, 1199-1206.

(191) Illescas, B. M.; Martín, N. *J. Org. Chem.* **2000**, *65*, 5986-5995.

(192) Abdel-Magid, A.; Carson, K. G.; Harris, B. D.; Maryanoff, C. A.; Shah, R. D. *J. Org. Chem.* **1996**, *61*, 3849-3862.

(193) Montague, D. C.; Rowland, F. S. *J. Am. Chem. Soc.* **1971**, *93*, 5381-5387.

(194) Fenwick, J.; Frater, G.; Ogi, K.; Strausz, O. P. *J. Am. Chem. Soc.* **1973**, *95*, 124-132.

(195) Berrué, F.; McCulloch, M. W. B.; Kerr, R. G. *Bioorg. Med. Chem.* **2011**, *19*, 6702-6719.

(196) Correa, H.; Aristizabal, F.; Duque, C.; Kerr, R. *Mar. Drugs* **2011**, *9*, 334-343.

(197) Fenical, W., & Jacobs, R. **1988**. *Pseudopterosin and synthetic derivatives thereof* A61K31/70; A61K31/7028; A61K31/7034; A61K31/704; A61P25/04; A61P29/00; A61P35/00; C07H15/256; (IPC1-7): C07H15/24.

(198) Reina, E.; Puentes, C.; Rojas, J.; Garcia, J.; Ramos, F. A.; Castellanos, L.; Aragon, M.; Ospina, L. F. *Bioorg. Med. Chem. Lett.* **2011**, *21*, 5888-5891.

(199) Lindel, T.; Jensen, P. R.; Fenical, W.; Long, B. H.; Casazza, A. M.; Carboni, J.; Fairchild, C. R. *J. Am. Chem. Soc.* **1997**, *119*, 8744-8745.

(200) Pellissier, H. *Tetrahedron* **2004**, *60*, 5123-5162.

(201) Anslyn, E. V.; Dougherty, D. A. In *Modern Physical Organic Chemistry;* University Science: **2006**.

(202) Zweifel, G.; Nagase, K.; Brown, H. C. *J. Am. Chem. Soc.* **1962**, *84*, 183-189.

(203) Hunsen, M.; Long, D. A.; D'Ardenne, C. R.; Smith, A. L. *Carbohydr. Res.* **2005**, *340*, 2670-2674.

(204) Marchbank, D. H.; Kerr, R. G. *Tetrahedron* **2011**, *67*, 3053-3061.

(205) Completo, G. C.; Lowary, T. L. *J. Org. Chem.* **2008**, *73*, 4513-4525.

(206) Williams, R. J.; McGill, N. W.; White, J. M.; Williams, S. J. *J. Carbohydr. Chem.* **2010**, *29*, 236-263.

(207) Karplus, M. *J. Am. Chem. Soc.* **1963**, *85*, 2870-2871.

(208) Lambert, J. B.; Netzel, D. A.; Sun, H.; Lilianstrom, K. K. *J. Am. Chem. Soc.* **1976**, *98*, 3778-3783.

(209) San Feliciano, A.; Medarde, M.; Lopez, J. L.; Salinero, M. A.; Rodriguez, M. L. *J. Org. Chem.* **1993**, *58*, 7942-7944.

(210) Madhunapantula, S. V.; Desai, D.; Sharma, A.; Huh, S. J.; Amin, S.; Robertson, G. P. *Mol. Cancer. Ther.* **2008**, *7*, 1297-1308.

(211) Mach, M.; Schlueter, U.; Mathew, F.; Fraser-Reid, B.; Hazen, K. C. *Tetrahedron* **2002**, *58*, 7345-7354.

(212) Kharitonov, Y. V.; Shul´ts, E. E.; Gatilov, Y. V.; Bagryanskaya, I. Y.; Shakirov, M. M.; Tolstikov, G. A. *Chemistry of Natural Compounds* **2012**, *48*, 250-257.

(213) - Hudlicky, T.; Reed, J. W. *Chem. Soc. Rev.* **2009**, *38*, 3117-3132.

(214) Wang, Y.; Tan, T.; Tan, G. K.; Connolly, J. D.; Harrison, L. J. *Phytochemistry* **2006**, *67*, 58-61.

(215) Hashimoto, T.; Noma, Y.; Gotoh, Y.; Tanaka, M.; Takaoka, S.; Asakawa, Y. *Heterocycles* **2004**, *62*, 655-666.

(216) Krugener, S.; Krings, U.; Zorn, H.; Berger, R. G. *Bioresour. Technol.* **2010**, *101*, 457-462.

(217) Choudhary, M.; Musharraf, S.; Sami, A.; Atta-ur-Rahman *HCA* **2004**, *87*, 2685-2694.

(218) Hashimoto, T.; Noma, Y.; Gotoh, Y.; Tanaka, M.; Takaoka, S.; Asakawa, Y. *Heterocycles* **2004**, *62*, 655-655-666.

(219) Buchanan, G. O.; Williams, L. A.; Reese, P. B. *Phytochemistry* **2000**, *54*, 39-45.

(220) Garcia-Granados, A.; Martinez, A.; Rivas, F.; Onorato, M. E.; Arias, J. M. *J. Nat. Prod.* **1990**, *53*, 436-440.

(221) Collins, D. O.; Reese, P. B. *Phytochemistry* **2002**, *59*, 489-492.

(222) Abraham, W.; Riep, A.; Hanssen, H. *Bioorg. Chem.* **1996**, *24*, 19.

(223) Garcia Granados, A.; Gutierrez, M. C.; Rivas, F. *J Molec Catal B* **2004**, *27*, 133.

(224) Furusawa, M.; Hashimoto, T.; Noma, Y.; Asakawa, Y. *Chemical and Pharmaceutical Bulletin* **2005**, *53*, 1423-1429.

(225) Bienapfl, J. C.; Floyd, C. M.; Percich, J. A.; Malvick, D. K. *Plant Dis.* **2012**, *96*, 1700-1700.

(226) Degenhardt, J.; Köllner, T. G.; Gershenzon, J. *Phytochemistry* **2009**, *70*, 1621-1637.

(227) Kakeya, H.; Takahashi-ando, N.; Kimura, M.; Onose, R.; Yamaguchi, I.; Osada, H. *Biosci. Biotechnol. Biochem.* **2002**, *66*, 2723-2726.

(228) García-Granados, A.; Gutiérrez, M. C.; Parra, A.; Rivas, F. *J. Nat. Prod.* **2002**, *65*, 1011-1015.